Vertical Migration: Structure and function of pelagic ecosystems

Pinti, Jerome Pierre Alexandre

Publication date:
2020

Document Version
Publisher's PDF, also known as Version of record

DTU Aqua
National Institute of Aquatic Resources

PhD Thesis

Vertical Migration

Structure and function of pelagic ecosystems

Jérôme Pinti

Supervisor:
André W. Visser

Co-supervisors:
Thomas Kiørboe
Patrizio Mariani

Kongens Lyngby, Denmark 2020

Centre for Ocean Life
VKR Centre of Excellence

DTU Aqua
National Institute of Aquatic Resources
Technical University of Denmark

Kemitorvet
Building 202
2800 Kongens Lyngby
www.dtu.dk/english

Abstract

Diel Vertical Migration (DVM) is the daily movement of marine organisms as diverse as zooplankton, fish and squids between the depths and the surface of the oceans. DVM is primarily an antipredator response, organisms typically hiding from visual predation in deep waters during daytime before ascending to feed in food-rich surface waters at night. DVM is such a widespread phenomenon that it is believed to be the largest natural daily movement of biomass of the planet (only potentially exceeded by human commuters).

Behind this apparent simplicity, a vast diversity of patterns can be observed in the oceans. The day residency depth, the night residency depth, the speed and timing of ascent and descent all vary according to the environmental conditions considered. In addition, DVM being an anti-predator response, trophic interactions and the food-web structure have important consequences on the realised migration patterns. Consequently, prey and predator can react to each other and adapt their behaviours simultaneously. Most studies modelling DVM usually consider varying environmental conditions (e.g. light levels) but keep predator and prey fields constant, omitting the cascading effects that changes in the DVM patterns of one population can have on other populations.

The first aim of this PhD thesis was to consider explicitly these feedbacks to understand mechanistically the drivers of DVM patterns (especially day and night residency depths). We merged notions of game theory, trait-based approach and classic ecology to reproduce DVM patterns observed in nature. Each organism is seen as a player that tries to optimize its fitness. Its fitness depends on its traits, but also on its own behaviour and on the behaviours of its prey and predators. Organisms modify their vertical position in the water column, exposing themselves to different light levels, i.e. different growth opportunities and mortality risks. We compute simultaneously the optimal behaviour of all organisms by finding the Nash equilibrium of the system – the point at which no organism can get a better fitness by changing unilaterally its behaviour. We first apply this method to a system consisting of a zooplankton prey and its visual predator, and investigate how changes in predator traits impact prey (and predators) DVM patterns. Then, we apply this method to a size-based zooplankton food-web. We divide the zooplankton community in 100 sub-populations based on their size and feeding modes and recreate size-based non-linear DVM patterns observed in the oceans.

Further, as a feature modifying food intake and mortality risks, DVM can potentially impact population dynamics. We investigate the consequences of behaviour at the

individual time scale on population dynamics (taking place at a larger time scale). We show that considering the adaptive behaviour of prey and predator affects population dynamics, but also ecosystem functions such as trophic transfer efficiency and active carbon export.

Indeed, if DVM is a fascinating feature by itself, it is also important globally as it has cascading consequences for marine ecosystem and the global carbon cycle. Global marine phytoplankton biomass represents "only" about 3 PgC (compared with 60 PgC for terrestrial vegetation), but they both fix carbon at a comparable rate (60 PgC/yr for terrestrial vegetation vs. approx. 50 PgC/yr for marine phytoplankton). Of these 50 PgC/yr, between 5 and 11 PgC/yr are transported below the euphotic zone, either through sinking (dead organisms, fecal material) or active transport of vertically migrating organisms. This carbon export rate is crucial for the global carbon cycle as carbon reaching the ocean depths is sequestrated for extended periods, consequently helping to reduce atmospheric CO_2 concentrations. It is estimated that active transport of carbon by organisms performing DVM represents approx. 15% of this total. However, this estimation is mainly for migrating zooplankton, and the exact global contribution of other functional groups such as fish is blurry.

In the final part of this thesis, we develop a model of DVM for different functional groups of zooplankton and fish that provides us with global DVM patterns. This enables us to disentangle the relative contribution of each functional group to the carbon export flux below the euphotic zone, as well as the relative importance of DVM in the carbon export mediated by each functional group. We couple these outputs with a global ocean circulation model and generate global estimates of carbon sequestrated through the different pathways of the active biological pump. We estimate that higher trophic levels (mesozooplankton and up) sequestrate around 751 PgC.

Dansk resumé

Daglig Vertikal Migration (DVM) er den daglige bevægelse af marine organismer, herunder dyreplankton, fisk og blæksprutter, mellem dybder og havenes overflade. DVM er primært en anti-prædationsrespons, hvor organismer, der typisk skjuler sig for visuel prædation i dybe farvande om dagen, stiger op til det fødevarerige overfladevand om natten for at spise. DVM er et så udbredt fænomen, at det antages at være den største naturlige daglige bevægelse af biomasse på hele planeten (kun potentielt overskredet af menneskelige pendlere).

Gennem dette tilsyneladende enkle fænomen kan man observere en lang række forskellige mønstre i verdenshavene. Dybden for de henholdsvis daglige og natlige ophold, samt både hastigheden og tidspunktet for opstigning og nedstigning, varierer alt sammen med de miljømæssige forhold. I kraft af, at DVM er en anti-prædationsrespons, har trofiske interaktioner og fødevarestrukturen vigtige konsekvenser for de realiserede migrationsmønstre. Derfor kan bytte og rovdyr reagere og tilpasse sig hinandens adfærd samtidig. De fleste studier, som modellerer DVM, tager normalt højde for forskellige miljøforhold (f.eks. niveauet af lys), men holder rovdyr- og byttesfærer konstant. Dette betyder dog, at man udelader den kaskade af effekter, som ændringer i en populations DVM-mønster kan have på andre populationer.

Det første mål med denne ph.d.-afhandling er eksplicit at overveje disse effekter, for mekanisk at forstå hvad der driver DVM-mønstrene (især dybder om dagen og natten). For at gengive DVM-mønstrene observeret i naturen, anvender vi både spilteori, en træk-baseret tilgang samt klassisk økologi. Dette betyder, at hver organisme bliver set som en spiller, der forsøger at optimere dens fitness. Dens fitness afhænger af dens træk, men også af dens egen adfærd, samt adfærden af dens bytte og rovdyr. Organismer ændrer deres vertikale position i vandsøjlen og udsætter sig for forskellige lysniveauer, dvs. forskellige vækstmuligheder og dødelighedsrisici. Vi beregner samtidig den optimale adfærd for alle organismer ved at finde den så kaldte Nash-ligevægt i systemet – altså det punkt, hvor ingen organisme kan få en bedre fitness ved udelukkende at ændre dens adfærd. Vi anvender først denne metode på et system, der består af et dyreplanktonbytte og dets visuelle rovdyr, og undersøger, hvordan ændringer i rovdyrsegenskaber kan have konsekvenser for byttedyrs (og rovdyrs) DVM-mønstre. Derefter anvender vi denne metode til et størrelsesbaseret fødenet af dyreplankton. Vi deler dyreplanktonsamfundet i 100 underpopulationer baseret på deres størrelse og måde at skaffe føde på og genskaber størrelsesbaserede ikke-lineære DVM-mønstre observeret i verdenshavene.

Som en funktion, der ændrer fødevareindtagelse og dødelighedsrisici, kan DVM endvidere potentielt på virke populationsdynamikker. Vi undersøger konsekvenserne af adfærd på den individuelle tidsskala på populationsdynamikker (som finder sted på en større tidsskala). Som forventet viser vi, at inklusionen af byttedyrs og rovdyrets adaptive opførsel på virker befolkningsdynamikken, men også økosystemfunktioner så som trofisk overførselseffektivitet og aktiv kulstofeksport.

Udover at være et fascinerende fænomen i sig selv, er DVM også vigtigt på globalt plan, da det har enorme konsekvenser for det marine økosystem og den globale kulstofcyklus. Den globale marine planteplanktonbiomasse repræsenterer "kun" ca. 3 PgC (sammenlignet med 60 PgC for terrestrisk vegetation), men de fikserer lige store mængder af kulstof (60 PgC/år for jordvegetation vs. ca. 50 PgC/år for marint planteplankton). Af disse 50 PgC/år transporteres mellem 5 og 11 PgC/ år til under den oplyste zone, enten gennem synkende (døde organismer, fækalt materiale) eller aktiv transport af vertikalt migrerende organismer. Denne kulstofeksportrate er afgørende for den globale kulstofcyklus, da det kulstof, som når dybhavet, lagres i længere perioder. Dette medvirker til at reducere den atmosfæriske CO_2-koncentration og derved til at reducere klimaændringerne. Det estimeres, at aktiv transport af kulstof fra organismer, der udfører DVM, repræsenterer ca. 15 % af den samlede kulstofmængde. Dette skøn er dog hovedsageligt beregnet på migrering af dyreplankton, og det nøjagtige globale bidrag fra andre funktionelle grupper, såsom fisk, er uklart.

I den sidste del af denne afhandling udvikler vi en DVM-model for forskellige funktionelle grupper af dyreplankton og fisk, som giver os globale DVM-mønstre. Dette gør det muligt for os at skille det relative bidrag fra hver funktionel gruppe til kulstofeksporten ned under den oplyste zone, såvel som den relative betydning af DVM i kulstofeksporten udført af hver enkel funktionel gruppe. Vi sammenholder disse resultater med en global havcirkulationsmodel og genererer globale estimater for kulstof, som bliver lagret gennem de forskellige dele af den aktive biologiske pumpe. Vi estimerer, at højere trofiske niveauer (fra mesodyreplankton og op) lagrer omkring 751 PgC.

Résumé en français

Les migrations verticales journalières (MVJ) désignent la mouvement journalier d'organismes aussi divers que le zooplancton, les poissons et les calamars entre les profondeurs et la surface des océans. Les MVJ sont principalement une réponse contre les prédateurs, où les organismes se cachent des prédateurs visuels pendant la journée en allant en profondeur, avant de migrer vers la surface riche en nourriture à la nuit tombée. Les MVJ sont un phénomène si courant qu'elles sont considérées comme le plus important mouvement de biomasse journalier de la planète (à l'exception peut-être des travailleurs humains). Derrière cette simplicité apparente se cache une grande diversité de MVJ dans les océans: de nombreux facteurs (tels que la profondeur de résidence durant le jour et la nuit, la vitesse et l'horaire de migration) varient selon les conditions environnementales. En plus, les MVJ étant une réponse anti-prédateurs, elles peuvent être grandement influencées par les interactions prédateur-proie et la structure du réseau trophique. Ainsi, les proies et prédateurs réagissent l'un à l'autre et adaptent leur comportement simultanément. La plupart des études qui modélisent les MVJ prennent en compte des changements de conditions environnementales (comme le niveau de lumière) mais gardent les distributions des proies et prédateurs constantes. De fait, ces études ignorent le fait que des changements de comportement d'une population peut se répercuter sur une autre, et vice-versa.

Le premier but de cette thèse de doctorat était de considérer explicitement ces rétroactions pour comprendre de manière méchanistique les MVJ observées (et en particulier la profondeur de résidence durant le jour et la nuit). Nous avons mélangé des notions de théorie des jeux, d'écologie classique et une approche basée sur les traits des organismes pour reproduire les MVJ observées. Chaque organisme est considéré comme un « joueur » qui essaye d'optimiser sa valeur adaptative (à quel point est-il efficace et adapté à son environnement ?). Cette valeur dépend des traits de l'individu considéré, mais elle dépend aussi de son comportement et du comportement de ses proies et de ses prédateurs. Les organismes modifient leur position verticale dans la colonne d'eau, s'exposant ainsi à différents niveaux d'illumination, c'est-à-dire différentes opportunités de se nourrir mais aussi différents risques de se faire capturer par des prédateurs. Nous calculons simultanément le comportement optimal de tous les organismes du réseau trophique considéré en trouvant l'équilibre de Nash du système, c'est-à-dire le point auquel aucun organisme ne peut augmenter sa valeur adaptative en changeant unilatéralement de comportement. Nous avons commencé à appliquer cette méthode à un système comprenant une population de zooplancton et une population de prédateurs visuels (des poissons planctivores) dans le but de

comprendre les conséquences qu'un changement de traits du prédateur peut avoir sur les MVJ de ses proies (mais aussi de lui-même). Ensuite, nous avons appliqué cette méthode à un réseau trophique de zooplancton. Nous avons divisé le zooplancton en 100 sous-populations (sur des critères de taille et de mode d'alimentation), ce qui nous a permis de recréer des motifs non-linéaires de MVJ observés dans les océans.

Ensuite, étant donné que les MVJ changent le taux d'alimentation et les risques de mortalité, elles ont aussi le potentiel d'impacter les dynamiques des populations. Nous avons exploré quelles conséquences les MVJ des individus (qui se produisent à une échelle de temps rapide) pouvaient avoir sur les dynamiques des populations (se produisant à une échelle de temps beaucoup plus lente). Comme suspecté, nous avons trouvé que considérer le comportement adaptatif des proies et des prédateurs affecte les dynamiques de populations, mais aussi des fonctions écosystémiques comme l'efficacité de transfert trophique et le transport actif de carbone.

En effet, si les MVJ sont un phénomène fascinant en elles-mêmes, elles sont aussi importantes d'un point de vue global étant donné qu'elles ont des conséquences pour les écosystèmes marins et le cycle global du carbone. La biomasse de phytoplancton marin ne représente «que» 3 PgC (à comparer aux 60 PgC de la végétation terrestre), mais les deux fixent le carbone à un taux comparable (60 PgC/an pour la végétation terrestre contre environ 50 PgC/an pour la phytoplancton marin). Sur ces 50 PgC/an, entre 5 et 11 PgC/an sont transportés sous la zone photique, soit grâce à la chute de particules (organismes morts, matière fécale), soit grâce au transport actif d'organismes effectuant des MVJ. Cet export de carbone est crucial pour le cycle global du carbone, étant donné que le carbone qui arrive en profondeur est séquestré pendant longtemps et aide donc à réduire la concentration atmosphérique de CO_2 et le changement climatique anthropogénique. Il est estimé que le carbone transporté par les organismes effectuant des MVJ représente environ 15 % du total du carbone exporté. Cependant, cette estimation concerne principalement le zooplancton performant les MVJ et la contribution exacte des autres populations (comme les poissons) est peu précisément établie.

Dans la dernière partie de cette thèse, nous avons développé un modèle qui génère les MVJ optimales de différents groupes fonctionnels de zooplancton et de poissons à l'échelle globale. Ce modèle nous a permis d'estimer les contributions relatives des MVJ pour chaque groupe fonctionnel considéré au flux de carbone sous la zone photique. Nous avons ensuite couplé ces résultats à un modèle de circulation océanique global, dans le but d'estimer le stockage global de carbone généré par chacun des groupes fonctionnels considérés. Au total, nous estimons que le mesozooplancton et les niveaux trophiques supérieurs contribuent à la séquestration d'environ 751 PgC.

Preface

This thesis was submitted as part of the requirements to fulfil the Doctor of Philosophy Degree (PhD) at the Technical University of Denmark (DTU). The research presented was carried out between October 2017 and September 2020 at the National Institute of Aquatic Resources (DTU Aqua) in Kongens Lyngby, except for manuscript I (Predator-prey games in multiple habitats reveal mixed strategies in diel vertical migration). This first manuscript was initiated as I was a master student at DTU, but a substantial part of the analysis and the writing were done during the period of employment as a PhD student at DTU Aqua.

This PhD project was part of the Centre for Ocean Life, a VKR centre for excellence funded by the Villum Foundation. Additional support was received from the Otto Mønsteds Fond for conferences participation in Hamburg, Germany (ICES Annual Science Conference); Chicheley Hall, England, United Kingdom (4^{th} International Workshop on trait-based approaches to Ocean Life); and San Diego, USA (Ocean Sciences Meeting 2020). EuroMarine (European Marine Research Network) is also acknowledged for funding a conference participation (4^{th} International Workshop on trait-based approaches to Ocean Life) and participation in a course (Life-history adaptations to seasonality, 1 month and a half at UNIS, Svalbard). The FILAMO network is further acknowledged for funding participation to the workshop on Movement Ecology of Marine Organisms in Cape Town, South Africa, in September 2018.

The PhD project was supervised by Prof. Dr. André W. Visser as well as Prof. Dr. Thomas Kiørboe and Dr. Patrizio Mariani. The project included two research stays abroad: a four week stay onboard RV Kronprins Haakon (cruise leader Dr. Webjørn Melle from IMR, Norway) in May 2019, and a six week stay at the University of California in Santa Barbara in collaboration with Prof. Dr. David Siegel and Prof. Dr. Timothy DeVries in January-February 2020.

Kongens Lyngby, Denmark, September 2020

Jérôme Pinti

Acknowledgements

Even though there is no scientific content in acknowledgements, they are traditionally the most-read section of a thesis – I hope you will enjoy reading them, but I also encourage you to skim through my thesis' chapters, I tried to make them at least as interesting as this section. I know only three persons that will for sure read the remaining of this thesis: the members of my PhD assessment committee. Asbjørn Christensen, Josefin Titelman and Olivier Maury, thank you so much for taking the time to evaluate my PhD work.

Many thanks to my supervisor André W. Visser. Andy, it was a real pleasure to work under your supervision. Among many things, I really appreciated the freedom you gave me to explore my own paths, but also your ways of asking me the good questions when what I wanted at first was just an answer. On a more personal note, I will be missing one of the best (and most prolific!) story tellers I've ever met.

I also thank my other supervisor, Thomas Kiørboe. Your supervision style perfectly complemented Andy's and I am really grateful to know that I could always rely on you. I will miss your motivation, efficiency, and your vast knowledge — even though I know we will stay in touch.

In complement to Andy and Thomas, I want to give a special thanks to my colleagues of the "Moore meetings", Ken H. Andersen and Camila Serra Pompei (as well as Subhendu Chakraborty, Mathilde Cadier and Anton Almgren when our presence at DTU coincided). I enjoyed the format of these meetings, and my PhD greatly benefited from our informal discussions. Camila, my "co-PhD" (and co-MSc!), an extra-special acknowledgement to you. It was great to have someone to share progress and issues with, and to grumble with about many maybe-not-so-important things.

The Centre for Ocean Life, the Section for Ocean and Arctic, and DTU Aqua will always have a special place in my heart. It was a pleasure to pursue my PhD there. I am grateful to everyone at DTU Aqua for always keeping their doors open whenever needed. I will keep many memories from our weekly ocean life meetings and annual retreats, but also from our many social activities: Friday drinks, international dinners, and of course cookie breaks and foosball games. DTU Aqua's foosball table deserves a shout out here, as it helped me to release so much pressure during these three years. But the table would have been of little help without all the foosball players (should I really give all the names here?): Subhendu, Daniel, Neil, Rocío, Fredrik, Rémy, Aurore, Kristian, Mridul, and probably a few more. Thanks for the perpetual fun! Mridul, I also want to thank you personally for the great advice you've given me in

many different situations, both scientifically and personally. Tommy and Neil, thank you for the squash and all the Friday drinks (Helle, Stefan, and all the other Friday drinkers, thank you too!). Lilian, thanks a lot for helping us on so many things and for making our lives at DTU Aqua so much easier! Josephine and Hanna, thank you for helping me with the Danish résumé of this thesis.

Away from Denmark, I thank David Siegel and Tim DeVries from the University of California in Santa Barbara, who welcomed me in their institute during my external stay. It was a pleasure to work with both of you. I am very grateful for the time you devoted to me and my project, and I am very happy to see that our collaboration really improved my last PhD chapter. Thank you also to Webjørn Melle from IMR and all the crew and scientific staff of R/V Kronprins Haakon for welcoming me onboard during their mesopelagic survey in the North Atlantic. It was such a fantastic experience to see with my own eyes what I used to model behind my computer. I learnt a lot during this month, and I hope I will keep on going in the field in the future! Stefan, thank you so much for helping me set this up.

I want to thank all my friends, from France, Denmark, and other countries for their support and for the time we spend together: my former housemates (Théo, Baltazar, Sam), Cécile, Alexandre, Nicolas, Berthe, members of KUSO (and especially the cello section of the best orchestra of Copenhagen), and of course all Brasspackers. Thanks also to my parents and Eloïse for their continuous support and encouragement despite my will to always discover new places and wander far away. Last, but clearly not least, thank you Aurore for always being there for me. These three years would not have been half as fun and interesting without you, and I can't wait to see what our next chapter will hold.

List of publications

This PhD thesis is based on the following publications:

I. **Pinti, J.** and A.W. Visser (2019). Predator-prey games in multiple habitats reveal mixed strategies in diel vertical migration. The American Naturalist 193(3):E65-E77, doi:10.1086/701041

II. **Pinti J.,** K.H. Andersen, and A.W. Visser. Co-adaptive behavior of interacting populations significantly impacts ecosystem function. (*under review*)

III. **Pinti J.,** T. Kiørboe, U.H. Thygesen, and A.W. Visser (2019). Trophic interactions drive the mergence of diel vertical migration patterns: a game-theoretic model of copepod communities. Proceedings of the Royal Society B 286:20191645, doi:10.1098/rspb.2019.1645

IV. **Pinti, J.,** T. DeVries, T. Norin, C. Serra-Pompei, R. Proud, D.A. Siegel, T. Kiørboe, C.M. Petrik, K.H. Andersen, A. Brierley, and A.W. Visser. Active carbon sequestration potential of different populations of a pelagic food-web. (*in preparation*)

Additionally, the following manuscripts represent minor contributions to the thesis:

- **Pinti J.,** A. Celani, U.H. Thygesen, and P. Mariani (2020). Optimal navigation and behavioural traits in oceanic migrations. Theoretical Ecology, doi:10.1007/s12080-020-00469-4

- C. Serra-Pompei, B. Ward, **J. Pinti,** A.W. Visser, T. Kiørboe, and K.H. Andersen. Role of zooplankton trophic dynamics in driving carbon export efficiency (*in preparation*)

Contents

CHAPTER 1

Introduction

1.1 Background

The oceans cover 70.9% of our planet. 93% of the oceans are deeper than 200 m, making the open ocean the largest bio-accessible environment on Earth. To better apprehend this immense volume, the oceans are divided into several zones (figure 1.1). From the surface to 200 m lies the photic zone, where light penetrates and photosynthesis happens – supporting most animals present in the oceans.

In the open ocean, the photic zone is also called the epipelagic zone. Below the epipelagic starts the mesopelagic zone, extending from roughly 200 m to 1000 m. Below that lies the bathyal, abyssal and hadal zones. Despite the large physical differences of these zones (in terms of light, temperature, and pressure), they are heavily connected through the global overturning circulation, a "conveyor belt" largely based on temperature and salinity differences that moves water masses all around the ocean basins (Schmitz Jr., 1996a,b).

Living organisms inhabit all these different zones and many move commonly between them, enhancing the connectivity of the different habitats. Horizontally, planktonic organisms can be advected by currents from oceanic to neritic waters (Isaacs and Schwartzlose, 1965), and nektonic organisms routinely migrate between coastal and offshore areas (Block et al., 2011). Vertically, many organisms use several zones as well, for instance during ontogenic habitat shift (Fuiman, 1997), annual dormancy (Jónasdóttir et al., 2015; Visser et al., 2017), rapid movements (Thygesen et al., 2016), or lastly diel vertical migrations, the main focus of this thesis.

Understanding how organisms are distributed within and move between these zones is important, as organisms and their movements determine ecosystem functions and services. For instance, organisms moving vertically actively transport carbon between the surface and the depths, influencing the global carbon cycle and playing a role in regulating our climate. Additionally, fish migrations and distribution determines their production, consequently impacting fishing activities. Understanding how organisms use different habitats is also critical to conservation purposes—without proper knowledge, the commercial exploitation of certain zones (e.g. for fishing or mining) may be very detrimental to some species and the ecosystem.

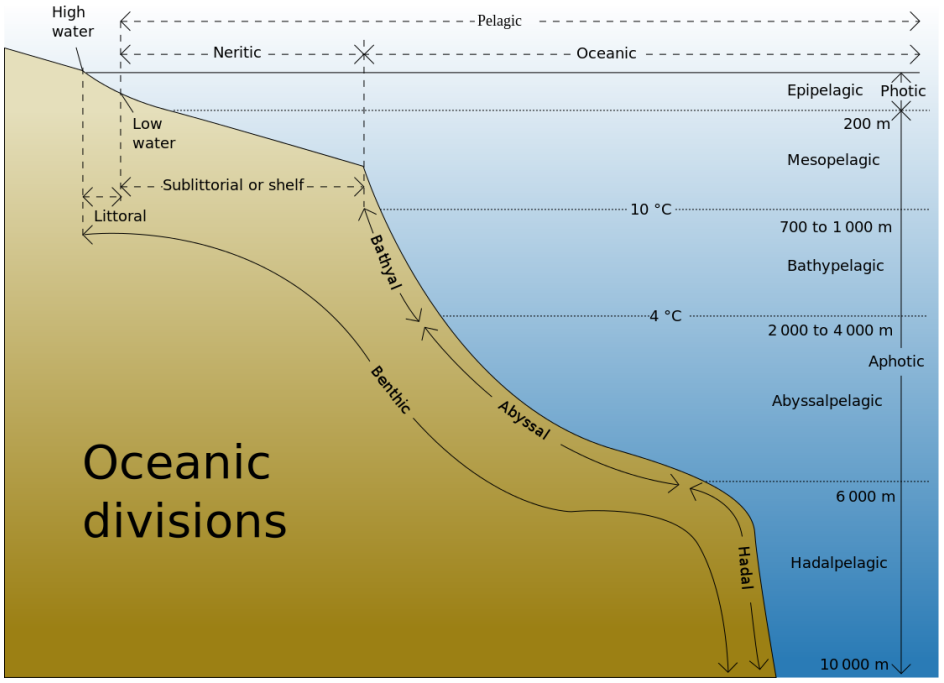

Figure 1.1: The major oceanic zones. Credit: K. Aainsqatsi.

1.2 A trait-based approach to ocean life

Considering all organisms previously mentioned and their behaviours can be an infinitely complex task. The classical approach to describe organisms and global ecological mechanisms is through taxonomy: organisms are first grouped into *species*, species are then grouped into *genus*, genus into *family*... up to the *domain* organisms belong to. In the marine world, this sums up to an estimated 0.7-1 million species in the eukarya domain (organisms whose cells have a nucleus bound by membranes, Appeltans et al. (2012)). If taxonomy is essential to describe the complexity of life and the proximity between different species, it becomes overwhelming when addressing more global ecological questions.

Biotic interactions do not occur between species or genus, but between individuals. A forage fish eating different plankton organisms will not differentiate between different prey species (unless they have different characteristics which makes them different to their predator). Similarly, the environment does not select for species, but for different combinations of characteristics in organisms.

These characteristics is what we call *traits*. A trait is "a well-defined, measurable property of organisms, usually measured at the individual level and used comparatively across species" (McGill et al., 2006). For example, the size of an organism is an obvious trait capturing the tremendous diversity of marine organisms. Marine organisms range

from 0.15 μm for the smallest living cells to over 30 m for the biggest blue whales (Andersen et al., 2016). The trait-based approach to ecology consists in ignoring the classical grouping of organisms into species and considers organisms as having a collection of traits (Kiørboe et al., 2018). This approach allows to discard many details that are taken into account when all taxonomic units are considered, but includes the necessary information for the description of species interactions and distributions.

A key consideration of the trait-based approach is that the different traits of an organism are usually related through trade-offs. For example, a plankton organism with a shell will likely decrease its predation risk, but growing and maintaining this shell will also increase metabolic costs (Pančić and Kiørboe, 2018). Ultimately, there is no free lunch: trade-offs ensure that no organism can be superior at all times (Litchman and Klausmeier, 2008).

For organisms, no matter their traits, life boils down to three main missions: eat, survive, reproduce (Kiørboe et al., 2018). A successful combination of traits is one that allows its carrier to fulfil these three missions and create a new generation of trait carriers. How well an organism performs is generally measured using Darwinian fitness, i.e. the total number of offsprings produced over an individual's life (see section 3.3 for further fitness considerations).

1.3 Behaviour, movement, and migrations

If behavioural ecology is a well-developed discipline within biology, the term "behaviour" appears to be used in a diversity of contexts, and the many definitions can be imprecise and self-contradicting (Levitis et al., 2009). An early definition by Nobel Prize recipient and co-founder of modern ethology Nikolaas Tinbergen considered behaviour as "The total movement made by the intact animal" (Tinbergen, 1955). More complex definitions include the one of Grier and Burk: behaviour is "all observable or otherwise measurable muscular and secretory responses (or lack thereof in some cases) and related phenomena such as changes in blood flow and surface pigments in response to changes in an animal's internal and external environment" (Grier and Burk, 1992). In the following of this thesis, I will consider behaviour in the light of traits: I define behaviour as **a set of traits that can be altered more or less rapidly, and potentially only temporarily.**

To increase their fitness, organisms need to change their behaviour and adapt to their surrounding environment and to their internal condition. For example, a puffer fish threatened will inflate almost instantly to appear much bigger and less palatable (figure 1.2). It will take a few hours to recover from the metabolic expenditure this behaviour triggered (McGee and Clark, 2014), but if this behaviour enables it to avoid predation, the net fitness gain is ultimately highly positive as it stays alive and can still produce offsprings in the future.

An example of behaviour that can be observed in most living organisms is movement. Movements can happen at different temporal and spatial scales, from a bacterium

Figure 1.2: A puffer fish threatened can inflate almost instantly to look much less palatable to its predator. Photo credit: Bill Eichenlaub, US National Park Service.

using its flagellum as a helical propeller (a few tens of μm/s, for a duration between 0.1 and 0.3 s, Johansen et al. (2002)) to an arctic tern migrating more than 80,000 km annually at speeds up to 500 km/day (Egevang et al., 2010) to long-legged flies that can produce escape jumps less than 5 ms after a stimulus (Sourakov, 2011). In the course of its life, a single individual is likely to experience several kinds of movements, that can be classified according to their goals (figure 1.3). The goal of movement is driven by a combination of internal drivers (i.e. the need to eat, reproduce, seek refuge...) and external stimuli (Nathan et al., 2008).

Migration is a special kind of periodic movement, whose goal is to relocate in order to find more favourable conditions (Dingle and Drake, 2007). Among others, these more favourable conditions may be a decrease in predation pressure, the need for more abundant better-quality food (for example in ungulates, Hebblewhite and Merrill (2007); Fryxell and Sinclair (1988)), and/or the need to find breeding or nesting sites to reproduce (for species such as whales, sea turtles or birds, Slijper (1962); Carr (1975); McKinnon et al. (2010)).

The world most important migration in terms of biomass involved (maybe exceeded by human commuters) is the diel vertical migration (DVM) of aquatic organisms (Brierley, 2014). Every day, in all oceans of the globe (as well as most freshwater lakes and reservoirs), marine organisms migrate between the surface of the water column and the deep. Most of the time, organisms remain at depth during daytime and

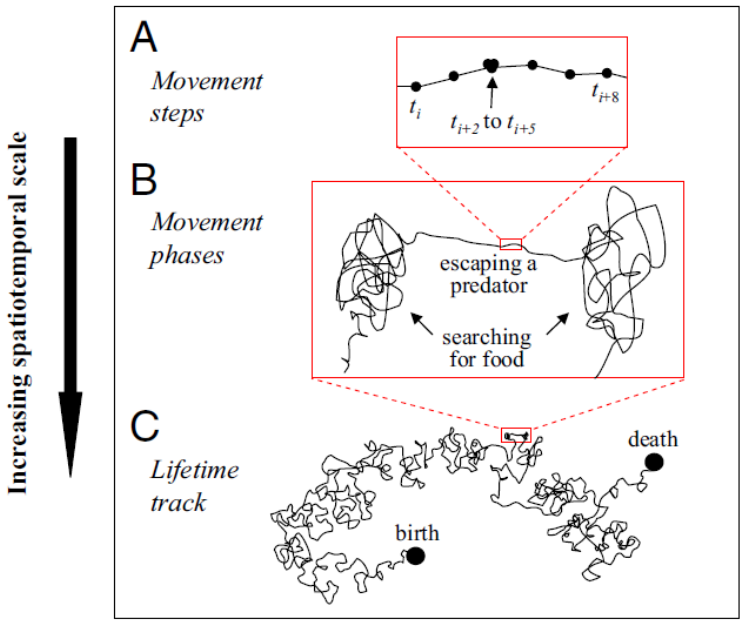

Figure 1.3: In the course of its life, an individual will experience different kinds of movement to satisfy different goals. It will forage for food, escape predators, but also look for mates, defend its territory, or migrate to more favourable environments. Reproduced from Nathan et al. (2008).

ascend to the surface at night, but other patterns can also emerge (Klevjer et al., 2016; Ohman, 1990). As movement is costly, this migration must yield some benefits. The primary explanation for DVM is the predator-avoidance hypothesis: as most predators are visual, seeking a dark habitat decreases the predator's visual range, thus prey are less likely to be encountered and captured. But, then, why migrate to the surface during nighttime? Zooplanktonic organisms feed on phytoplankton, and migrating up at night enables zooplankton to feed while remaining in a relatively dark and safe environment (Cohen and Forward Jr, 2009).

1.4 Framework and focus of this thesis

This thesis was carried out within the Centre for Ocean Life, an interdisciplinary and collaborative centre of excellence, spanning five research departments at three universities. The goal of the centre is to develop a trait-based approach to marine life, in order to get a fundamental understanding and a predictive capacity of marine ecosystems (Kiørboe et al., 2018).

The Centre is divided in four different research areas (figure 1.4):

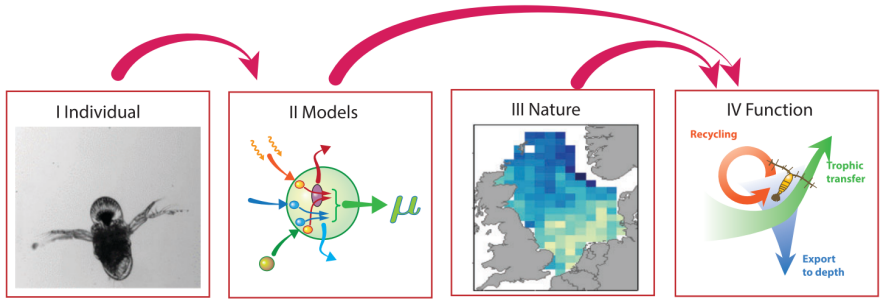

Figure 1.4: The four themes (research areas) of the Centre for Ocean Life. Research on theme I (individuals) feeds research on theme II (models), and theme II and III (nature) are used to assess and predict ecosystem functions (theme IV). Reproduced from Kiørboe et al. (2018).

- Individual: How do organisms perform? How do they interact? This research area aims at providing a mechanistic understanding of organisms based on their key traits and associated trade-offs.
- Models: Based on the key traits and trade-offs identified in the first research area, trait-based models aim at describing community structure and function. Models consider individuals interacting together to assess the trait distribution in an ecosystem, i.e. the biomass or abundance of individuals with a given trait assemblage.
- Nature: This research area aims at describing the trait distribution in nature and its variation with time and space. If this collection and interpretation of data is important by itself, it also provides great support to research area II (Models), as it allows validating model outputs.
- Function: The function of an ecosystem depends on the environmental conditions of the ecosystem, but also on the biomass and traits of organisms in the ecosystem (Kiørboe et al., 2018). What do the observed or modelled trait distribution mean for ecosystem function? How will ecosystems respond to the effects of global change from a mechanistic point of view?

This thesis uses a trait-based approach to diel vertical migrations. It is rooted in all research areas of the centre. I quantify the benefits and trade-offs of moving and performing vertical migrations. To do so, I develop models to assess the optimal vertical migration patterns of organisms from several trophic levels simultaneously, and I compare my model predictions with field observations. Finally, I use model outputs to compute ecosystem functions resulting from this process, such as trophic transfer efficiency and carbon export.

This work is based on four manuscripts, with the general aim of contributing to a better mechanistic understanding of diel vertical migrations and their consequences for ecosystem functions. In particular, we explored the following aspects:

- Mechanistic feedbacks between migrating prey and predators, and the interplay between environmental and biological drivers for DVM: chapter 5 and 7.

- The interplay between behaviour (fast time scale) and population dynamics (slower time scale): chapter 6.
- Ecosystem functions driven by diel vertical migrations: chapter 6 and 8.

Bibliography

Andersen, K. H., Berge, T., Gonçalves, R., Hartvig, M., Heuschele, J., Hylander, S., Jacobsen, N., Lindemann, C., Martens, E., Neuheimer, A., Olsson, K., Palacz, A., Prowe, A., Sainmont, J., Traving, S., Visser, A. W., Wadhwa, N., and Kiørboe, T. (2016). Characteristic Sizes of Life in the Oceans, from Bacteria to Whales. *Annual Review of Marine Science*, 8(1):217–241.

Appeltans, W., Ahyong, S. T., Anderson, G., Angel, M. V., Artois, T., Bailly, N., Bamber, R., Barber, A., Bartsch, I., Berta, A., Błażewicz-Paszkowycz, M., Bock, P., Boxshall, G., Boyko, C. B., Brandão, S. N., Bray, R. A., Bruce, N. L., Cairns, S. D., Chan, T.-Y., Cheng, L., Collins, A. G., Cribb, T., Curini-Galletti, M., Dahdouh-Guebas, F., Davie, P. J., Dawson, M. N., De Clerck, O., Decock, W., De Grave, S., de Voogd, N. J., Domning, D. P., Emig, C. C., Erséus, C., Eschmeyer, W., Fauchald, K., Fautin, D. G., Feist, S. W., Fransen, C. H., Furuya, H., Garcia-Alvarez, O., Gerken, S., Gibson, D., Gittenberger, A., Gofas, S., Gómez-Daglio, L., Gordon, D. P., Guiry, M. D., Hernandez, F., Hoeksema, B. W., Hopcroft, R. R., Jaume, D., Kirk, P., Koedam, N., Koenemann, S., Kolb, J. B., Kristensen, R. M., Kroh, A., Lambert, G., Lazarus, D. B., Lemaitre, R., Longshaw, M., Lowry, J., Macpherson, E., Madin, L. P., Mah, C., Mapstone, G., McLaughlin, P. A., Mees, J., Meland, K., Messing, C. G., Mills, C. E., Molodtsova, T. N., Mooi, R., Neuhaus, B., Ng, P. K., Nielsen, C., Norenburg, J., Opresko, D. M., Osawa, M., Paulay, G., Perrin, W., Pilger, J. F., Poore, G. C., Pugh, P., Read, G. B., Reimer, J. D., Rius, M., Rocha, R. M., Saiz-Salinas, J. I., Scarabino, V., Schierwater, B., Schmidt-Rhaesa, A., Schnabel, K. E., Schotte, M., Schuchert, P., Schwabe, E., Segers, H., Self-Sullivan, C., Shenkar, N., Siegel, V., Sterrer, W., Stöhr, S., Swalla, B., Tasker, M. L., Thuesen, E. V., Timm, T., Todaro, M. A., Turon, X., Tyler, S., Uetz, P., van der Land, J., Vanhoorne, B., van Ofwegen, L. P., van Soest, R. W., Vanaverbeke, J., Walker-Smith, G., Walter, T. C., Warren, A., Williams, G. C., Wilson, S. P., and Costello, M. J. (2012). The Magnitude of Global Marine Species Diversity. *Current Biology*, 22(23):2189–2202.

Block, B. A., Jonsen, I. D., Jorgensen, S. J., Winship, A. J., Shaffer, S. A., Bograd, S. J., Hazen, E. L., Foley, D. G., Breed, G. A., Harrison, A.-L., Ganong, J. E., Swithenbank, A. M., Castleton, M. R., Dewar, H., Mate, B. R., Shillinger, G. L., Schaefer, K. M., Benson, S. R., Weise, M. J., Henry, R. W., and Costa, D. P. (2011). Tracking apex marine predator movements in a dynamic ocean. *Nature*, 475(7354):86–90.

Brierley, A. S. (2014). Diel vertical migration. *Current Biology*, 24(22):R1074–R1076.

Carr, A. (1975). The Ascension Island Green Turtle Colony. *Copeia*, 3:547–555.

Cohen, J. H. and Forward Jr, R. B. (2009). Zooplankton Diel Vertical Migration — A Review Of Proximate Control. *Oceanography and Marine Biology*, 47:77–110.

Dingle, H. and Drake, V. A. (2007). What Is Migration ? *BioScience*, 57(2):113–121.

Egevang, C., Stenhouse, I. J., Phillips, R. A., Petersen, A., Fox, J. W., and Silk, J. R. D. (2010). Tracking of Arctic terns Sterna paradisaea reveals longest animal migration. *Proceedings of the National Academy of Sciences*, 107(5):2078–2081.

Fryxell, J. M. and Sinclair, A. R. (1988). Causes and consequences of migration by large herbivores. *Trends in Ecology and Evolution*, 3(9):237–241.

Fuiman, L. A. (1997). What can flatfish ontogenies tell us about pelagic and benthic lifestyles? *Journal of Sea Research*, 37(3-4):257–267.

Grier, J. W. and Burk, T. (1992). *Biology of animal behaviour*. Times Mirror, Mosby college, St Louis, Missouri.

Hebblewhite, M. and Merrill, E. H. (2007). Multiscale wolf predation risk for elk: does migration reduce risk? *Oecologia*, 152(2):377–387.

Isaacs, J. D. and Schwartzlose, R. A. (1965). Migrant Sound Scatterers: Interaction with the Sea Floor. *Science*, 150(3705):1810–1813.

Johansen, J. E., Pinhassi, J., Blackburn, N., Zweifel, U. L., and Hagström, Å. (2002). Variability in motility characeristics among marine bacteria. *Aquatic Microbial Ecology*, 28:229–237.

Jónasdóttir, S. H., Visser, A. W., Richardson, K., and Heath, M. R. (2015). Seasonal copepod lipid pump promotes carbon sequestration in the deep North Atlantic. *Proceedings of the National Academy of Sciences*, 112(39):12122–12126.

Kiørboe, T., Visser, A., and Andersen, K. H. (2018). A trait-based approach to ocean ecology. *ICES Journal of Marine Science*.

Klevjer, T. A., Irigoien, X., Røstad, A., Fraile-Nuez, E., Benítez-Barrios, V. M., and Kaartvedt, S. (2016). Large scale patterns in vertical distribution and behaviour of mesopelagic scattering layers. *Scientific Reports*, 6(1):19873.

Levitis, D. A., Lidicker, W. Z., and Freund, G. (2009). Behavioural biologists do not agree on what constitutes behaviour. *Animal Behaviour*, 78(1):103–110.

Litchman, E. and Klausmeier, C. A. (2008). Trait-Based Community Ecology of Phytoplankton. *Annual Review of Ecology, Evolution, and Systematics*, 39(1):615–639.

McGee, G. E. and Clark, T. D. (2014). All puffed out: do pufferfish hold their breath while inflated? *Biology Letters*, 10(12):20140823.

McGill, B. J., Enquist, B. J., Weiher, E., and Westoby, M. (2006). Rebuilding community ecology from functional traits. *Trends in Ecology & Evolution*, 21(4):178–185.

McKinnon, L., Smith, P. A., Nol, E., Martin, J. L., Doyle, F. I., Abraham, K. F., Gilchrist, H. G., Morrison, R. I., and Bêty, J. (2010). Lower predation risk for migratory birds at high latitudes. *Science*, 327(5963):326–327.

Nathan, R., Getz, W. M., Revilla, E., Holyoak, M., Kadmon, R., Saltz, D., and Smouse, P. E. (2008). A movement ecology paradigm for unifying organismal movement research. *Proceedings of the National Academy of Sciences*, 105(49):19052–19059.

Ohman, M. D. (1990). The Demographic Benefits of Diel Vertical Migration by Zooplankton. *Ecological Monographs*, 60(3):257–281.

Pančić, M. and Kiørboe, T. (2018). Phytoplankton defence mechanisms: traits and trade-offs. *Biological Reviews*, 93(2):1269–1303.

Schmitz Jr., W. J. (1996a). On the World Ocean Circulation: Volume I - Some global features / North Atlantic circulation. Technical report, Woods Hole Oceanographic Institution.

Schmitz Jr., W. J. (1996b). On the World Ocean Circulation: Volume II - The Pacific and Indian Oceans / A global update. Technical report, Woods Hole Oceanographic Institution.

Slijper, E. J. (1962). *Whales*. New York: Basic Books.

Sourakov, A. (2011). Faster than a Flash: The Fastest Visual Startle Reflex Response is Found in a Long-Legged Fly, Condylostylus sp. (Dolichopodidae) . *Florida Entomologist*, 94(2):367–369.

Thygesen, U. H., Sommer, L., Evans, K., and Patterson, T. A. (2016). Dynamic optimal foraging theory explains vertical migrations of Bigeye tuna. *Ecology*, 97(7):1852–1861.

Tinbergen, N. (1955). *The study of instinct*. Oxford: Clarendon.

Visser, A. W., Grønning, J., and Jónasdóttir, S. H. (2017). Calanus hyperboreus and the lipid pump. *Limnology and Oceanography*, 62(3):1155–1165.

CHAPTER 2

Ecological and biological background

2.1 Observing diel vertical migrations

Diel vertical migration (DVM) is the daily movement of plankton and nekton up and down the water column. The classical pattern was originally described by Cushing (1951), who decomposed it into five components (figure 2.1): (1) an ascent towards the surface during sunset, (2) a departure from the surface, at or before midnight usually referred to as midnight sink, (3) a return to the surface just before dawn, (4) a descent to the day depth and (5) the variable day depth. Steps (2) and (3) can be very weak or nonexistent, meaning that the night behaviour is effectively a surface residency. Other patterns can emerge such as reverse vertical migrations, where organisms spend the day in well lit waters before returning to the depths at night (Ohman et al., 1983).

DVM of planktonic organisms is known to the scientific community since at least the XIXth century and observations from Cuvier in 1817 (Bayly, 1986). However, fishermen have known about fish vertical migrations for centuries (Pearre, 2003; Woodhead, 1966), and any serious angler knows that it is best to consider the time of the day when going fishing.

On a technical level, the first way to investigate DVM was through net sampling (Pearre, 2003). Then came World War II and the development of sonars for submarine detection. This unexpectedly led to the discovery of the deep scattering layer (also called sound scattering layer, Brierley (2014)). This layer, primarily mistaken for the ocean bottom, is a very dense aggregations of organisms (mainly euphausiids and

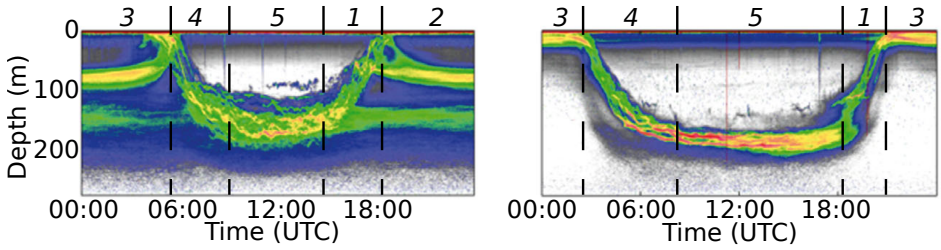

Figure 2.1: Typical DVM patterns observed with echosounder in Masfjorden, Norway in March and August. If all stages described by Cushing (1951) can be observed in March, there seem to be no midnight sink or morning rise in August, with organisms remaining at the surface throughout the night . Modified from Prihartato et al. (2015).

small fish) that echoes back the acoustic signals sent by sonars, thus providing better knowledge of the biomass[1] distribution in the water column. In the second half of the XX^{th} century, advances in acoustic and data storage tags enabled to follow large individual organisms (Yuen, 1970; Thygesen et al., 2016): diel vertical population was not only a large scale process anymore, it was also a behaviour that could be investigated at the individual level. The recent development of more advanced acoustic (e.g. submerged echosounders (Solberg and Kaartvedt, 2017; Kaartvedt et al., 2009, 2020) or broadband acoustics (Horne, 2000)) or imaging (e.g. ROVs (Ohman et al., 2019)) techniques allows for individual detection and fine-scale behavioural studies. Of course, the different methods work in synergy, and combining them capitalises on the strengths of each of them. For example, echosounders can give a good representation of the vertical distribution of forage fish and net sampling helps identifying plankton species composition (Onsrud and Kaartvedt, 1998), allowing to investigate changes in trophic interactions and biodiversity with depth.

Finally, several mechanistic models—such as the ones presented in this thesis (chapters 6, 7, 8 and 9)—were also developed to study diel vertical migrations. These models are very useful in that they allow testing different hypothesis and predicting how DVM patterns may change in the future. One of the prerequisite of mechanistic models is to have some understanding of the drivers of the processes considered. As discussed in the next section, this is not necessarily obvious in the case of diel vertical migration and it deserves some consideration.

2.2 Proximate and ultimate causes of diel vertical migration

When observing an unexpected or unexplained phenomenon, one of the first questions that usually come to mind is "Why?", followed generally by "How?". DVM research made no exception, and many researchers thought about the possible **ultimate** and **proximate** causes behind it (Worthington, 1931; Ringelberg and Gool, 2003; Cohen and Forward Jr, 2009; Hays, 2003).

Here, ultimate refers to the reason behind the process ("why?"), which can be an evolutionary or adaptive benefit. Proximate relates to the drivers of the process ("how?"), i.e. what behavioural and physiological mechanisms trigger organisms to perform DVM. Even if these two questions are closely related, it is important to avoid any confusion between the two in order to understand correctly the particulars of diel vertical migration (Ringelberg and Gool, 2003).

[1] Or more exactly of the backscatter, which cannot be so easily related to the biomass of a system (Iida et al., 1996).

2.2.1 Ultimate causes of diel vertical migration

Early planktonic DVM research tried to understand the ultimate causes of DVM, or "*why they [organisms] behaved the way [researchers] observed*" (Worthington, 1931). In light of the diversity of patterns observed, a variety of causes was postulated (Kikuchi, 1930). The fact that many causes may be responsible for DVM is still acknowledged, especially considering the vast number of species and systems involved (Hays, 2003). DVM was explained as a light avoidance mechanism as early as 1912 (Murray and Hjort, 1912), but many other reasons were postulated in parallel: the direction of the wind driving plankton inshore and offshore, the eye adaptation of planktonic organisms for night vision, a specific temperature preference or an interplay between light preference and gravity[2] (Kikuchi, 1930). Once it was argued that it was difficult to decide on any factor (or several factors) accounting for DVM, Worthington (Worthington, 1931) stated:

> *It is remarkable that not all species have adapted to light to save the trouble of migrating.*

Thinking about adaptation to justify DVM is the good approach, but we now know that Worthington's conclusions are wrong. However, it is useful to think about what organisms need to adapt to. As stated section 1.2, organisms need to optimize their behaviour to satisfy the three missions of life (eat, survive, reproduce) and maximise their life-time reproductive output. They do not necessarily need to adapt to life in light conditions, but they need to find a way to optimize their fitness (defined, for example, as the life-time reproductive output) in any available habitat. If optimising fitness is *the* ultimate cause for DVM, it is very generic and does not provide any further mechanistic understanding of the migration process, so we can instead define the ultimate cause as the mechanism that yields this fitness benefit.

Being at the surface at all times is beneficial in that it allows organisms to feed on phytoplankton continuously, but there must be a cost in staying there at all times. In other words, it is a trade-off that triggers migration behaviours. This trade-off is the ultimate reason for DVM behaviours. Lampert (1989) summarised the two most plausible hypotheses[3] concerning the ultimate reason of DVM:

- Residing in cold water has a metabolic advantage ;
- The predator avoidance hypothesis: organisms migrate at depth to decrease the risk of visual predation.

The first hypothesis postulates that there is an advantage in feeding in warm water but residing during daytime in cold waters (McLaren, 1963), as it decreases metabolic and

[2]Some of these reasons are in fact proximate causes and not ultimate causes, as we will see in section 2.2.2.

[3]In addition to these two hypothesis, the reduction of UV damage may be a justification for DVM in shallow lakes (Leech and Williamson, 2001). Due to the vertical attenuation of UV radiations, this is very unlikely to be the case for migrations of tens to hundreds of meters in the oceans.

digestion rates. However, most experiments and models indicate that the reverse is true (Lampert et al., 1988; Lampert, 1989; Aksnes and Giske, 1990) and this hypothesis fails to explain why depth residency should primarily occur during daytime.

The predator avoidance hypothesis was first explicitly formulated by Zaret and Suffern (1976). The pelagic is a homogeneous environment, with no physical refuge to escape predation. If most of the predation is visual (e.g. planktivorous fish), zooplankton can decrease their predation risk by hiding in deep dark waters. However, zooplankton also have to feed on phytoplankton that rely on light and therefore grow close to the surface. Nighttime offers an ideal window of opportunity: by migrating to the surface at dusk, zooplankton can feed in relatively safe waters during the night, before returning to their deep refuge at dawn until the next night. As Kremer and Kremer (1988) stated, these zooplankton embraced the mantra "*better hungry than dead*".

There is considerable support for this hypothesis in the literature (Frost, 1988; Bollens et al., 1992; De Robertis et al., 2000; Hays, 2003). In both experimental and natural systems, zooplankton migrate only when fish predators appeared (Bollens and Frost, 1989a; Bollens et al., 1992; Luecke, 1986). The time at which zooplankton arrive at the surface depends on their size, and therefore on their sensitivity to predation: more sensitive animals are more cautious and can venture in surface waters later than less susceptible organisms (De Robertis et al., 2000)[4]. Satiated organisms do not need to risk going to the surface and can remain at depth (Fiksen and Carlotti, 1998; Sekino and Yoshioka, 1995). Finally, this mechanism can even explain reverse vertical migration. Indeed, if a predator is performing normal vertical migration patterns because it needs to hide from visual predators, avoiding overlap with it (i.e. adopting a reverse migration pattern) decreases mortality risks (Ohman et al., 1983; Ohman, 1990).

Most of this development was tailored to zooplankton DVM, but it also applies to fish (as well as cephalopods, and other groups performing DVM). Even if zooplanktivorous predators do not need to go to the surface to feed on phytoplankton, it is beneficial for them to follow their zooplanktonic prey. Predators are imposing a control on prey through fear, to which zooplankton react by adapting their behaviour. The fact that predators can in turn adapt their behaviour (Lima, 2002) is important to consider, as it can have unexpected consequences (such as reverse vertical migrations).

2.2.2 Proximate causes of diel vertical migration

Organisms mainly migrate to decrease their vulnerability to predators, but potential factors triggering DVM are numerous.

[4]Transition times seem to be the most dangerous time of the day for migrating prey. It was shown that up to 90% of cod feeding on sprat in the Baltic happened at dawn and dusk (Andersen et al., 2017).

2.2.2.1 Light levels

As DVM seeks to reduce visual predation, it is natural that light is the primary proxy for DVM (Cohen and Forward Jr, 2009; Lampert, 1989; Dodson, 1990; Widder and Frank, 2001). Three main hypothesis exist for the prevailing underlying mechanism (Cohen and Forward Jr, 2009):

- The preferendum (or isolume) hypothesis: organisms reside at constant light levels.
- The absolute intensity threshold: movement is initiated only once the light level reaches a critical threshold.
- The relative rate-of-change hypothesis: The movement is initiated only when the light intensity relative rate of change reaches a certain value.

The preferendum hypothesis is not always validated in the field when looking at the migration pathway. While Widder and Frank (2001) showed that shrimps were following the isolume (corrected for the critter's eye spectral sensitivity), Onsrud and Kaartvedt (1998) found that krill could only follow the isolume during part of the migration, and other studies could not find any evidence of the hypothesis (Haney et al., 1990; Abello et al., 2005). However, when applied to the day residency depths of the organisms, the preferendum hypothesis seems to hold (Cohen and Forward Jr, 2009): the water clarity is a good predictor of daytime residence depth (Dodson, 1990), and the deep scattering layer rises with sudden influx of turbid waters to remain at a constant isolume (Frank and Widder, 2002).

The absolute intensity threshold is a variant of the preferendum hypothesis. By definition, it can only be applied to the onset of migrations and not to residency depths, and, as the preferendum hypothesis, it showed conflicting results. Some studies found partial justification of the hypothesis (Cohen and Forward, 2005; Yoshida et al., 2004), while others did not (Haney et al., 1990).

Similar to the previous hypothesis, the relative rate-of-change hypothesis only applies to the initiation of the migration. This hypothesis seems to find some evidence in the literature, especially for *Daphnia* in freshwater reservoirs (Ringelberg, 1991, 1995a; McFarland et al., 1999; Ringelberg, 1999). However, the results appear to vary significantly, suggesting that there are other parameters to consider.

2.2.2.2 Predation pressure

After light, predation pressure is probably the most important driver of DVM globally. There is plenty of evidence that zooplankton can adapt their behaviour in response to predator cues (Lass and Spaak, 2003; Vaughn, 2007; Vaughn and Strathmann, 2008; Bollens and Frost, 1991; Frost and Bollens, 1992), and DVM is no exception. Predator cues can alter the magnitude of migration (Bollens and Frost, 1989b), trigger migration in previously non-migrating species (Luecke, 1986), or even cause organisms to perform reverse migrations (Ohman et al., 1983; Ohman, 1990). It is important to

note, however, that predator cues alone do not trigger DVM, and that light cycles are a necessary condition for vertical movements (Loose, 1993). Consequently, predator cues do not modify the behaviour directly, but they modify the response to the light stimulus (Van Gool and Ringelberg, 1997; Forward and Rittschof, 2000). This is consistent with the predator avoidance hypothesis: lowering visual predation risk in changing predator abundances requires to reduce detectability.

What precisely are "predator cues" is still unclear. If chemical cues (fish kairomones) were recognised to trigger DVM of freshwater copepods (Neill, 1990, 1992), the mechanism is not only linked to chemical cues but also potentially to visual and/or mechanical cues for marine zooplankton (Bollens and Frost, 1989a). Another study showed the importance of mechanical cues (Bollens et al., 1994) in zooplankton DVM, but other researchers contested the validity of the experimental protocol (Ringelberg, 1995b) (a summary of the discussion is provided by Cohen and Forward Jr (2009)). If a complete understanding of the mechanism is still lacking, the conclusion of Bollens et al. (1994) that the predator stimuli triggering DVM are multiple and may vary between species probably still holds.

2.2.2.3 Food abundance

The counterpart of predator abundance is prey abundance. The predator avoidance hypothesis is a trade-off between eating and being eaten, and as such the incentive to hide at depth and migrate to the surface does not depend only on predation risk but also on the feeding opportunities in the different parts of the water column (Hardy, 1936; Cushing, 1951; Sainmont et al., 2013).

2.2.2.4 Oxygen concentration

In highly productive areas (such as in the California Current, the Humboldt current or the Benguela current), strong bacterial degradation of sinking material consumes a lot of oxygen, resulting in sub-surface waters with very low oxygen concentration called oxygen minimum zones (OMZ).

Below a certain oxygen concentration, organisms can struggle to meet their oxygen requirements. Therefore, areas of the water column with low oxygen concentrations can be inaccessible to some zooplanktonic organisms (Auel and Verheye, 2007; Criales-Hernández et al., 2008), but may provide a refuge for species adapted to low oxygen conditions (Auel and Verheye, 2007). OMZs can be fatal to some species: if they are unable to sustain low oxygen conditions for some time, they may not be able to cross it to perform DVM and end up with only a restricted portion of the water column as potential habitat.

Mesopelagic fish constituting the deep scattering layer (DSL) are also impacted by low oxygen conditions, and the depth of the deep scattering layer correlates with the oxygen concentration in the upper pelagic zone (Bianchi et al., 2013). With increasing OMZ, the DSL is expected to shoal and expend as the lower part of the DSL is moving upward slower than the upper part (figure 2.2, Netburn and Koslow (2015)).

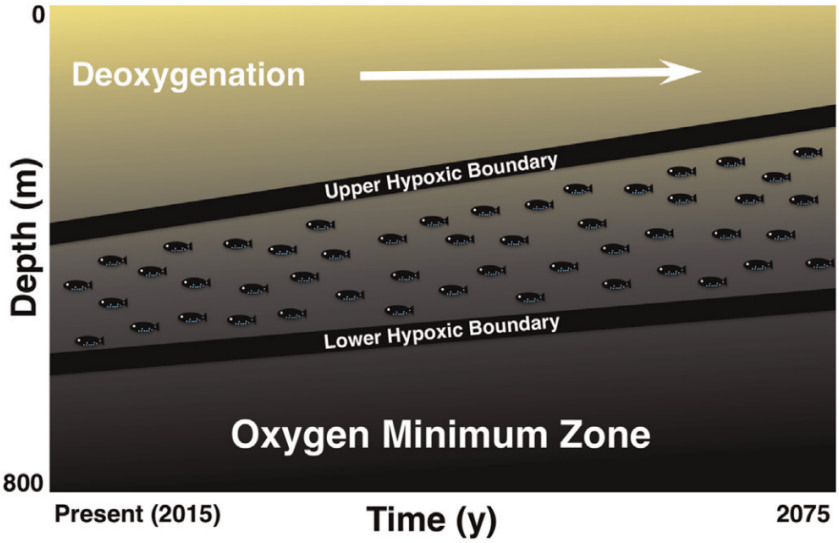

Figure 2.2: Scheme of the DSL under increasing deoxygenation and light attenuation. The upper DSL boundary is expected to shoal faster than the lower boundary, effectively expending the DSL width. Redrawn from Netburn and Koslow (2015).

2.2.2.5 Others

In addition to these proximate drivers of DVM, other factors worth mentioning here are hypothesised to play a role in triggering vertical migrations:

- Endogenous rhythms. Zooplankton have internal clocks triggering the onset of DVM (Forward et al., 2007; Duchêne and Queiroga, 2001; Cohen and Forward, 2005). This was hypothesised to be redundant, as organisms also rely on external cues to initiate DVM (Cohen and Forward, 2005). However, bathypelagic organisms also perform DVM (Kaartvedt et al., 2020). There, internal clocks are likely to be proximate causes of DVM, as no light penetrates that deep in the water column.

- Weather and turbulence. Cushing (1951) hypothesised that wind stress affects zooplankton DVM. A recent study proved this hypothesis right, but only for ambush-feeding copepods and not filter-feeders (Tanaka, 2019). Moreover, their results only concerned surface waters (<10m), and this is probably anecdotal in the pelagic.

- Temperature. Temperature is probably a limiting agent of DVM only at the extremes of the organism's tolerance range (Cushing, 1951). It can prevent organisms from accessing certain parts of the water column (Cushing, 1951), but

it can also have consequences on life history as temperature directly controls metabolic rates (Loose and Dawidowicz, 1994).

2.3 Individual variability in DVM

If DVM is (generally) a predation avoidance mechanism, many different proximate factors can play a role in triggering the movement or defining the residence depth, resulting in a vast array of patterns. The fact that DSLs have varying widths or that multiple scattering layers can be present shows that there is not necessarily a unique optimal pattern at a given location.

Individual variations can arise for several reasons. Organisms from different species or with different traits experience different trade-offs, and as such may have different optimal DVM patterns. For example, a strong pigmentation changes visual detectability and increases predation risk in surface waters (De Robertis, 2002; Hylander et al., 2009; Hylander and Hansson, 2013).

Individuals can also exhibit multiple DVM behaviours throughout their lifetime, for example through ontogenic shifts (De Robertis et al., 2000; Kaartvedt, 2010). On an even faster time scale, the body condition of an individual plays a role in its willingness to migrate up to feed and expose itself to predation (Fiksen and Carlotti, 1998; Sekino and Yoshioka, 1995).

More subtle is the dependency of DVM patterns to the DVM patterns of other organisms, through frequency-dependent and density-dependent effects. Indeed, as more individuals or a higher fraction of the population adopts a pattern, the benefit of this strategy may change (chapters 6 and 7). On the one hand, being with other conspecifics decreases predation risks as it spreads the risk among organisms at the same location. On the other hand, it may reduce feeding opportunity, and a high concentration of individuals can spark predators' interests.

One of the questions that arise from these considerations is the plasticity of diel vertical migrations. Is it a behaviour that is fixed for each individual, or can it vary based on the environmental conditions? Many studies highlighted the rapid changes in DVM due to changing conditions and attributed it to phenotypic plasticity (Bollens and Frost, 1991; Frost and Bollens, 1992; Loose and Dawidowicz, 1994; Cresswell et al., 2009)[5]. Moreover, a constant behaviour in the field (in general only varying with light, Aksnes et al. (2017); Norheim et al. (2016); Langbehn et al. (2019)) may be the consequence of low variations in environmental conditions (other than the daily cycle of light) rather than a non-plastic behaviour. Finally, optimal fitness considerations, ontogeny of organisms and seasonality of resources and environmental conditions indicate that phenotypic plasticity in DVM should be expected as it gives individuals

[5]Natural selection may also be responsible for observed changes in DVM patterns in some cases (Cousyn et al., 2001), but this is not incompatible with individual plasticity in DVM behaviours (Neill, 1992).

a distinctive advantage in any non constant environment (Fiksen and Carlotti, 1998; Boriss and Gabriel, 1998).

All of this considered, it becomes clear that one needs to take into account individual behaviours and trade-offs to understand optimal DVM patterns at the individual level. In the field, this is possible to do (Kaartvedt et al., 2007, 2008), but technically challenging to implement in the open ocean. Models provide the adequate framework to investigate individual responses in the water column.

2.4 Other behaviours in the pelagic

DVM is a very efficient way to deal with spatio-temporal heterogeneity in the pelagic. But other behaviours also exist—often in concert with DVM— to deal with this heterogeneity.

DVM is described as a 1D movement in the water column, but if it is profitable, organisms can also perform diel horizontal migrations. Resource abundance may be somehow homogeneous in the pelagic, but there can be large gradients of food availability perpendicularly to shores. As a consequence, forage fish can exhibit large inshore-offshore movements: they migrate up and inshore during night time in rich but risky places, and migrate down offshore at dawn (Robinson et al., 1995).

Schooling (for fish, usually called swarming for krill and other zooplankton) is another antipredator adaptation in the water column. Rather than looking for darkness, organisms group together to decrease their population-level encounter rate (figure 2.3, (Partridge, 1982)). As an added benefit for prey, predators seem to be less efficient at catching prey when they are clustered in a school (Partridge, 1982). Schooling is a widespread behaviour in fish and krill (Seghers, 1974; Prihartato et al., 2015; Kaartvedt, 2010), often associated with DVM (Kaartvedt et al., 1998; Nilsson et al., 2003). It is an efficient way to reduce the predation risk when it is not possible to find shelter in dark waters (for example at high latitudes during summertime (Kaartvedt et al., 1998) or in shallow areas during daytime (Nilsson et al., 2003)). Note that for large predators, schooling can be used to increase foraging efficiency: individuals distribute as to maximise their collective encounter rate, and work together to outmanoeuvre prey schools encountered and increase food uptake (Partridge, 1982).

Diel Seasonal Migration is a behaviour which is seen in zooplankton, especially at high latitudes (Hirche, 1996). When conditions become unfavorable, zooplankton migrate in deep waters and reduce severely their metabolism to survive periods of food shortage (Varpe, 2012). They enter diapause, during which they use their lipid reserves (figure 2.4). At the onset of spring, organisms migrate up and reproduce, trying to match their ascent with the phytoplankton spring bloom to maximise growth opportunities[6].

[6] An original alternative strategy can be found in the one-year life cycle of *Neocalanus tonsus* in the Southern Ocean: after diapause, organisms do not migrate up but release buoyant eggs that float back to the surface (Bradford-Grieve, 2001).

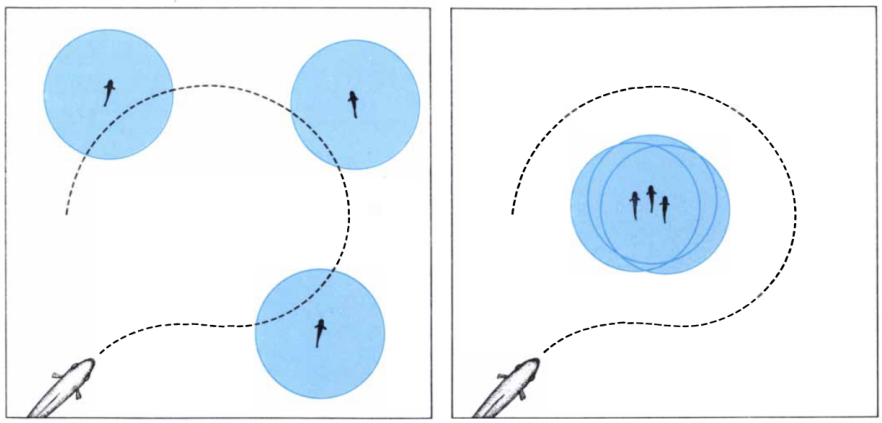

Figure 2.3: Prey group together to reduce the risk of being encountered and therefore eaten. Redrawn from Partridge (1982).

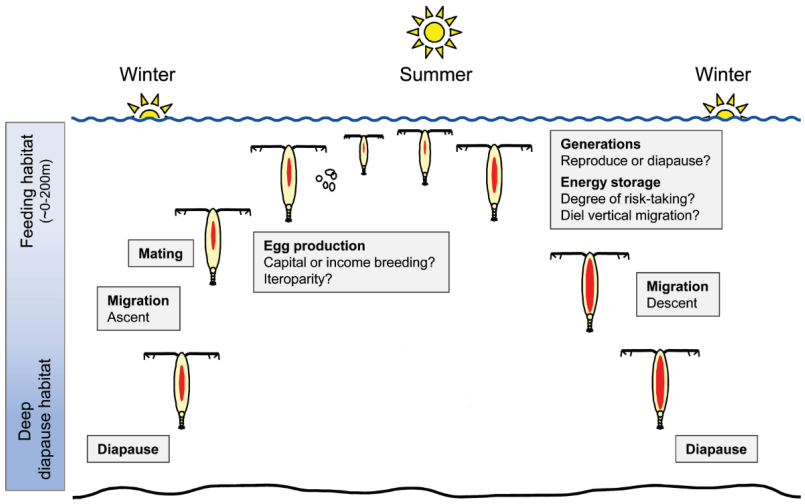

Figure 2.4: Zooplankton annual routine. Energy reserves are represented by the extent of their lipid sac (red). When conditions become unfavourable and organisms have enough reserve, they migrate deep to enter diapause and wait for the next spring to reproduce. Modified from Varpe (2012).

2.5 Ecosystem consequences of diel vertical migration

Carbon export is an important ecosystem function directly linked to DVM (Hansen and Visser, 2016; Davison et al., 2013; Aumont et al., 2018; Archibald et al., 2019, chapter 9). Organisms feeding at the surface and migrating to deeper water actively bring carbon below the euphotic zone, where they respire or excrete it as fecal pellets. In the current climate change context, carbon export is an important topic: carbon removal from the surface waters is equivalent to carbon removal from the atmosphere—DVM thus helps to reduce atmospheric CO_2 concentration and mitigates the effects of anthropogenic carbon emissions. Global estimates of carbon flux below the euphotic zones are around 6-9 PgC/yr (Siegel et al., 2016; DeVries and Weber, 2017). Recent studies estimate that DVM exports 1.05 PgC/yr, contributing to around 18% of sinking particles below 150 m (Aumont et al., 2018). The contribution of migrating zooplankton would be around 13% of the total export flux (Archibald et al., 2019). The contribution of migrating mesopelagic fish has not been assessed on a global scale yet, but is likely to be significant considering the total biomass involved (Irigoien et al., 2014). In the California Current, export mediated by mesopelagic fish accounts for 15-17% (22-24 mgC/m^2/day) of total export (Davison et al., 2013).

As organisms migrate, they also use more energy, therefore impacting their growth and decreasing their trophic transfer efficiency compared to resident organisms (chapter 7). This has cascading effects on the growth of predators and then on potential fisheries yields. Moreover, fisheries are also impacted by DVM: nets target specific fishing depths, and fishing during daytime in deep scattering layers is more energy-demanding than fishing at night closer to the surface. The fact that different organisms choose different depth residencies provides opportunities to target specific species or to avoid them and reduce by-catch, both actions being advantageous to fisheries operations (Coelho et al., 2015).

Bibliography

Abello, H. U., Shellito, S. M., Taylor, L. H., and Jumars, P. A. (2005). Light-cued emergence and re-entry events in a strongly tidal estuary. *Estuaries*, 28(4):487–499.

Aksnes, D. L. and Giske, J. (1990). Habitat profitability in pelagic environments. *Marine Ecology Progress Series*, 64:209–215.

Aksnes, D. L., Røstad, A., Kaartvedt, S., Martinez, U., Duarte, C. M., and Irigoien, X. (2017). Light penetration structures the deep acoustic scattering layers in the global ocean. *Science Advances*, 3(5):1–6.

Andersen, N. G., Lundgren, B., Neuenfeldt, S., and Beyer, J. E. (2017). Diel vertical interactions between Atlantic cod Gadus morhua and sprat Sprattus sprattus in a stratified water column. *Marine Ecology Progress Series*, 583:195–209.

Archibald, K. M., Siegel, D. A., and Doney, S. C. (2019). Modeling the impact of zooplankton diel vertical migration on the carbon export flux of the biological pump. *Global Biogeochemical Cycles*.

Auel, H. and Verheye, H. M. (2007). Hypoxia tolerance in the copepod Calanoides carinatus and the effect of an intermediate oxygen minimum layer on copepod vertical distribution in the northern Benguela Current upwelling system and the Angola-Benguela Front. *Journal of Experimental Marine Biology and Ecology*, 352(1):234–243.

Aumont, O., Maury, O., Lefort, S., and Bopp, L. (2018). Evaluating the potential impacts of the diurnal vertical migration by marine organisms on marine biogeochemistry. *Global Biogeochemical Cycles*, pages 1–22.

Bayly, I. A. E. (1986). Aspects of Diel Vertical Migration in Zooplankton, and Its Enigma Variations. In De Dekker, P. and Williams, W. D., editors, *Limnology in Australia*, pages 349–368. CSIRO Australia.

Bianchi, D., Galbraith, E. D., Carozza, D. A., Mislan, K. A. S., and Stock, C. A. (2013). Intensification of open-ocean oxygen depletion by vertically migrating animals. *Nature Geoscience*, 6(7):545–548.

Bollens, S. and Frost, B. W. (1989a). Predator-induced diel vertical migration in a planktonic copepod. *Journal of Plankton Research*, 11(5):1047–1065.

Bollens, S. M. and Frost, B. W. (1989b). Zooplanktivorous fish and variable diel vertical migration in the marine planktonic copepod Calanus pacificus. *Limnology and Oceanography*, 34(6):1072–1083.

Bollens, S. M. and Frost, B. W. (1991). Diel Vertical Migration in Zooplankton - Rapid Individual-Response to Predators. *Journal of Plankton Research*, 13(6):1359–1365.

Bollens, S. M., Frost, B. W., and Cordell, J. R. (1994). Chemical, mechanical and visual cues in the vertical migration behavior of the marine planktonic copepod Acartia hudsonica. *Journal of Plankton Research*, 16(5):555–564.

Bollens, S. M., Frost, B. W., Thoreson, S. D., and Watts, S. J. (1992). Diel vertical migration in zooplankton : field evidence in support of the predator avoidance hypothesis. *Hydrobiologia*, 234:33–39.

Boriss, H. and Gabriel, W. (1998). Vertical migration in Daphnia: the role of phenotypic plasticity in the migration pattern for competing clones or species. *Oikos*, 83(1):129–138.

Bradford-Grieve, J. M. (2001). Potential contribution that the copepod Neocalanus tonsus makes to downward carbon flux in the Southern Ocean. *Journal of Plankton Research*, 23(9):963–975.

Brierley, A. S. (2014). Diel vertical migration. *Current Biology*, 24(22):R1074–R1076.

Coelho, R., Fernandez-Carvalho, J., and Santos, M. N. (2015). Habitat use and diel vertical migration of bigeye thresher shark: Overlap with pelagic longline fishing gear. *Marine Environmental Research*, 112:91–99.

Cohen, J. H. and Forward, R. B. (2005). Diel vertical migration of the marine copepod Calanopia americana. II. Proximate role of exogenous light cues and endogenous rhythms. *Marine Biology*, 147(2):399–410.

Cohen, J. H. and Forward Jr, R. B. (2009). Zooplankton Diel Vertical Migration — A Review Of Proximate Control. *Oceanography and Marine Biology*, 47:77–110.

Cousyn, C., De Meester, L., Colbourne, J. K., Brendonck, L., Verschuren, D., and Volckaert, F. (2001). Rapid, local adaptation of zooplankton behavior to changes in predation pressure in the absence of neutral genetic changes. *Proceedings of the National Academy of Sciences of the United States of America*, 98(11):6256–6260.

Cresswell, K. A., Tarling, G. A., Thorpe, S. E., Burrows, M. T., Wiedenmann, J., and Mangel, M. (2009). Diel vertical migration of Antarctic krill (Euphausia superba) is flexible during advection across the Scotia Sea. *Journal of Plankton Research*, 31(10):1265–1281.

Criales-Hernández, M. I., Schwamborn, R., Graco, M., Ayón, P., Hirche, H. J., and Wolff, M. (2008). Zooplankton vertical distribution and migration off Central Peru in relation to the oxygen minimum layer. *Helgoland Marine Research*, 62(2 SUPPL.1):85–100.

Cushing, D. H. (1951). The vertical migration of planktonic Crustacea. *Biological reviews*, 26(2):158–192.

Davison, P. C., Checkley, D. M., Koslow, J. A., and Barlow, J. (2013). Carbon export mediated by mesopelagic fishes in the northeast Pacific Ocean. *Progress in Oceanography*, 116:14–30.

De Robertis, A. (2002). Size-dependent visual predation risk and the timing of vertical migration: An optimization model. *Limnology and Oceanography*, 47(4):925–933.

De Robertis, A., Jaffe, J. S., and Ohman, M. D. (2000). Size-dependent visual predation risk and the timing of vertical migration. *Limnology and Oceanography*, 45(8):1838–1844.

DeVries, T. and Weber, T. (2017). The export and fate of organic matter in the ocean: New constraints from combining satellite and oceanographic tracer observations. *Global Biogeochemical Cycles*, 31(3):535–555.

Dodson, S. (1990). Predicting diel vertical migration of zooplankton. *Limnology and Oceanography*, 35(5):1195–1200.

Duchêne, J. C. and Queiroga, H. (2001). Use of an intelligent CCD camera for the study of endogenous vertical migration rhythms in first zoeae of the crab Carcinus maenas. *Marine Biology*, 139(5):901–909.

Fiksen, Ø. and Carlotti, F. (1998). A model of optimal life history and diel vertical migration in Calanus finmarchicus. *Sarsia*, 83:129–147.

Forward, R. B., Diaz, H., and Ogburn, M. B. (2007). The ontogeny of the endogenous rhythm in vertical migration of the blue crab Callinectes sapidus at metamorphosis. *Journal of Experimental Marine Biology and Ecology*, 348(1-2):154–161.

Forward, R. B. and Rittschof, D. (2000). Alteration of photoresponses involved in diel vertical migration of a crab larva by fish mucus and degradation products of mucopolysaccharides. *Journal of Experimental Marine Biology and Ecology*, 245(2):277–292.

Frank, T. M. and Widder, E. A. (2002). Effects of a decrease in downwelling irradiance on the daytime vertical distribution patterns of zooplankton and micronekton. *Marine Biology*, 140(6):1181–1193.

Frost, B. W. (1988). Variability and Possible Adaptive Significance of Diel Vertical Migration in Calanus-Pacificus, a Planktonic Marine Copepod. *Bulletin of Marine Science*, 43(3):675–694.

Frost, B. W. and Bollens, S. M. (1992). Variability of Diel Vertical Migration in the Marine Planktonic Copepod Pseudocalanus newmani in Relation to Its Predators. *Canadian Journal of Fisheries and Aquatic Sciences*, 49(6):1137–1141.

Haney, J. F., Craggy, A., Kimball, K., and Weeks, F. (1990). Light control of evening vertical migrations by Chaoborus punctipennis larvae. *Limnology and Oceanography*, 35(5):1068–1078.

Hansen, A. N. and Visser, A. W. (2016). Carbon export by vertically migrating zooplankton: An optimal behavior model. *Limnology and Oceanography*, 61(2):701–710.

Hardy, A. C. (1936). Plankton ecology and the hypothesis of animal exclusion. *Proceedings of the Linnean Society of London*, 148(2):64–70.

Hays, G. C. (2003). A review of the adaptive significance and ecosystem consequences of zooplankton diel vertical migrations. *Hydrobiologia*, 503:163–170.

Hirche, H.-J. (1996). Diapause in the marine copepod, Calanus finmarchicus - A review. *Ophelia*, 44(October):129–143.

Horne, J. K. (2000). Acoustic approaches to remote species identification: A review. *Fisheries Oceanography*, 9(4):356–371.

Hylander, S. and Hansson, L.-A. (2013). Vertical distribution and pigmentation of Antarctic zooplankton determined by a blend of UV radiation, predation and food availability. *Aquatic Ecology*, 47(4):467–480.

Hylander, S., Larsson, N., and Hansson, L.-A. (2009). Zooplankton vertical migration and plasticity of pigmentation arising from simultaneous UV and predation threats. *Limnology and Oceanography*, 54(2):483–491.

Iida, K., Mukai, T., and Hwang, D. J. (1996). Relationship between acoustic backscattering strength and density of zooplankton in the sound-scattering layer. *ICES Journal of Marine Science*, 53(2):507–512.

Irigoien, X., Klevjer, T. A., Røstad, A., Martinez, U., Boyra, G., Acuña, J. L., Bode, A., Echevarria, F., Gonzalez-Gordillo, J. I., Hernandez-Leon, S., Agusti, S., Aksnes, D. L., Duarte, C. M., and Kaartvedt, S. (2014). Large mesopelagic fishes biomass and trophic efficiency in the open ocean. *Nature communications*, 5:3271.

Kaartvedt, S. (2010). Diel Vertical migration behaviour of the Northern krill (Meganyctiphanes norvegica Sars). In *Advances in Marine Biology*, volume 57, pages 255–275.

Kaartvedt, S., Klevjer, T. A., Torgersen, T., Sørnes, T. A., and Røstad, A. (2007). Diel vertical migration of individual jellyfish (Periphylla periphylla). *Limnology and Oceanography*, 52(3):975–983.

Kaartvedt, S., Knutsen, T., and Holst, J. C. (1998). Schooling of the vertically migrating mesopelagic fish Maurolicus muelleri in light summer nights. *Marine Ecology Progress Series*, 170:287–290.

Kaartvedt, S., Røstad, A., Christiansen, S., and Klevjer, T. A. (2020). Diel vertical migration and individual behavior of nekton beyond the ocean's twilight zone. *Deep Sea Research Part I: Oceanographic Research Papers*, page 103280.

Kaartvedt, S., Røstad, A., Klevjer, T., and Staby, A. (2009). Use of bottom-mounted echo sounders in exploring behavior of mesopelagic fishes. *Marine Ecology Progress Series*, 395:109–118.

Kaartvedt, S., Torgersen, T., Klevjer, T. A., Røstad, A., and Devine, J. A. (2008). Behavior of individual mesopelagic fish in acoustic scattering layers of Norwegian fjords. *Marine Ecology Progress Series*, 360:201–209.

Kikuchi, K. (1930). Diurnal Migration of Plankton Crustacea. *The Quarterly Review of Biology*, 5(2):189–206.

Kremer, P. and Kremer, J. M. (1988). Energetic and behavioral implications of pulsed food availability for zooplankton. *Bulletin of Marine Science*, 43(3):797–809.

Lampert, W. (1989). The Adaptive Significance of Diel Vertical Migration of Zooplankton Author (s): W . Lampert Published by : British Ecological Society Stable URL : http://www.jstor.org/stable/2389671. *Functional Ecology*, 3(1):21–27.

Lampert, W., Schmitt, R.-D., and Muck, P. (1988). Vertical migration of freshwater zooplankton: test of some hypotheses predicting a metabolic advantage. *Bulletin of Marine Science*, 43(3):620–640.

Langbehn, T., Aksnes, D., Kaartvedt, S., Fiksen, Ø., and Jørgensen, C. (2019). Light comfort zone in a mesopelagic fish emerges from adaptive behaviour along a latitudinal gradient. *Marine Ecology Progress Series*, 623:161–174.

Lass, S. and Spaak, P. (2003). Chemically induced anti-predator defences in plankton: A review. *Hydrobiologia*, 491:221–239.

Leech, D. M. and Williamson, C. E. (2001). In situ exposure to ultraviolet radiation alters the depth distribution of Daphnia. *Limnology and Oceanography*, 46(2):416–420.

Lima, S. L. (2002). Putting predators back into behavioral predator -prey interactions. *Trends in Ecology and Evolution*, 17(2):70–75.

Loose, C. J. (1993). Daphnia diel vertical migration behavior: response to vertebrate predator abundance. *Archiv für hydrobiologie ergebnisse der limnologie*, 39:29–36.

Loose, C. J. and Dawidowicz, P. (1994). Trade-offs in diel vertical migration by zooplankton: The costs of predator avoidance. *Ecology*, 75(8):2255–2263.

Luecke, C. (1986). A change in the pattern of vertical migration of Chaoborus flavicans after the introduction of trout. *Journal of Plankton Research*, 8(4):649–657.

McFarland, W., Wahl, C., Suchanek, T., and McAlary, F. (1999). The behavior of animals around twilight with emphasis on coral reef communities. In Archer, S., Djamgoz, M. B. A., Loew, E. R., Partridge, J. C., and Valler, editors, *Adaptive Mechanisms in the Ecology of Vision*, pages 583–628. Springer-Science+Business Media.

McLaren, I. A. (1963). Effects of Temperature on Growth of Zooplankton, and the Adaptive Value of Vertical Migration. *Journal of the Fisheries Research Board of Canada*, 20(3):685–727.

Murray, J. and Hjort, J. (1912). *The depths of the ocean*. Macmillan, London.

Neill, W. E. (1990). Induced vertical migration in copepods as a defence against invertebrate predation. *Nature*, 345(6275):524–526.

Neill, W. E. (1992). Population variation in the ontogeny of predator-induced vertical migration of copepods. *Nature*, 356(6364):54–57.

Netburn, A. N. and Koslow, J. A. (2015). Dissolved oxygen as a constraint on daytime deep scattering layer depth in the southern California current ecosystem. *Deep-Sea Research Part I*, 104:149–158.

Nilsson, L. A., Thygesen, U. H., Lundgren, B., Nielsen, B. F., Nielsen, J. R., and Beyer, J. E. (2003). Vertical migration and dispersion of sprat (Sprattus sprattus) and herring (Clupea harengus) schools at dusk in the Baltic Sea. *Aquatic Living Resources*, 16(3):317–324.

Norheim, E., Klevjer, T. A., and Aksnes, D. L. (2016). Evidence for light-controlled migration amplitude of a sound scattering layer in the Norwegian Sea. *Marine Ecology Progress Series*, 551:45–52.

Ohman, M. D. (1990). The Demographic Benefits of Diel Vertical Migration by Zooplankton. *Ecological Monographs*, 60(3):257–281.

Ohman, M. D., Davis, R. E., Sherman, J. T., Grindley, K. R., Whitmore, B. M., Nickels, C. F., and Ellen, J. S. (2019). Zooglider: An autonomous vehicle for optical and acoustic sensing of zooplankton. *Limnology and Oceanography: Methods*, 17(1):69–86.

Ohman, M. D., Frost, B. W., and Cohen, E. B. (1983). Reverse diel vertical migration: An escape from invertebrate predators. *Science*, 220(4604):1404–1407.

Onsrud, M. S. and Kaartvedt, S. (1998). Diel vertical migration of the krill Meganyctiphanes norvegica in relation to physical environment, food and predators. *Marine Ecology Progress Series*, 171(Dvm):209–219.

Partridge, B. L. (1982). The structure and function of fish schools. *Scientific American*, 246(6):90–100.

Pearre, S. (2003). Eat and run? The hunger satiation hypothesis in vertical migration: history, evidence and consequences. *Biological Reviews*, 78:1–79.

Prihartato, P. K., Aksnes, D. L., and Kaartvedt, S. (2015). Seasonal patterns in the nocturnal distributionand behavior of the mesopelagic fish Maurolicus muelleri at high latitudes. *Marine Ecology Progress Series*, 521:189–200.

Ringelberg, J. (1991). A mechanism of predator-mediated induction of diel vertical migration in Daphnia hyalina. *Journal of Plankton Research*, 13(1):83–89.

Ringelberg, J. (1995a). Changes in light intensity and diel vertical migration: a comparison of marine and freshwater environments. *Journal of the Marine Biological Association of the U.K.*, 75:15–25.

Ringelberg, J. (1995b). Is diel vertical migration possible without a rhythmic signal? Comments on a paper by Bollens et al. (1994).

Ringelberg, J. (1999). The photobehaviour of Daphnia spp. As a model to explain diel vertical migration in zooplankton. *Biological Reviews*, 74(4):397–423.

Ringelberg, J. and Gool, E. V. (2003). On the combined analysis of proximate and ultimate aspects in diel vertical migration (DVM) research. *Hydrobiologia*, 491:85–90.

Robinson, C. J., Arenas, F. V., and Gomez, G. J. (1995). Diel vertical and offshore-inshore movements of anchovies off the central Baja California coast. *Journal of Fish Biology*, 47(5):877–892.

Sainmont, J., Thygesen, U. H., and Visser, A. W. (2013). Diel vertical migration arising in a habitat selection game. *Theoretical Ecology*, 6(2):241–251.

Seghers, B. H. (1974). Schooling behavior in the guppy (Poecilia reticulata): an evolutionary response to predation. *Evolution*, 28(3):486–489.

Sekino, T. and Yoshioka, T. (1995). The Relationship between Nutritional Condition and Diel Vertical Migration of Daphnia galeata. *Japanese Journal of Limnology*, 56(2):145–150.

Siegel, D. A., Buesseler, K. O., Behrenfeld, M. J., Benitez-Nelson, C. R., Boss, E., Brzezinski, M. A., Burd, A., Carlson, C. A., D'Asaro, E. A., Doney, S. C., Perry, M. J., Stanley, R. H., and Steinberg, D. K. (2016). Prediction of the export and fate of global ocean net primary production: The exports science plan. *Frontiers in Marine Science*, 3(MAR):1–10.

Solberg, I. and Kaartvedt, S. (2017). The diel vertical migration patterns and individual swimming behavior of overwintering sprat Sprattus sprattus. *Progress in Oceanography*, 151:49–61.

Tanaka, M. (2019). Changes in vertical distribution of zooplankton under wind-induced turbulence: A 36-year record. *Fluids*, 4(195):1–11.

Thygesen, U. H., Sommer, L., Evans, K., and Patterson, T. A. (2016). Dynamic optimal foraging theory explains vertical migrations of Bigeye tuna. *Ecology*, 97(7):1852–1861.

Van Gool, E. and Ringelberg, J. (1997). The effect of accelerations in light increase on the phototactic downward swimming of Daphnia and the relevance to diel vertical migration. *Journal of Plankton Research*, 19(12):2041–2050.

Varpe, Ø. (2012). Fitness and phenology: Annual routines and zooplankton adaptations to seasonal cycles. *Journal of Plankton Research*, 34(4):267–276.

Vaughn, D. (2007). Predator-induced morphological defenses in marine zooplankton: A larval case study. *Ecology*, 88(4):1030–1039.

Vaughn, D. and Strathmann, R. R. (2008). Predators induce cloning in echinoderm larvae. *Science*, 319(5869):1503.

Widder, E. A. and Frank, T. M. (2001). The speed of an isolume: A shrimp's eye view. *Marine Biology*, 138(4):669–677.

Woodhead, P. (1966). The behavior of fish in relation to light in the sea. *Oceanogr. Mar. Biol. Ann. Rev.*, 4:337–403.

Worthington, E. B. (1931). Vertical movements of fresh-water Macroplankton. *Internationale Revue der gesamten Hydrobiologie und Hydrographie*, 25(5-6):394–436.

Yoshida, T., Toda, T., Kuwahara, V., Taguchi, S., and Othman, B. H. (2004). Rapid response to changing light environments of the calanoid copepod Calanus sinicus. *Marine Biology*, 145(3):505–513.

Yuen, H. S. H. (1970). Behavior of Skipjack Tuna, Katsuwonus pelamis , as Determined by Tracking with Ultrasonic Devices . *Journal of the Fisheries Research Board of Canada*, 27(11):2071–2079.

Zaret, T. M. and Suffern, S. (1976). Vertical migration in zooplankton as a predator avoidance mechanism. *Limnology and Oceanography*, 21(6):804–813.

CHAPTER 3

Mathematical background

3.1 Ideal Free Distribution, Evolutionary Stable Strategy and Nash equilibrium

3.1.1 For single species

Understanding how organisms distribute spatially is arguably one of the ultimate goals of ecology (Morris, 2003; Křivan et al., 2008). Modern theoretical considerations of animal habitat distribution can be traced back to Fretwell and Lucas (1970), who introduced the concept of **Ideal Free Distribution** (IFD) for a single species. The IDF predicts how organisms from one population should distribute in a discrete habitat with several patches. The IFD states that all organisms should distribute to have an equal pay-off (or to say it differently, they distribute so that all occupied habitats are equally suitable). If we assume that (i) all animals are equal competitors, (ii) there is no resource or population dynamics, (iii) all animals have complete information and (iv) there is no migration cost between the different patches, the IFD means simply that the number of individuals in each patch is proportional to the amount of resources. Despite some debate, there seems to be indications that animals follow the IFD in nature, at least in some cases (Morris, 2006; Křivan et al., 2008).

The single-species IFD is important in ecology because it is also an ESS, i.e. an **Evolutionary Stable Strategy** (Cressman and Křivan, 2006). An ESS is a strategy that is stable under natural selection. If a strategy adopted by most members of a population is an ESS, no mutant strategy can invade and perform better than residents (Maynard Smith and Price, 1973). The fact that the IFD is an ESS is crucial in ecology, as its relevance would be negligible otherwise (Křivan et al., 2008). Indeed, if other patch selection strategies yields a higher reward, then after any random perturbation the system would be driven away from the equilibrium distribution.

The IDF is also a **Nash equilibrium** (Nash, 1951; Cressman and Křivan, 2006). Assuming complete information, a Nash equilibrium is a point where no individual can increase its pay-off by changing unilaterally its strategy. Formally, if we call V_i the pay-off received by the fraction of animals p_i in patch i, the Nash equilibrium is characterised by:

$$\begin{aligned} &V_i = V_j = V^* \text{ for all } p_i, p_j > 0, \\ &V_i \leq V^* \text{ for all } p_i = 0. \end{aligned} \tag{3.1}$$

There can be zero, one or several Nash equilibria in a system (Hofbauer and Sigmund, 2003).

For the single-species habitat selection game, the IFD is an ESS and is also a Nash equilibrium. Moreover, if the pay-off in each patch is a decreasing function of the population density (e.g. because of resource competition or density-dependent mortality), the habitat selection game has a unique Nash equilibrium, which is the IFD (Cressman and Křivan, 2006).

3.1.2 Extension to several species

As species interact, the single-species IFD cannot be applied anymore as feedback processes and indirect effects need to be considered. This led to the definition of the two-species IFD (Křivan et al., 2008). We consider two species M and N with the same set of pure strategies[1] H. p and q is the respective distribution of M and N, and V_i (resp. W_i) is the pay-off of an individual from species M (resp. N) following strategy i. The pay-offs V_i and W_i only depend on the fraction of the populations in patch i, i.e. on (p_i, q_i). The two-species IFD needs, at least, to conform to the single-species definition, meaning that the pay-off for all individuals (of the same species) in any patch must be the same, and higher than the pay-off they would get in unoccupied patches. Mathematically, this translates to:

$$\begin{aligned} V_i(p^*, q^*) = V_j(p^*, q^*) \leq V_k(p^*, q^*) \text{ for all } p_i^*, p_j^* > 0 \text{ and } p_k^* = 0, \\ W_i(p^*, q^*) = W_j(p^*, q^*) \leq W_k(p^*, q^*) \text{ for all } q_i^*, q_j^* > 0 \text{ and } q_k^* = 0. \end{aligned} \tag{3.2}$$

This can be related to the definition of the Nash equilibrium for a pair of (p^*, q^*) strategies (Křivan et al., 2008). This was used as the definition of two-species IFD (called "joint IFD") in several articles (Morris, 2004; Křivan and Sirot, 2002), but it was argued that this strategy set cannot be qualified an IFD because it lacks the ESS stability property that one-species IFD have (Cressman et al., 2004). As a consequence, Křivan et al. (2008) recommend to use the term Nash equilibria for strategies complying with equation 3.2, and to keep the term IFD for Nash equilibria that satisfy further stability conditions.

The work presented in this thesis deals only with multi-population systems (from 2 to 101 populations depending on the projects), and we kept referring to the equilibria presented as Nash equilibria and not IFD as no stability properties were formally investigated. However, many of the presented Nash equilibria are probably also IFD.

[1] A pure strategy (by opposition to a mixed strategy) is a strategy where the player chooses a fixed action and does not mix them. In our habitat selection game, a pure strategy means choosing a definite habitat, whereas a mixed strategy is a set of different habitats that can be chosen with certain probability (the sum of these probabilities is 1 as the animal has to be in a habitat).

3.2 Game theory and replicator dynamics

Game theory is defined as "the study of mathematical models of conflict and cooperation between intelligent rational decision-makers" (Myerson, 1991). Our approach to the habitat selection issue is deeply rooted in game theory, as we consider individuals from several interacting populations playing against each other for the highest possible pay-off (mathematical models of conflict) and investigate the equilibrium distribution of organisms in the strategy space (the Nash equilibrium). The fact that the definition of game theory includes "intelligent rational decision-makers" is not incompatible with our study of marine creatures. Indeed, we assume that evolution equipped individuals with the capacity to deal with a range of conditions encountered in an optimal way. Indeed, if it were possible to behave in a different way, organisms would have evolved differently and the initial set of strategies would have gone extinct. This is probably valid in constant or slowly varying environments. In fast changing environments, organisms would probably need some time to adjust to the new conditions, even though it was shown that organisms can react quite fast to stimuli such as the arrival of new predators (Godø et al., 2014).

Several techniques have been developed to find the Nash equilibria of a system: best response dynamics (Cressman, 2003), differential equations established thanks to mean-field game theory (Thygesen and Patterson, 2018), and the replicator equation (Schuster and Siegmund, 1983). Here, we will focus on the replicator equation, as it is the method used in this thesis.

The replicator equation is an algorithm that allows to get to the Nash equilibrium of a system. Let a system consist of n populations $X^1, X^2, ..., X^n$ with H possible pure strategies. At the time step t of the algorithm, the fraction of organisms from population i following strategy j is noted $X^i_j(t)$, and $W^i_j(t)$ is their associated pay-off. In essence, the replicator equation allows each subgroup of each population to grow according to its pay-off, before renormalization to ensure that there is no biomass increase in the system:

$$\begin{aligned} \tilde{X}^i_j(t+1) &= X^i_j(t)(1+W^i_j(t)), \\ X^i_j(t+1) &= \frac{\tilde{X}^i_j(t+1)}{\sum_{k=1}^{H} \tilde{X}^i_k(t+1)}. \end{aligned} \tag{3.3}$$

This scheme is run until steady state is reached. The replicator equation describes a selection process in which successful strategies (the ones leading to the highest pay-off) spread in the population (Hofbauer and Sigmund, 2003).

For normal form games (i.e. games that can be written out as matrix games), the Folk theorem of Evolutionary Game Theory (Hofbauer and Sigmund, 1998) asserts three statements relating to the stability of the system:

1. A stable rest point of the replicator equation is a Nash Equilibrium.

2. Any convergent trajectory of the replicator equation evolves to a Nash equilibrium.

3. A strict Nash equilibrium is asymptotically stable.

It is important to note that the reverse statements are not necessarily true. For example, the replicator equation is not assured to converge to all Nash equilibria of a system. Whether the Folk theorem holds in more "exotic" games depends on the games considered, but we can state that in our case its convergent trajectories evolve towards Nash equilibria.

The replicator equation is conceptually simple, and relatively easy to implement. Its big advantage is that it can deal with any form of pay-off function, enabling to describe species interactions as precisely as desired. However, drawbacks hampered its widespread implementation. The outcome of the replicator equation depends on the set of initial conditions used, and there is no guarantee that the replicator equation will be able to find all Nash equilibria of the system given different initial conditions. To address these problems, in the following chapter several runs were performed to assess whether the replicator equation would find multiple equilibria. In all the following of this thesis, it appears that each specific system could only lead to a single stable state of the replicator equation (strict equilibrium or attractor – in chapter 8). Finally, it should be noted that when the system becomes complex (either in terms of players involved or possible strategies), the algorithm can take a very long time to converge, limiting one's ability to perform many runs and sensitivity analysis of different parameters.

3.3 Fitness definitions

In sections 3.1 and 3.2, we related the players outcome of the habitat selection game to their "pay-off". The pay-off is what they gain from playing the game, i.e. their **fitness** in ecological terms. For an individual, the most exhaustive way to define fitness is typically the life-integrated expected reproductive output[2]. This is the number of offsprings that an organism will produce throughout its life. If an organism is very successful, it will pass on its genes (and traits) to many offsprings that will, in turn, pass on their genes to their offsprings. In a Darwinian sense, this fitness allows to know which individuals are the fittest and which genes (or traits, or strategies) will spread or go extinct in a population.

However, this definition of fitness can be technically challenging to implement in already complex numerical models as it requires to consider the full life cycle of the individuals. Consequently, many different criteria are used in the literature to

[2]For completeness, we can add that fitness definitions can be even more comprehensive and include the offsprings' condition or the number of offsprings that actually reach maturity. If all the offsprings produced by an organism die right after birth, this individual will not pass on any genes to the next generations, no matter how many offsprings it produces.

circumvent these issues, with different outcomes depending on the fitness measure used (Luttbeg and Sih, 2004). Among others, we can cite the venturous revenue (Liu et al., 2003), a predator avoidance function (Han and Straškraba, 2001), a decision criteria based on the internal state of the individual (Castellani et al., 2013), or the ratio energy gain over mortality also known as Gilliam's rule (Gilliam and Fraser, 1987; Houston et al., 1993; De Robertis, 2002; Sainmont et al., 2013). Gilliam's rule is probably one of the simplest to implement, as it is a myopic rule: it is only based on immediately available information and cues, and neglects potential changes due to variability such as seasonality. Nevertheless, it is still a good approximation of the Darwinian fitness. When the environment is constant (and ontogeny is ignored), Gilliam's rule performs as well as a life history optimization model (Sainmont et al., 2015). In a highly seasonal environment, Gilliam's rule is also a good approximation to Darwinian fitness, as Sainmont et al. (2015) showed that the total reproductive output differs only up to 25% compared to a model that considers life-history.

In the following chapters of this thesis (except chapters 6 and 7), the fitness used will be a slight variation of Gilliam's rule, based on the daily-averaged growth and mortality rates of the individual (Kiørboe et al., 2018). If the growth rate is positive, the fitness measure used is Gilliam's rule, i.e. growth *divided* by mortality, but if the growth rate is negative the measure used is growth *minus* mortality. This is because we assume that under averse conditions organisms try to maximise the time they can survive by minimising all possible losses (Kiørboe et al., 2018).

Bibliography

Castellani, M., Rosland, R., Urtizberea, A., and Fiksen, Ø. (2013). A mass-balanced pelagic ecosystem model with size-structured behaviourally adaptive zooplankton and fish. *Ecological Modelling*, 251:54–63.

Cressman, R. (2003). *Evolutionary dynamics and extensive form games*. MIT Press.

Cressman, R. and Křivan, V. (2006). Migration dynamics for the ideal free distribution. *American Naturalist*, 168(3):384–397.

Cressman, R., Křivan, V., and Garay, J. (2004). Ideal free distributions, evolutionary games, and population dynamics in multiple-species environments. *The American naturalist*, 164(4):473–489.

De Robertis, A. (2002). Size-dependent visual predation risk and the timing of vertical migration: An optimization model. *Limnology and Oceanography*, 47(4):925–933.

Fretwell, S. D. and Lucas, H. L. J. (1970). On theoretical behavior and other factors influencing habitat distribution in birds. *Acta Biotheoretica*, 19:16–32.

Gilliam, J. F. and Fraser, D. F. (1987). Habitat Selection Under Predation Hazard: Test of a Model with Foraging Minnows. *Ecology*, 68(6):1856–1862.

Godø, O. R., Macaulay, G. J., Kaartvedt, S., Johnsen, E., Handegard, N. O., Browman, H. I., Huse, G., Giske, J., and Ona, E. (2014). Marine ecosystem acoustics (MEA): quantifying processes in the sea at the spatio-temporal scales on which they occur. *ICES Journal of Marine Science*, 71(8):2357–2369.

Han, B. P. and Straškraba, M. (2001). Control mechanisms of diel vertical migration: Theoretical assumptions. *Journal of Theoretical Biology*, 210(3):305–318.

Hofbauer, J. and Sigmund, K. (1998). *Evolutionary games and population dynamics*. Cambridge University Press.

Hofbauer, J. and Sigmund, K. (2003). Evolutionary Game Dynamics. *Bulletin (New Series) of the American mathematical society*, 40(403):479–519.

Houston, A. I., McNamara, J. M., and Hutchinson, J. M. C. (1993). General results concerning the trade-off between gaining energy and avoiding predation. *Philosophical Transactions of the Royal Society of London. Series B: Biological Sciences*, 341(1298):375–397.

Kiørboe, T., Saiz, E., Tiselius, P., and Andersen, K. H. (2018). Adaptive feeding behavior and functional responses in zooplankton. *Limnology and Oceanography*, 63(1):308–321.

Křivan, V., Cressman, R., and Schneider, C. (2008). The ideal free distribution: A review and synthesis of the game-theoretic perspective. *Theoretical Population Biology*, 73(3):403–425.

Křivan, V. and Sirot, E. (2002). Habitat selection by two competing species in a two-habitat environment. *The American Naturalist*, 160(2):214–234.

Liu, S. H., Sun, S., and Han, B. P. (2003). Diel vertical migration of zooplankton following optimal food intake under predation. *Journal of Plankton Research*, 25(9):1069–1077.

Luttbeg, B. and Sih, A. (2004). Predator and prey habitat selection games: the effects of how prey balance foraging and predation risk. *Israel Journal of Zoology*, 50:233–254.

Maynard Smith, J. and Price, G. (1973). The logic of animal conflict. *Nature*, 246:15–18.

Morris, D. W. (2003). Shadows of predation: Habitat-selecting consumers eclipse competition between coexisting prey. *Evolutionary Ecology*, 17(4):393–422.

Morris, D. W. (2006). Moving to the ideal free home. *Nature*, 443(7112):645–646.

Morris, W. (2004). Some crucial consequences of adaptive habitat selection by predators and prey: apparent mutualisms, competitive ghosts, habitat abandonment, and spatial structure. *Israel Journal of Zoology*, 50:207–232.

Myerson, R. B. (1991). *Game Theory: Analysis of Conflict*. Harvard University Press.

Nash, J. (1951). Non-Cooperative Games. *The Annals of Mathematics*, 54(2):286.

Sainmont, J., Andersen, K. H., Thygesen, U. H., Fiksen, Ø., and Visser, A. W. (2015). An effective algorithm for approximating adaptive behavior in seasonal environments. *Ecological Modelling*, 311:20–30.

Sainmont, J., Thygesen, U. H., and Visser, A. W. (2013). Diel vertical migration arising in a habitat selection game. *Theoretical Ecology*, 6(2):241–251.

Schuster, P. and Siegmund, K. (1983). Replicator Dynamics. *Journal of Theoretical Biology*, 100:533–538.

Thygesen, U. H. and Patterson, T. A. (2018). Oceanic diel vertical migrations arising from a predator-prey game. *Theoretical Ecology*, pages 1–13.

CHAPTER 4

Synopsis

Paper I Diel Vertical Migration in a predator-prey system

Several studies investigated DVM of zooplankton and fish as a game being played out between prey and predator (Iwasa, 1982; Hugie and Dill, 1994; Sainmont et al., 2013), but all divided the habitats between a surface layer and a deep refuge. If this set-up was very useful for theoretical considerations, it could not provide any meaningful information as to the potential depth of the deep scattering layer. This paper investigates whether game theory and replicator dynamics are useful tools and methods to model precisely the behavioural dynamics of organisms migrating daily in the water column.

In this paper, I model the optimal habitat selection game of a zooplankton and a fish population in a water column, discretised in several ($n = 30$) water layers. Both species interact together, and each individual from both populations can change its behaviour to optimize its fitness. Behaviour is seen here as the set of day and night depths organisms reside at (I ignore the transition time between these two depths, even though the model includes a migration cost that is an increasing function of the depth travelled). I look for the Nash equilibrium of the system under different conditions.

Our results are satisfying, in that they display one clear Nash equilibrium for each set of parameters investigated. Moreover, our model performs relatively well at reconstructing the migration behaviour of *Meganyctiphanes norvegica* observed over a yearly cycle in the Mediterranean (Sardou et al., 1996), and provides information on the potential prey distribution. Further, I explore the optimal DVM patterns of prey and predator according to a predator trait, namely the predator clearance rate. An increase in clearance rate allows the predator to forage more efficiently, but also means that the prey will suffer an increased mortality rate. Would the prey hide deeper in response to an increased predator clearance rate, or would they remain at the same depth, enabling predators to feed more?

I find three different migration regimes as the predator clearance rate increases. First, at very low clearance rates, both prey and predator remain close to the surface. At a certain point, the predation risk for prey becomes too high during daytime and they start performing DVM. Predator follow the prey, and perform DVM as well. Finally, a third migration regime emerges when the mortality risk at the surface becomes too high for prey even at night: prey remain at depth at all times and

predator are scattered in the water column. The third migration regime results in a very low fitness for both prey and predators.

This last result is very surprising: natural selection would tend to favour predators with a higher clearance rate, meaning that they are able to feed more efficiently than their counterparts. As a consequence, the trait "higher clearance rate" would spread in the population, triggering a fitness collapse at the population level: predators would become "too accomplished for their own good" (Pinti and Visser, 2019). This curiosity is probably an artefact of the fixed population sizes, but how this would be resolved in a setting with population dynamics remains uncertain at this point.

Paper II Population game theory: the interplay between the individual and the population time scales

Following results from Paper I, I explore the coupling between the individual (fast) and the population (slower) time scale. The initial motivation was to understand what would happen to DVM patterns of prey and predators expressing high clearance rate, as I saw previously that the results with fixed population sizes are not satisfying in this case.

To that end, I adapted population game theory (Cressman et al., 2004) to our previous model of diel vertical migration for a prey and a predator in n water layers. In short, the dynamics happen at two time scales. On a fast time scale, the optimal behaviour of the organisms is determined by the Nash equilibrium of the system. On a slower time scale, the population sizes evolve following Lotka-Volterra dynamics. I assume that the system is always at equilibrium on the fast time scale, so I always update the optimal behaviour of the individuals before any change at the population time scale happens. I run the algorithm until equilibrium is reached at both time scales.

This method helped us to solve the issue raised by Paper I. It appears that normal DVM patterns are much more widespread when population dynamics are considered. A change in predator clearance rate does not influence much the DVM pattern but rather the equilibrium population sizes. As predator clearance rate increases, equilibrium population sizes of zooplankton and fish decrease.

Furthermore, I use this model to assess the cascading effect of adaptive behaviour for ecosystem functions. It appears that considering explicitly the adaptive behaviour of predators and prey in population dynamics model does not only impact population dynamics, but it also has cascading consequences for ecosystem functioning. When organisms perform DVM, they spend energy migrating, reducing trophic transfer efficiency. They also bring actively carbon to the depths, where they respire it or excrete it as fecal pellets. As such, they increase the efficiency of the biological pump. With this theoretical study, I stress that it is important to consider the adaptive behaviour of organisms when using population models to draw conclusions about ecosystem functioning.

Paper III Non-linear diel vertical migration patterns of a copepod community

Copepods are among the most important diel vertical migrators, and many modelling studies investigated their migration patterns (Hansen and Visser, 2016; Fiksen, 1995; Varpe et al., 2007). However, most disregarded is the plurality of patterns that can be observed at a given point in time and space, such as the ones observed by Ohman and Romagnan (2016) in the California Current. Ohman and Romagnan (2016) investigated the DVM patterns of copepods distinguished according to their size. They found that (i) small copepods (<1 mm) did not migrate and remain close to the surface at all times, (ii) big copepods (around 1 cm) did not migrate either but remain at depth, (iii) intermediate copepods (between 1 mm and 1 cm) are performing DVM. The depth residency of the biggest copepods and the extent of the amplitude of DVM for intermediate copepods vary with the location investigated within the California Current.

Paper III investigates the size-based DVM patterns of a copepod community. Following the same methodological framework as project I (but with many more subpopulations), I reproduce DVM patterns observed in the California Current, enabling to get a mechanistic understanding of the behavioural dynamics in focus. For small copepods, migration is not worth the cost: they are so small that they do not really suffer from visual predators, and can remain close to the surface at all times. On the contrary, large copepods experience a higher mortality risk due to visual predation at the surface even during nighttime, constraining them to remain at depth at all times. Finally, intermediate copepods perform DVM: visual predation is too high during daytime, but nighttime enables them to migrate back to the surface. It is interesting to note that our model also divides copepods according to their feeding mode. I show that active-feeding copepods represent the vast majority of organisms responsible for DVM, while passive-feeding organisms do not migrate much, corroborating previous observations (Irigoien et al., 2004; Moraitou-Apostolopoulou, 1971).

Finally, this paper also investigate a more exotic DVM pattern reported to occur in fjords (Ohman et al., 1983; Ohman, 1990) with a characteristic tri-trophic food-chain. Visual predators impose a top-down control on tactile predators, that perform normal DVM to reduce their mortality rate. Smaller organisms, when tactile predators are abundant, need to hide more from tactile predators than from visual predators. Consequently, they perform reverse diel vertical migration to decrease as much as possible the overlap with the former. With limited tuning, our model managed to reproduce these dynamics, enabling to explain from a mechanistic viewpoint this counter-intuitive pattern.

Paper IV Global carbon export of a pelagic community

The biological pump is the biologically-driven carbon sequestration from the surface of the ocean to its interior. The active part of the biological pump is the carbon that is not just sinking below the euphotic zone but actively brought at depth by migrating individuals (either daily or seasonally). Once at depth, these organisms respire or excrete carbon as fecal pellets. It is estimated that the biological pump exports between 6-9 PgC/yr on a global scale (Siegel et al., 2014; DeVries and Weber, 2017), of which between $13 - 18\%$ are due to the active part of the biological pump (mainly zooplankton, Archibald et al. (2019); Aumont et al. (2018)). With the exception of a few particular locations (Davison et al., 2013), the relative contribution of different functional groups such as forage fish or mesopelagic fish to the biological pump is currently unknown.

Paper IV explores this knowledge gap and aims at providing global estimates of active carbon export worldwide for different pelagic functional groups. Using game theoretic methods as in Paper I and III, I set up a pelagic food-web model and compute the optimal DVM patterns for all components of the food-web (meso and macro zooplankton, forage fish, mesopelagic fish, top predators and jellyfish). In the pelagic, light is not the only environmental driver of DVM as organisms can be limited by temperature and oxygen concentrations, and these potential limitations are included in the model. Using global estimates of the different populations as well as environmental variables (Petrik et al., 2019; Stock et al., 2017; Proud et al., 2018; Locarnini et al., 2019), I compute the optimal DVM patterns for each functional group at each point of the global ocean.

This global set of distributions enables us to compute the active carbon transport below the euphotic zone as well as its breakdown by functional groups. I find that overall, mesozooplankton and higher trophic levels export 4.8 PgC/yr below the euphotic zone due to fecal pellets sinking alone.

Additionally, I couple the results to a global ocean circulation inverse model (DeVries and Primeau, 2011; DeVries, 2014) to estimate the global carbon sequestrated via the different pathways, and as such the direct importance of each functional group for the global carbon cycle. I find that the total carbon sequestration mediated by organisms of our model is 875 PgC. Zooplankton are responsible for most of it (561 PgC), but our results suggest that mesopelagic fish and forage fish are much more important to the active biological pump than currently thought (responsible for the sequestration of 158 and 94 PgC respectively).

Bibliography

Archibald, K. M., Siegel, D. A., and Doney, S. C. (2019). Modeling the impact of zooplankton diel vertical migration on the carbon export flux of the biological pump. *Global Biogeochemical Cycles*.

Aumont, O., Maury, O., Lefort, S., and Bopp, L. (2018). Evaluating the potential impacts of the diurnal vertical migration by marine organisms on marine biogeochemistry. *Global Biogeochemical Cycles*, pages 1–22.

Cressman, R., Křivan, V., and Garay, J. (2004). Ideal free distributions, evolutionary games, and population dynamics in multiple-species environments. *The American naturalist*, 164(4):473–489.

Davison, P. C., Checkley, D. M., Koslow, J. A., and Barlow, J. (2013). Carbon export mediated by mesopelagic fishes in the northeast Pacific Ocean. *Progress in Oceanography*, 116:14–30.

DeVries, T. (2014). The oceanic anthropogenic CO2 sink: Storage, air-sea fluxes, and transports over the industrial era. *Global Biogeochemical Cycles*, 28(7):631–647.

DeVries, T. and Primeau, F. (2011). Dynamically and observationally constrained estimates of water-mass distributions and ages in the global ocean. *Journal of Physical Oceanography*, 41(12):2381–2401.

DeVries, T. and Weber, T. (2017). The export and fate of organic matter in the ocean: New constraints from combining satellite and oceanographic tracer observations. *Global Biogeochemical Cycles*, 31(3):535–555.

Fiksen, Ø. (1995). Vertical distribution and population dynamics of copepods by dynamic optimization. *ICES Journal of Marine Science*, 52(3-4):483–503.

Hansen, A. N. and Visser, A. W. (2016). Carbon export by vertically migrating zooplankton: An optimal behavior model. *Limnology and Oceanography*, 61(2):701–710.

Hugie, D. M. and Dill, L. M. (1994). Fish and Game: a game theoretic approach to habitat selection by predators and prey. *Journal of Fish Biology*, 45(Supplement A):151–169.

Irigoien, X., Conway, D. V., and Harris, R. P. (2004). Flexible diel vertical migration behaviour of zooplankton in the Irish Sea. *Marine Ecology Progress Series*, 267(2):85–97.

Iwasa, Y. (1982). Vertical migration of zooplankton: a game between predator and prey. *The American naturalist*, 120(2):171–180.

Locarnini, R., Mishonov, A., Baranova, O., Boyer, T., Zweng, M., Garcia, H., Reagan, J., Seidov, D., Weathers, K., Paver, C., and Smolyar, I. (2019). World Ocean Atlas, Volume 1: Temperature.

Moraitou-Apostolopoulou, M. (1971). Vertical distribution, diurnal and seasonal migration of copepods in Saronic Bay, Greece. *Marine Biology*, 9(2):92–98.

Ohman, M. D. (1990). The Demographic Benefits of Diel Vertical Migration by Zooplankton. *Ecological Monographs*, 60(3):257–281.

Ohman, M. D., Frost, B. W., and Cohen, E. B. (1983). Reverse diel vertical migration: An escape from invertebrate predators. *Science*, 220(4604):1404–1407.

Ohman, M. D. and Romagnan, J.-B. (2016). Nonlinear effects of body size and optical attenuation on Diel Vertical Migration by zooplankton. *Limnology and Oceanography*, 61(2):765–770.

Petrik, C. M., Stock, C. A., Andersen, K. H., van Denderen, P. D., and Watson, J. R. (2019). Bottom-up drivers of global patterns of demersal, forage, and pelagic fishes. *Progress in Oceanography*, 176(June):102124.

Pinti, J. and Visser, A. W. (2019). Predator-Prey Games in Multiple Habitats Reveal Mixed Strategies in Diel Vertical Migration. *The American Naturalist*, 193(3):E000–E000.

Proud, R., Cox, M. J., Handegard, N. O., Kloser, R. J., and Brierley, A. S. (2018). From siphonophores to deep scattering layers: an estimation of global mesopelagic fish biomass. *ICES Journal of Marine Science*, (May).

Sainmont, J., Thygesen, U. H., and Visser, A. W. (2013). Diel vertical migration arising in a habitat selection game. *Theoretical Ecology*, 6(2):241–251.

Sardou, J., Etienne, M., and Andersen, V. (1996). Seasonal abundance and vertical distributions of macroplankton and micronekton in the Northwestern Mediterranean Sea. *Oceanologica acta*, 19(6):645–656.

Siegel, D. A., Buesseler, K. O., Doney, S. C., Sailley, S. F., Behrenfeld, M. J., and Boyd, P. W. (2014). Global assessment of ocean carbon export by combining satellite observations and food-web models. *Global Biogeochemical Cycles*, 28(3):181–196.

Stock, C. A., John, J. G., Rykaczewski, R. R., Asch, R. G., Cheung, W. W., Dunne, J. P., Friedland, K. D., Lam, V. W., Sarmiento, J. L., and Watson, R. A. (2017). Reconciling fisheries catch and ocean productivity. *Proceedings of the National Academy of Sciences of the United States of America*, 114(8):E1441–E1449.

Varpe, Ø., Jørgensen, C., Tarling, G. A., and Fiksen, Ø. (2007). Early is better: Seasonal egg fitness and timing of reproduction in a zooplankton life-history model. *Oikos*, 116(8):1331–1342.

CHAPTER 5

Discussion and perspectives

This thesis evolves around two main topics, behavioural ecology and game theory, linked together by the mechanistic study of diel vertical migration. In this thesis, I demonstrate that game theory can be used to compute optimal DVM patterns of marine organisms (chapters 6 and 7), and that it is important to consider the interplay between different trophic levels to understand how various patterns can arise in the pelagic (chapter 8). I use these results to investigate an important question in global biogeochemical cycles: what is the importance of fish to the global carbon pump? My results indicate that fish, especially forage fish and mesopelagic fish, are more important than previously believed (chapter 9). In addition to these findings, my work opens up possibilities for future research and raises further ecological questions.

5.1 Optimality of DVM and game theory

Many modelling studies use the preferendum hypothesis (organisms reside around a preferred light level – see section 2.2.2.1) to derive the depth of the deep scattering layer (Aumont et al., 2018), sometimes modulating it with oxygen levels (Archibald et al., 2019). Aksnes et al. (2017) showed that globally, organisms remain at light levels $\sim 10^{-7}$ W/m^2 during daytime, while Aumont et al. (2018) selected a preferred light level of 10^{-4} W/m^2 and Archibald et al. (2019) a light level of 10^{-3} W/m^2. If there is no doubt that predation pressure is a secondary factor modifying DVM after illumination (Dickson, 1972; Langbehn et al., 2019), there is still debate on whether it can be completely ignored. The previously mentioned global studies of DVM ignore predation (Aumont et al., 2018; Archibald et al., 2019), whereas this thesis considers this factor explicitly. The validity of this simplification probably depends on the accuracy with which we want to model the system, and on the variability of the other factors in the ecosystem in focus. For example, light levels alone would not explain how multiple behaviours can emerge in a single system (Ohman and Romagnan, 2016).

Another question related to these considerations is whether individual organisms actually react to changes in environmental cues (such as temperature or predator levels), and if so, how fast they can respond to such changes. Considering DVM to be a behaviour implies that individual DVM patterns can be altered more or less rapidly, and potentially only temporarily. The plasticity of DVM at the community level is now well documented (Kampa, 1975; Frank and Widder, 2002; Godø et al., 2014), but as far

as I know the last studies of DVM at the individual level date back from the 90s, and left many unanswered questions (see section 2.2.2.2). Further experimental investigations of the adaptation capacity and adaptation speed of zooplankton **individuals** (and fish individuals, even if it is technically harder to implement) to changes in external cues would be interesting. In particular, the recent development of an automated hydrodynamic trademill – a water-filled hamster wheel designed for zooplankton[1] – enables unlimited vertical tracking of planktonic organisms (Krishnamurthy et al., 2020). Varying external stimuli while tracking single organisms has the potential to reveal many hidden drivers of vertical migration at the individual level, and to verify directly if single organisms behave optimally.

On a technical level, the method used throughout this thesis to find the Nash equilibrium of a system is the replicator equation (Hofbauer and Sigmund, 2003). However, this method has many pitfalls that limits its widespread application in ecology. First, nothing guarantees that the replicator equation will converge to a Nash equilibrium, and different initial conditions may lead to different Nash equilibria. Throughout this thesis, however, only a single Nash equilibrium was found for each system – though in some instances (chapter 8) the replicator equation reached limit cycles around the equilibrium and not a strict equilibrium. Second, the replicator equation is an inefficient algorithm to run, especially when many players are involved (for example, a single simulation in chapter 8 took around 24 hours to converge) or when it is coupled with population dynamics as in chapter 7. Another method that deserves consideration for game theoretic approaches is **mid-field games** (Lasry and Lions, 2007). In short, mid-field games consider that the optimal strategies depend on the behaviour of the entire community and not on the behaviour of all other players, simplifying the problem when many players are considered compared to game theoretic approaches looking for Nash equilibria. An example of mid-field games used to study the behaviour of a prey and a predator can be found in Thygesen and Patterson (2018), and I believe that this kind of approach will develop in the future, enabling for example better temporal resolution.

5.2 The active biological pump

My last chapter (chapter 9) builds on the results of my previous chapters and investigates in detail one of the most important ecosystem functions related to diel vertical migrations, active carbon export. I do not only consider how much carbon sinks below an arbitrary depth, but I take into account global ocean circulation to understand how much carbon can be sequestered in the oceans (DeVries and Primeau, 2011; DeVries, 2014). For example, carbon sinking close to an upwelling area may resurface very quickly and not be stored very efficiently, and carbon sinking in a

[1] To be precise, the first apparatus of this kind is more than 60 years old (Hardy and Bainbridge, 1954). At that time, organisms had to be visually and manually tracked, making the experiment itself very cumbersome and difficult to carry on for more than a few hours.

downwelling area may be sequestered for a very long time. I think that the **amount of carbon sequestered** is a better indicator of the efficiency of the global biological pump than an export flux (often reported at an arbitrary depth, Buesseler et al. (2020)), and it would be beneficial to generalize its systematic use in future global modelling studies. This carbon sequestered is the dynamic storage due to the pump in focus, i.e. the amount of carbon that would ultimately be released in the atmosphere should this pump be stopped.

I consider **oxygen levels** in the last chapter of this thesis only, even though it was recognized as a more important factor than light levels to predict deep scattering layer depths (Bianchi et al., 2013). Modelling mechanistically the interplay between temperature and oxygen levels proved difficult, especially because of the lack of data. A better mechanistic understanding of how different species / functional groups react to changes in temperature and oxygen conditions simultaneously is important if we want to model water columns precisely. More precisely, this will help resolve the impacts of climate change on the biological pump – oxygen minimum zones are anticipated to be a driving force in shaping deep scattering layer depths in the future (Bianchi et al., 2013; Netburn and Koslow, 2015).

My work suggests that carbon export mediated by a functional group scales almost linearly with the biomass of that group. Refining **global biomass estimates** of several functional groups (e.g. mesopelagic fish and jellyfish) would immediately refine carbon export estimates. In particular, the biomass of gelatinous organisms is still very weakly constrained. Another factor to consider with gelatinous organisms is their large spatial and temporal variability. Jelly **blooms** can export a significant amount of carbon to the seafloor, but due to their limited spatial and temporal occurrence they are rarely recorded in the field (Luo et al., 2020). Gelatinous organisms form a wide paraphyletic group encompassing, among others, cnidarians, ctenophores and tunicates (including appendicularians and salps). Tunicates feed on very small organisms for their size with a very high clearance rate and create fast sinking fecal pellets. During blooms, they can completely dominate the particulate flux (Smith et al., 2014; Stone and Steinberg, 2016). A good understanding and modelling capacity of these bloom events is necessary to unravel the importance of gelatinous organisms to the carbon pump.

Finally, my global study (chapter 9) was limited to annual averages of behaviour in temperate and tropical areas. Better estimates of DVM patterns and of carbon export fluxes would require the consideration of seasonal patterns, but also the inclusion of polar areas. Both these issues are related to my fitness definition: I only use myopic rules (Sainmont et al., 2015), whereas organisms living in **seasonal environments** require the inclusion of life-history events. Annual routines are now very well described in one player optimization models (Fiksen and Carlotti, 1998; Varpe et al., 2007), but have to my knowledge not been considered in multi-player (game theoretic) approaches yet. Considering the annual routine of organisms in my game theoretic framework is possible in theory, but the computing power required for such a project makes it unrealistic in practice. The advance of more efficient methods may allow the inclusion of annual routines in game theoretic models.

In a world with constantly increasing anthropogenic pressures on marine ecosystems, understanding the functioning of pelagic ecosystems and the services they provide is key to motivate their adequate management and conservation. As such, this thesis provides a framework with which the consequences of trophic interactions on the vertical structure of pelagic food-webs can be investigated, and provides a first global estimate of the importance of fish (and, in particular, mesopelagic fish) for the biological carbon pump. Estimating how global change will affect the biological carbon pump and other ecosystem functions in the pelagic is an important question for future ecological research.

Bibliography

Aksnes, D. L., Røstad, A., Kaartvedt, S., Martinez, U., Duarte, C. M., and Irigoien, X. (2017). Light penetration structures the deep acoustic scattering layers in the global ocean. *Science Advances*, 3(5):1–6.

Archibald, K. M., Siegel, D. A., and Doney, S. C. (2019). Modeling the impact of zooplankton diel vertical migration on the carbon export flux of the biological pump. *Global Biogeochemical Cycles*.

Aumont, O., Maury, O., Lefort, S., and Bopp, L. (2018). Evaluating the potential impacts of the diurnal vertical migration by marine organisms on marine biogeochemistry. *Global Biogeochemical Cycles*, pages 1–22.

Bianchi, D., Galbraith, E. D., Carozza, D. A., Mislan, K. A. S., and Stock, C. A. (2013). Intensification of open-ocean oxygen depletion by vertically migrating animals. *Nature Geoscience*, 6(7):545–548.

Buesseler, K. O., Boyd, P. W., Black, E. E., and Siegel, D. A. (2020). Metrics that matter for assessing the ocean biological carbon pump. *Proceedings of the National Academy of Sciences*, 117(18):201918114.

DeVries, T. (2014). The oceanic anthropogenic CO2 sink: Storage, air-sea fluxes, and transports over the industrial era. *Global Biogeochemical Cycles*, 28(7):631–647.

DeVries, T. and Primeau, F. (2011). Dynamically and observationally constrained estimates of water-mass distributions and ages in the global ocean. *Journal of Physical Oceanography*, 41(12):2381–2401.

Dickson, R. R. (1972). On the relationship between ocean transparency and the depth of sonic scattering layers in the north atlantic. *ICES Journal of Marine Science*, 34(3):416–422.

Fiksen, Ø. and Carlotti, F. (1998). A model of optimal life history and diel vertical migration in Calanus finmarchicus. *Sarsia*, 83:129–147.

Frank, T. M. and Widder, E. A. (2002). Effects of a decrease in downwelling irradiance on the daytime vertical distribution patterns of zooplankton and micronekton. *Marine Biology*, 140(6):1181–1193.

Godø, O. R., Macaulay, G. J., Kaartvedt, S., Johnsen, E., Handegard, N. O., Browman, H. I., Huse, G., Giske, J., and Ona, E. (2014). Marine ecosystem acoustics (MEA): quantifying processes in the sea at the spatio-temporal scales on which they occur. *ICES Journal of Marine Science*, 71(8):2357–2369.

Hardy, A. C. and Bainbridge, R. (1954). Experimental observations on the vertical migrations of plankton animals. *Journal of the Marine Biological Association of the United Kingdom*, 33(2):409–448.

Hofbauer, J. and Sigmund, K. (2003). Evolutionary Game Dynamics. *Bulletin (New Series) of the American mathematical society*, 40(403):479–519.

Kampa, E. M. (1975). Observations of a sonic-scattering layer during the total solar eclipse 30 June, 1973. *Deep-Sea Research and Oceanographic Abstracts*, 22(6).

Krishnamurthy, D., Li, H., Benoit du Rey, F., Cambournac, P., Larson, A. G., Li, E., and Prakash, M. (2020). Scale-free vertical tracking microscopy. *Nature Methods*.

Langbehn, T., Aksnes, D., Kaartvedt, S., Fiksen, Ø., and Jørgensen, C. (2019). Light comfort zone in a mesopelagic fish emerges from adaptive behaviour along a latitudinal gradient. *Marine Ecology Progress Series*, 623:161–174.

Lasry, J. M. and Lions, P. L. (2007). Mean field games. *Japanese Journal of Mathematics*, 2(1):229–260.

Luo, J. Y., Condon, R. H., Stock, C. A., Duarte, C. M., Lucas, C. H., Pitt, K. A., and Cowen, R. (2020). Gelatinous zooplankton-mediated carbon flows in the global oceans: a data-driven modeling study. *Global Biogeochemical Cycles*, 34(e2020GB006704).

Netburn, A. N. and Koslow, J. A. (2015). Dissolved oxygen as a constraint on daytime deep scattering layer depth in the southern California current ecosystem. *Deep-Sea Research Part I*, 104:149–158.

Ohman, M. D. and Romagnan, J.-B. (2016). Nonlinear effects of body size and optical attenuation on Diel Vertical Migration by zooplankton. *Limnology and Oceanography*, 61(2):765–770.

Sainmont, J., Andersen, K. H., Thygesen, U. H., Fiksen, Ø., and Visser, A. W. (2015). An effective algorithm for approximating adaptive behavior in seasonal environments. *Ecological Modelling*, 311:20–30.

Smith, K. L., Sherman, A. D., Huffard, C. L., McGill, P. R., Henthorn, R., Von Thun, S., Ruhl, H. A., Kahru, M., and Ohman, M. D. (2014). Large salp bloom export from the upper ocean and benthic community response in the abyssal northeast Pacific: Day to week resolution. *Limnology and Oceanography*, 59(3):745–757.

Stone, J. P. and Steinberg, D. K. (2016). Salp contributions to vertical carbon flux in the Sargasso Sea. *Deep-Sea Research Part I: Oceanographic Research Papers*, 113:90–100.

Thygesen, U. H. and Patterson, T. A. (2018). Oceanic diel vertical migrations arising from a predator-prey game. *Theoretical Ecology*, pages 1–13.

Varpe, Ø., Jørgensen, C., Tarling, G. A., and Fiksen, Ø. (2007). Early is better: Seasonal egg fitness and timing of reproduction in a zooplankton life-history model. *Oikos*, 116(8):1331–1342.

CHAPTER 6

Predator prey games in multiple habitats reveal mixed strategies in diel vertical migration

Pinti J., Visser A.W. (2019) The American Naturalist 193(3):E65-E77.

The American Naturalist

Abstract

Prey and predators continuously react to each other and to their environment, adjusting their behaviour to maximize their fitness. In a pelagic environment, organisms can optimize their fitness by performing diel vertical migrations (DVM). We applied a game theoretic approach to investigate the emergent patterns of optimal habitat selection strategies in a multiple habitat arena. Our set-up allows both players to choose their position at day and at night in the water column. The model reproduces features of vertical migrations observed in nature, including residency at depth or at the surface, vertical migrations, mixed strategies and bimodal distributions within a population. The mixed strategies appear as a consequence of frequency-dependent processes and not of any intra-species difference between individuals. The model also reveals a curious feature, where natural selection on individuals can provoke distinct regime shifts and precipitate an irreversible collapse in fitness. In the case presented here, the increasing voracity of the predator triggers a behavioural shift in the prey reducing the fitness of all members of the predator population.

Keywords— Diel Vertical Migration, Game theory, Habitat selection, Predator-prey interactions, Deep scattering layer, Optimal strategies.

6.1 Introduction

Diel vertical migration (DVM) is a behaviour exhibited by a large number of marine species from plankton to marine mammals. The most conspicuous of these are the migrations carried out by mesopelagic fish (O'Driscoll et al., 2009; Dypvik et al., 2012), krill (Onsrud et al., 2004; Zhou and Dorland, 2004), copepods (McLaren, 1963; Frost and Bollens, 1992; Hays et al., 2001) and jellyfish (Kaartvedt et al., 2007). These migrations are particularly evident in the daily variations in the depth of the deep scattering layer (Barham, 1966; Isaacs et al., 1974), the signature of aggregations of acoustically reflective marine organisms which typically alternate between a surface layer during night time and a deeper layer during day light hours. While deep scattering layers are ubiquitous features of the world's oceans, the patterns they exhibit vary considerably from place to place and over seasons (Plueddemann and Pinkel, 1989; Klevjer et al., 2016). There are, for instance, large variations in the depth of the deep, daylight layer — from a few dozens to several hundred meters. Further, there is seldom a single well-defined scattering layer and a wide variety of daily patterns is observed. There can for instance be multiple strata displaying different vertical cycles, double layers that remain resident near surface and at depth with daily exchange, layers that disperse and re-aggregate, and any number of combinations of these. With the advent of more advanced acoustics that are able to track individual organisms (Kaartvedt et al., 2007, 2008), the picture becomes even more complex, with individuals of apparently the same species displaying quite different behaviours. While these patterns are of interest in themselves and the trophic interactions they mediate (Bollens et al., 2011), they also contribute to the biological pump and have

an important consequence for the biogeochemistry of the world's oceans (Longhurst and Harrison, 1989; Steinberg et al., 2000; Bianchi et al., 2013). Vertically migrating organisms actively transport organic carbon out of the surface ocean, often to depths of 100 m or more, where it is respired and excreted by the migrator itself, or consumed by their predators – giving rise to a drawdown of carbon from the surface ocean (Ducklow et al., 2001; Hansen and Visser, 2016), an associated depletion of surface nutrients (Dam et al., 1995; Steinberg et al., 2002) and a depletion of subsurface oxygen (Bianchi et al., 2013). The importance of DVM in ocean biogeochemistry stems in part from the sheer numbers of organisms involved. In particular, that these patterns show up in acoustic profiles indicates that a significant fraction of the pelagic biomass is involved. Indeed, it has been estimated that the vertical migration of zooplankton constitutes one of the largest mass movements of biomass on earth (Hays, 2003). The daily cycles in the distribution of biomass into different depth strata of the oceans, the mechanisms which drive this partitioning and how they are affected by biotic and abiotic factors is thus a question of some relevance for the carbon, nutrient and oxygen dynamics of the ocean.

As with many phenomena in behavioural ecology, the imperative for DVM can be seen in a fitness trade-off between growth and mortality risk (Lima and Dill, 1990). For zooplankton grazers, this is a balance between feeding at the surface on their phytoplankton prey and avoiding the attention of visual predators. The optimal strategy is thus to feed in the surface at night and take refuge at depth during the day (Zaret and Suffern, 1976) where the cost of migration and lost growth potential are offset by increased survivorship. Different patterns can in part be explained by different zooplankton species, for each of which migration contributes to their fitness trade-off in a somewhat different way (Stich and Lampert, 1981).

The predators that in some sense provoke the migration of grazers, have in turn their own imperatives to optimize fitness; they can follow their prey or not, or adopt some other distinct migration pattern depending for instance on water clarity, competition with non-visual predators, and their own mortality risk. This triggers a cascade of interlinked migration patterns throughout the food web (Bollens et al., 2011). Indeed, seen in this light, it becomes evident that in a predator-prey system, the optimal choice of strategy for one affects the optimal choice of strategy for the other (Hugie and Dill, 1994) and vice versa. That is, there is a game of strategies being played out between predators and prey that ultimately shapes the patterns of DVM that emerge in nature.

In ecology, game theory has been used widely to describe everything from sex ratios (Fisher, 1930; Maynard Smith, 1976) to distribution of competitors (Sih, 1998; Cressman et al., 2004) and social arrangements (Reeve and Holldobler, 2007). In this work, we extend predator-prey game from a two habitats arena (Iwasa, 1982; Gabriel and Thomas, 1988; Sainmont et al., 2013) into a multiple habitat arena in which prey and predators can adjust their position in a water column divided into several layers, and are not just obliged to choose between the surface and some deep habitat. This radically increases the number of potential competing strategies.

In addition to implications for the biogeochemistry of the oceans, the multiple habitat

arena also allows us to capture the vertical variability of the proximate causes of DVM, namely food availability and light intensity. In particular, the trade-off will be different in different depth strata even without frequency dependence.

6.2 Methods

We consider two populations of fixed size: one of prey (N) and one of predators (P). These populations live in a water column divided into M layers of Δz [m] thickness, ordered from the shallowest to the deepest. Each organism is free to move within the water column. To illustrate the model, we cast it in terms of zooplankton grazers as prey and planktivorous fish as predators. The fish rely on vision, and thus light, to locate their zooplankton prey. The resources for prey are located in the surface simulating phytoplankton. This setting is one of the most common in the pelagic ocean, but it should be noted that the method outlined here can be tailored to any trophic arrangement given suitable mechanistic descriptions of the growth, interaction and mortality terms.
We define the matrices $\mathbf{n} = n_{ij}$ and $\mathbf{p} = p_{ij}$ as the frequency of ij strategies in prey and predator populations respectively; i.e. the strategy in which the individual chooses its daytime position in layer j and its night time position in layer i. By definition, n_{ij} and p_{ij} conform to the identities

$$\begin{aligned} \sum_{i=1}^{M}\sum_{j=1}^{M} n_{ij} &= 1, \\ \sum_{i=1}^{M}\sum_{j=1}^{M} p_{ij} &= 1. \end{aligned} \tag{6.1}$$

In terms of abundance, if we write N_0 $[m^{-3}]$ and P_0 $[m^{-3}]$ the mean concentration of prey and predators throughout the water column, then the prey and predator concentration in layer i at night time is

$$\begin{aligned} N_{i,night} &= MN_0 \sum_{j=1}^{M} n_{ij}, \\ P_{i,night} &= MP_0 \sum_{j=1}^{M} p_{ij}, \end{aligned} \tag{6.2}$$

with similar expressions for the day time concentrations.
Time wise, the day is divided between a fraction σ of daylight hours, and a fraction $1-\sigma$ of darkness, neglecting the periods of dawn and dusk. The general depth varying factors governing the fitness of individuals in the respective populations are the potential growth rate of the prey, and the mortality risk posed by the predators. Depth variations in potential prey growth rates reflect for instance the vertical distribution of phytoplankton food resource, or temperature. For convenience, we write individual

growth rate as $g'(z) = g_{max}g(z)$ [day^{-1}] where $g(z)$ is a dimensionless function indicating the depth structure, and g_{max} [day^{-1}] is the maximum growth rate that can vary depending on temperature and resource (phytoplankton) abundance.
The ability of the visual predator to detect prey depends on light intensity $L(z,t)$ [W m^{-2}] equal to $L_{max}\exp(-\kappa z)$ during daytime and $\rho L_{max}\exp(-\kappa z)$ during nighttime. We assume a uniform extinction coefficient κ [m^{-1}]. We note that the factor ρ is not necessarily 0, as illumination by moonlight can be significant for visual predators (Bollens and Frost, 1991; Webster et al., 2013). The clearance rate β [m^3 s^{-1}] of the predator is defined to mimic a saturation condition at high light intensities (Aksnes and Utne, 1997; Titelman and Fiksen, 2004; Bianchi et al., 2013). Defining the constant b_{max} [m^3 day^{-1}] allows us to write the clearance rates as $\beta_{day} = b_{max}b_{day}(z)$ and $\beta_{night} = b_{max}b_{night}(z)$, where b_{day} and b_{night} are two dimensionless functions given by

$$\begin{aligned} b_{day}(z) &= \frac{L_{max}\exp(-\kappa z)}{L_0+L_{max}\exp(-\kappa z)}, \\ b_{night}(z) &= \frac{\rho L_{max}\exp(-\kappa z)}{L_0+\rho L_{max}\exp(-\kappa z)}, \end{aligned} \tag{6.3}$$

where L_0 [Wm^{-2}] is the half saturation light intensity.
The fitness of a specific strategy ij is defined as the difference between the specific growth rate and the potential mortality rate that an organism is exposed to over a daily cycle. For migrating animals, an extra term modelling the cost of migration is added. For simplicity, we assume feeding interactions to follow a type I (linear) functional response, as in the natural environment, organisms are generally under saturated in food supply (Kiørboe, 2011).
For the prey, net growth for strategy ij is

$$G_{ij}^N = g_{max}((1-\sigma)g_i + \sigma g_j) - c_N\delta_{ij}, \tag{6.4}$$

where the net migration cost is assumed to be a linear function of the migration distance, with c_N the cost to migrate $1m$ and $\delta_{ij} = \Delta z|i-j|$.
For this strategy, the corresponding mortality risk from visual predators is proportional to the probability (i.e. sum of frequencies) of predators being in the same layer at the same time:

$$\begin{aligned} D_{ij}^N &= (1-\sigma)\beta(i,night)P_{i,night} + \sigma\beta(j,day)P_{j,day} \\ &= b_{max}MP_0((1-\sigma)b_{night,i}\sum_{k=1}^{M}p_{ik} + \sigma b_{day,j}\sum_{k=1}^{M}p_{kj}). \end{aligned} \tag{6.5}$$

Mortality risk for prey is conversely a component of the potential growth rate for the predator. For the strategy ij, this growth rate can be written

$$G_{ij}^P = b_{max}\eta MN_0((1-\sigma)b_{night,i}\sum_{k=1}^{M}n_{ik} + \sigma b_{day,j}\sum_{k=1}^{M}n_{kj}) - c_P\delta_{ij}. \tag{6.6}$$

In this, η represents the conversion efficiency – how much a single prey contributes to the reproduction rate of a predator. As with prey, we include a cost of migration proportional to migration distance. Finally, for closure, we require a mortality risk for predators. We choose a density dependent function to reflect reduced fitness at high abundances, to mimic possible interference with each other and attraction of top predators at high concentration (Hixon and Carr, 1997):

$$D_{ij}^{P} = \mu M P_0((1-\sigma)\sum_{k=1}^{M} p_{ik} + \sigma \sum_{k=1}^{M} p_{kj}). \tag{6.7}$$

In summary, the fitness of prey and predator following strategy ij are

$$\begin{aligned} F_{ij}^{N}(\mathbf{p}) = \quad & g_{max}((1-\sigma)g_i + \sigma g_j) - c_N \delta_{ij} \\ & -b_{max} M P_0((1-\sigma) b_{night,i} \sum_{k=1}^{M} p_{ik} + \sigma b_{day,j} \sum_{k=1}^{M} p_{kj}), \end{aligned} \tag{6.8}$$

$$\begin{aligned} F_{ij}^{P}(\mathbf{n},\mathbf{p}) = \quad & b_{max}\eta M N_0((1-\sigma) b_{night,i} \sum_{k=1}^{M} n_{ik} + \sigma b_{day,j} \sum_{k=1}^{M} n_{kj}) - c_P \delta_{ij} \\ & -\mu M P_0((1-\sigma) \sum_{k=1}^{M} p_{ik} + \sigma \sum_{k=1}^{M} p_{kj}). \end{aligned} \tag{6.9}$$

These fitness functions describe a non-cooperative game, where all individuals within each population are trying to maximize their fitness. This game is solved when a Nash equilibrium is reached which means no organism has an advantage in unilaterally changing its strategy. In such a solution, only a subset of all strategies might be populated (i.e. those for which $n_{ij} > 0$ and $p_{ij} > 0$), and at equilibrium, all populated strategies within the prey and predator populations will have identical fitness

$$F_{ij}^{N}(\mathbf{p}) = F_0^N \text{ for all } n_{ij} > 0 \text{ and } F_{ij}^{P}(\mathbf{n},\mathbf{p}) = F_0^P \text{ for all } p_{ij} > 0, \tag{6.10}$$

while all unpopulated strategies will have inferior fitness

$$F_{ij}^{N}(\mathbf{p}) \leq F_0^N \text{ for all } n_{ij} = 0 \text{ and } F_{ij}^{P}(\mathbf{n},\mathbf{p}) \leq F_0^P \text{ for all } p_{ij} = 0. \tag{6.11}$$

The system has polymorphic-monomorphic equivalency (Broom and Rychtář, 2014) discussed further in section 6.6. That is, the matrices $\mathbf{n}$ and $\mathbf{p}$ denote the frequency distribution of strategies but are mute on how these distributions arise; either in terms of different proportions of the population playing pure strategies (polymorphic), or all individuals playing the same mixed strategy (monomorphic) or indeed some combination of these two extremes. Any individual playing against resident ($\mathbf{n}$,$\mathbf{p}$) is indifferent to whether these represent polymorphic or monomorphic strategies.
We find the Nash equilibrium of the system numerically by solving the replicator equation (Schuster and Siegmund, 1983; Hofbauer and Sigmund, 2003). Essentially,

each subpopulation of strategy ij is allowed to grow according to its growth rate (i.e. fitness) before renormalization to satisfy constraint 6.1. For details, see supplementary material section 6.6. In general, not all situations solved with replicator dynamics lead to a steady state solution. In this particular case, all simulations of the replicator dynamics converged to a stable equilibrium. We ensured this by iterating over a large number of time steps (typically 10^6) and different initial conditions, and assessed stability by estimating the variance in fitness and strategies.
The MATLAB code to run the examples discussed is deposited in the Dryad Digital Repository: http://doi.org/10.5061/dryad.19n37d1 (Pinti and Visser, 2018).

Table 6.1: Glossary of parameters. Values and equations were taken from the literature: detection distance (Bianchi et al., 2013), light-related parameters (Aksnes and Utne, 1997), maximum growth rate (Hirst and Sheader, 1997), and copepod rates and costs (Titelman and Fiksen, 2004; Visser, 2007).

Variable	**Description**	**Value (default)**	**Unit**
b_{max}	Absolute maximum clearance rate (voracity) of predator	10^{-2} to 100	$m^3\ day^{-1}$
g_{max}	Maximum growth rate of prey	0.1	day^{-1}
N_0	Average concentration of prey in water column	5000	m^{-3}
P_0	Average concentration of predator in water column	1	m^{-3}
M	Number of depth bins, leading to M^2 different pure strategies per trophic level	30	-
β	Clearance rate of predator	-	$m^3\ day^{-1}$
$b_{day}(z)$ $b_{night}(z)$	Vertical structure function for maximum clearance rate of predator at day and night	eq. 6.3	-
$g(z)$	Vertical structure function for maximum growth rate of prey	eq. 6.12	-
L	Light intensity at depth z and time t	-	$W\ m^{-2}$
L_{max}	Typical light level at the surface during daylight hours	100	$W\ m^{-2}$
L_0	Half saturation level for visual predator	1	$W\ m^{-2}$
μ	Density dependent mortality rate of predators. If all predators are uniformly distributed throughout the water column, they each suffer a mortality of $\mu P_0\ day^{-1}$. If they are all concentrated into a single bin, they each suffer a mortality of $M\mu P_0\ day^{-1}$.	10^{-3}	$m^3\ day^{-1}$
c_N	The cost in terms of growth rate of migrating	10^{-5}	$m^{-1}\ day^{-1}$
c_P	1m for prey — same for predator	10^{-5}	
δ_{ij}	Migration distance for strategy ij	$\Delta z\|i-j\|$	m

Table 6.1 – continued from previous page

Variable	Description	Value	Unit
σ	Fraction of daylight hours per day	0 to 1	-
κ	Attenuation coefficient for light	0.07	m^{-1}
ρ	Fractional difference between night and day light levels	10^{-3}	-
η	Predator growth efficiency	10^{-2}	-
z	Depth coordinate	0 to 300	m
Δz	Thickness of depth bins	10	m
H	Depth of the water column	300	m
z_0	Depth of the mixed layer	50	m
z_s	Thickness of the mixed layer transition zone	10	m
G^N_{ij}, G^P_{ij}	Growth rate of prey (predator) following strategy ij	eq. 6.4 and 6.6	day^{-1}
D^N_{ij}, D^P_{ij}	Death rate of prey (predator) following strategy ij	eq. 6.5 and 6.7	day^{-1}

6.3 Results

We choose a set of parameters (Table 6.1) that are illustrative for a planktonic system of a zooplankton grazer (the prey) feeding on a phytoplankton resource, and preyed upon in turn by a visual predator such as a fish. The vertical variation in maximum prey growth rate is given by

$$g(z) = \frac{1}{2}(1 - \tanh(\frac{z - z_0}{z_s})), \tag{6.12}$$

where z_0 is the depth of the surface mixed layer (hence resource availability), and z_s is the thickness of the transition zone to a depleted deep layer (Ji and Franks, 2007). Figure 6.1 shows the vertical functional form of both the growth conditions as well as the predator clearance rate for both day and night conditions.

Maximum clearance rate

Among many of the governing parameters, both environmental and those determining trophic interactions and efficiency, one that can exhibit large variation in nature is the maximum clearance rate of the predator. This is a function not only of light and the visual acuity of the predator, but also the conspicuousness of the prey (is it pigmented, does it have a full gut, is it moving?), the swimming behaviour of the predator, as well as the escape ability of the prey. Figure 6.2 shows the change in predatory-prey strategies as a function of b_{max}, the maximum clearance rate of the predator, all other

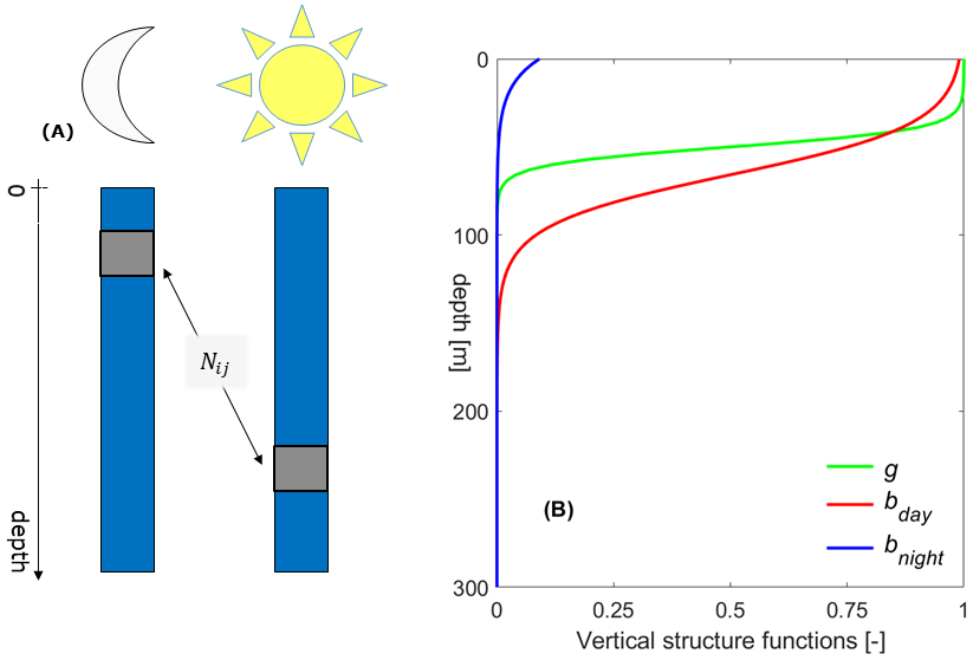

Figure 6.1: (A) Prey following the strategy ij will alternate between the layer i at night and the layer j during daytime. (B) The vertical structure function of the growth g (in green), of the clearance rate during daytime b_{day} (red) and during nighttime b_{night} (blue). A summary of the parameters used to plot these profiles is given in table 6.1.

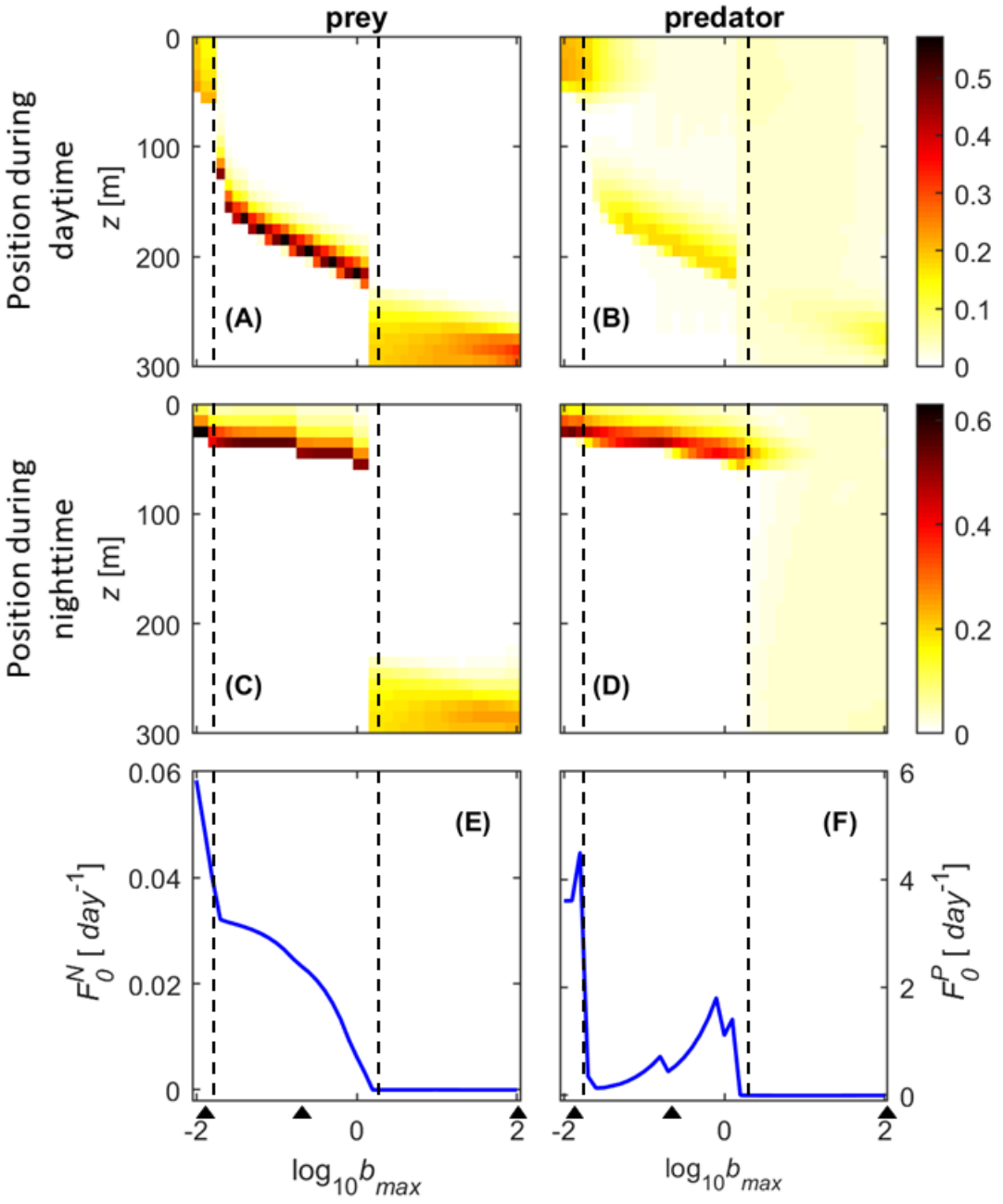

Figure 6.2: The vertical distribution of the prey during day (A) and night (C), and the corresponding distribution for predator during day (B) and night (D) for a range of predator maximum clearance rate b_{max} from 0.01 m^3 day^{-1} to 100 m^3 day^{-1}. Parameters values are set according to the values given in Table 6.1. The variation of fitness for the prey (E) and predator (F) as a function of the predator maximum clearance rate b_{max} corresponding to vertical distribution patterns given above. Small dark triangles show the value of b_{max} for which the strategy occupancy diagrams are plotted (figure 6.3). Dashed lines show the theoretical migration regime shifts.

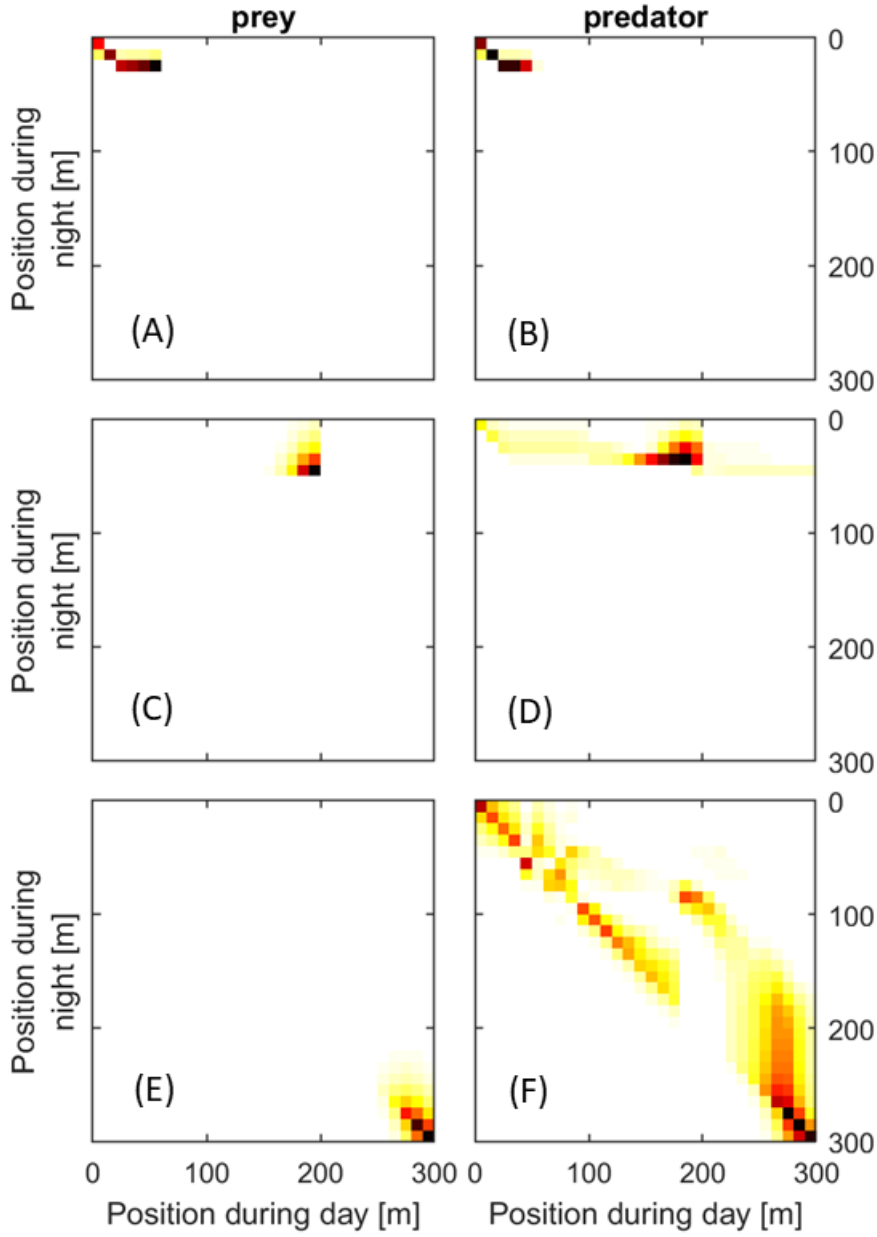

Figure 6.3: The strategy occupancy of prey (A, C and E) and predator (B, D and F) in the three different migration regimes. These examples are for the specific $b_{max} = 0.0126$ (A & B), $b_{max} = 0.1995$ (C & D) and $b_{max} = 100$ (E & F).

parameters being held constant. It shows three general patterns of strategies:
Strategy 1. For very low clearance rates ($b_{max} < 0.02$) essentially both predators and prey exhibit no significant DVM, and reside exclusively in the surface layer. They both alternate between a diffuse day-time distribution (figure 6.2 A & B) and are more concentrated during night time (figure 6.2 C & D). During this phase, the fitness of the prey decreases while that of the predator increases with increasing b_{max} (figure 6.2 E & F).
Strategy 2. For intermediate clearance rates ($0.02 < b_{max} < 1.6$) both prey and predators start to migrate alternating between a deep day time depth and a shallow night time depth. This pattern is most clear in the prey, where the whole population subscribes to DVM albeit to slightly different depths. For the predator though, while the major part of the population follows the prey between the surface and depth, there is a small fraction that remains resident in the surface, and another fraction that follows the prey at night, but chooses some intermediate depth during the day. This small fraction at intermediate depth is a consequence of the game, as it prevents prey remaining higher in the water column during daytime to "cheat". It would not be encountered in analysis without game theory. The depth of both the night time surface layer and the deep day time layer gradually deepen as b_{max} increases. In this phase, while the prey fitness (figure 6.2 E) continues to decrease with increasing b_{max}, it does so at a lower rate than when $b_{max} < 0.02$. The predator fitness (figure 6.2 F) suffers a significant decrease at the point where the prey start migrating. Thereafter, the predator maximum fitness increases again with increasing b_{max}.
Strategy 3. For large values of clearance rate ($b_{max} > 1.6$) prey and predators both essentially stop migrating, with prey retreating to a permanent residence at depth (figure 6.2 A & C), and predators becoming uniformly distributed in the water column throughout the day (figure 6.2 B & D). For this range of b_{max}, the maximum fitness for both prey and predator drops to zero (figure 6.2 E & F).
In Figure 6.3, we present the strategy occupancy of prey and predators in the three different migration regimes. These examples are for the specific $b_{max} = 0.0126\,\mathrm{m}^3\ \mathrm{day}^{-1}$ (figure 6.3 A & B), $b_{max} = 0.1995\,\mathrm{m}^3\ \mathrm{day}^{-1}$ (figure 6.3 C & D) and $b_{max} = 100\,\mathrm{m}^3\ \mathrm{day}^{-1}$ (figure 6.3 E & F). Although certain strategies are adopted by the majority of individuals, the full range of strategies for both predator and prey for which fitness is equal and maximized is quite extensive.
Transitions between different migrations regimes for prey can be estimated from simple theoretical considerations of migrations between a feeding and a resting layer, for example by calculating when the risk of remaining at the surface during daytime becomes greater than the net gain in growth (see section 6.6 for details). With the parameter set used here, this results in approximate migration regime shifts at thresholds $b_{max} = 0.0167\,\mathrm{m}^3\ \mathrm{day}^{-1}$ and $b_{max} = 2.7\,\mathrm{m}^3\ \mathrm{day}^{-1}$ which is consistent with the values observed in figure 6.2.

Day length

Day–night differences in light is a primary driver of DVM (Zaret and Suffern, 1976; Hays, 2003). Figure 6.4 illustrates the DVM strategies emerging for varying daytime fraction σ in this game. For most of the values of σ , results in terms of distribution during day and night in the water column change very little ($0.1 < \sigma < 0.9$); both prey and predator undertake regular DVM from the depth to the surface. However, the results are different for extreme values of σ. If σ is small (< 0.1), which means there is almost no daytime, prey stay at the surface all the time. As the risk of being preyed upon is very low and the resources maximum, it is not beneficial to migrate (figure 6.4 A & C). Predators also stay at the surface to catch prey where they are (figure 6.4 B & D). When the fraction of daytime is close to 1 (i.e. almost no night), prey stop migrating and spend all their time at depth, whereas predators distribute themselves evenly in the water column. This is a direct consequence of the fact that the players are distributed as to follow a Nash equilibrium; since there is plenty of light, predators would be able to catch any prey in the upper layers of the water column. The predators remove the possibilities for the prey to escape the game and be in more profitable water layers by being evenly distributed in the water column. This situation also corresponds to a minimum fitness for the prey, as the predator confines them at depths with the slower growth. The fitness of the prey decreases linearly as σ increases (figure 6.4 E); they are staying less and less at the surface, and therefore benefit less and less from the resources they can find there. The fitness of the predator also decreases linearly with the day length. When the day length increases, prey spend more time in the depth, and cannot be captured as easily as in the mixed layer, even at night. Indeed, this can be summarized from the ratio of predator clearance rates $b_{day}(200\,\mathrm{m}) \simeq 10^{-2} b_{night}(50\,\mathrm{m})$.

Seasonality

Daytime fraction σ alone is only one of several seasonally varying factors driving DVM. Additional factors include the maximum irradiance L_{max}, the mixed layer depth z_0, the maximum growth rate for the prey g_{max} and the average prey concentration in the water column N_0. We select typical patterns of the seasonal variation of these (Table 6.2) to illustrate the DVM patterns that emerge (Figure 6.5). From shallow DVM in the winter months, the DVM almost disappears in the summer where organisms are almost evenly scattered in the water column. This corresponds to a strong fitness minimum for both species.

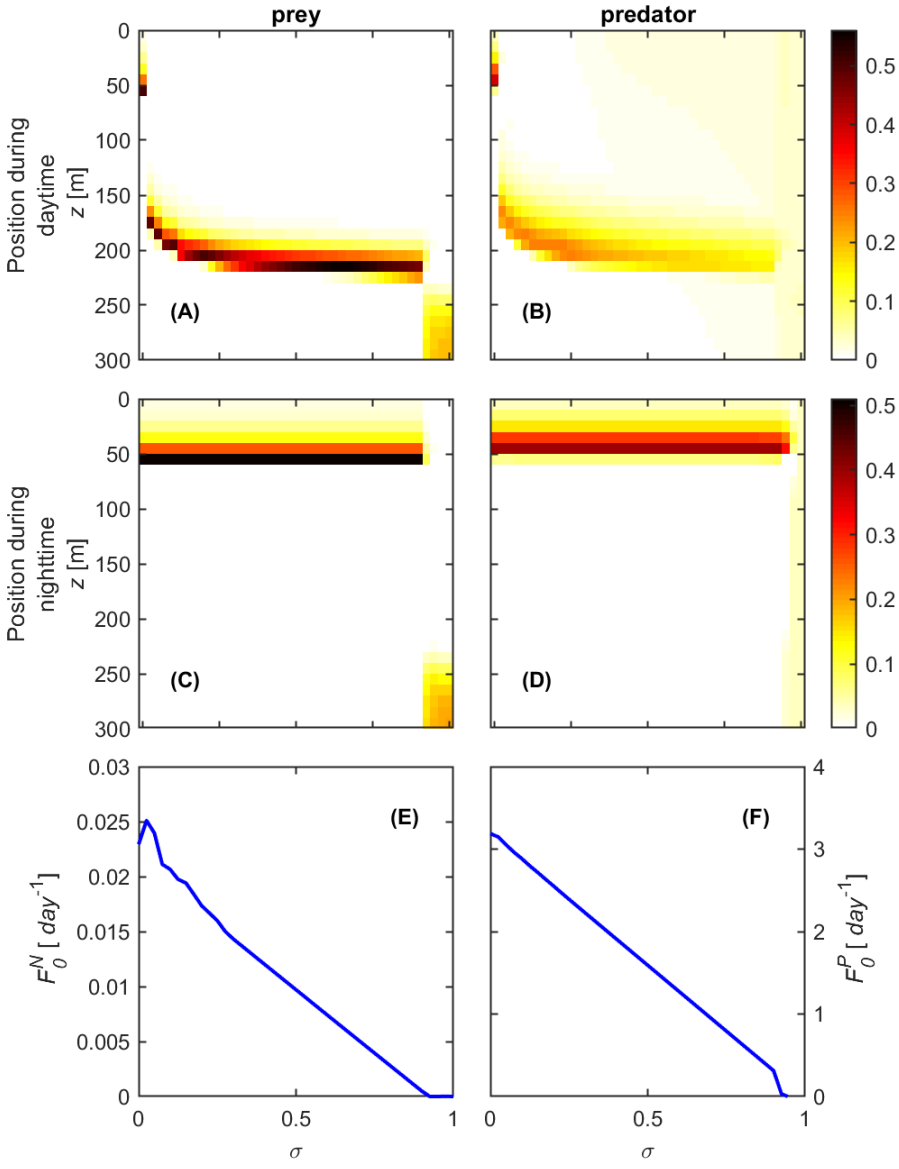

Figure 6.4: The vertical distribution of the prey during day (A) and night (C), the corresponding distribution for predator during day (B) and night (D), and the associated prey (E) and predator fitnesses (F) for a range of day light fractions σ from 0 (total 24 hour darkness) to 1 (total 24 hour light).

Table 6.2: Seasonal values of the parameters used to produce figure 6.5. Solar irradiance was calculated using the Solar Electricity Handbook (Boxwell, 2017), and other variables taken from literature: prey average concentration (Sardou et al., 1996), prey maximum growth rates and chlorophyll (Morel and André, 1991) and mixed layer depth (D'Ortenzio et al., 2005).

Parameter	Jan	Feb	Mar	Apr	May	Jun	Jul	Aug	Sep	Oct	Nov	Dec
σ [−]	0.39	0.44	0.50	0.56	0.61	0.64	0.63	0.58	0.52	0.46	0.40	0.37
L_{max} [W m^{-2}]	81.25	120.0	175.0	211.25	250.83	293.75	296.25	248.75	188.75	120.42	82.92	65.0
z_0 [m]	80	00	60	30	10	10	10	10	10	20	30	50
N_0 [m^{-3}]	33750	45000	12500	7500	2500	7500	1250	22500	2500	15000	11250	6250
g_{max} [day^{-1}]	0.35	0.35	0.63	0.88	1.0	0.63	0.55	0.55	0.55	0.63	0.5	0.5
L_0 [W m^{-2}]	0.5	0.5	0.5	0.5	0.5	0.5	0.5	0.5	0.5	0.5	0.5	0.5

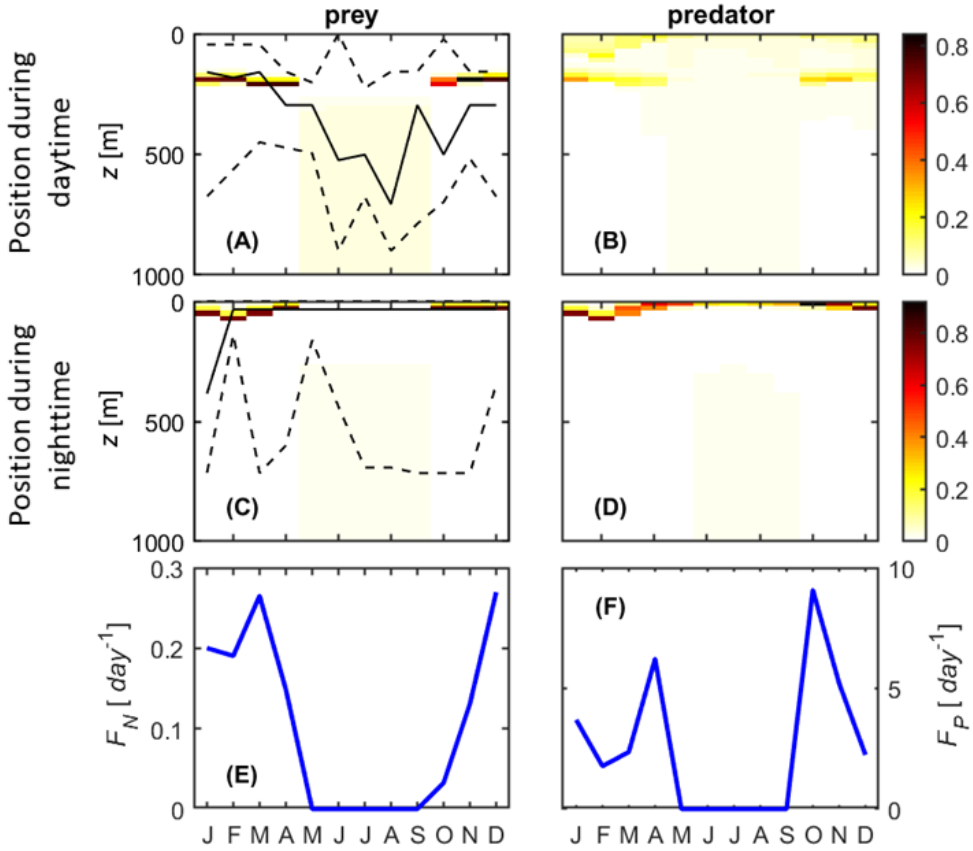

Figure 6.5: Variations in the vertical distribution of the prey during day (A) and night (C), the corresponding distribution for predator during day (B) and night (D), and the associated prey (E) and predator fitness (F) during an annual cycle. The full (resp. dashed) lines in (A) and (C) shows the mean (resp. minimum and maximum) observed depth of *Meganyctiphanes norvegica* (Sardou et al., 1996).

6.4 Discussion

Game theory as a way to investigate migration patterns

Our method based on game theory principles is effective as it can reproduce the main migration patterns observed in nature. Among all the known regimes of DVM (normal, residency, reverse migration), only reverse migration (i.e. surface at night, depth during the day) is not reproduced by our model; a migration pattern arising from additional trophic levels, or the presence of non-visual predators (Ohman, 1990). Moreover, the model reproduces the DVM patterns of both prey and predators, who can choose to follow their prey or not, depending on the ensuing benefit. To our knowledge, this is the first time that a model provides the distribution of two trophic levels in a multi-layered water column. Several models looked at DVM (Fiksen, 1995; Giske et al., 1997; De Robertis et al., 2000; Batchelder et al., 2002; Fiksen et al., 2005; Hansen and Visser, 2016), but only a game theoretic set-up enables consideration of the movements of two trophic layers (Fiksen et al., 2005). There exists some game theoretic set ups focusing on DVM, but either they considered the migration of only one trophic layer (Gabriel and Thomas, 1988), or they divided the water column in only two layers – namely surface and depth – (Iwasa, 1982; Sainmont et al., 2013) thus giving a very crude approximation of the positions and strategies of the players.

Mixed strategies emerge from frequency-dependent processes

Our model also illustrates the importance of frequency dependent processes as they drive the emergence of mixed strategies. That is, even though players within a population are identical, they display different strategies. The distribution of individuals amongst strategies ensures that all players within a population have identical fitness — the defection of any one player from a given strategy will invariably reduce its fitness. Indeed, this variation of strategies within a population has been observed, but are usually explained as state dependent (maturity, hunger) or as a manifestation of personality syndromes (boldness, aggression) (Ohman, 1990). We show here that mixed strategies are a feature of the underlying interactions, and are not due to a variability in trade-offs experienced by different members of populations. This is one of the strength of our approach, as these frequency dependent processes and thus mixed strategies cannot be addressed in a fixed environment with optimal fitness techniques based on simpler rules such as Gilliam's rule or even with more complex life history optimization (e.g. dynamic programming, but without a game theoretic approach).

Clearance rates and behaviour changes

The different migration regimes as a function of predator clearance rate demonstrated by our model can be validated from field findings. For instance, different clearance rates for predators can be related to prey size (reduced detectability of smallest prey, and thus reduced clearance (Aksnes and Utne, 1997)) so these results can be compared to observed size-dependent DVM patterns (Ohman and Romagnan, 2016). Indeed,

observed size-dependent DVM patterns (Sardou et al., 1996) indicate that intermediate sized prey exhibit the largest migration amplitude while small prey remain resident in the surface and large prey remain resident at depth. While other factors can be involved, this pattern is entirely consistent with our model results where size can be equated with clearance rate.
Clearance rate can also be influenced by the predator's visual range and hence changes in water turbidity. Observations of the vertical movement of marine organisms in response to an inflow of turbid water (Frank and Widder, 2002) showed that smaller organism (small euphausiids) migrated upward, whereas larger organisms (large euphausiids, salps, myctophids) did not change their distribution. As for observed size-dependent patterns (Ohman and Romagnan, 2016), this is consistent with an upward migration in response to a decrease in risk whereas larger organisms with a relatively smaller decrease in risk did not change their behaviour. While empirically this behaviour can be related to organisms following a specific isolume (Schmitz et al., 2004), the functional rationale can be posited in terms of reduced risk for which irradiance serves as a easily sensed proxy. In a similar manner, different migration patterns of the krill *Meganyctiphanes norvegica* in different Norwegian fjords can be related to different concentrations of dissolved organic matter (Onsrud and Kaartvedt, 1998) in effect changing the clearance rate of their predators.

Changes with seasonality

The equilibrium distributions for extreme values of σ points out that variation in day length cannot explain the observed seasonality in DVM in and of itself. Indeed, the only place where such fractions of daylight can occur is the high Arctic, where many more factors come into play (e.g. diapause during the polar night is as much about temperature and low primary production as it is about darkness and predator avoidance (Varpe, 2012)).
We investigated the seasonal variation (table 6.2, figure 6.5) in a temperate water column, specifically the Northwestern Mediterranean. This enabled us to compare our results with the monthly study of DVM (Sardou et al., 1996) exhibited by the krill *Meganyctiphanes norvegica*. The general pattern produced by the model is in broad agreement with field findings (figure 6.5). Observed monthly distribution of the predatory fish are also in general agreement. Predators gather at the surface at night, and perform DVM throughout the year except during summer where both predator and prey are scattered through the water column. Predators follow a bimodal distribution during the day (200m depth and the surface) between October and April. Such bimodal distributions have been exhibited before, for example with the analysis of acoustic scattering layers (Klevjer et al., 2016).

Nash equilibrium, Evolutionary Stable Strategy and Ideal Free Distribution

The coupling presented here provides a way to assess optimal distributions of prey and predators in terms of Nash Equilibria. For a game with a single player, the ideal free distribution (IFD) is the Nash equilibrium of the habitat selection game, and provided that the fitness is negatively density dependent it is also an evolutionary stable strategy (ESS) (Cressman and Křivan, 2006; Křivan et al., 2008; Křivan, 2014). However, for two or more players, the Folk Theorem (Cressman, 2003) states that a stable equilibrium of the replicator equation is a Nash equilibrium but is not necessarily an ESS, the very definition of which is clouded for two-species games with more than two strategies as considered here (Křivan et al., 2008). As we consider the equilibrium distribution of the population at a given period, and no group of the population will change its behaviour at the same time, we believe the replicator equation gives a reasonable representation of nature. Trophic rearrangements and seasonal variations of environmental parameters surely occur, but we assume that organisms have learnt through evolution to deal with these changes. Of greater concern is the fact that our model might have several Nash equilibria or can oscillate around equilibria. In order to check that, for each set of parameters used, several runs with different initial conditions were performed. No significant differences between runs were observed, which validates the robustness of our model in providing us with stable equilibria mimicking animal distribution in the water column. Moreover, our results were quite stable with little (or no) oscillations across equilibrium points, both for the fitness and the distribution. Figure 6.6 displays an example of convergence to the equilibrium with the replicator equation. The variances in fitness over the last 20,000 iterations were very low, ranging between 10^{-3} and 10^{-11}.

Natural selection triggers fitness collapse

A curious consequence of the frequency dependent processes described here is that evolution by natural selection can drive a species to a collapse in realized fitness. Evolution is shaped after all by the advantage an individual gets from adaptations, and it would seem that an individual would benefit from having a superior attribute, let's say for example a higher clearance rate which would enable it to capture more prey. This trait would thus be favoured, and would then spread within the predator population. However, this can induce a sharp decline in realized predator fitness (figure 6.2 F) — in a sense they become too accomplished for their own good. Furthermore, such a change is irreversible in that a reduction in clearance rate for an individual always reduces its fitness compared to its conspecifics, and thus cannot be favoured evolutionarily. The proximate cause for this is the switch in behaviour of the prey as increasing predator voracity drives them to seek refuge in a process akin to behaviourally mediated trophic relationships (Schmitz et al., 2004). It remains unclear how this process would play out in an evolutionary setting that includes population dynamics.

6.5 Conclusion and perspectives

DVM is more than just a key behavioural component of marine life, it has far reaching effects on the productivity, community structure and population dynamics of marine ecosystems (Cushing, 1951; Hays, 2003), as well as the ocean's biogeochemistry (Longhurst et al., 1990; Bianchi et al., 2013). Our work provides a mechanistic understanding of DVM, and particularly the cascading migrations of the upper trophic layers (Bollens et al., 2011) that also play a significant role in the biological pump. It is becoming increasingly evident that the active transport of carbon by consumers such as zooplankton (Jónasdóttir et al., 2015; Hansen and Visser, 2016) and fish (Davison et al., 2013) constitute an important component of the biological pump. Our model provides a tool to dynamically describe the vertical positioning of these consumer species in terms of readily prescribed (or modelled) environmental parameters. Furthermore, the modelling framework can be readily expanded to include additional consumer populations with different feeding modes (e.g. tactile predators such as jellyfish). A clear conclusion that can be drawn from this work is that behaviour is an important factor in determining how marine ecosystems function, and that optimality of behaviour, as we see in DVM, is strongly controlled by a strategic play-off between predators and their prey.

Acknowledgements

We thank Uffe H. Thygesen for useful discussions during the study. This work was supported by the Centre for Ocean Life, a VKR Centre of excellence supported by the Villum Foundation, and by the Gordon and Betty Moore Foundation (grant #5479). Finally, we would like to thank Vlastimil Křivan, Burt P. Kopler and an anonymous reviewer of the manuscript, whose comments and suggestions helped us to improve this work.

6.6 Supplementary information

The polymorphic-monomorphic equivalence

Monomorphic-polymorphic equivalence means that an individual cannot distinguish whether it is playing against a monomorphic population (mixed strategy) or a polymorphic population of fixed strategies (Broom and Rychtář, 2014). So far, we considered individuals playing fixed strategies where the distribution of strategies in the strategy space was given by $\mathbf{n}$ and $\mathbf{p}$, and the fitness of an individual following strategy ij was given by $F_{ij}^N(\mathbf{p})$ and $F_{ij}^P(\mathbf{n},\mathbf{p})$. Any individual playing a mixed strategy, i.e. a combination of different behaviours ij will have a fitness corresponding to the mean fitness of the strategies used.
Now, we consider a population where individuals can play mixed strategies. If we ordinate prey and predator from 1 to N_0 (respectively P_0 for predators), each prey (predator) plays a strategy

$$\tilde{n}_k = (\alpha_{ij}^k), \tag{6.13}$$

$$\tilde{p}_k = (\beta_{ij}^k), \tag{6.14}$$

where α_{ij}^k is the frequency at which prey k displays behaviour ij, and β_{ij}^k is the frequency at which predator k displays behaviour ij. The frequency at which the behaviour ij is played in the population of prey (and predator) is:

$$n_{ij} = \frac{1}{N_0} \sum_{k=1}^{N_0} \alpha_{ij}^k, \tag{6.15}$$

$$p_{ij} = \frac{1}{P_0} \sum_{k=1}^{P_0} \beta_{ij}^k. \tag{6.16}$$

With the same reasoning as the one which led to equation 6.8, we can express the fitness of a prey displaying the behaviour ij as:

$$\begin{aligned} F_{ij}^N(\tilde{p}) = \quad & g_{max}[(1-\sigma)g_i + \sigma g_j] - c_N\delta_{ij} - (1-\sigma)b_{max}b_{night,i}P_{night,i} \\ & -\sigma b_{max}b_{day,j}P_{day,j}. \end{aligned} \tag{6.17}$$

$P_{night,i}$ (resp. $P_{day,j}$) here represents the total probabilistic abundance of predators at night time (resp. daytime) in the layer i (resp. j). Similarly to equation 6.2, we can express it as:

$$\begin{aligned} P_{night,i} &= \sum_{k=1}^{P_0} M \sum_{q=1}^{M} \beta_{iq}^k, \\ P_{day,j} &= \sum_{k=1}^{P_0} M \sum_{q=1}^{M} \beta_{qj}^k. \end{aligned} \tag{6.18}$$

We can then rewrite the fitness of the prey as:

$$\begin{aligned} F_{ij}^N(\tilde{p}) = \quad & g_{max}[(1-\sigma)g_i + \sigma g_j] - c_N\delta_{ij} - (1-\sigma)b_{max}b_{night,i} \sum_{k=1}^{P_0} M \sum_{q=1}^{M} \beta_{iq}^k \\ & -\sigma b_{max}b_{day,j} \sum_{k=1}^{P_0} M \sum_{q=1}^{M} \beta_{qj}^k \\ = \quad & g_{max}[(1-\sigma)g_i + \sigma g_j] - c_N\delta_{ij} - (1-\sigma)b_{max}b_{night,i} \sum_{q=1}^{M} M\tfrac{P_0}{P_0} \sum_{k=1}^{P_0} \beta_{iq}^k \\ & -\sigma b_{max}b_{day,j} \sum_{q=1}^{M} M\tfrac{P_0}{P_0} \sum_{k=1}^{P_0} \beta_{qj}^k \\ = \quad & g_{max}[(1-\sigma)g_i + \sigma g_j] - c_N\delta_{ij} - (1-\sigma)b_{max}b_{night,i}MP_0 \sum_{q=1}^{M} p_{iq} \\ & -\sigma b_{max}b_{day,j}MP_0 \sum_{q=1}^{M} p_{qj}. \end{aligned} \tag{6.19}$$

p_{ij} is the mean population strategy now, as individual organisms are "playing the field". This fitness has the same form as the fitness of equation 6.8. By linear combination, the payoff of an individual prey $\tilde{n}$ is the linear combination of the fitness of its possible behaviours ij. We replicate the same reasoning for the predators. The fitness associated with behaviour ij can

be expressed as:

$$\begin{aligned} F_{ij}^{P}(\tilde{n},\tilde{p}) = \quad & b_{max}\eta[(1-\sigma)b_{night,i}N_{night,i} + \sigma b_{day,j}N_{day,j}] - c_P\delta_{ij} \\ & -\mu(1-\sigma)P_{night,i} - \mu\sigma P_{day,j}, \end{aligned} \tag{6.20}$$

where $N_{night,i}$ and $N_{day,j}$ are defined similarly to $P_{night,i}$ and $P_{day,j}$ in equation 6.18. We can then develop the fitness:

$$\begin{aligned} F_{ij}^{P}(\tilde{n},\tilde{p}) = \quad & b_{max}\eta[(1-\sigma)b_{night,i}\sum_{k=1}^{N_0} M\sum_{q=1}^{M}\alpha_{iq}^{k} + \sigma b_{day,j}\sum_{k=1}^{N_0} M\sum_{q=1}^{M}\alpha_{qj}^{k}] \\ & -c_P\delta_{ij} - \mu(1-\sigma)\sum_{k=1}^{P_0} M\sum_{q=1}^{M}\beta_{iq}^{k} - \mu\sigma\sum_{k=1}^{P_0} M\sum_{q=1}^{M}\beta_{qj}^{k} \\ = \quad & b_{max}\eta[(1-\sigma)b_{night,i}\sum_{q=1}^{M} M\tfrac{N_0}{N_0}\sum_{k=1}^{N_0}\alpha_{iq}^{k} + \sigma b_{day,j}\sum_{q=1}^{M} M\tfrac{N_0}{N_0}\sum_{k=1}^{N_0}\alpha_{qj}^{k}] \\ & -c_P\delta_{ij} - \mu(1-\sigma)\sum_{q=1}^{M} M\tfrac{P_0}{P_0}\sum_{k=1}^{P_0}\beta_{iq}^{k} - \mu\sigma\sum_{q=1}^{M} M\tfrac{P_0}{P_0}\sum_{k=1}^{P_0}\beta_{qj}^{k} \\ = \quad & b_{max}\eta MN_0[(1-\sigma)b_{night,i}\sum_{q=1}^{M} n_{iq} + \sigma b_{day,j}\sum_{q=1}^{M} n_{qj}] \\ & -c_P\delta_{ij} - \mu MP_0(1-\sigma)\sum_{q=1}^{M} p_{iq} - \mu MP_0\sigma\sum_{q=1}^{M} p_{qj}. \end{aligned} \tag{6.21}$$

This equation is also similar to the fitness of equation 6.9. By linear combination, the payoff of an individual predator $\tilde{p}$ is the linear combination of the fitness of its possible behaviours ij. Therefore, any individual, prey or predator, cannot distinguish whether it is playing against a monomorphic population consisting of mixed strategies or a polymorphic population with fixed strategies: we have the polymorphic-monomorphic equivalence.

The Replicator equation

As mentioned in the manuscript, we first allow each population to grow according to its fitness.

$$\begin{aligned} n'_{ij}(t+dt) &= n_{ij}(t) + dt\cdot F_{ij}^{N}\cdot n_{ij}(t), \\ p'_{ij}(t+dt) &= p_{ij}(t) + dt\cdot F_{ij}^{P}\cdot p_{ij}(t). \end{aligned} \tag{6.22}$$

Here, dt is a time step that is chosen to ensure a rapid but smooth transition to equilibrium (see figure 6.6 for a figure showing the convergence of the algorithm to equilibrium, and further down in this section for how we define dt). Moreover, since we are only interested in the relative abundance of strategies and not total population size (which in all likelihood comes under the control of other non-modelled constraints), we renormalize at each iteration

$$\begin{aligned} n_{ij}(t+dt) &= \frac{n'_{ij}(t+dt)}{\sum_k\sum_l n'_{kl}(t+dt)}, \\ p_{ij}(t+dt) &= \frac{p'_{ij}(t+dt)}{\sum_k\sum_l p'_{kl}(t+dt)}. \end{aligned} \tag{6.23}$$

This process insures that constraint 6.1 is satisfied at all times. dt is a factor used to keep the increase in populations within reasonable limits at each iteration, hence its precise numerical

value is not of immediate interest. It is chosen at each iteration according to

$$dt \cdot \max(|F^N|, |F^P|) = \lambda < 1. \tag{6.24}$$

As a practical compromise, we choose $\lambda = 0.1$. This means that any subpopulation following any strategy ij cannot grow of more than 10% of its size between each iteration. Preventing big changes in subpopulation sizes smoothens the convergence to equilibrium.

Theoretical calculations of regime shifts

The transitions from resident surface to DVM for prey can be derived by simple considerations of a migration between two layers (a feeding and a resting layer). The first regime shift occurs when the risk of remaining in the surface during the day becomes greater than the net gain in growth. Specifically, when:

$$b_{max} P_0 H \sigma b_{surf} / z_0 > g_{max} \sigma g_{surf} - c_N \delta_{surf-deep}, \tag{6.25}$$

where the assumed prey, and hence predator distribution is relatively uniform over the surface mixed layer of thickness z_0. Further, since near surface values of both structure functions are close to unity ($g_{surf} \approx 1$ and $b_{surf} \approx 1$) and assuming minimal cost, this reduces to a relatively simple criterion

$$b_{max} P_0 H / z_0 > g_{max}. \tag{6.26}$$

Likewise, the transition from DVM to permanent residence in the deep occurs when the risk of remaining within the mixed layer during night time exceeds the net gain in growth.

$$b_{max} P_0 H (1-\sigma) b_{night,feeding} / z_0 > g_{max} (1-\sigma) g_{feeding} - c_N \delta_{surf-deep}. \tag{6.27}$$

Assuming negligible cost, we get

$$b_{max} P_0 \rho H b_{night,feeding} / z_0 > g_{max} g_{feeding}. \tag{6.28}$$

Our parameter set leads to thresholds at $b_{max} = 0.0167\,\mathrm{m}^3\ \mathrm{day}^{-1}$ and $b_{max} = 2.7\,\mathrm{m}^3\ \mathrm{day}^{-1}$ (assuming that the feeding layer is around 50m depth before the transition, figure 6.2 C), which is consistent with values of figure 6.2.

Convergence of the replicator equation

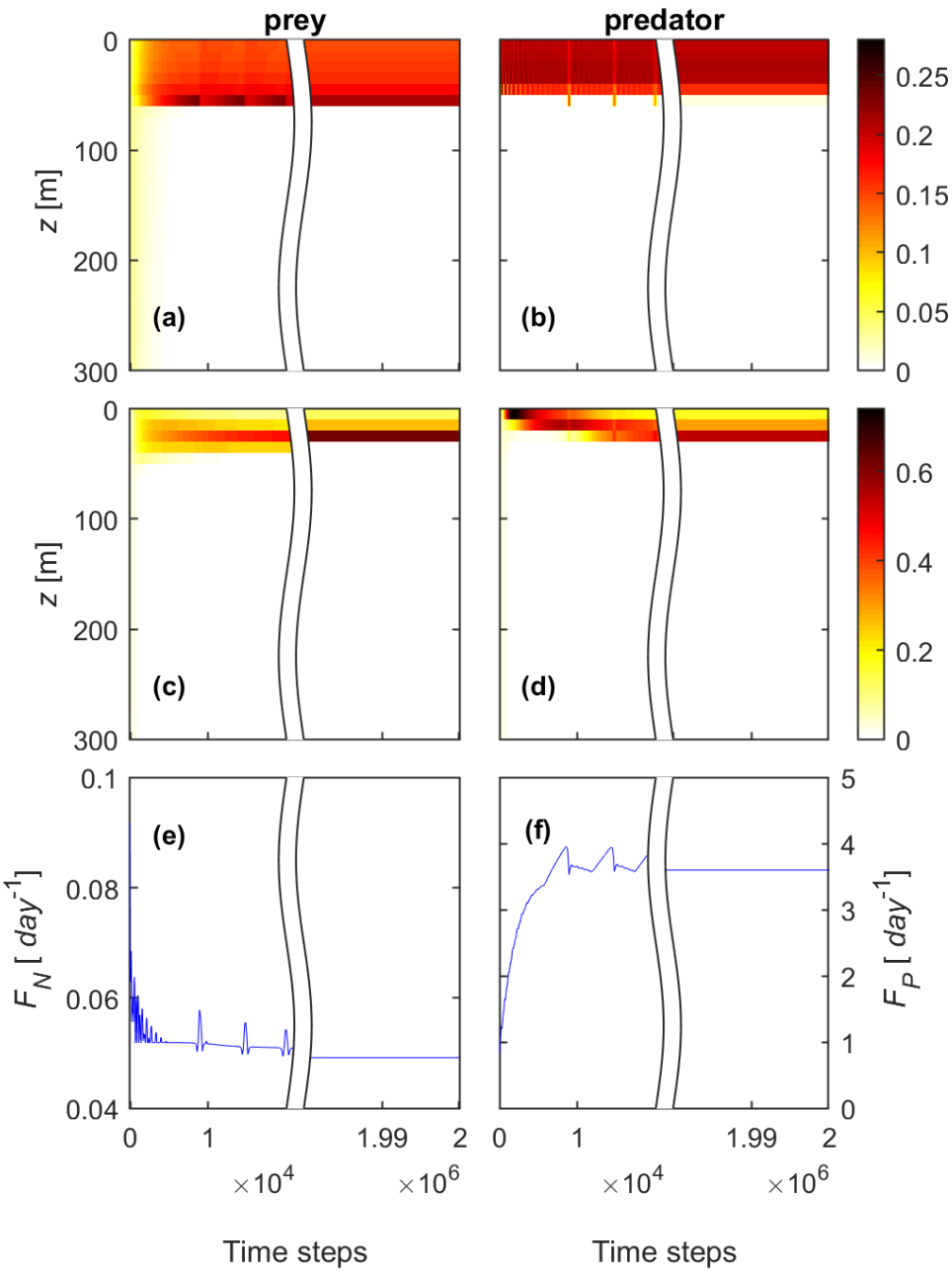

Figure 6.6: Example of convergence to the equilibrium with the replicator equation. The parameter set used is detailed in table 6.1, with the exception of b_{max} equal to 0.0126. Note the gap in time steps, created to illustrate more clearly the initial dynamics and the converged solution.

Bibliography

Aksnes, D. L. and Utne, A. C. W. (1997). A revised model of visual range in fish. *Sarsia*, 4827(September):37–41.

Barham, E. G. (1966). Deep scattering layer migration and composition: observations from a diving saucer. *Science*, 151(3716):1399–1403.

Batchelder, H. P., Edwards, C. A., and Powell, T. M. (2002). Individual-based models of copepod populations in coastal upwelling regions: implications of physiologically and environmentally influenced diel vertical migration on demographic success and nearshore retention. *Progress in Oceanography*, 53(2-4):307–333.

Bianchi, D., Stock, C., Galbraith, E. D., and Sarmiento, J. L. (2013). Diel vertical migration: Ecological controls and impacts on the biological pump in a one-dimensional ocean model. *Global Biogeochemical Cycles*, 27(2):478–491.

Bollens, S. M. and Frost, B. W. (1991). Diel Vertical Migration in Zooplankton - Rapid Individual-Response to Predators. *Journal of Plankton Research*, 13(6):1359–1365.

Bollens, S. M., Rollwagen-Bollens, G., Quenette, J. A., and Bochdansky, A. B. (2011). Cascading migrations and implications for vertical fluxes in pelagic ecosystems. *Journal of Plankton Research*, 33(3):349–355.

Boxwell, M. (2017). *The Solar Electricity Handbook: A Simple, Practical Guide to Solar Energy - Designing and Installing Solar Photovoltaic Systems.* Greenstream Publishing, 11th revis edition.

Broom, M. and Rychtář, J. (2014). Asymmetric Games in Monomorphic and Polymorphic Populations. *Dynamic Games and Applications*, 4(4):391–406.

Cressman, R. (2003). *Evolutionary dynamics and extensive form games.* MIT Press.

Cressman, R. and Křivan, V. (2006). Migration dynamics for the ideal free distribution. *American Naturalist*, 168(3):384–397.

Cressman, R., Křivan, V., and Garay, J. (2004). Ideal free distributions, evolutionary games, and population dynamics in multiple-species environments. *The American naturalist*, 164(4):473–489.

Cushing, D. H. (1951). The vertical migration of planktonic Crustacea. *Biological reviews*, 26(2):158–192.

Dam, H. G., Roman, M. R., and Youngbluth, M. J. (1995). Downward export of respiratory carbon and dissolved inorganic nitrogen by diel-migra1nt mesozooplankton at the JGOFS Bermuda time-series station. *Deep Sea Research Part I: Oceanographic Research Papers*, 42(7):1187–1197.

Davison, P. C., Checkley, D. M., Koslow, J. A., and Barlow, J. (2013). Carbon export mediated by mesopelagic fishes in the northeast Pacific Ocean. *Progress in Oceanography*, 116:14–30.

De Robertis, A., Jaffe, J. S., and Ohman, M. D. (2000). Size-dependent visual predation risk and the timing of vertical migration. *Limnology and Oceanography*, 45(8):1838–1844.

D'Ortenzio, F., Iudicone, D., de Boyer Montegut, C., Testor, P., Antoine, D., Marullo, S., Santoleri, R., and Madec, G. (2005). Seasonal variability of the mixed layer depth in the Mediterranean Sea as derived from in situ profiles. *Geophysical Research Letters*, 32(12):1–4.

Ducklow, H. W., Steinberg, D. K., and Buesseler, K. O. (2001). Upper Ocean Carbon Export and the Biological Pump. *Oceanography*, 14(4):50–58.

Dypvik, E., Klevjer, T. A., and Kaartvedt, S. (2012). Inverse vertical migration and feeding in glacier lanternfish (Benthosema glaciale). *Marine Biology*, 159(2):443–453.

Fiksen, Ø. (1995). Vertical distribution and population dynamics of copepods by dynamic optimization. *ICES Journal of Marine Science*, 52(3-4):483–503.

Fiksen, Ø., Eliassen, S., and Titelman, J. (2005). Multiple predators in the pelagic: Modelling behavioural cascades. *Journal of Animal Ecology*, 74(3):423–429.

Fisher, R. A. (1930). The genetical theory of Natural Selection.

Frank, T. M. and Widder, E. A. (2002). Effects of a decrease in downwelling irradiance on the daytime vertical distribution patterns of zooplankton and micronekton. *Marine Biology*, 140(6):1181–1193.

Frost, B. W. and Bollens, S. M. (1992). Variability of Diel Vertical Migration in the Marine Planktonic Pseudocalanus newmani in Relation to Its Predators. *Canadian Journal of Fisheries and Aquatic Sciences*, 49:1137–1141.

Gabriel, W. and Thomas, B. (1988). Vertical Migration of Zooplankton as an Evolutionarily Stable Strategy. *The American Naturalist*, 132(2):199–216.

Giske, J., Rosland, R., Berntsen, J., and Fiksen, Ø. (1997). Ideal free distribution of copepods under predation risk. *Ecological Modelling*, 95(1):45–59.

Hansen, A. N. and Visser, A. W. (2016). Carbon export by vertically migrating zooplankton: An optimal behavior model. *Limnology and Oceanography*, 61(2):701–710.

Hays, G. C. (2003). A review of the adaptive significance and ecosystem consequences of zooplankton diel vertical migrations. *Hydrobiologia*, 503:163–170.

Hays, G. C., Kennedy, H., and Frost, B. W. (2001). Individual variability in diel vertical migration of a marine copepod: Why some individuals remain at depth when others migrate. *Limnology and Oceanography*, 46(8):2050–2054.

Hirst, A. G. and Sheader, M. (1997). Are in situ weight specific growth rates body-size independent in marine planktonic copepods? A re-ananlysis of the global syntheses and a new empirical model. *Mar. Ecol. Prog. Ser*, 154:155–165.

Hixon, M. A. and Carr, M. H. (1997). Synergistic predation, density dependance, and population regulation in marine fish. *Science*, 277(August):946–949.

Hofbauer, J. and Sigmund, K. (2003). Evolutionary Game Dynamics. *Bulletin (New Series) of the American mathematical society*, 40(403):479–519.

Hugie, D. M. and Dill, L. M. (1994). Fish and Game: a game theoretic approach to habitat selection by predators and prey. *Journal of Fish Biology*, 45(Supplement A):151–169.

Isaacs, J. D., Tont, S. A., and Wick, G. L. (1974). Deep scattering layers: vertical migration as a tactic for finding food. *Deep-Sea Research and Oceanographic Abstracts*, 21(8):651–656.

Iwasa, Y. (1982). Vertical migration of zooplankton: a game between predator and prey. *The American naturalist*, 120(2):171–180.

Ji, R. and Franks, P. (2007). Vertical migration of dinoflagellates: model analysis of strategies, growth, and vertical distribution patterns. *Marine Ecology Progress Series*, 344:49–61.

Jónasdóttir, S. H., Visser, A. W., Richardson, K., and Heath, M. R. (2015). Seasonal copepod lipid pump promotes carbon sequestration in the deep North Atlantic. *Proceedings of the National Academy of Sciences*, 112(39):12122–12126.

Kaartvedt, S., Klevjer, T. A., Torgersen, T., Sørnes, T. A., and Røstad, A. (2007). Diel vertical migration of individual jellyfish (Periphylla periphylla). *Limnology and Oceanography*, 52(3):975–983.

Kaartvedt, S., Torgersen, T., Klevjer, T. A., Røstad, A., and Devine, J. A. (2008). Behavior of individual mesopelagic fish in acoustic scattering layers of Norwegian fjords. *Marine Ecology Progress Series*, 360:201–209.

Kiørboe, T. (2011). How zooplankton feed: Mechanisms, traits and trade-offs. *Biological Reviews*, 86(2):311–339.

Klevjer, T. A., Irigoien, X., Røstad, A., Fraile-Nuez, E., Benítez-Barrios, V. M., and Kaartvedt, S. (2016). Large scale patterns in vertical distribution and behaviour of mesopelagic scattering layers. *Scientific Reports*, 6(1):19873.

Křivan, V. (2014). The Allee-type ideal free distribution. *Journal of Mathematical Biology*, 69(6-7):1497–1513.

Křivan, V., Cressman, R., and Schneider, C. (2008). The ideal free distribution: A review and synthesis of the game-theoretic perspective. *Theoretical Population Biology*, 73(3):403–425.

Lima, S. L. and Dill, L. M. (1990). Behavioral decisions made under the risk of predation: a review and prospectus. *Canadian Journal of Zoology*, 68:619–640.

Longhurst, A., Bedo, A., Harrison, W., Head, E., and Sameoto, D. (1990). Vertical flux of respiratory carbon by oceanic diel migrant biota. *Deep Sea Research Part A. Oceanographic Research Papers*, 37(4):685–694.

Longhurst, A. R. and Harrison, W. G. (1989). The biological pump: Profiles of plankton production and consumption in the upper ocean. *Progress in Oceanography*, 22(1):47–123.

Maynard Smith, J. (1976). Evolution and the Theory of Games. *American Scientist*, 64(1):41–45.

McLaren, I. A. (1963). Effects of Temperature on Growth of Zooplankton, and the Adaptive Value of Vertical Migration. *Journal of the Fisheries Research Board of Canada*, 20(3):685–727.

Morel, A. and André, J.-M. (1991). Pigment distribution and Primary Production in the Western Mediterranean as Derived and Modeled From Coastal Zone Color Scanner Observations. *Journal of Geophysical Research*, 96(C7):12685–12698.

O'Driscoll, R. L., Gauthier, S., and Devine, J. A. (2009). Acoustic estimates of mesopelagic fish: as clear as day and night? *ICES Journal of Marine Science*, 66(6):1310–1317.

Ohman, M. D. (1990). The Demographic Benefits of Diel Vertical Migration by Zooplankton. *Ecological Monographs*, 60(3):257–281.

Ohman, M. D. and Romagnan, J.-B. (2016). Nonlinear effects of body size and optical attenuation on Diel Vertical Migration by zooplankton. *Limnology and Oceanography*, 61(2):765–770.

Onsrud, M. S. and Kaartvedt, S. (1998). Diel vertical migration of the krill Meganyctiphanes norvegica in relation to physical environment, food and predators. *Marine Ecology Progress Series*, 171(Dvm):209–219.

Onsrud, M. S. R., Kaartvedt, S., Røstad, A., and Klevjer, T. A. (2004). Vertical distribution and feeding patterns in fish foraging on the krill Meganyctiphanes norvegica. *ICES Journal of Marine Science*, 61(8):1278–1290.

Pinti, J. and Visser, A. W. (2018). Data from: Predator-prey games in multiple habitats reveal mixed strategies in diel vertical migration. *American Naturalist, DRYAD Digital Repository*.

Plueddemann, A. J. and Pinkel, R. (1989). Characterization of the patterns of diel migration using a Doppler sonar. *Deep Sea Research Part A, Oceanographic Research Papers*, 36(4):509–530.

Reeve, H. K. and Holldobler, B. (2007). The emergence of a superorganism through intergroup competition. *Proceedings of the National Academy of Sciences*, 104(23):9736–9740.

Sainmont, J., Thygesen, U. H., and Visser, A. W. (2013). Diel vertical migration arising in a habitat selection game. *Theoretical Ecology*, 6(2):241–251.

Sardou, J., Etienne, M., and Andersen, V. (1996). Seasonal abundance and vertical distributions of macroplankton and micronekton in the Northwestern Mediterranean Sea. *Oceanologica acta*, 19(6):645–656.

Schmitz, O. J., Křivan, V., and Ovadia, O. (2004). Trophic cascades: The primacy of trait-mediated indirect interactions. *Ecology Letters*, 7(2):153–163.

Schuster, P. and Siegmund, K. (1983). Replicator Dynamics. *Journal of Theoretical Biology*, 100:533–538.

Sih, A. (1998). Game theory and predator–prey response races. In Dugatkin, L. A. and Reeve, H. K., editors, *Game theory and animal behavior.*, chapter Game theor, pages 221–238. Oxford University Press.

Steinberg, D. K., Carlson, C. A., Bates, N. R., Goldthwait, S. A., Madin, L. P., and Michaels, A. F. (2000). Zooplankton vertical migration and the active transport of dissolved organic and inorganic carbon in the Sargasso Sea. *Deep Sea Research Part I*, 47(1):137–158.

Steinberg, D. K., Goldthwait, S. A., and Hansell, D. A. (2002). Zooplankton vertical migration and the active transport of dissolved organic and inorganic nitrogen in the Sargasso Sea. *Deep Sea Research Part I*, 49:1445–1461.

Stich, H.-B. and Lampert, W. (1981). Predator evasion as an explanation of diurnal vertical migration by zooplankton. *Nature*, 293(5831):396–398.

Titelman, J. and Fiksen, Ø. (2004). Ontogenetic vertical distribution patterns in small copepods: field observations and model predictions. *Marine Ecology Progress Series*, 284(1):49–63.

Varpe, Ø. (2012). Fitness and phenology: Annual routines and zooplankton adaptations to seasonal cycles. *Journal of Plankton Research*, 34(4):267–276.

Visser, A. W. (2007). Motility of zooplankton: Fitness, foraging and predation. *Journal of Plankton Research*, 29(5):447–461.

Webster, C. N., Varpe, Ø., Falk-Petersen, S., Berge, J., Stübner, E., and Brierley, A. S. (2013). Moonlit swimming: vertical distributions of macrozooplankton and nekton during the polar night.

Zaret, T. M. and Suffern, S. (1976). Vertical migration in zooplankton as a predator avoidance mechanism. *Limnology and Oceanography*, 21(6):804–813.

Zhou, M. and Dorland, R. D. (2004). Aggregation and vertical migration behavior of Euphausia superba. *Deep-Sea Research Part II: Topical Studies in Oceanography*, 51(17-19):2119–2137.

CHAPTER 7

Co-adaptive behaviour of interacting populations significantly impacts ecosystem function

Pinti J., Andersen K.H., Visser A.W. (*under review*)

Abstract

Mechanistic descriptions of ecosystem function are based on population models that seldom take behaviour into account. However, individuals of different interacting populations often adapt to prevailing conditions by changing their behaviour simultaneously, with consequences for trophic relationships throughout the system. Here, we present a model that combines the population dynamics and adaptive behaviour of organisms of two populations. We illustrate this for the case of diel vertical migration (DVM), the daily movement of marine organisms between food-depleted but safe dark depths and more risky nutrition-rich surface waters. DVM in a marine community is rich in adaptive behaviours, as the optimal pattern of each individual is linked to the optimal migration pattern of its conspecifics, its prey and its predators. We show that population sizes at equilibrium are significantly different if organisms can adapt their behaviour, and that optimal DVM behaviours within the community vary significantly if population dynamics are considered. As a consequence, ecosystem function estimates such as trophic transfer efficiency and vertical carbon export differ greatly when fitness seeking behaviour is included. Ignoring the role of behaviour in multi-trophic population modeling can potentially lead to inaccurate predictions of population biomasses and ecosystem functions.

Keywords— Game theory, Population dynamics, Predator-prey interactions, Trophic cascade, Diel vertical migration, Ecosystem function

7.1 Introduction

A central challenge in mechanistic ecological modelling is to predict how the functioning of ecosystems will respond to global change (Steffen et al., 2018; Kiørboe et al., 2018). This requires a sound theoretical basis for not only how populations respond numerically to change, but also how they may adapt behaviourally (Schmitz et al., 2008; Sih et al., 2011). In essence, this calls for ecosystem models to simultaneously capture processes that take place at very different time scales: notably the time scale at which individual organisms behave, the time scale at which populations interact with each other and fluctuate in abundance, and the evolutionary time scale at which traits or species emerge or go extinct (Křivan and Cressman, 2009). It is well known that the processes at one time scale can have phenomenological effects at other time scales (Pelletier et al., 2009; Schoener, 2011). For example, re-introducing wolves in an ecosystem had cascading consequences not only on the abundance of the two trophic levels below them, but also on the behaviour of their prey (Ripple and Larsen, 2000; Ripple et al., 2001). Similarly, if dragonfly larvae have a plastic behaviour, the presence of predators modifies the larvae behaviour and abundance, but also the abundance and species assemblage of the larvae's prey (Start, 2020). However, modelling these time scales conjointly proves difficult, especially if several interacting populations are involved.

For a single species, the link between behavioural and population time scales is fairly well established, usually by allowing individuals to optimize a specific behaviour (e.g. Lima, 1985; Houston et al., 1993; Titelman and Fiksen, 2004; Visser et al., 2012). Adaptive behaviour can have various theoretical consequences such as reducing a food-chain length (Kondoh and Ninomiya, 2009), promoting coexistence of prey (Křivan and Sikder, 1999), altering the stability of a system (Abrams, 2007; Křivan and Cressman, 2009; Visser et al., 2012) or changing the amplitude of population cycles (Křivan, 2007). Multiple interacting populations increases complexity as different populations can evolve simultaneously or adapt their behaviour in response to the reciprocal responses adopted by other populations. This mutual inter-dependence of individual responses is usually solved by finding the Nash equilibrium of the system (Iwasa, 1982; Hugie and Dill, 1994; Bouskila, 2001). Evolutionary game theory assesses how the frequency of traits (or strategies) in a population evolves, but rarely considers the evolution of the population size which generally only receives a qualitative mention (Brown et al., 1999; Bouskila, 2001; Pinti and Visser, 2019).

Merging individual and population time scales (and to some extent evolutionary time scales) for a multi-species system leads to population game theory (Cressman et al., 2004). Specifically, at the fastest time scale, individuals behave adaptively to optimize their behaviour in terms of Darwinian fitness. They do so in response to both the abundance of conspecifics, predators and prey (density dependence) as well as the various strategies these players adopt (frequency dependence). The rationale here is that evolution has equipped individuals with rules that provide an optimal behaviour in any given situation. The ensuing population dynamics then follow Lotka-Volterra dynamics. Most population game theory studies have focused on a predator and one or two prey in a two-patch environment, where prey and/or predators can adapt their behaviours (Křivan and Sikder, 1999; Křivan and Schmitz, 2003; Cressman et al., 2004; Křivan, 2007; Křivan and Cressman, 2009; Cressman and Křivan, 2010). How behaviour and population dynamics interact in realistic systems where both multiple trophic levels and multiple behavioural strategies are possible remains unresolved. Perhaps more critical and less well understood, are the controls these interactions have on emergent ecosystem functions.

Diel Vertical Migration (DVM) is a well studied behaviour in aquatic systems. Every day, a significant fraction of marine organisms migrate to depth to hide from visual predators, but ascend at night to feed in nutrient-rich surface waters (Mehner and Kasprzak, 2011; Klevjer et al., 2016; Ohman and Romagnan, 2016). Many modelling studies have investigated the optimal migration strategy of a particular organism depending on environmental conditions (Giske and Aksnes, 1992; Rosland and Giske, 1994; Titelman and Fiksen, 2004). Game theory extends this by predicting the optimal strategies that prey and predator use while playing against each other (Iwasa, 1982; Hugie and Dill, 1994; Sainmont et al., 2015; Thygesen and Patterson, 2018; Pinti and Visser, 2019; Pinti et al., 2019), but they all considered fixed population sizes and none quantitatively examined the coupling of emerging optimal fitness-seeking behaviour on population dynamics.

We consider a tri-trophic food chain consisting of a phytoplankton resource, a zooplankton consumer and a visual predator, the last two playing against each other in a water column by adjusting their vertical position at day and at night. Using population game theory, we incorporate the plasticity of rational behaviours (i.e. each animal changes its migrating strategy to behave optimally at all times) in predator-prey dynamics, effectively reconciling the individual and population time scales for a game played out between two populations in multiple arenas. This allows us to compare population sizes with and without games, behaviour of populations computed with or without population dynamics, and the resulting ecosystem function estimates.

7.2 Methods

We consider a tri-trophic chain (phytoplankton – also called the resource –, zooplankton, and fish) and two time scales: the behavioural time scale, and the population time scale. We investigate three different models: model A considers only the behavioural time scale, model B considers only the population time scale, and model C considers both the behavioural and the population time scale (figure 7.1).

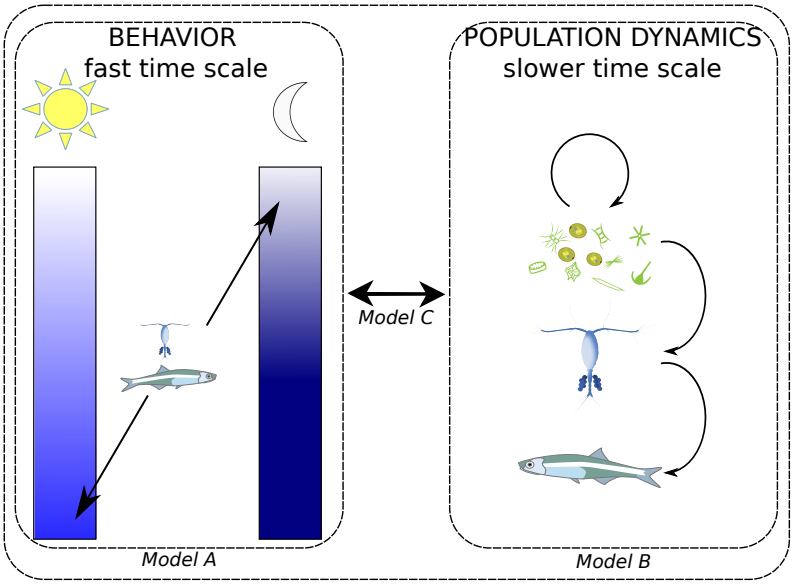

Figure 7.1: Representation of the three different models considered here. Model A consider behaviour but not population dynamics (Pinti and Visser, 2019). Model B considers population dynamics but not behaviour. Model C combines behaviour and population dynamics, merging both the individual and the population time scale.

The organisms reside in a water column divided into M water layers. For model A and C, days are divided into two periods: daylight hours (a fraction σ of the time) and night ($1 - \sigma$ of the time). Phytoplankton cannot perform diel vertical migration, whereas zooplankton and visual predators can adapt their position at day and at night (DVM strategy) to maximise their fitness.

Model A derives the optimal behaviour of zooplankton and fish by computing the Nash equilibrium of the system following Pinti and Visser (2019), with the exception that phytoplankton are now an explicit resource grazed upon by zooplankton (details of all equations can be found section 7.6, and all parameters are summarised table 7.1).

Model B is a simple 1D water column model of the population dynamics. In this model, we allow phytoplankton, zooplankton and fish to grow according to Lotka-Volterra equations. We do not consider population exchanges or diffusion between the different water layers, and phytoplankton grow following a chemostat. Their carrying capacity as well as their instantaneous growth rate are depth-dependent, to mimic the effects of light in the water column.

Model C combines model A and B: on a fast time scale, zooplankton and fish change their behaviour as to always behave following their Nash equilibrium. On a slower time scale, population sizes vary similarly to model B, following Lotka-Volterra dynamics.

We compare these three models based on the resulting behaviour and biomasses of the populations considered, but also based on two ecosystem functions: trophic transfer efficiency and active carbon export.

Details of the equations of the 3 models and ecosystem functions are available section 7.6. The MATLAB code necessary to run these models is available on the following repository: `https://gitlab.gbar.dtu.dk/jppi/Frequency-dependent_behaviour_of_interacting_populations_significantly_impacts_ecosystem_function`.

7.3 Results

We compare three models (figure 7.1): adaptive behaviour with fixed population sizes (model A), population dynamics with fixed behaviour (model B), and both behaviour and population dynamics (model C). We explore the influence of the phytoplankton carrying capacity on the system. These three models are compared in terms of two predicted ecosystem functions: trophic transfer efficiency and active carbon export flux.

Games with and without population dynamics

With fixed population sizes (model A), three migration regimes emerge (figure 7.2 a-b and figure 7.4 a-b-c-d). At low resource carrying capacity, prey remain at depth

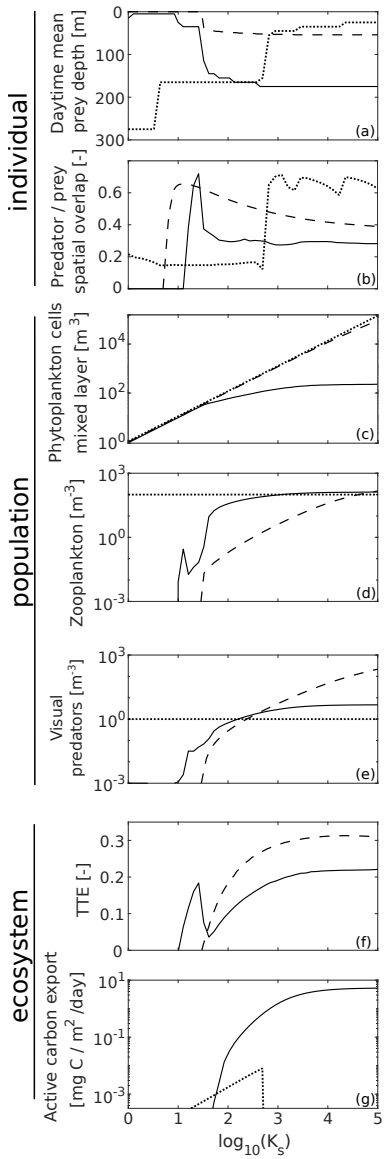

Figure 7.2: (a) Day mean prey position, (b) Spatial overlap between predator and prey, (c) phytoplankton concentration in the mixed layer, (d) mean zooplankton concentration in the water column, (e) mean fish concentration, (f) trophic transfer efficiency and (g) active carbon export as a function of the phytoplankton carrying capacity. Dotted lines for the model with only behaviour (model A), dashed lines for the model with no behaviour considerations (model B) and plain lines are for the model where both behaviour and population dynamics are considered (model C).

at all times and predator are scattered through the water column (figure 7.4 b-d). At intermediate values of the two parameters, prey exhibit DVM patterns and predators are scattered throughout the water column. Finally, at high resource carrying capacity, fish and zooplankton reside close to the surface with a high spatial overlap (figure 7.2 b).

The vertical distribution in model C allows only two regimes (figure 7.3). Counter to a model with fixed population sizes (model A, Pinti and Visser, 2019), there is no complete depth residency, as organisms go extinct without feeding. In addition, population dynamics drives the emergence of prey DVM across most of their existence range (figure 7.3 and figure 7.4 a-c). Predators, in contrast, are scattered throughout the water column during the day and gather only during nighttime at the surface (figure 7.3 and figure 7.4 b-d).

Population dynamics with and without games

Population sizes at equilibrium are considerably different when adaptive behaviour is included or not (model B and C, figure 7.2 c-d-e). An adaptive behaviour (model C) allows a wider range of coexistence for all three populations. Varying the phytoplankton carrying capacity (figure 7.2) exhibits an enrichment ladder, where successively higher trophic levels are admitted as productivity surpasses certain levels (Oksanen et al., 1981). Adaptive behaviours reduce the productivity levels necessary for the emergence of consumers and predators. The equilibrium population sizes at high carrying capacity are also different when considering adaptive behaviours: the resource biomass does not grow exponentially but saturates, causing the saturation of the zooplankton and fish biomass as well.

Trophic transfer efficiency

The trophic transfer efficiency (TTE) is very low when predator start to emerge (figure 7.2 f), but when considering behaviour the TTE increases at first, falls down (when prey start to perform DVM, see figure 7.2 a) and then increases again as the the population sizes increase, to saturate around 0.22. The TTE of model B increases much slower, as the predator population needs a higher resource carrying capacity to establish. But the TTE saturates around 0.3, higher than for model C. This is because all energy is transferred to the higher trophic level (except for a small background mortality term), as zooplankton cannot defend themselves against predation by migrating deeper during daytime.

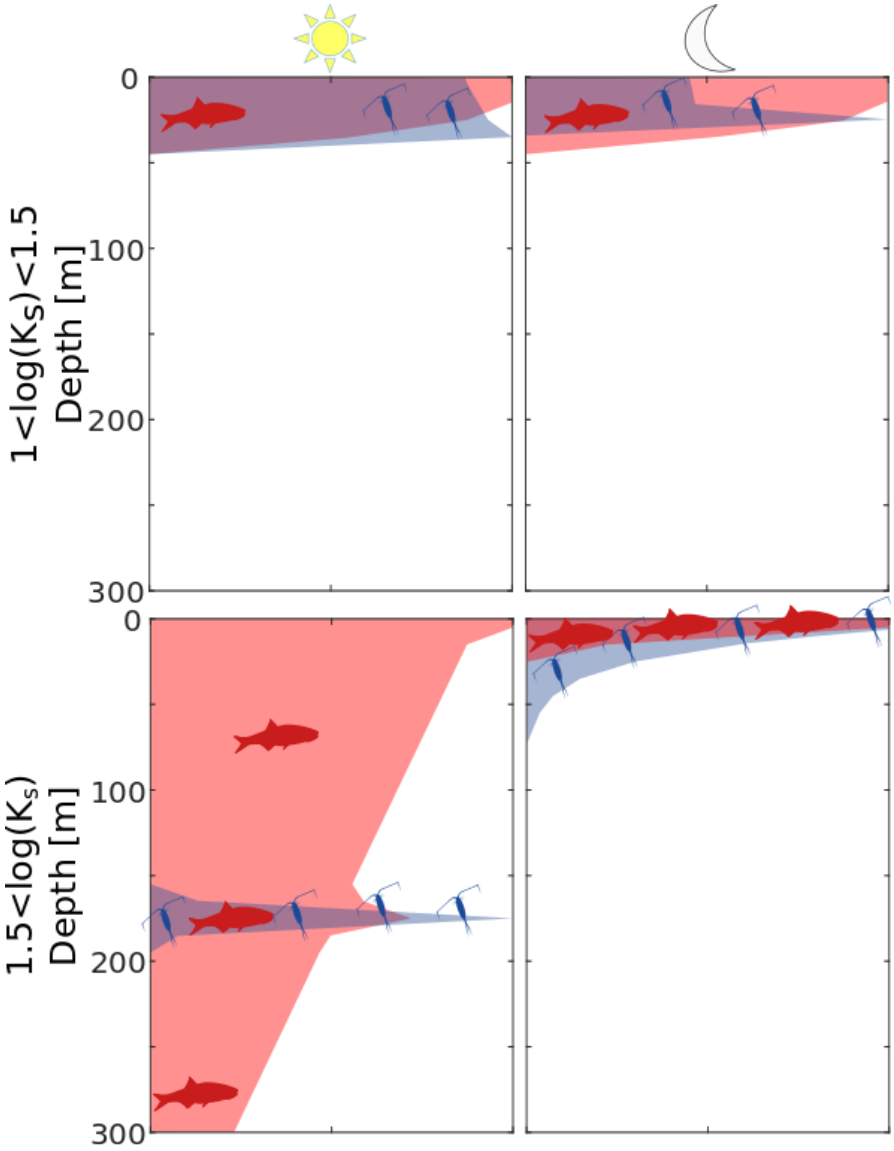

Figure 7.3: Two examples of typical vertical distribution of organisms during day and night for model C. Top panels: predation pressure is very low (beginning of the existence range of predators). Bottom panels: after $\log_{10}(K_s) = 1.5$, predation pressure is higher and prey perform DVM.

Carbon Export

As for TTE, the different models yield very different active carbon export estimates. Except when predator start to emerge, the active carbon export in model C (with population dynamics, figure 7.2 g) is higher than in model A (no population dynamics), because predators are more abundant (figure 7.2 e) and because a more important fraction of the population performs DVM (figure 7.4).

At low phytoplankton carrying capacity (and high carrying capacity for the model A without population dynamics), the active export is null, either because the populations went extinct, or because they do not migrate and remain at depth or at the surface at all times.

7.4 Discussion

Our method successfully couples the effects of the behavioural and the population time scales on two populations. By considering the individual and population time scales, our model unravels effects at both time scales simultaneously. The results are different than when a single time scale is considered, whether it be the individual or the population time scale. Crucially, our simulations demonstrate that an adaptive behaviour alters ecosystem functions. The trophic transfer efficiency (TTE) is lowered when adaptive behaviour is considered, especially at high resource carrying capacity. This is because zooplankton mortality risk directly depends on the behaviour adopted. The general top-down control of consumers, especially in productive areas (Hairston et al., 1960; Oksanen et al., 1981) seem to indicate that TTE would typically be reduced when consumer adopt an adaptive behaviour as the incurred energy cost is lost for the next trophic level.

More generally, behaviour can affect multiple ecosystem functions (trophic transfer, nutrient cycling and carbon export), and a failure to identify and consider possible adaptive behaviours may lead to severely biased estimates. Population games are an efficient way to couple behaviour and population dynamics, and the method can be used to compute meticulously emergent ecosystem functions.

We framed our study as a game played out between predator and prey in a diel vertical migration context, but we stress that provided with adequate description of the population interactions our method can be tailored to reproduce other systems, such as the adaptive behaviour and trophic cascades in pond invertebrates (Start, 2020), the succession of color morphs in a lizard species (Sinervo and Lively, 1996), or the competition between owls and snakes preying on rodents (Bouskila, 2001). More generally, previous studies pointed the importance of considering risk consequences in predator prey interactions (Lima and Bednekoff, 1999; Lima, 2002), and a more systematic inclusion of behaviour in population dynamics and ecosystem functions studies would probably be beneficial to the mechanistic understanding of the systems in focus.

It is not straightforward to anticipate what behaviour would emerge in the population from models without behaviour implemented, or what happens at the population level from static games. A high or low fitness does not necessarily mean that a population will grow or go extinct, as behaviours can change and individuals can adapt to new constraints through density and frequency dependent effects with repercussions for the fitness of all other players in the system. For example, considering the behaviour of individuals from a single population can have a range of consequences, such as relaxing the predation pressure on some species (Holt and Lawton, 1994) or stabilizing the food-web structure (Kondoh and Ninomiya, 2009). In addition, a more realistic description of ecosystem processes would consider real time dynamics. Our study only considered population dynamics when the equilibrium was reached, but population sizes vary with seasonal cycles in nature. Implementing this game to describe real time dynamics requires considering these natural variations. In addition, one should consider expected reproductive output as well as life history strategies and not just the instantaneous fitness in seasonal studies.

Moreover, the evolutionary time scale (not explicitly considered in this work), would also be relevant for the system. If we consider the evolution of the predator clearance rate as a trait (for example, through improved eye performances or increased swimming speed), the predator surprisingly does worse as it becomes more efficient – in the dynamic models (B and C) the population size decreases (figures S3 and S4). For an individual, it would always be beneficial to increase clearance rate providing a competitive edge over conspecifics, and as such, all individuals should evolve following red queen dynamics toward better performances (Dieckmann et al., 1995). In this light, the population will then drive itself to extinction, being "too accomplished for their own good" (Pinti and Visser, 2019). However, there is invariably some trade-off to balance (Stearns, 1989). An increased eye capacity or swimming ability would, for example, come at the cost of an increased metabolic rate for predatory fish. As a consequence, there may be an optimum trait value for the clearance rate, which would ultimately control the state of our system.

There is also the real possibility that this trait optimization could lead to speciation. Conceivably, different subgroups of a polymorphic population (i.e. a population where different individuals can have different strategies) may diverge. In our illustrative example, for instance, polymorphism could lead to the emergence of two predator types, such as high light - low light specialists. Such considerations would provide insight into the types of traits and behavioural strategies expressed in a given community, with cascading consequences for biodiversity and ecosystem function estimates.

7.5 Conclusion

In addition to the abundance and diversity of its constituent species, the functioning of an ecosystem also depends on how its indigenous organisms behave. Particularly with regards to trophic interactions, behavioural strategies form an inter-connected

network, predicated by game-theory and honed by evolution – the etho-web – where a small change in conditions can trigger a restructuring of behavioural strategies across large sectors of the ecosystem, precipitating a significant change in ecosystem function. We have demonstrated this for the pelagic ecosystem where daily cycles of risk and opportunity drive a rich mosaic of populations and behavioural strategies, and where predicted ecosystem functions show significant density and frequency dependence. For the case of the pelagic ocean, these dependencies impact directly on two of the most important ecosystem services of the global ocean, namely fisheries production and carbon sequestration. How such abundance-frequency dependencies play out in other ecosystems remains an open question, but we contend that trophic relationships almost invariably have co-evolved with behavioural strategies that mitigate risk and maximise opportunity for all individuals in their concurrent roles as competitors, predators and prey.

Acknowledgements
This work was supported by the Centre for Ocean Life, a Villum Kann Rasmussen Centre of Excellence supported by the Villum Foundation, and by the Gordon and Betty Moore Foundation (grant 5479).

7.6 Supplementary information

Model A

Model A refers to the model where organisms have an adaptive behaviour, but where population sizes are fixed, similar to most game theoretic studies. Here, we fixed the consumer concentration to $N = 100\,\mathrm{m}^{-3}$ and the predator concentration to $P = 1\,\mathrm{m}^{-3}$. Most of the following equations are taken from (Pinti and Visser, 2019), and adapted to fit with our explicit description of the phytoplankton resources. For simplicity and readability, we drop the time dependencies of all variables, and i and j can either refer to a specific water bin (when used as an index) or to its corresponding depth (when used as a function variable).

We define the strategy matrices $\mathbf{n} = n_{ij}$ and $\mathbf{p} = p_{ij}$ as the frequency of the prey and predator population respectively, that follows strategy ij, i.e. being in layer j during day and i during night. By definition, we have:

$$\sum_{i=1}^{M}\sum_{j=1}^{M} n_{ij} = \sum_{i=1}^{M}\sum_{j=1}^{M} p_{ij} = 1. \tag{7.1}$$

If N and P are the mean concentration of prey and predators in the water column (in m^{-3}), the prey concentration in layer j during daytime is:

$$N_{j,day} = MN\sum_{i=1}^{M} n_{ij}, \tag{7.2}$$

with similar expressions for predator and for nighttime concentrations. The clearance rate g of prey is constant, but the clearance rate b of visual predators varies with light levels:

$$\begin{aligned} b(day, z) &= \frac{L_{max} \exp(-\kappa z)}{L_0 + L_{max} \exp(-\kappa z)}, \\ b(night, z) &= \frac{\rho L_{max} \exp(-kz)}{L_0 + \rho L_{max} \exp(-\kappa z),} \end{aligned} \tag{7.3}$$

with L_{max} the daytime irradiance at the surface, L_0 the half-saturation light intensity and ρ the attenuation coefficient between day and night.
Fitness is defined as the difference between specific growth and potential mortality over a 24h cycle. For prey, growth is equal to:

$$G_{ij}^N = \varepsilon_Z \frac{M_\varphi}{M_Z} g(\sigma\varphi(j) + (1-\sigma)\varphi(i)) - C(i,j), \tag{7.4}$$

with φ the resource concentration (varying with depth but not time in this model), $C(i,j)$ the migration cost between layer i and j, taken equal to $2c\Delta z|i-j|$, Δz the width of a bin and c the cost to migrate $1m$, ε_Z the assimilation efficiency of zooplankton and $\frac{M_\varphi}{M_Z}$ the weight ratio of phytoplankton and zooplankton organisms. For such strategy ij, the corresponding mortality risk is:

$$D_{ij}^N = MP((1-\sigma)b(night, i)\sum_{k=1}^{M} p_{ik} + \sigma b(day, j)\sum_{k=1}^{M} p_{kj}) - \mu, \tag{7.5}$$

with μ a background mortality rate. The mortality risk for prey is conversely a component of the predator's growth rate. For strategy ij, if we call η the conversion efficiency between prey and predator, the predator growth rate is then:

$$G_{ij}^P = \eta MN(\sigma b(day, j)\sum_{k=1}^{M} n_{kj} + (1-\sigma)b(night, i)\sum_{k=1}^{M} n_{ik}) - C(i,j). \tag{7.6}$$

The density-dependent mortality rate of predators is as follow:

$$D_{ij}^P = \mu_0 MP(\sigma\sum_{k=1}^{M} p_{kj} + (1-\sigma)\sum_{k=1}^{M} p_{ik}). \tag{7.7}$$

The fitness of prey is then $F_{ij}^N = G_{ij}^N - D_{ij}^N$, with a similar expression for the predator fitness F^P. The Nash equilibrium of the system is found using the replicator equation (Schuster and Siegmund, 1983; Hofbauer and Sigmund, 2003). In short, each strategy is allowed to grow proportionally to its fitness, before renormalization of the strategy matrices to ensure that condition 7.1 is satisfied.

$$\begin{cases} n'_{ij}(\tau + \Delta\tau) &= n_{ij}(\tau) + \Delta\tau F_{ij}^N(\tau), \\ p'_{ij}(\tau + \Delta\tau) &= p_{ij}(\tau) + \Delta\tau F_{ij}^P(\tau). \end{cases} \tag{7.8}$$

$$\begin{cases} n_{ij}(\tau+\Delta\tau) = \dfrac{n'_{ij}(\tau+\Delta\tau)}{\sum_k \sum_l n'_{kl}(\tau+\Delta\tau)}, \\ p_{ij}(\tau+\Delta\tau) = \dfrac{p'_{ij}(\tau+\Delta\tau)}{\sum_k \sum_l p'_{kl}(\tau+\Delta\tau)}. \end{cases}$$

$\Delta\tau$ is a factor selected to keep the increase or decrease of strategy frequencies within reasonable limits at each iteration. It is chosen at each iteration according to:

$$\Delta\tau \cdot \max(|F^N|, |F^P|) = \lambda. \tag{7.9}$$

As a practical compromise, we chose $\lambda = 0.1$. For all simulations, equilibrium was reached before $2 \cdot 10^6$ time steps.

Model B

Model B refers to a simple 1D tri-trophic model, considering population dynamics but not the behaviour of the different organisms. This model does not include light cycle nor organism migrations. The differential equations governing phytoplankton, zooplankton and fish dynamics are:

$$\begin{aligned} \frac{\partial \varphi}{\partial t} &= r(z)\left(1 - \frac{\varphi(z,t)}{K(z)}\right)\varphi(z,t) - \frac{M_\varphi}{M_Z} g N(z,t)\varphi(z,t), \\ \frac{\partial N}{\partial t} &= \varepsilon_Z \frac{M_\varphi}{M_Z} g N(z,t)\varphi(z,t) - m_0(z) N(z,t) P(z,t) - \mu N(z,t), \\ \frac{\partial P}{\partial t} &= \varepsilon_P m_0(z) N(z,t) P(z,t) - \mu_0 P(z,t)^2 - \mu_1 P(z,t), \end{aligned} \tag{7.10}$$

where r is the depth-dependent growth rate of phytoplankton, K its depth-dependent carrying capacity, g the clearance rate of copepods and m_0 the clearance rate of fish defined as $b_{max}\exp(-\kappa z)$. To mimic the growth description of zooplankton in Pinti and Visser (Pinti and Visser, 2019), the carrying capacity of phytoplankton was set as:

$$K(z) = \frac{K_0}{2}\left(1 - \tanh\left(\frac{z - z_0}{z_s}\right)\right), \tag{7.11}$$

with K_0 the surface carrying capacity, z_0 the depth of the mixed layer and z_s the thickness of the transition zone to a depleted layer. The growth rate $r(z)$ of phytoplankton depends on light:

$$r(z) = r_0 \exp(-\kappa z), \tag{7.12}$$

with r_0 the surface growth rate and κ the light attenuation coefficient.

The equilibrium distributions can then be derived analytically, and are (if we omit for readability the dependencies in time and depth)

$$\begin{aligned} N &= \frac{r\mu_0 \left[\varepsilon_Z \frac{M_\varphi}{M_Z} gK - \mu + m_0\mu_1/\mu_0\right]}{\varepsilon_P m_0^2 r + \varepsilon_Z \frac{M_\varphi^2}{M_Z^2} g^2 K \mu_0}, \\ P &= \frac{\varepsilon_P m_0 N - \mu_1}{\mu_0}, \\ \varphi &= \frac{m_0 F + \mu}{\varepsilon_Z \frac{M_\varphi}{M_Z} g} \end{aligned} \tag{7.13}$$

if all populations co-exist,

$$\begin{aligned} \varphi &= \frac{\mu}{\varepsilon_Z \frac{M_\varphi}{M_Z} g}, \\ N &= \frac{r(1-\varphi/K)}{\frac{M_\varphi}{M_Z} g} \end{aligned} \tag{7.14}$$

if only phytoplankton and zooplankton are present, and

$$\varphi = K \tag{7.15}$$

if only phytoplankton is present in the system.

In the particular case of an enrichment setting where the carrying capacity K of phytoplankton increases, the system consecutively admits (i) only phytoplankton, (ii) phytoplankton and zooplankton, and (iii) all three species. The transition from one regime to the next can be derived analytically. Zooplankton appear at:

$$K_1 = \frac{\mu}{\varepsilon_Z \frac{M_\varphi}{M_Z} g}, \tag{7.16}$$

and visual predators at:

$$K_2 = \frac{\varepsilon_P \mu r m_0}{\varepsilon_Z \frac{M_\varphi}{M_Z} g \left[\varepsilon_P m_0 r - \mu_1 \frac{M_\varphi}{M_Z} g\right]}. \tag{7.17}$$

The consecutive appearance of the three regimes depends on the set of parameters chosen, and happens only if $0 < K_1 < K_2$. With our set of parameters, we have $K_1 = 30$ and $K_2 = 30.001$, making the second regime indistinguishable on the figures.

Model C

Model C combines models A and B to consider both behaviour and population dynamics. In essence, we start by computing the Nash equilibrium in the strategy space as in model A, before updating the population sizes as in model B. At the behavioural time scale, we assume that processes are going much faster than at the population time scale, so the system should always be at equilibrium before any change at the population time scale takes place.

The clearance rate of zooplankton on prey is chosen such that the corresponding zooplankton growth rate when the resource is at its carrying capacity K_0 is equal to the growth rate of zooplankton at the surface in Pinti and Visser (2019). Zooplankton also suffer a low background mortality rate, to ensure that the absence of food drives them to extinction even without predation. The details of the game dynamics and the fitness definition are similar to model A. We call F^N (resp. F^P) the prey (resp. predator) fitness at the Nash equilibrium. We can define one such value for all organisms as, by definition of the Nash equilibrium, all organisms from the same population have the same fitness. Since phytoplankton have no behaviour, their fitness is of no interest other than in population dynamics.

At the population time scale, populations can grow and decay. Phytoplankton cannot change position, but as they are grazed upon by zooplankton their population sizes can also change. For simplicity, we ignore physical mixing between the different layers, and the concentration of phytoplankton in each layer is independent from the other layers and follows a chemostat. The population sizes are updated following functional responses type I:

$$\begin{aligned}
\frac{\partial}{\partial t}\varphi(z,t) &= \varphi(z,t)\left(r(z)\left(1-\frac{\varphi(z,t)}{K(z)}\right) - \sigma\frac{M_\varphi}{M_Z}gN_{day}(z) - (1-\sigma)\frac{M_\varphi}{M_Z}gN_{night}(z)\right)\\
\frac{d}{dt}N(t) &= N(t)F^N\\
\frac{d}{dt}P(t) &= P(t)F^P,
\end{aligned} \tag{7.18}$$

with r and K defined as in model B. Thereafter, the behavioural and population dynamic processes are looped until steady state is reached, for both population sizes and migration strategies.

Ecosystem functions

Trophic transfer efficiency

For models B and C, the trophic transfer efficiency was defined as the total consumption of zooplankton by fish divided by the total consumption of phytoplankton by zooplankton (Lindeman, 1942; Andersen, 2019) integrated over the total zooplankton population:

$$TTE = \int_{z=0}^{z=z_{max}} \frac{m_0 N(z,t)P(z,t)}{M_\varphi/M_Z gN(z,t)\varphi(z,t)}N(z,t)dz \tag{7.19}$$

The TTE was not defined for model A: because of the fixed population sizes, the system is not at equilibrium in terms of population sizes, and it is therefore unsure if the extra food eaten (i.e., the fitness in our set-up) is made available to the next trophic level through growth and reproduction or if it is simply egested.

Active carbon export

The active carbon export of prey and predators was defined as the amount of carbon that active migrants bring below a fixed depth (here set as 100m). It is therefore:

$$C^X_{exp} = (1-\sigma)\varepsilon_D m_{c,x-1}\tau_D \int_{z=0}^{z=100m} I_X(z,night)X_{night}(z,t)X_{migr}\Delta z dz. \tag{7.20}$$

X is a placeholder for prey and predator. $m_{c,x-1}$ is the carbon mass of the prey of X, ε_D is the fraction of ingested food I_X which is egested, and τ_D is the fraction of the food ingested at the surface that is egested at depth (to take into account e.g. digestion time). X_{migr} is the fraction of night surface residents that migrate back below 100 m:

$$X_{migr} = \frac{\int_{z=0}^{z=100m} X_{night}(z,t)dz - \int_{z=0}^{z=100m} X_{day}(z,t)dz}{\int_{z=0}^{z=100m} X_{night}(z,t)dz} \tag{7.21}$$

The total active carbon export of the food-web is defined as $C^N_{exp} + C^P_{exp}$.

The active carbon export for model B is always null: as there are no migrants in this model no carbon is actively transported below 100 m.

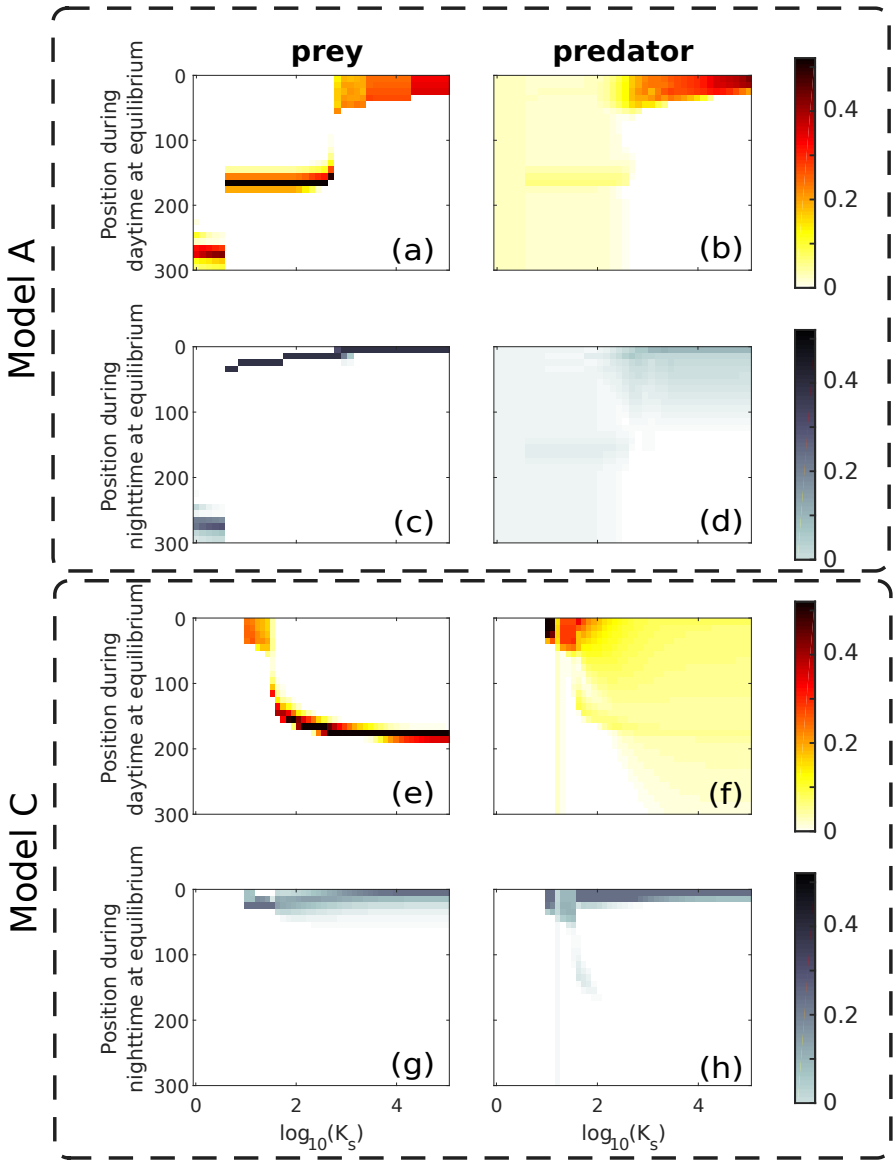

Figure 7.4: Distribution of zooplankton (panel a-c-e-g) and fish (panel b-d-f-h) during day (red) and night (blue) in model A and C as the phytoplankton carrying capacity increases.

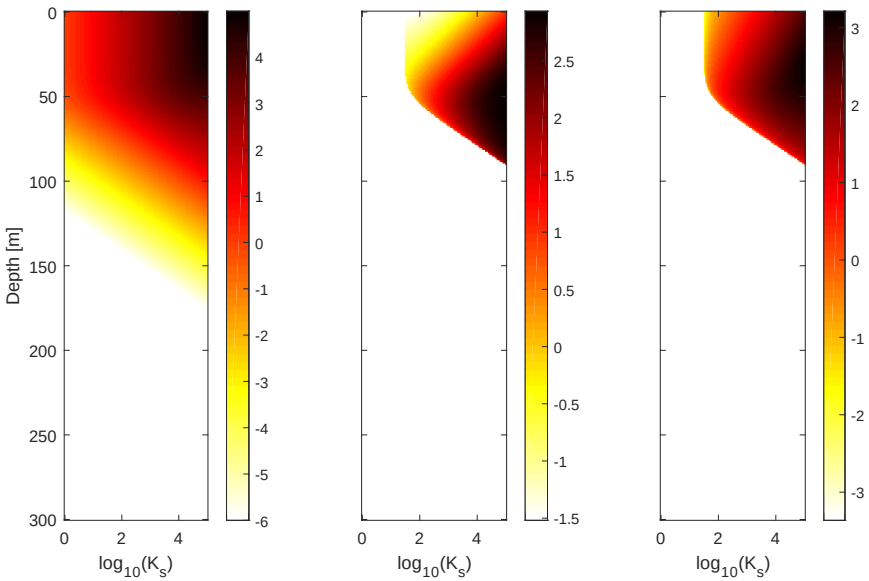

Figure 7.5: Distribution of phytoplankton, zooplankton and fish in model B (no behaviour) at equilibrium as the phytoplankton carrying capacity at the surface K_s varies. Note the logarithmic scale of the colour bars (unit is $\log_{10}(\mathrm{m}^{-3})$).

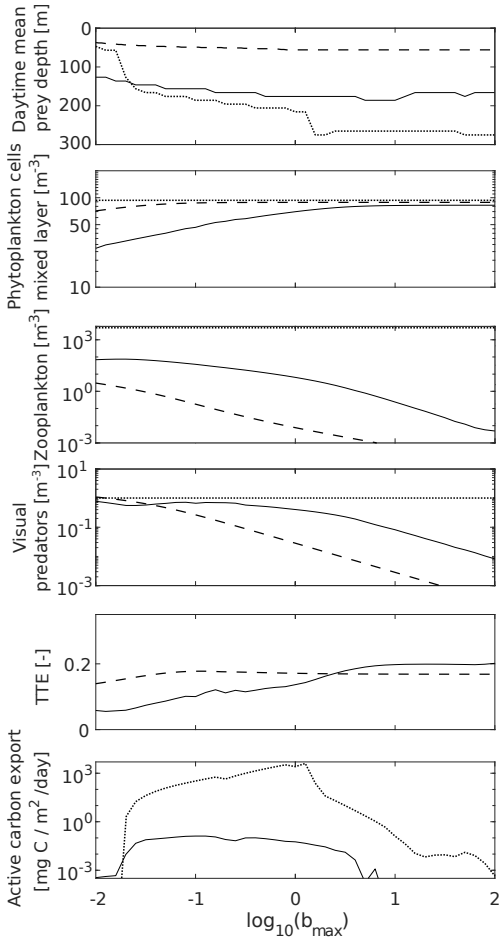

Figure 7.6: From top to bottom: Day mean prey position; phytoplankton, zooplankton and fish abundance; trophic transfer efficiency and active carbon export as a function of the predator maximum clearance rate b_{max}. Dotted lines for the model with only behaviour (model A), dashed lines for the model with no behaviour considerations (model B) and plain lines are for the model where both behaviour and population dynamics are considered (model C).

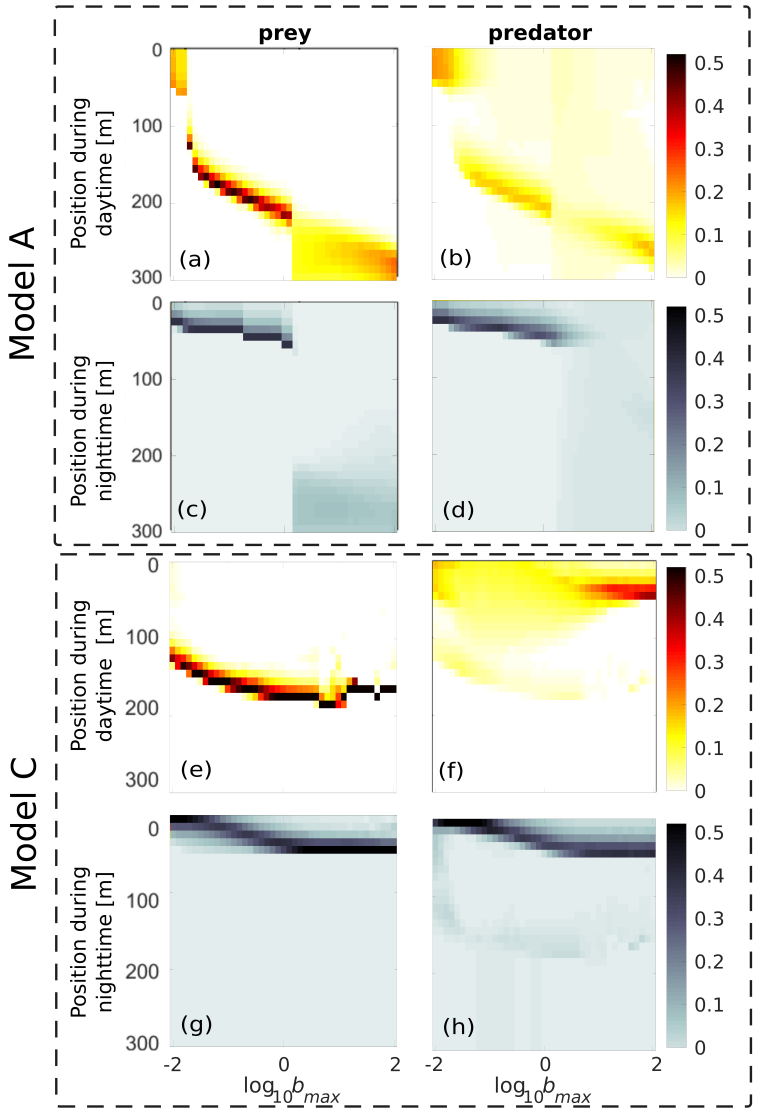

Figure 7.7: Distribution of zooplankton (panel a-c-e-g) and fish (panel b-d-f-h) during day (red) and night (blue) in model A and C as the predator maximum clearance rate b_{max} increases.

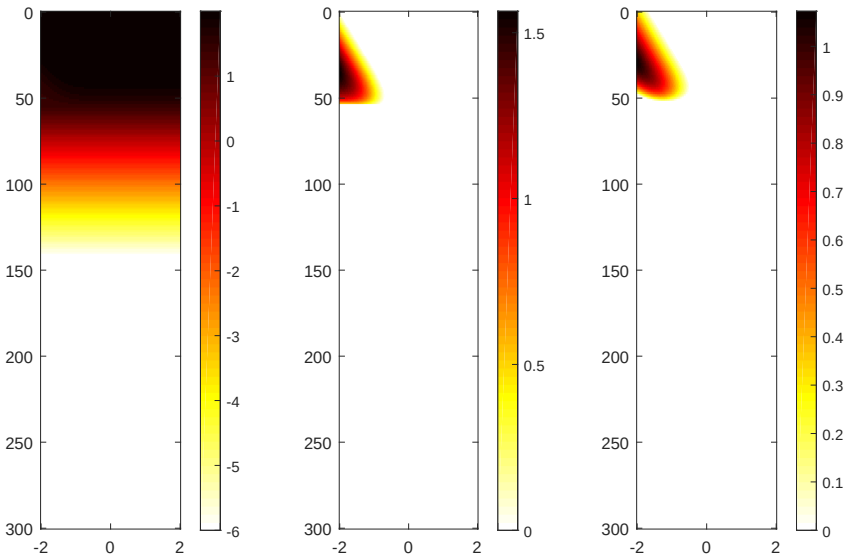

Figure 7.8: Distribution of phytoplankton, zooplankton and fish in model B (no behaviour) at equilibrium as predator maximum clearance rate b_{max} varies. Note the logarithmic scale of the colour bars (unit is $\log_{10}(\,\mathrm{m}^{-3})$).

Summary of all parameters used

Table 7.1: Glossary of parameters

Variable	Description	Value	Unit
t	Time	-	day
z	Depth	-	m
M	Number of water layers	30	-
Δz	Thickness of depth bins	10	m
z_{max}	Total depth of the water column	$M \cdot \Delta z = 300$	m
σ	Fraction of daylight hours per day	0.65	-
$N_{day/night}(z,t)$	Concentration of prey during day (night) at depth z	eq. 7.2	m^{-3}
$P_{day/night}(z,t)$	Concentration of predator during day (night) at depth z	eq. 7.2	m^{-3}
$\varphi(z,t)$	Concentration of resources at depth z	eq. 7.18	m^{-3}
$N(t)$	Mean prey concentration in the water column	eq. 7.18	m^{-3}
$P(t)$	Mean predator concentration in the water column	eq. 7.18	m^{-3}
$K(z)$	Carrying capacity for phytoplankton	eq. 7.11	m^{-3}
K_0	Surface carrying capacity for phytoplankton	10^4	m^{-3}
z_0	Mixed layer depth	50	m
z_s	Sharpness of the transition zone	10	m
$r(z)$	Growth rate of phytoplankton	eq. 7.12	day^{-1}
κ	Light attenuation coefficient of water	0.07	m^{-1}
r_0	Maximum growth rate of phytoplankton	1	day^{-1}
$F_N(t)$	Fitness of the prey population at time t	-	day^{-1}
$F_P(t)$	Fitness of the predator population at time t	-	day^{-1}
g	Clearance rate of zooplankton	10^{-1}	$\mathrm{m}^3\mathrm{day}^{-1}$
$\frac{M_\varphi}{M_Z}$	Weight ratio between phytoplankton and zooplankton	0.01	-
δt	Time step	0.01	day
$\mathbf{n} = n_{ij},\ \mathbf{p} = p_{ij}$	Frequency matrix of prey (predator) strategies	-	-
$\tau, \Delta\tau$	Time and time steps of the replicator dynamics	-	-
λ	Factor for the increase rate of the replicator equation	0.1	-
b	Predator clearance rate	eq. 7.3	$\mathrm{m}^3\mathrm{day}^{-1}$
L_{max}	Surface irradiance during daytime	100	Wm^{-2}
L_0	Half-saturation light intensity for visual predators	1	Wm^{-2}
ρ	Fractional difference between day and night light levels	10^{-3}	-
$G_{ij}^N,\ G_{ij}^P$	Growth rate of prey (predators)	eq. 7.4 and 7.6	day^{-1}
$D_{ij}^N,\ D_{ij}^P$	Mortality rate of prey (predators)	eq. 7.5 and 7.7	day^{-1}
$C(i,j)$	Migration cost for strategy ij	$2c\Delta z\lvert i-j\rvert$	day^{-1}
c	Cost to migrate 1m	10^{-5}	$\mathrm{m}^{-1}\mathrm{day}^{-1}$
μ	Background mortality rate of prey	0.01	day^{-1}
μ_0	Density-dependent mortality rate of predators	10^{-3}	$\mathrm{m}^3\mathrm{day}^{-1}$
μ_1	Mortality rate of predators	10^{-3}	day^{-1}
ε_Z	Zooplankton assimilation efficiency	1/3	-
ε_P	Fish assimilation efficiency	1/3	-
η	Predator growth efficiency	10^{-2}	-
m_0	Clearance rate of fish for zooplankton	$b_{max}\exp(-\kappa z)$	$\mathrm{m}^3\mathrm{day}^{-1}$
P_0	Mean concentration of fish in the water column	0.1	m^{-3}
b_{max}	Clearance rate of fish at the surface	-	$\mathrm{m}^3\mathrm{day}^{-1}$
TTE	Trophic transfer efficiency	eq. 7.19	-
C_{exp}^X	Active carbon export mediated by X	eq. 7.20	$\mathrm{gCm}^{-2}\mathrm{day}^{-1}$
X_{migr}	Fraction of DVM migrants between the epipelagic and the depths	eq. 7.21	-
ε_D	Fraction of ingested food egested	1/3	-
τ_D	Fraction of food ingested at the surface egested at depth	1/2	-
$m_{c,\varphi}$	Carbon weight of a resource	10^{-8}	gC
$m_{c,N}$	Carbon weight of a consumer	10^{-5}	gC
$I_X(z,t)$	Ingestion rate of an individual X	-	day^{-1}

Code accessibility

All MATLAB codes necessary to run the models are available online at `https://gitlab.gbar.dtu.dk/jppi/Frequency-dependent_behavior_of_interacting_populations_significantly_impacts_ecosystem_function`.

Bibliography

Abrams, P. A. (2007). Habitat choice in predator-prey systems: Spatial instability due to interacting adaptive movements. *American Naturalist*, 169(5):581–594.

Andersen, K. H. (2019). *Fish Ecology, Evolution, and Exploitation : A New Theoretical Synthesis*. Princeton University Press, monographs edition.

Bouskila, A. (2001). A habitat selection game of interactions between rodents and their predators. *Annales Zoologici Fennici*, 38(January 2001):55–70.

Brown, J. S., Laundre, J. W., and Gurung, M. (1999). The Ecology of Fear: Optimal Foraging, Game Theory, and Trophic Interactions. *Journal of Mammalogy*, 80(2):385–399.

Cressman, R. and Křivan, V. (2010). The ideal free distribution as an evolutionarily stable state in density-dependent population games. *Oikos*, 119(8):1231–1242.

Cressman, R., Křivan, V., and Garay, J. (2004). Ideal free distributions, evolutionary games, and population dynamics in multiple-species environments. *The American naturalist*, 164(4):473–489.

Dieckmann, U., Marrow, P., and Law, R. (1995). Evolutionary cycling in predator-prey interactions: population dynamics and the red queen. *Journal of Theoretical Biology*, 176(1):91–102.

Giske, J. and Aksnes, D. L. (1992). Ontogeny , season and trade-offs : Vertical distribution of the mesopelagic fish Maurolicus muelleri. *Sarsia*, 77:253–261.

Hairston, N. G., Smith, F. E., and Slobodkin, L. B. (1960). Community Structure , Population Control , and Competition. *The American Naturalist*, 94(879):421–425.

Hofbauer, J. and Sigmund, K. (2003). Evolutionary Game Dynamics. *Bulletin (New Series) of the American mathematical society*, 40(403):479–519.

Holt, R. D. and Lawton, J. H. (1994). The Ecological Consequences of Shared Natural Enemies. *Annual Review of Ecology and Systematics*, 25(1):495–520.

Houston, A. I., McNamara, J. M., and Hutchinson, J. M. C. (1993). General results concerning the trade-off between gaining energy and avoiding predation. *Philosophical Transactions of the Royal Society of London. Series B: Biological Sciences*, 341(1298):375–397.

Hugie, D. M. and Dill, L. M. (1994). Fish and Game: a game theoretic approach to habitat selection by predators and prey. *Journal of Fish Biology*, 45(Supplement A):151–169.

Iwasa, Y. (1982). Vertical migration of zooplankton: a game between predator and prey. *The American naturalist*, 120(2):171–180.

Kiørboe, T., Visser, A., and Andersen, K. H. (2018). A trait-based approach to ocean ecology. *ICES Journal of Marine Science*.

Klevjer, T. A., Irigoien, X., Røstad, A., Fraile-Nuez, E., Benítez-Barrios, V. M., and Kaartvedt, S. (2016). Large scale patterns in vertical distribution and behaviour of mesopelagic scattering layers. *Scientific Reports*, 6(1):19873.

Kondoh, M. and Ninomiya, K. (2009). Food-chain length and adaptive foraging. *Proceedings of the Royal Society B: Biological Sciences*, 276(1670):3113–3121.

Křivan, V. (2007). The Lotka Volterra Predator Prey Model with Foraging Predation Risk Trade-Offs. *The American Naturalist*, 170(5):771–782.

Křivan, V. and Cressman, R. (2009). On evolutionary stability in predator–prey models with fast behavioural dynamics. *Evolutionary Ecology Research*, 11(2):227–251.

Křivan, V. and Schmitz, O. J. (2003). Adaptive foraging and flexible food web topology. *Evolutionary Ecology Research*, 5(5):623–652.

Křivan, V. and Sikder, A. (1999). Optimal Foraging and Predator Prey Dynamics, II. *Theoretical Population Biology*, 55:111–126.

Lima, S. L. (1985). Maximizing feeding efficiency and minimizing time exposed to predators: a trade-off in the black-capped chickadee. *Oecologia*, 66(1):60–67.

Lima, S. L. (2002). Putting predators back into behavioral predator -prey interactions. *Trends in Ecology and Evolution*, 17(2):70–75.

Lima, S. L. and Bednekoff, P. A. (1999). Temporal Variation in Danger Drives Antipredator Behavior: The Predation Risk Allocation Hypothesis. *The American Naturalist*, 153(6):649–659.

Lindeman, R. L. (1942). The trophic aspect of ecology. *Ecology*, 23:399–418.

Mehner, T. and Kasprzak, P. (2011). Partial diel vertical migrations in pelagic fish. *Journal of Animal Ecology*, 80(4):761–770.

Ohman, M. D. and Romagnan, J.-B. (2016). Nonlinear effects of body size and optical attenuation on Diel Vertical Migration by zooplankton. *Limnology and Oceanography*, 61(2):765–770.

Oksanen, L., Fretwell, S. D., Arruda, J., and Niemelä, P. (1981). Exploitation Ecosystems in Gradients of Primary Productivity. *American Naturalist*, 118(2):240–261.

Pelletier, F., Garant, D., and Hendry, A. (2009). Eco-evolutionary dynamics. *Philosophical Transactions of the Royal Society B: Biological Sciences*, 364(1523):1483–1489.

Pinti, J., Kiørboe, T., Thygesen, U. H., and Visser, A. W. (2019). Trophic interactions drive the emergence of diel vertical migration patterns: a game-theoretic model of copepod communities. *Proceedings of the Royal Society B: Biological Sciences*, 286(1911):20191645.

Pinti, J. and Visser, A. W. (2019). Predator-Prey Games in Multiple Habitats Reveal Mixed Strategies in Diel Vertical Migration. *The American Naturalist*, 193(3):E000–E000.

Ripple, W. J. and Larsen, E. J. (2000). Historic aspen recruitment, elk, and wolves in northern Yellowstone National Park, USA. *Biological Conservation*, 95(3):361–370.

Ripple, W. J., Larsen, E. J., Renkin, R. A., and Smith, D. W. (2001). Trophic cascades among wolves, elk and aspen on Yellowstone National Park's northern range. *Biological Conservation*, 102(3):227–234.

Rosland, R. and Giske, J. (1994). A dynamic optimization model of the diel vertical distribution of a pelagic planktivorous fish. *Prog. Oceanogr.*, 34:1–43.

Sainmont, J., Andersen, K. H., Thygesen, U. H., Fiksen, Ø., and Visser, A. W. (2015). An effective algorithm for approximating adaptive behavior in seasonal environments. *Ecological Modelling*, 311:20–30.

Schmitz, O. J., Grabowski, J. H., Peckarsky, B. L., Preisser, E. L., Trussell, G. C., and Vonesh, J. R. (2008). From individuals to ecosystem function: toward an integration of evolutionary and ecosystem ecology. *Ecology*, 89(9):2436–2445.

Schoener, T. W. (2011). The newest synthesis: Understanding the interplay of evolutionary and ecological dynamics. *Science*, 331(6016):426–429.

Schuster, P. and Siegmund, K. (1983). Replicator Dynamics. *Journal of Theoretical Biology*, 100:533–538.

Sih, A., Ferrari, M. C., and Harris, D. J. (2011). Evolution and behavioural responses to human-induced rapid environmental change. *Evolutionary Applications*, 4(2):367–387.

Sinervo, B. and Lively, C. M. (1996). The rock-paper-scissors game and the evolution of alternative male strategies. *Nature*, 380(6571):240–243.

Start, D. (2020). Phenotypic plasticity and community composition interactively shape trophic interactions. *Oikos*, 00:1–11.

Stearns, S. C. (1989). Trade-Offs in Life-History Evolution. *Functional Ecology*, 3(3):259.

Steffen, W., Rockström, J., Richardson, K., Lenton, T. M., Folke, C., Liverman, D., Summerhayes, C. P., Barnosky, A. D., Cornell, S. E., Crucifix, M., Donges, J. F., Fetzer, I., Lade, S. J., Scheffer, M., Winkelmann, R., and Schellnhuber, H. J. (2018). Trajectories of the Earth System in the Anthropocene. *Proceedings of the National Academy of Sciences of the United States of America*, 115(33):8252–8259.

Thygesen, U. H. and Patterson, T. A. (2018). Oceanic diel vertical migrations arising from a predator-prey game. *Theoretical Ecology*, pages 1–13.

Titelman, J. and Fiksen, Ø. (2004). Ontogenetic vertical distribution patterns in small copepods: field observations and model predictions. *Marine Ecology Progress Series*, 284(1):49–63.

Visser, A. W., Mariani, P., and Pigolotti, S. (2012). Adaptive behaviour, tri-trophic food-web stability and damping of chaos. *Journal of The Royal Society Interface*, 9(71):1373–1380.

CHAPTER 8

Trophic interactions drive the emergence of diel vertical migration patterns: a game-theoretic model of copepod communities

Pinti J., Kiørboe T., Thygesen U.H., Visser A.W. (2019) Proceedings of the Royal Society B: Biological Sciences 286(1911): 20191645.

THE ROYAL SOCIETY PUBLISHING

PROCEEDINGS OF THE ROYAL SOCIETY B

BIOLOGICAL SCIENCES

Abstract

Diel Vertical Migration (DVM), the daily movement of organisms through oceanic water columns, is mainly driven by spatio-temporal variations in light affecting the intensity of predator-prey interactions. Migration patterns of an organism are intrinsically linked to the distribution of its conspecifics, its prey, and its predators, each with their own fitness seeking imperatives. We present a mechanistic, trait-based model of DVM for the different components of a pelagic community. Specifically we consider size, sensory mode, and feeding mode as key traits, representing a community of copepods that prey on each other and are, in turn, preyed upon by fish. Using game theoretic principles, we explore the optimal distribution of the main groups of a planktonic pelagic food-web simultaneously. Within one single framework, our model reproduces a whole suite of observed patterns, such as size-dependent DVM patterns of copepods and reverse migrations. These patterns can only be reproduced when different trophic levels are considered at the same time. This study facilitates a quantitative understanding of the drivers of DVM, and is an important step towards mechanistically underpinned predictions of DVM patterns and biologically mediated carbon export.

Keywords— Diel Vertical Migrations, Trait-based ecology, Food-webs, Game theory, Optimal strategies

8.1 Introduction

Diel Vertical Migration (DVM) is the daily movement of marine organisms between the surface and deep layers (Klevjer et al., 2016). The most common pattern consists of daytime residency at depth and night-time residency in the upper part of the water column (Klevjer et al., 2016). But this pattern can vary considerably, with respect to residency depths, the time spent at various depths, and the speed of ascent and descent (De Robertis et al., 2000; Holliland et al., 2012). These variations occur both within and between geographical locations, and the frequent presence of two or more densely populated layers reveals the existence of multiple migrating strategies in communities (Klevjer et al., 2016; Netburn and Koslow, 2015; Sourisseau et al., 2008).

Precisely what patterns of DVM emerge in an ecosystem depends on a variety of factors. The type of organisms involved in terms of species (Netburn and Koslow, 2015; Ariza et al., 2016), their means of detecting prey (e.g. visual or tactile) (Andersen and Sardou, 1992), life stages (Holliland et al., 2012) and size (Ohman and Romagnan, 2016; Falkenhaug et al., 1997) all influence the risk-benefit trade-off that an individual experiences at each depth during day and night, and thus its optimal DVM strategy. More subtly, the most fit strategy of an individual also depends on the abundance of the other players in the system – predators, prey and conspecifics – and the variety of strategies they undertake. With all players seeking to maximise their fitness, it is clear that all DVM strategies within an ecosystem can be interlocked giving rise to the multiple and varied patterns seen in nature.

Open ocean food-webs are usually complex, with a wide size-range of primary producers,

zooplankton, and fish. A study in the California current (Ohman and Romagnan, 2016) explored the DVM strategies of copepods and found that the day and night residency depths of these copepods varied systematically with their size. The smallest copepods, probably too small to be readily detected by visual predators, remain close to the surface at all times. The largest copepods, on the contrary, are likely to be conspicuous to predators even at night, and thus remain at depth all the time. In between, intermediate-sized copepods perform daily migrations of up to a hundred meters. Further, this size dependent pattern of copepod DVM varied spatially in the California Current in concert with environmental parameters such as phytoplankton biomass, stratification and water clarity. Understanding quantitatively the mechanisms behind these migrations patterns is important not only in itself, but also because DVM is a direct driver of several ecosystem functions. For example, trophic interactions within a food-web are greatly affected by migration and by the spatial and temporal overlap of predators and prey. Active carbon transport (Aumont et al., 2018) is directly linked to the migration patterns of the different individuals in the water column, as they actively transport resources to the depths, providing deeper residents with valuable food resources (Trueman et al., 2014) and ultimately promoting pelagic - benthic coupling. Assessing different ecosystem functions on a global scale is difficult and estimates are poorly constrained: for instance, active carbon flux in the North Atlantic ocean was found to vary between 0.3 and 7.7 $\mathrm{gC\ m^{-2}\ yr^{-1}}$ (Hansen and Visser, 2016; Morales, 1999). The first step to refining such estimates is to better understand the drivers of the migration patterns and of their variability.

In this work, we present a simple framework based on three fundamental traits that determine trophic interactions in the plankton, namely an organism's size, whether it is a visual or tactile predator, and its feeding mode as either an active or ambush predator. We use game theory to assess the equilibrium distribution and daily migration patterns of all groups simultaneously. Given fixed population sizes, individuals of each population can choose their position in the water column at day and at night. Their choice does not only affect their own fitness, but also the fitness of their conspecifics and of individuals from other populations. To our knowledge, this is the first time that a model recreates diel vertical migration patterns for such a wide spectrum of planktonic organisms. The model is validated by reproducing observed size-dependent patterns of copepod migrations from different locations in the California Current Ecosystem (Ohman and Romagnan, 2016), and we show examples of how multiple optimal positions in the water column as well as reverse diel migration may emerge. We believe that this is also the first time that a mechanistic model is able to reproduce reverse migrations.

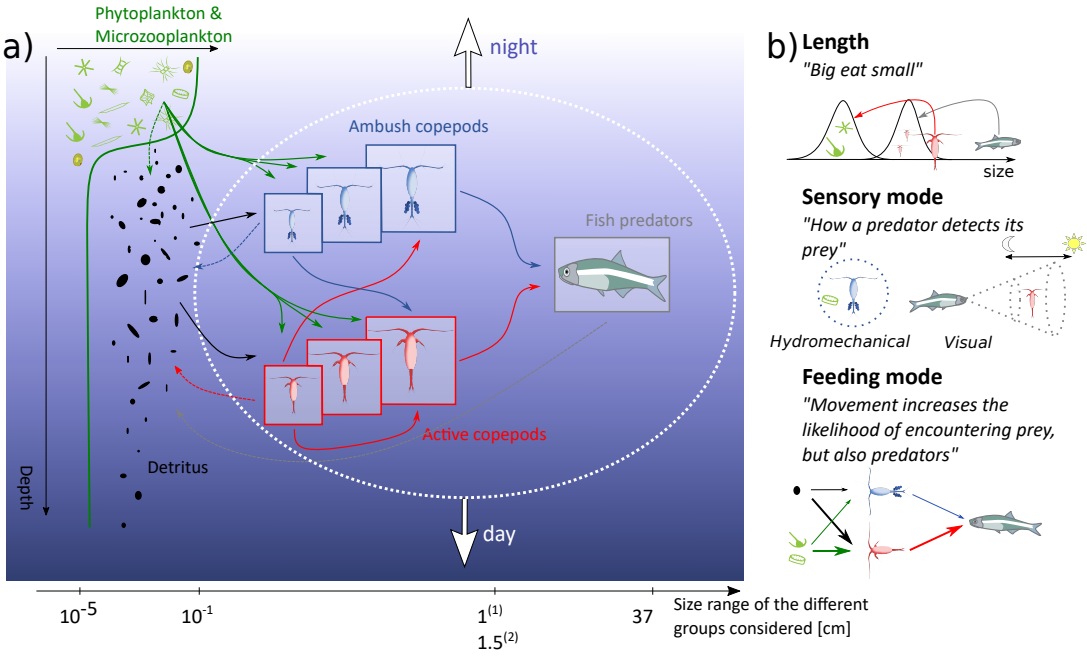

Figure 8.1: (a) Schematic representation of the model. We consider two classes of copepods, ambush (blue) and active (red) feeding, each sub-divided into k size classes. Copepods (tactile predators) can feed on phytoplankton, microzooplankton, detritus and smaller copepods. They are preyed upon by larger copepods and fish (visual predators). Note that the arrows indicate interactions but not their intensities, which are dictated by many factors (e.g., environmental conditions such as light levels, abundances of the different groups in the layer considered, size-preference functions). In order to maximise their fitness, all copepods and fish can adjust their vertical position individually at day and at night (example arrows here are for normal migration patterns, but reverse migrations and residency are also possible strategies). $^{(1)}$ in the body-length axis is for environmental scenarios 1-5, and $^{(2)}$ for environmental scenario 6. (b) The main influences of the three key traits (length, sensory mode, feeding mode) on predator-prey interactions.

8.2 Methods

Community set-up

The model considers a simple pelagic food-web consisting of phytoplankton, microzooplankton, copepods, and fish. We include particulate detritus created by the various components of this food web. The copepod community is divided into two feeding modes (ambush and active feeding), each further divided into a number of size classes (figure 8.1 (a)). Copepods can feed on phytoplankton and microzooplankton that are abundant near the surface, on smaller copepods (depending on size and feeding mode), and on the rain of particulate detritus produced by the overlaying community. In turn, copepods are predated by larger copepods (again, size and feeding mode rules apply) and visually feeding fish. Throughout the water column, copepods experience different conditions (concentration of phytoplankton, microzooplankton and detritus, light levels) that impact both their access to food and exposure to predators. Light conditions vary between day and night, and copepods and fish are all allowed to undertake DVM, each seeking their optimal strategy balancing feeding opportunity against risk. Since population dynamics are not considered, we make the simplification that the size distribution of organisms follows a Sheldon spectrum (i.e. equal biomass in groups of equal logarithmic size ranges (Sheldon and Parsons, 1967)). We note that the general approach is not dependent on this assumption, although it does reduce our parameter space in that fixing the phytoplankton biomass in the water column also fixes the biomass of all other groups. We also make the simplifying assumption that active feeding copepods constitute about 65% of the smallest size classes (total length 1mm) but almost 100% of the largest (total length 1cm), consistent with observations reported in a copepod database (Brun et al., 2016) (see section 8.6 for more details). The vertical distribution of phytoplankton (and microzooplankton) is prescribed with a typical profile - high in the surface and depleted at depths (Pinti and Visser, 2019), while all other organisms in the model can adjust their position in the water column freely at day and at night. The goal of an organism's DVM strategy is to maximise its fitness, which is defined as a trade-off between growth and mortality (Kiørboe et al., 2018a; Visser, 2007). Growth and mortality terms are derived from feeding interactions between all individuals (figure 8.1 (a)) that are described mechanistically with simple assumptions (prey size spectra, visual or tactile predation defining the clearance rates of organisms), see figure 8.1 (b) for a schematic representation of how traits influence these interactions and section 8.6 for a complete mathematical description of these interactions. Growth is equal to the assimilation rate (the ingestion rate modulated by an assimilation efficiency) minus a metabolic cost and a migration cost. Mortality is due to direct predation and to a background mortality term (i.e. predation from higher non-modelled trophic levels). Active copepods have a high encounter rate with prey as they sweep out a greater search volume per unit time than passive copepods that have to rely solely on the movement of their prey to bring about encounters (figure 8.1 (a)). Active feeding, however, has a downside in that it also increases the encounter rate with predators as well as incurring a higher metabolic cost (Visser

and Kiørboe, 2006). Preference functions of active and passive copepods are also different, active copepods generally eating relatively bigger prey than passive copepods (Kiørboe, 2016). Moreover, all organisms create detrital particulate material, which sinks and can be taken up again by flux feeding copepods (Stamieszkin et al., 2015). All things being equal, the encounter of flux feeding copepods with detrital material increases with depth due to coagulation that increases particle size and sinking speed (Jackson and Checkley Jr, 2011). A comprehensive description of the different rates, interactions and parameters is provided section 8.6.

Optimal migration patterns

For each group of migrating organisms (i.e., within the same size range and feeding mode; each "organism box" of figure 8.1 (a)), we want to know the proportion that follows each possible strategy ij (that is, being in water layer i during daytime and j during night-time). To this end, each group λ is allocated a strategy matrix $\mathbf{n}^{\lambda} = n_{ij}^{\lambda}$, where n_{ij}^{λ} is the proportion of organisms from the group λ following strategy ij. The optimal distribution is the set of matrices $\mathbf{n}^{\lambda *}$ that simultaneously maximise the fitness of all groups, with the additional property that within each group, the fitness for each occupied strategy (i.e. $\mathbf{n}^{\lambda *} > 0$) is identical and greater than the fitness for each unoccupied strategy (i.e. $\mathbf{n}^{\lambda *} = 0$). The optimal distribution of one group is obviously dependent on the distribution of all other groups, and the equilibrium of all groups is termed the Nash equilibrium (Nash, 1951). This equilibrium is the point where no individual from any group can change its strategy without decreasing its own fitness.

The Nash equilibrium is derived using the replicator equation (Hofbauer and Sigmund, 2003; Pinti and Visser, 2019). In short, the replicator equation allows each subgroup of individuals following a particular strategy to grow proportionally to its corresponding fitness. At each iteration, the biomass of all groups is renormalized to ensure that no biomass is added to the system. The algorithm is iterated many times (approx. $2 \cdot 10^6$), until it has converged. Because of the complexity of our model, the system reached an attractor but not a perfectly stable equilibrium in the presented simulations: some groups exhibited oscillations around an average distribution (see section 8.6 and figure 8.5 for more details). As a consequence, the results we present are averages of the distributions when the system has converged. Sensitivity analyses were performed on the most uncertain parameters (light saturation parameter for fish visual range, slope of the size spectrum, depth-dependent detritus preference function, size-dependent proportion of ambush and active copepods) of the model to test its robustness (section 8.6).

Definition of environmental scenarios

As a test case, we use size-dependent migration patterns observed in the California Current Ecosystem (Ohman and Romagnan, 2016). We created 5 environmental scenarios

(ES) corresponding to the environmental conditions encountered at 5 different oceanic locations, ordered from clear, oligotrophic conditions to more eutrophic, turbid ones. These environmental scenarios corresponded to the oceanic conditions encountered by Ohman and Romagnan at the time and locations of their study (Ohman and Romagnan, 2016). They assessed these patterns with a fine depth and size resolution, providing an ideal test of the robustness of our model to different oceanic conditions (figure 8.2 (a)). Between the different scenarios, only a few environmental parameters varied: the surface phytoplankton concentration, the depth of the mixed layer z_0, the extent of the transition zone z_m from nutrient-rich to nutrient poor waters, the total biomass of the system, the light attenuation coefficient, and the surface detritus concentration (table 9.17). These environmental parameters match the measured oceanic conditions reported when the migration patterns were observed (Ohman and Romagnan, 2016; Taylor and Landry, 2018). A 6^{th} environmental scenario was created, reflecting conditions observed in a temperate fjord, Dabob Bay (Washington, USA). This environmental scenario is particularly interesting as reverse migration of small copepods was observed in this fjord (Ohman et al., 1983; Ohman, 1990). Tactile predators up to 1.5cm long have been reported there, and we increased our size-range of zooplankton for that scenario so that our model matches the observed distribution.

Table 8.1: Glossary of parameters used for the 6 Environmental Scenarios (ES)

Parameter	Unit	Signification	ES 1	ES 2	ES 3	ES 4	ES 5	ES 6
P_0	gC m^{-3}	Phytoplankton surface concentration	0.042	0.16	0.27	0.65	0.74	0.23
z_0	m	Mixed layer depth	100	100	60	50	50	30
z_m	m	Sharpness of the transition zone	60	60	30	10	10	10
k_{light}	m^{-1}	Attenuation coefficient	0.03	0.07	0.1	0.2	0.6	0.1
SD	gC m^{-3}	Surface detritus concentration	0.005	0.02	0.03	0.06	0.1	0.05

8.3 Results

The general trends of the DVM patterns of copepods observed in the California Current (figure 8.2(a), (Ohman and Romagnan, 2016)) are reproduced by our model (figure 8.2(b)) under similar environmental conditions (table 9.17). The smallest copepods remain close to the surface (between 0 and 20m) without performing DVM. Their residency in this layer is more or less constant across environmental scenarios. The biggest copepods do not migrate either, remaining at depth day and night. Their

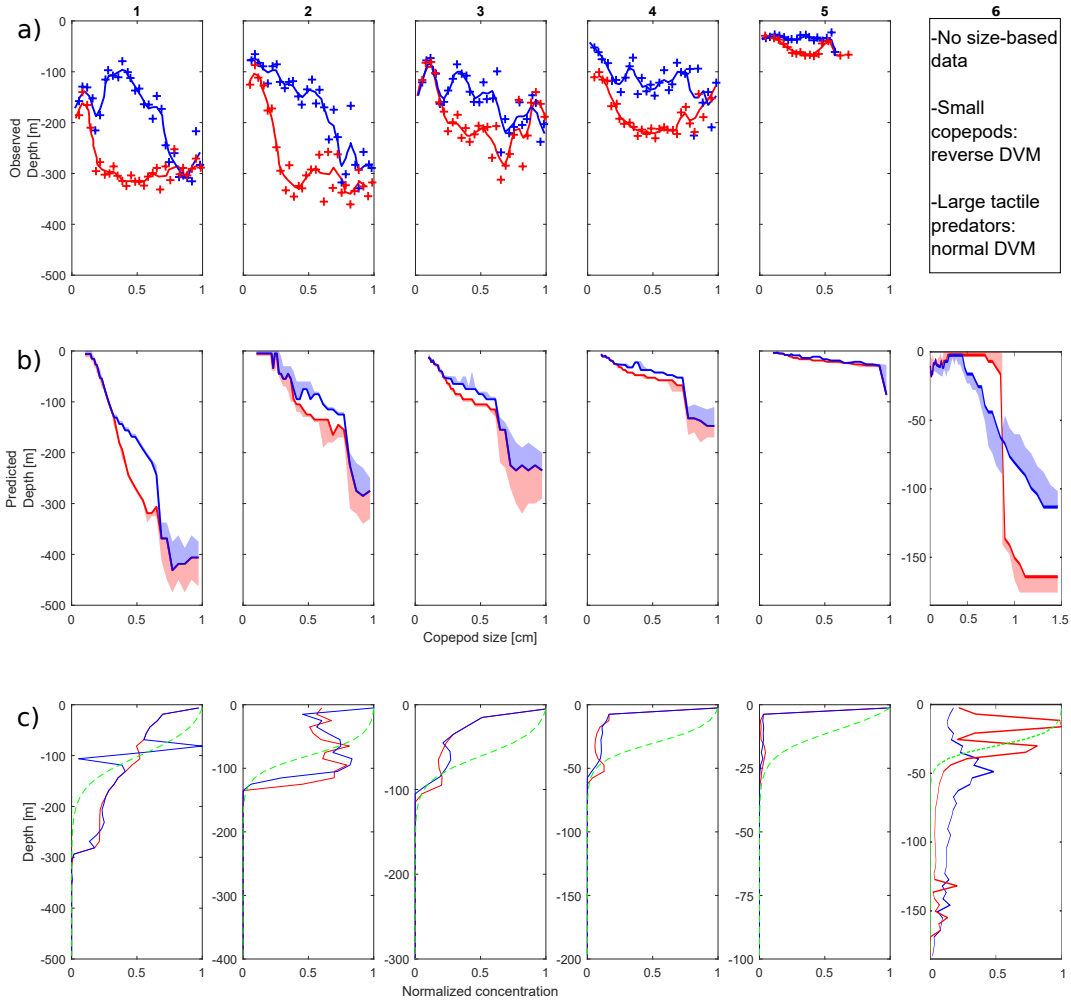

Figure 8.2: (a) Weighted mean depth as a function of copepod body size by day (red) and night (blue) at five different locations in the California Current. Points indicate means of duplicate profiles, and lines loess fits. Migration patterns are arranged from offshore clear water (left) to onshore more turbid waters (right). Data redrawn from Ohman and Romagnan (2016). (b) Simulated size-dependent median (and 1^{st} and 3^{rd} quartile—shaded areas) position of copepods at day (red) and night (blue) for conditions similar to the ones of the 5 experimental migration patterns of panel (a). (c) Simulated day (red) and night (blue) normalized fish distribution as well as prescribed normalized abundance of phytoplankton and microzooplankton (dashed green) in the water column. Note the change in vertical axis scale in the different figures of panel (c).

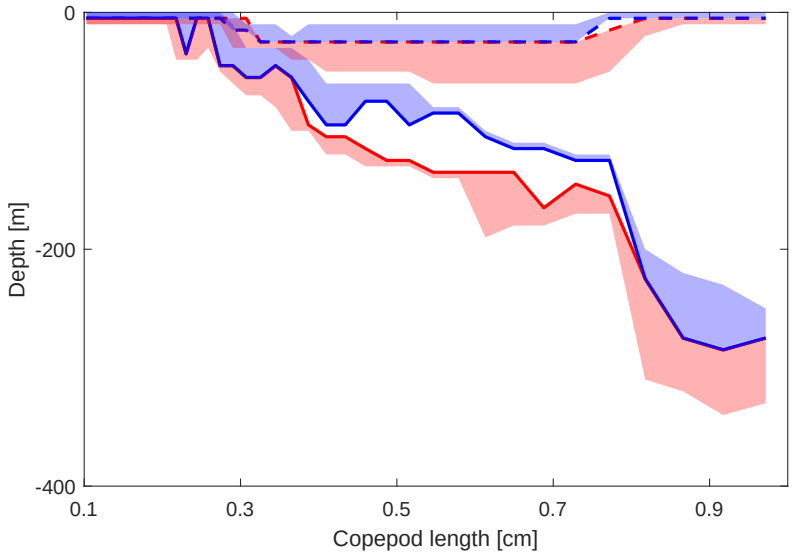

Figure 8.3: Modelled day (red) and night (blue) distribution of active and passive copepods in ES 2. Active copepods exhibit DVM (solid lines), while passive copepods remain at the surface (dashed lines).

residency varies from more than 400m for the open ocean to less than 100m for the most nearshore, turbid location. In between, intermediate-sized copepods (total length between approximately 2 and 7mm) undertake DVM. The day and night positions of these copepods get closer to the surface as the conditions get more eutrophic (i.e. more turbid), and the amplitude of migration also decreases: the biggest migration amplitude decreases from almost 100m (offshore-like conditions) to about 10m. With regards to feeding mode, it is active copepods that primarily undertake DVM, while passive feeders remain close to the surface at day and at night (figure 8.3).

Fish on the contrary display different behaviours depending on the conditions, but with very little or no clear DVM patterns. For very clear waters (ES 1), they display no major difference in their distribution between day and night: they are most numerous close to the surface, and their abundance steadily decreases until 300m, where their concentration suddenly becomes very low. In the 2^{nd} ES, fish do not exhibit strong DVM either, with day and night distributions confined to the upper 120 m with a weak maximum at around 80–100m deep. ES 3 displays a peak concentration around 30m, and decreases up to 100m, beyond which the concentration is almost null. The distribution of fish in ES 4 shows a peak at the surface before a strong decline, but with day-night differences: the day distribution is bimodal, with a second (lower) maximum around 80m. At night, fish that are part of this second peak migrate up

between 0 and 50m. In the last environmental scenario, fish mainly remain close to the surface, and a few remain day and night at depths up to 50m.

For the environmental scenario 6, three migration regimes are observed: no migration patterns and residency close to the surface for the smallest organisms (between 0.1 and 0.4cm), reverse migration patterns for intermediate-sized organisms (between 0.4 and 0.8cm), and normal DVM patterns for the biggest ones (0.8 to 1.5cm). Note that no residency at depth was found here for the biggest organisms.

8.4 Discussion

Our model successfully recreates the migration trends observed for different size classes of interacting copepods across a gradient of environmental conditions (Ohman and Romagnan, 2016; Ohman et al., 1983). The few discrepancies between observed and modelled patterns can be due to simplifications in our setup or uncertainties in the model parametrisation. For example, our vertical structure of phytoplankton and microzooplankton distribution near the surface is highly idealised. In particular, it is relatively common that the maximum phytoplankton abundance (and indeed maximum primary production) is sub-surface (Davis et al., 2008; Richardson, 2000). The maximum depth available to fish (and probably to large copepods) could also be limited by an Oxygen Minimum Zone (Netburn and Koslow, 2015). Further, we opted for a simple myopic fitness measure (Sainmont et al., 2015) and we do not consider ontogeny; but different life stages have different fitness goals, and their fitness measure varies accordingly. Despite these simplifications, our model captures the DVM behaviours of a full community only driven by environmental conditions and trophic interactions.

Trophic interactions as a DVM driver

To our knowledge, only two previous mechanistic models investigated DVM for more than one trophic level with a fine depth resolution, and both considered zooplankton prey interacting with planktivorous fish (Pinti and Visser, 2019; Thygesen and Patterson, 2018). Pinti and Visser (2019), in agreement with our study, found that zooplankton have three main migration regimes: surface residency under low predation pressure, DVM under intermediate predation pressure and residency at depth under high predation pressure. However, when the food-web becomes more complex (e.g. figure 8.2), it can be difficult to judge which organisms will have the highest predation pressure, and, thus, which migration regimes will emerge. Nevertheless, it is clear that organisms can only remain at depth if there is food available there. In our case, sinking detritus provided the largest copepods with the resources they need to survive at depth without migrating (cf. sensitivity analysis in the supplementary material). DVM patterns of fish are also very different from those reported in this previous

study and in many field studies (see e.g. Ariza et al. (2016); Mehner and Kasprzak (2011)): fish generally exhibit a much more pronounced DVM than our results show. This may be because DVM of forage fish is not only driven by prey abundance but also by their predators. While zooplankton in our model are effectively subject to frequency-dependent mortality (i.e. a dense layer of prey attracts more predators), fish are not subject to the same process, being exposed only to a constant mortality risk representing top predators. The absence of these potentially migrating top predators in our simulations may explain why only few fish undertake DVM. Planktivorous fish DVM is here only triggered by a bottom-up approach, and adding explicitly top predators may induce a stronger DVM response due to an added top-down control.

There have been only a few observational studies of DVM distinguishing between the multiple groups or species within (and across) different layers. In the Atlantic, it was found that multiple densely populated layers were mainly due to different species of fish and cephalopods having distinct DVM behaviours (Ariza et al., 2016). In contrast, multiple dense layers in the St-Lawrence were due only to krill (Sourisseau et al., 2008) that could switch between the different layers, suggesting that they had the same fitness in all these layers, possibly because of the presence of different prey (as it is the case for fish in our study). Organisms from very similar species can have different migration strategies (Longhurst, 1985), and organisms from the same species can have completely different DVM patterns – e.g. normal and reverse – in the coastal or open ocean (Irigoien et al., 2004). Also, while many copepods migrate, a substantial proportion of the community can remain resident at depth day and night, for example in the North East Atlantic (Roe, 1984) or in the Irish Sea (Irigoien et al., 2004). A common rule validated by our study is that bigger organisms migrate deeper (Longhurst, 1985; Irigoien et al., 2004; Holliland et al., 2012) and that the large organisms usually do not migrate at all (Longhurst, 1985; Irigoien et al., 2004) – even though the contrary is possible (Atkinson et al., 1992).

The biggest copepods, resident at depth, require a resource at depth to be able to survive. We hypothesised that this resource is a flux of detritus produced by the discard of the overlaying zooplankton community. While other non-modelled sources of food (extra zooplankton, benthic organisms in shallow water columns) might also play a role, our modelled particle flux is sufficient to support these big copepods at depth. In this, the coagulation process by which small detrital particles coalesce into larger faster sinking particles was an important factor to provide a sufficient flux to fuel the residency of the biggest copepods at depth. Model runs where this process was not included failed to replicate the non-migratory deep-residence of large copepod (cf. sensitivity analysis of the depth-dependent detritus preference function in the supplementary material) suggesting that their migration patterns may be substantially different in areas where detritus does not coagulate or where it gets broken down quickly.

An important feature highlighted by this study is that trophic interactions can lead to distinctly different DVM patterns for different organisms within the same water column, providing a possible explanation for the multi-modal distributions that are consistently observed in the world ocean basins (Klevjer et al., 2016), but

also for singular patterns such as reverse migrations. Our study focused on a few oceanic conditions where size-dependent DVM patterns are known, but we believe that provided with the correct set of environmental parameters the model could very well reproduce other patterns, and they should be investigated more systematically. For example, if the largest copepods consistently remain at depth, global estimates of DVM-mediated carbon exports could be very biased if the entire community is thought to behave alike (such as in Aumont et al. (2018)). In a context of global change where copepods are likely to become smaller in general (Garzke et al., 2015, 2016; Daufresne et al., 2009), our model indicates that active carbon exports by migrating copepods could decrease if the abundance of intermediate-sized copepods migrating vertically decreases as well. But many other factors have to be taken into account (such as higher metabolism at increased temperatures), and the future of active carbon transport by zooplanktonic migrants remains uncertain (Steinberg and Landry, 2017; Passow and Carlson, 2012).

Trait-dependent DVM

Size is often recognised as a master trait (Kiørboe et al., 2018b), governing the main vital rates of organisms (Kiørboe and Hirst, 2014a) as well as trophic interactions, and thus greatly influencing DVM patterns of plankton.

In addition to size, feeding mode shapes trade-offs that are different enough to trigger very different behaviours (figure 8.3); while active feeding copepods migrate, passive (i.e. ambush) feeding copepods remain resident at the surface. We are not aware of any study that looked specifically at the relation between DVM and feeding mode, but a few studies investigating DVM patterns at the species level corroborate our findings (Irigoien et al., 2004; Longhurst, 1985; Moraitou-Apostolopoulou, 1971): active copepods predominantly perform DVM, while ambush copepods tend to remain resident at a particular depth. In areas where a particular species dominates (active or passive feeder) this difference could cause very different migratory patterns at the community level, impacting in turn the magnitude of the biological pump.

Further, male and female copepods seem to have a different behaviour (Roe, 1984). It is unclear if this difference is only due to a significant size difference between males and females changing their respective trade-offs, or if the trade-off itself is different irrespective of size, for example because of different reproductive investments. In many calanoid species, males feed less than females (or not at all) (Gilbert and Williamson, 1983) and can thus remain deeper. In egg-carrying species, females do not risk only their own lives but also their offspring's, and seem to remain deeper than the individuals without eggs (Bollens and Frost, 1991b).

Traits and trait-based approaches are proving more and more useful to solve complex issues in marine ecosystems (Kiørboe et al., 2018b). Predator-prey interactions often occur between many different species simultaneously, and trait-based approaches can be particularly useful in these cases as they can reduce the system complexity

significantly. For example, trait-based approaches allow drawing conclusions on predator-prey interactions in little-studied ecosystems such as fresh waters (Boukal, 2014), considering complex feeding interactions between marine mammals and many different prey species (Spitz et al., 2014), predicting the outcome of potential invasive species in coral reefs (Green and Côté, 2014), as well as estimating ecosystem functions at an oceanic scale (Brun et al., 2019).

The role of light and proxies of DVM

Light levels are of great importance for the depth distribution of organisms in the water column (Frank and Widder, 2002), but the underlying mechanism is quite uncertain (Onsrud and Kaartvedt, 1998; Cohen and Forward Jr, 2009). Several studies explored the role of light in triggering DVM, mostly through the isolume hypothesis: zooplankton always remain at a constant light level (Cohen and Forward Jr, 2009). However, studies considering this hypothesis only partially validate it, either because zooplankton follow the isolume only during part of the day (Onsrud and Kaartvedt, 1998) since they cannot keep up with a rapid change in light intensity (Kampa, 1975), or because only organisms of particular stages and species follow an isolume (Daase et al., 2008). The isolume hypothesis also fails to explain the quick response of zooplankton to the presence of predators in the water column (Bollens and Frost, 1991a), the emergence of reverse migration patterns, or even the presence of complete residency at certain depths. While light is a very important driver of DVM (Cohen and Forward Jr, 2009), and can be an important sensory proxy for migrating animals, it cannot be considered its only driver without oversimplifying the DVM process.

Variations in the light attenuation coefficient alone could not explain the differences between the five environmental scenarios from the California Current. A combination of different factors such as productivity and mixed layer depth is important when it comes to understanding the observed patterns. For high food abundance for instance, copepods can reduce their foraging time or feed in somewhat deeper waters, reducing their presence in light waters and thus their mortality risk. Abundance of food reduces the need for DVM. Our study emphasises the importance of prey and predator abundance as drivers of DVM patterns, but a justification on how organisms effectively sense and react to such abundance changes remains to be found.

Alternative defence mechanisms for pelagic organisms

While DVM is a key defence mechanism against predation in the pelagic, alternative defence strategies also exist. For example, schooling is seen as a way to decrease predation risk (Partridge, 1982), and can thus be understood as a potential way to overcome the need for DVM. Schooling behaviours can also be adopted in complement to DVM, and often depend on the period of the day. Fish tend to disaggregate at night (O'Driscoll and McClatchie, 1998; Solberg and Kaartvedt, 2017), sometimes in concert with an upward migration (Solberg and Kaartvedt, 2017). However, schooling is not

always an appropriate strategy, as it can also attract predators and increase predation pressure (Nicol and O'dor, 1985). But this very fact may also attract the predator's predator, a process known as indirect trophic interaction. Piscivorous fish have been reported to patrol within krill swarms, on the look-out for potential planktivorous fish attracted by the swarms (Kaartvedt et al., 2005). Here, the krill strategy can be compared with a strategy of reverse diel vertical migration: in both cases, the association with a dangerous area or species for predators offers some protection against them.

Moreover, we consider only two periods during a day: daytime and night-time. But light levels between these two periods vary smoothly, and this can provide fish with an extra incentive to change their distribution during transitions between day and night. Transition periods are risky for copepods whose visibility would suddenly increase if they do not time their ascent or descent optimally with light levels. Feeding rates increase tremendously at dawn and dusk (Thygesen and Patterson, 2018), and for some fish up to 90% of the feeding has been found to take place during these transition times (Andersen et al., 2017). Thus, bigger copepods suffer a higher mortality risk at dawn and at dusk than smaller ones, and the smaller copepods spend significantly more time at the surface than their bigger counterparts (De Robertis, 2002). We decided not to include this extra complexity in the model, as it would increase computation time tremendously.

While DVM is one strategy that seeks to balance feeding opportunity with risk, other strategies, often used in concert with DVM, are also found. For instance, as visual predation is a main driver of copepod DVM, organism transparency can offset part of the risk of feeding at the surface. This is a strategy followed by some otherwise transparent species which migrate in tune to their gut fullness; digesting a meal at depth and returning to the surface to feed with an empty gut (Tsuda et al., 1998; Onsrud and Kaartvedt, 1998). Alternatively, some zooplankton species are adapted to survive in low oxygen conditions. Indeed, OMZs (Oxygen Minimum Zones, zones depleted of oxygen where most fish cannot survive for long (Sewell and Fage, 1948)) are present in some marine ecosystems, primarily in upwelling regions. Copepods adapted to low oxygen conditions can take refuge in OMZs shallower than their "normal" migration depths (Netburn and Koslow, 2015; Flint et al., 1991), thus remaining inaccessible to predators non-adapted to low oxygen conditions while shortening their DVM amplitude. This can explain why our copepod distributions in the clearest environmental scenarios (1–2) are more spread than observed in the California Current (Ohman and Romagnan, 2016; Netburn and Koslow, 2015). Being in cold waters at depth also reduces metabolism (Brown et al., 2004) and is thus a way to increase fitness (Fiksen, 1995). The internal state of a copepod can also be an incentive to migrate or not: a starving organism may be willing to face more risk and go closer to the surface than one with a full stomach, or additionally, an organism with a full gut would be more conspicuous to a visual predator than one with an empty gut. This idea gave rise to the "foray hypothesis" (Leising et al., 2005): if a copepod already has a full stomach there is no benefit in staying at the surface. The migration patterns of an individual then depend on the time it takes the individual to fill and empty its

stomach, and will consist of many ascents to feeding areas followed by descents into safe depths as soon as its stomach is full.

8.5 Conclusion

Using game theory, we have shown that DVM patterns of zooplankton and planktivorous fish do not depend only on light levels and environment conditions but also on the structure of the pelagic food-web. Within a single framework, we provide an explanation for the wide variety of migratory patterns observed in nature, including multi-modal distributions and reverse migrations (Klevjer et al., 2016; Ohman et al., 1983). To our knowledge, this is the first time that a model provides such an explanation, and the first time that a model provides DVM patterns for so many different organisms at the same time. It shows the importance of considering trophic interactions when modelling DVM in general.
Understanding and quantifying the drivers of vertical migratory behaviours under different oceanic conditions is vital as it can lead to more precise estimates of DVM patterns worldwide, and of carbon actively transported to the depths by migrating organisms, which can be a substantial part of the carbon pump (Hansen and Visser, 2016; Aumont et al., 2018). It is clear from this work that all aspects of the marine food-web are implicated in this active transport, not just as primary agents but also in setting the environmental parameters which govern DVM and its associated flux. How climate change will affect the emergent community structure of marine ecosystems and its cascading effects for the active carbon flux remains an important question for Earth system research.

Data, code and material

The source code (written in MATLAB) supporting this article has been uploaded as part of the supplementary material.

Competing interests

The authors declare to have no conflict of interest.

Author's contributions

J.P., T.K. and A.W.V designed the study; J.P. conceptualized the model with help from U.H.T. and A.W.V.; J.P. coded the model; J.P. analyzed the results with the help of all authors. J.P. wrote the paper with contributions from all authors.

Acknowledgements

We thank Ken H. Andersen and Mark Ohman for fruitful discussions throughout the development of this project, as well as Hans van Someren Gréve for the copepod drawings of figure 8.1. We are grateful to three anonymous reviewers, whose comments and suggestions helped us to improve this manuscript.

Funding

This work was supported by the Centre for Ocean Life, a VKR Centre of excellence funded by the Villum Foundation, and by the Gordon and Betty Moore Foundation (grant #5479).

8.6 Supplementary material

This supplementary material refers to the article Trophic interactions drive the emergence of diel vertical migrations: a game-theoretic model of copepod communities, published in 2019 in Proceedings B. The article doi is: 10.1098/rspb.2019.1645 .

Size distribution and abundance of different classes

As this is a static model, the total abundance of all groups in the water column is fixed. The size-distribution of organisms is meant to be simple and follows a Sheldon spectrum (same biomass in intervals of the same length on a logarithmic axis) (Sheldon and Parsons, 1967; Sheldon et al., 1972). For all groups, we fix the minimum and maximum size (table 8.2), and the concentration is then derived from the Sheldon spectrum (eq. 8.1). As a boundary condition, we fix the concentration of phytoplankton to P_0, measured in gC m^{-3} (grams of carbon per cubic meter). Phytoplankton are distributed over a size interval, from $l_{P,min}$ to $l_{P,max}$. The concentration X of a generic class of minimum size l_{min} and maximum size l_{max} is then:

$$X = \int_{l_{min}}^{l_{max}} \frac{1}{l} \frac{P_0}{\ln(l_{P,max} l_{P,min})} \mathrm{d}l = P_0 \frac{\ln(l_{max}/l_{min})}{\ln(l_{P,max}/l_{P,min})} \qquad [\,\mathrm{gC\ m^{-3}}]. \tag{8.1}$$

For simplicity (and to decrease computing time), we then compute the average size within the classes or populations and consider that each class is only constituted of average individuals. While this can lead to substantial bias when the size classes are very wide, as we increase the number of size classes (i.e. decrease the width of each size class) the approximation becomes more and more accurate.

For copepods, there is an extra layer of complexity. Firstly, the distribution of copepods between ambush feeders and active feeders is defined by the fraction of active feeders $\beta(l)$. This fraction is found by dividing the 162 copepod species for which the feeding regime and the length is available from Brun et al.'s database (Brun et al., 2016) into 16 logarithmically-sized

Table 8.2: Size ranges of the different components of the food web (note that copepods are further divided in 40 logarithmically spaced size classes). (1) is for environmental scenarios (ES) 1-5, (2) is for ES 6.

Group	Min. size [cm]	Max. size [cm]
Phytoplankton	10^{-5}	10^{-3}
Microzooplankton	10^{-3}	10^{-1}
Copepods	0.1	$1^{(1)}$, $1.5^{(2)}$
Fish	$1^{(1)}$, $1.5^{(2)}$	37

bin classes (figure 8.4). The fraction of active feeders for each bin is computed, and the following function is fitted to the resulting data:

$$\beta(l) = \frac{l^a + b}{l^a + c}, \tag{8.2}$$

yielding $a = 9.2951$, $b = 157.132$ and $c = 241.4225$ ($R^2 = 0.83$). Note that the choice of this function is empirical rather than mechanistic.
Secondly, the copepods are divided into size classes. There is the same biomass in all size classes, so the length span of the size classes is increasing logarithmically with individual length in agreement with Sheldon's hypothesis.

Conversion factors

Conversion factors between length, wet weight and carbon weight are assumed to be the same for fish and zooplankton (table 8.3). Unless stated differently, all units are in gC (carbon weight), g (wet weight) and cm (length).

Table 8.3: Conversion factors (Andersen, 2019)

plankton and fish	From length (cm)	From wet weight (g)
To carbon weight (gC)	$1.25 \cdot 10^{-3} l^3$	$0.125 Ww$
To wet weight (g)	$0.01 l^3$	Ww

Phytoplankton and microzooplankton

We ignore the large-scale motility of these communities (both vertically and horizontally), so their distribution in the water column is fixed. Phytoplankton cannot swim, whereas microzooplankton do swim (but do not move much in total, as we assume that they cannot change their vertical position). Their distributions in the water column are given by the functions $P(z)$ and $M_Z(z)$, defined as Pinti and Visser (2019):

$$\begin{cases} P(z) &= \frac{P_0}{2} \quad (1 - \tanh(\frac{z - z_0}{z_m})) \\ M_Z(z) &= \frac{M_{Z_0}}{2} \quad (1 - \tanh(\frac{z - z_0}{z_m})). \end{cases} \tag{8.3}$$

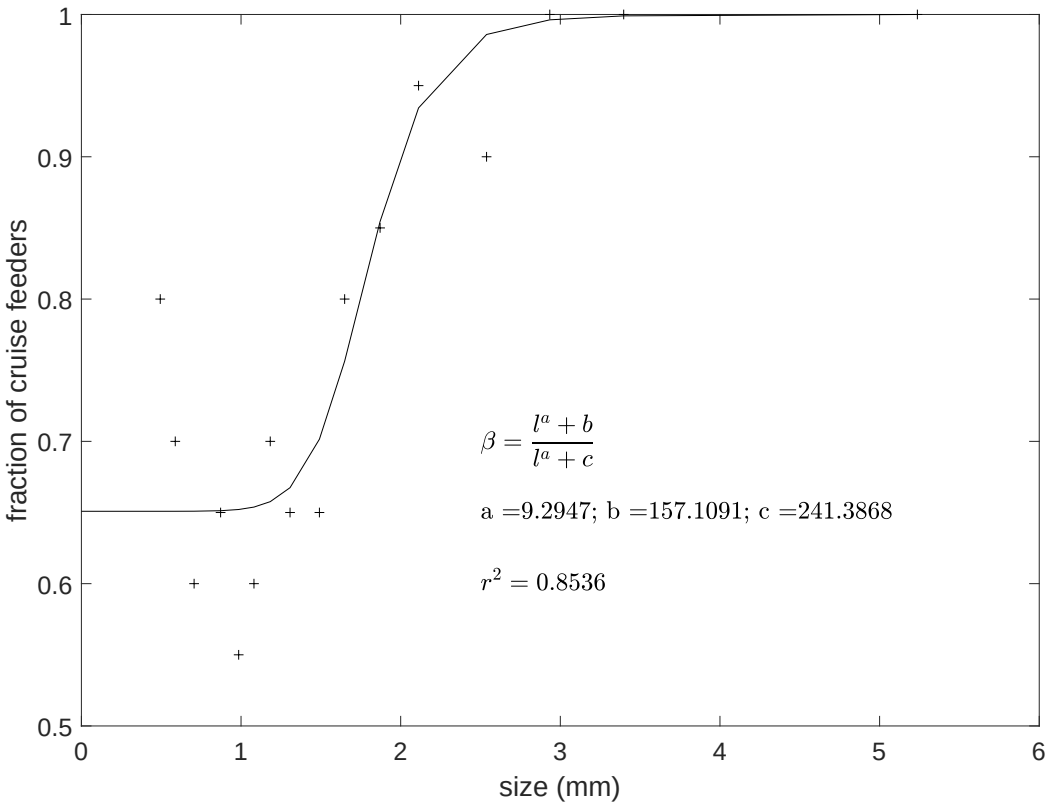

Figure 8.4: Proportion of cruise feeders species as their average size increases. Data extracted from (Brun et al., 2016).

From P_0 we may derive the mean phytoplankton P_{mean}, given by:

$$P_{mean} = \frac{\int_0^Z P(z)\mathrm{d}z}{Z}, \tag{8.4}$$

where Z is the total depth of the water column. We assume that the Sheldon spectrum (Sheldon and Parsons, 1967; Sheldon et al., 1972) holds for all size classes of our model, and not only in the smallest phytoplankton. Moreover, all communities have non-overlapping size ranges, so $M_{Z,mean}$ and P_{mean} are related by:

$$M_{Z,mean} = P_{mean}\frac{\log_{10}(l_{MZ,max}/l_{MZ,min})}{\log_{10}(l_{P,max}/l_{P,min})}. \tag{8.5}$$

Vital rates

(i) Fitness

The optimal behaviour that we are interested in is the one that maximises the reproductive output of the individual. To avoid complicated and tedious life-time calculations, we use a fitness proxy based on the growth and mortality of the individual, either Gilliam's rule (Gilliam and Fraser, 1987) or the difference between growth and mortality depending on the sign of the growth rate (Kiørboe et al., 2018a):

$$\begin{cases} Fit = \frac{Growth}{Mortality} \text{ if } Growth > 0 \\ Fit = \frac{Growth - Mortality}{\mu} \text{ if } Growth < 0, \end{cases} \tag{8.6}$$

with μ a constant mortality rate (to ensure that the fitness always has the same unit) taken equal to μ_0 for zooplankton and 1 day^{-1} for fish.

The growth rate is defined as the assimilation rate subtracted by the metabolic rate and a migration cost accounting for the strategy chosen by the individual. The mortality rate is the sum of the predation rate (when applicable) and of a constant background mortality rate. For migrating organisms, the fitness is defined as the weighted mean of their fitness at their day and night residency (minus the migration cost). For simplicity, we assume that daytime occurred during a fraction $\sigma = 0.6$ of a day and nighttime during $1 - \sigma = 0.4$, thus neglecting the transition periods at dawn and at dusk.

(ii) Assimilation rate

The assimilation rate ν_k of a predator k depends on the ingestion rate of the predator for each prey type F_k^i in the following way:

$$\nu_k = \sum_{preyi} \varphi_k F_k^i \qquad [\text{gC day}^{-1}], \tag{8.7}$$

where φ_k is the assimilation efficiency of the predator(equal to 0.65 for fish and 0.7 for copepods (Acuña et al., 2011a)).
Predators (copepods or fish) cannot feed as much as they want, and we assume that their

ingestion rate is modulated with a Holling type II functional response (Holling, 1959). The ingestion rate of a predator k on a prey i is then:

$$F_k^i = \frac{I_{max}^k E_k^i}{I_{max}^k + \sum_{prey} E_k^i} \qquad [\text{gC day}^{-1}]. \tag{8.8}$$

I_{max}^k is the maximum ingestion rate of the predator k,and E_k^i is the attack rate of predator k for prey i. The maximum ingestion rate is a size-dependent function (Andersen, 2019):

$$I_{max} = 33.3Ww^{0.75}\,\text{g year}^{-1} = 0.054Wc^{0.75}\,\text{gC day}^{-1} = 3.6 \cdot 10^{-4} l^{2.25}\,\text{gC day}^{-1}. \tag{8.9}$$

The attack rate of a predator depends on its clearance rate V_k^i, the prey concentration Z_i and a preference function Φ as follows:

$$E_k^i = V_k^i \Phi(k,i) Z_i \qquad [\text{gC day}^{-1}]. \tag{8.10}$$

The clearance rate of an organism k on a prey i depends on its feeding mode, as detailed below. The preference function depends on the size and on the feeding mode of the predator (Kiørboe, 2016) and is defined as (Hartvig et al., 2011):

$$\Phi(k,i) = \exp\left(\frac{-\log_{10}\left(\frac{l_i}{l_k \psi}\right)^2}{2\sigma_{pref}^2}\right). \tag{8.11}$$

The preferred ratios ψ and their standard deviation σ_{pref} is given table 8.4.

Table 8.4: Preference parameters for predators (Kiørboe, 2016; Andersen, 2019)

Predator	ψ	σ_{pref}
Ambush copepods	0.16	0.1155
Active copepods	0.06	0.3091
Fish	0.10	0.33

Clearance rate of copepods:
The clearance rate of a copepod k on a prey i depends on its size and on both feeding modes (i.e. swimming habits) of the prey and the predator (van Someren Gréve et al., 2017):

$$V_k^i = (3600 \cdot 24 \quad \text{s day}^{-1}) \cdot \pi R_{k,i}^2 \sqrt{u_i^2 + u_k^2} \qquad [\text{m}^3\ \text{day}^{-1}]. \tag{8.12}$$

u is the swimming speed of the organism, prey or predator, and is defined as (Huntley and Zhou, 2004):

$$u = 0.483(10^{-3}Ww)^{0.275} = 0.128Wc^{0.275} = 0.0204l^{0.825} \qquad [\text{m s}^{-1}], \tag{8.13}$$

if the animal is moving (i.e. if it is an active microzooplankton, a cruising copepod, or a fish). In all other cases (i.e. phytoplankton and ambush predators), the swimming speed of the organism is set to 0 $\quad \text{m s}^{-1}$.
$R_{k,i}$ is the detection distance of the prey i by the predator k. This detection distance depends

on the size and the feeding modes of both organisms (van Someren Gréve et al., 2017):

$$R_{k,i} = (10^{-2} \quad \text{m cm}^{-1}) \cdot (r_k + r_i) \qquad [\text{m}]. \tag{8.14}$$

r_k is the encounter radius of the predator, $r_k = 1.4 l_k^{1.24}$ (Andersen et al., 2016) and r_i is the extension of the prey fluid signal if it is moving (taken equal to $2l$) or the radius of the prey $l_i/2$ if it does not (van Someren Gréve et al., 2017).

Clearance rate of fish:

The fish we consider in this model are planktivorous fish, that rely on light levels to detect prey, but that can also filter-feed if their visual range is too low. The visual clearance rate of a fish is as follows (Titelman and Fiksen, 2004):

$$V_{is-i,fish} = (3600 \cdot 24 \quad \text{s day}^{-1}) \cdot \gamma \pi R_{i,fish}^2 u_f \qquad [\text{m}^3 \text{ day}^{-1}], \tag{8.15}$$

with γ the fraction of cross-sectional area efficiently scanned (taken equal to 0.5), u_f the swimming speed of the fish as defined in equation 8.13 and $R_{i,fish}$ the light-dependent detection distance of a prey by a fish taken as (Bianchi et al., 2013b):

$$R_{i,fish} = R_0 \frac{l_i}{l_{ref}} \sqrt{\frac{\Lambda(z, day)}{K_e + \Lambda(z, day)}} \qquad [\text{m}]. \tag{8.16}$$

R_0 is the maximum detection distance for a prey of size l_{ref}, K_e a composite light-saturation parameter and $\Lambda(z, day)$ the light level (in W m^{-2}) at depth z and at time *day* (for us, day will be a simple boolean to express day and night). The light level can be expressed as (Bianchi et al., 2013b):

$$\Lambda(z, day) = \rho_l(day) \cdot L_0 \exp(-k_{light} z) \qquad [\text{W m}^{-2}], \tag{8.17}$$

with L_0 the surface illumination at day, k_{light} the light attenuation coefficient and ρ_l a factor equal to 1 at day and 10^{-5} at night, as illumination by moonlight can be significant for visual predators (Bollens and Frost, 1991a; Webster et al., 2013).
The filtering potential of a fish was modelled simply as the clearance rate of an organism with a filtering efficiency ζ cruising at a speed u:

$$F_{ilt-i,fish} = (3600 \cdot 24 \text{ s day}^{-1}) \cdot u_f \pi \cdot \zeta \cdot ((10^{-2} \text{ m cm}^{-1}) l_k/2)^2 \qquad [\text{m}^3 \text{ day}^{-1}]. \tag{8.18}$$

The clearance rate of a fish on a prey i is then the maximum of both terms:

$$V_{fish}^i = \max(V_{is-i,fish}, F_{ilt-i,fish}) \qquad [\text{m}^3 \text{ day}^{-1}]. \tag{8.19}$$

(iii) Metabolic rate

Metabolic rates are taken from group-specific regressions (Kiørboe and Hirst, 2014b). We took the original data and forced the slopes to be -1/4, as the authors acknowledge that deviations from this slope in their regressions is likely due to bias in measurements or a lack of data points (Kiørboe and Hirst, 2014b). For copepods, this yields the following regression:

$$T_k = 0.0052 W c_k^{-0.25} \qquad [\,\mathrm{day}^{-1}], \tag{8.20}$$

and for fish it yields:

$$T_{fish} = 0.0148 W c_k^{-0.25} \qquad [\,\mathrm{day}^{-1}]. \tag{8.21}$$

These regressions are in accordance with canonical expressions usually used (Andersen et al., 2017). Using group-specific equations prevents over-estimating metabolic cost of the smaller individuals (and the contrary for bigger ones): the slope is identical for all groups but the intercepts are group-specific (Kiørboe and Hirst, 2014b). For ambush predators, we decreased the metabolic cost by a rather arbitrary factor of 0.5, because they spend less energy than active predators as they are not moving around to encounter food.

(iv) Migration cost

The power related to the movement of a body in a fluid is related to the hydrodynamic drag D_r (Kiørboe et al., 2010):

$$D_r = \frac{1}{2}\pi C_D \rho \frac{((10^{-2}\ \mathrm{m\ cm}^{-1})l)^2}{4} u^2 \qquad [\,\mathrm{kg\ m\ s}^{-2}], \tag{8.22}$$

with ρ the density of the fluid, u the speed of the organism and C_D its drag coefficient. Approximating the organisms to steadily translating spheres, we can relate their drag coefficient to their Reynolds number Re (Kiørboe et al., 2010):

$$C_D = \frac{24}{Re} + \frac{5}{\sqrt{Re}} + \frac{2}{5}. \tag{8.23}$$

The Reynolds number is defined as:

$$Re = \frac{10^{-2} l u}{\nu_w}, \tag{8.24}$$

with ν_w the kinematic viscosity of sea water. The energy spent migrating is then:

$$\begin{aligned} C_{migr} &= \tfrac{1}{46 \cdot 10^3} \textstyle\int_{migrevent} \tfrac{D_r}{\epsilon} u \mathrm{d}t \\ &= \tfrac{D_r}{46 \cdot 10^3 \epsilon} \Delta Z \qquad [\mathrm{gC}]. \end{aligned} \tag{8.25}$$

ϵ is the efficiency with which internal energy is converted to motion (here set to 0.01) (Visser, 2007) and ΔZ is the distance migrated. The migration cost is converted to grams of carbon using a generic ratio of 46 $kJ\ gC^{-1}$ (Salonen et al., 1976). It also needs to be multiplied by two to have the total daily expenditure due to migration (migration at dawn and at dusk).

(v) Growth

The growth rate of an individual is then a combination of equations 8.7, 8.20 or 8.21 and 8.25:

$$Growth_k = \frac{\nu_k}{Wc_k} - T_k - \frac{2C_{migr,k}}{Wc_k} \tag{8.26}$$

(vi) Mortality

Mortality arises from direct predation from other predators (bigger copepods, fish), or from parasites and diseases in the form of a background mortality (Visser, 2007). In this model, fish do not have an explicit predator, so their mortality is only a background mortality term (Hartvig et al., 2011):

$$Mortality_{fish} = 0.0014 Wc^{-0.25} \qquad [\,\mathrm{day}^{-1}]. \tag{8.27}$$

Copepod mortality arises from a background mortality term (Visser, 2007) and from predation from the higher trophic levels (the expression is similar to equation 8.7):

$$Mortality_i = \mu_0 + \frac{1}{Z_i} \sum_{pred.k} F_k^i \frac{Z_k}{Wc_k} \qquad [\,\mathrm{day}^{-1}]. \tag{8.28}$$

Detritus

Because biggest copepods residing at depth (Ohman and Romagnan, 2016) need something that they can feed upon, we implemented a detritus flux providing them with extra food. $D(l, z)$ refers to the concentration of particles of size l (without taking aggregation into consideration) at depth z. The smallest detritus particle come from a detritus flux of dead phytoplankton at the surface, and the other particles come from the sinking of fecal pellets of migrating organisms in the water column.
The background detritus flux is implemented as to follow a Martin curve (Martin et al., 1987):

$$D_0 = S_D z^{-0.86} \qquad [\,\mathrm{gC\ m}^{-3}], \tag{8.29}$$

with S_D the Surface Detritus concentration. As for the second part of the flux, all organisms playing the game (i.e. copepods and fish) are creating detritus in the form of fecal pellets: it is the part of the resource which is ingested but not assimilated (so $(1-\varphi)\sum F_k^i$). We consider that all organisms of the same size class of organisms create fecal pellets of the same size (Stamieszkin et al., 2015). For an individual of length l, the volume of its fecal pellet $F_{PV}(l)$ is defined by (Stamieszkin et al., 2015):

$$\log_{10}(F_{PV}(l)) = \eta + \theta \log_{10}(10l), \qquad F_{PV}(l) \text{ in } \mu\mathrm{m}^3. \tag{8.30}$$

The sinking rate of a particle is (Stamieszkin et al., 2015):

$$\log_{10}(S_R(l)) = \tau + \phi \log_{10}(F_{PV}(l)), \quad S_R \text{ in m day}^{-1}. \tag{8.31}$$

Values of the parameters are given table 8.5.
If an individual ingests $x\,\mathrm{gCday}^{-1}$, it produces $(1-\varphi)x\,\mathrm{gC\ day}^{-1}$ of fecal pellets. Given a concentration of N individuals of the same class per m^3 at a given layer, the concentration of fecal pellets created by individuals of this class in this layer i will be (Stamieszkin et al., 2015):

$$F_{PC}(l, z_i) = \frac{(1-\varphi)xN}{\alpha + S_R(l)/\Delta Z} \qquad [\mathrm{gC\ m}^{-3}], \tag{8.32}$$

with α the degradation rate of the particles (taken as 0.1 day^{-1}) and ΔZ the thickness of the water layer.
The concentration of fecal pellets at depth z_j due to the sinking of this source is then:

$$F_{PC}(l, z_j) = F_{PC}(l, z_i) e^{-\frac{\alpha}{S_R(l)}(z_j - z_i)} \qquad [\mathrm{gC\ m}^{-3}]. \tag{8.33}$$

Table 8.5: Fecal pellet parameters (Stamieszkin et al., 2015)

Parameter	Value
η	5.4
θ	2.58
τ	-0.03
ϕ	0.32
α	0.1 /day

Moreover, detritus created from phytoplankton and microzooplankton can coagulate to create marine snow (Kiørboe et al., 1990). This results in bigger particles (Jackson and Checkley Jr, 2011). This increased particle size influences the encounter rate in two direct ways, as can be seen from equation 8.12: bigger particles sink faster, but they are also detected from further away. This has very little influence in the upper levels of the water column, as the characteristic size of detritus is much smaller than the characteristic size of copepods, but it becomes increasingly important with depth as particles are getting bigger and bigger. Zooplankton may also be able to sense aggregates from further away due to an increased odour plume (Jackson and Kiørboe, 2004).
To account for this coagulation process, we introduced a depth-dependent preference function on the encounter rate of detritus:

$$\Phi_{det}(z) = \begin{cases} 1 + \frac{19z}{200} & \text{if } z < 200\,\mathrm{m} \\ 20 & \text{if } z > 200\,\mathrm{m}. \end{cases} \tag{8.34}$$

This means that the average size of background detritus increases from the surface to 200m by a factor of 20 before remaining constant from 200m to the seafloor. The exact evaluation of this function is quite hard, especially because of the lack of data on particle size increase with depth (which can also vary spatially, but see (Jackson and Checkley Jr, 2011) for data on the first 100m of the water column). Therefore, a sensitivity analysis on it was performed (see section 8.6 of the supplementary material).

The total concentration of detritus of a certain size is then found by summing at each layer the production of this layer and the detritus which sink there (we assume that the

detritus distribution is at steady state the whole time), and by removing from the equation the detritus that are eaten. Detritus are considered regular prey items for our copepods (with a motility equal to their sinking speed), but cannot be fed upon by fish. A rescaling of the consumption rate of detritus by all copepods is done if the total daily consumption exceeds a fraction $\lambda = 0.5$ of the available detritus, so that the total consumption per day is λD. This rescaling also impacts the ingestion rates of other resources by copepods as it modifies the denominator of the functional response.

Definition of the 6 environmental scenarios

The first five different environmental scenarios (ES) were intended to reproduce a gradient of different oceanic conditions, from a very clear oligotrophic water column to a quite eutrophic and turbid one. As a consequence, what varied in the runs is the light attenuation coefficient, the total biomass of the system, the structure of the water column (i.e. the depth and sharpness of the mixed layer depth through the two parameters z_0 and z_m that define it, cf. equation 8.3) and the surface concentration of detritus. The sixth ES was performed to reproduce conditions similar to Dabob Bay (Washington, USA), were reverse migration patterns have been observed (Ohman, 1990). Therefore, the same environmental parameters were also changed (the different values used are summarised in table 8.6), and the size range of zooplankton was extended to match observations (cf. table 8.2).

Table 8.6: Glossary of values used for the 6 environmental scenarios

Parameter	Unit	Signification	ES 1	ES 2	ES 3	ES 4	ES 5	ES 6
P_0	gC m^{-3}	Phytoplankton surface concentration	0.042	0.16	0.27	0.65	0.74	0.23
z_0	m	Mixed layer depth	100	100	60	50	50	30
z_m	m	Sharpness of the transition zone	60	60	30	10	10	10
k_{light}	m^{-1}	Attenuation coefficient	0.03	0.07	0.1	0.2	0.6	0.1
S_D	gC m^{-3}	Surface detritus concentration	0.005	0.02	0.03	0.06	0.1	0.05

The Nash equilibrium and the replicator equation

In order to find the optimal distribution of organisms in the water column, we find the Nash equilibrium of the system. The Nash equilibrium means that no organism has any advantage in changing unilaterally its strategy. As a consequence, all organisms from the same guild have the same fitness at the equilibrium.
To compute it, we define for each class of players k (i.e. copepods in different size classes and with different feeding modes and fish, see figure 1 of the manuscript) a matrix $\mathbf{n}^k = n_{ij}^k$ of strategies. n_{ij}^k is the proportion of organisms k that follow strategy ij, meaning which are

at layer i during daytime and at layer j during nighttime. As an immediate consequence of that, we have:

$$\sum_{i=1}^{M}\sum_{j=1}^{M} n_{ij}^{k} = 1, \tag{8.35}$$

with M the number of water layers considered in the system.
With Z_k the average concentration of organisms from class k in the system, the concentration of organisms in a layer i at day is $Z_k \sum_{j=1}^{n} n_{ij}^{k}$, and similarly for the concentrations of organisms at night in a layer j.
We use the replicator equation (Hofbauer and Sigmund, 2003; Schuster and Siegmund, 1983) to find the Nash equilibrium. In short, each subpopulation following a strategy ij is allowed to grow according to its fitness, before a renormalisation to satisfy constraint 8.35:

$$\begin{aligned} n'^{k}_{ij}(t+1) &= n_{ij}^{k}(t) + \delta t \cdot Fit_{n_{ij}^{k}}\, n_{ij}^{k}(t) \\ n_{ij}^{k}(t+1) &= \frac{n'^{k}_{ij}(t+1)}{\sum_v \sum_w n'^{k}_{vw}(t+1)}. \end{aligned} \tag{8.36}$$

The fitness $Fit_{n_{ij}^{k}}$ of an organism k following strategy ij depends on n_{ij}^{k} but also on the distributions in the strategy space of all other players players from all communities. To keep the notations simple, we dropped these dependencies in the equation above. δt is a (class-specific) dynamic parameter taken as to keep the increase in population within reasonable bounds at each iteration. It is chosen at each iteration according to:

$$\delta t \max(Fit_{n^{k}}) = \lambda_{inc} \tag{8.37}$$

As a practical compromise, we chose $\lambda_{inc} = 0.05$. This means that a subpopulation following strategy ij cannot grow more than 5% of its size at each iteration.
Moreover, recalculating the detritus concentration assuming steady state at each iteration may create oscillatory cycles, where the creation of detritus at a previous time step enhances the increase in population at the next time, which can then completely deplete the detritus resource. To prevent these oscillations, a damper was installed in the system: the concentration of detritus at the next time step is a weighted average of the calculated steady-state concentration D' and of the concentration of detritus at the previous time step:

$$D(t+1) = p \cdot D(t) + (1-p) \cdot D'(t+1) \tag{8.38}$$

Here, we took $p = 0.1$.
We note that the Nash equilibrium provides us with matrices of strategies, but is mute on how these strategies distribute in the population: organisms could follow the same strategy all the time, or could use an array of strategies with different probabilities (provided that the sum of all strategies is equal to the global strategy matrix). This does not matter, as our model has a polymorphic - monomorphic equivalence (Broom and Rychtář, 2014). The derivation of the proof of this equivalence is very similar to the one done in Pinti and Visser (2019).
Due to the complexity of the model, in many cases the system could not converge to an equilibrium but reached an attractor (see figure 8.5). This is typical of organisms for which fitness is not varying much when changing strategy. While this attractor cannot be rigorously termed a "Nash equilibrium", we argue that it is still relevant with regards to the optimal behaviour of the organisms. Oscillations in effective distributions are relatively small, and

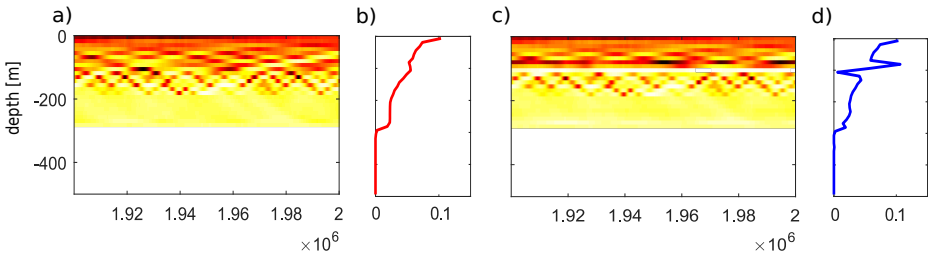

Figure 8.5: a) Steady state distribution of fish during day (last 200 000 iterations of the replicator equation). b) Averaged proportion of fish at each depth during day based on the steady state distribution. c) Steady state distribution of fish during night (last 200 000 iterations of the replicator equation). b) Averaged proportion of fish at each depth during night based on the steady state distribution.

most appear for groups with very low abundance (e.g. big ambush copepods). Many different, random initial distributions were used to explore different steady states or equilibrium, but simulations always led to the same attractor.

Sensitivity analysis

Because of the high computation cost of such a model (with the resolution of our set-up, 2 million iterations of the replicator equation take more than 24 hours on a high performance computer), we did not conduct a proper sensitivity analysis but investigated the sensitivity of the model to some parameters that are hard to define (most of the time because of a lack of available data to estimate them). The parameters that we varied are:

- The surface irradiance during daytime L_{max}. We tested values within the range 100 to 1000 Wm^{-2}.
- The composite light saturation parameter K_e. We tested values within the range 0.01 to 10 Wm^{-2}.
- The depth-specific preference function for detritus Φ_{det}. We varied both the threshold depth from 0 to 500 m, and the factor of increase from 1 to 100 (a factor of increase of 1 means that detritus do not change size).
- The assumption that the different groups follow a Sheldon spectrum. There are indications that some times the Sheldon spectrum can be slightly tilted (Sprules and Munawar, 1986; Woodworth-Jefcoats et al., 2013), with less biomass in the biggest size classes. We scaled linearly the total concentration of organisms so that the biomass of the highest trophic level considered (fish) represents a fraction ξ of the phytoplankton biomass, with ξ varying between 0.1 and 1.
- The distribution of equally sized copepods between ambush and active feeders $\beta(l)$. We redefined a function β to compare more systematically the investigated specifically the effect of an equal distribution between active and ambush feeders:

$$\beta(l) = \frac{1-a}{2} \tanh(\frac{l-l_c}{\Delta l}). \tag{8.39}$$

a is the minimum proportion of active feeders, l_c is length at which we are at the mid-increase in active feeders (i.e. when the proportion of active feeders is $\frac{1+a}{2}$ and the proportion of passive feeders is $\frac{1-a}{2}$) and Δl is the sharpness in the transition zone (see figure 8.13). We also investigated the effects of extreme proportions of active and passive feeders, i.e. if they are all active or all passive feeders.

Light

Maximum irradiance

The effect of the maximum irradiance on the optimal migration patterns is rather small. The

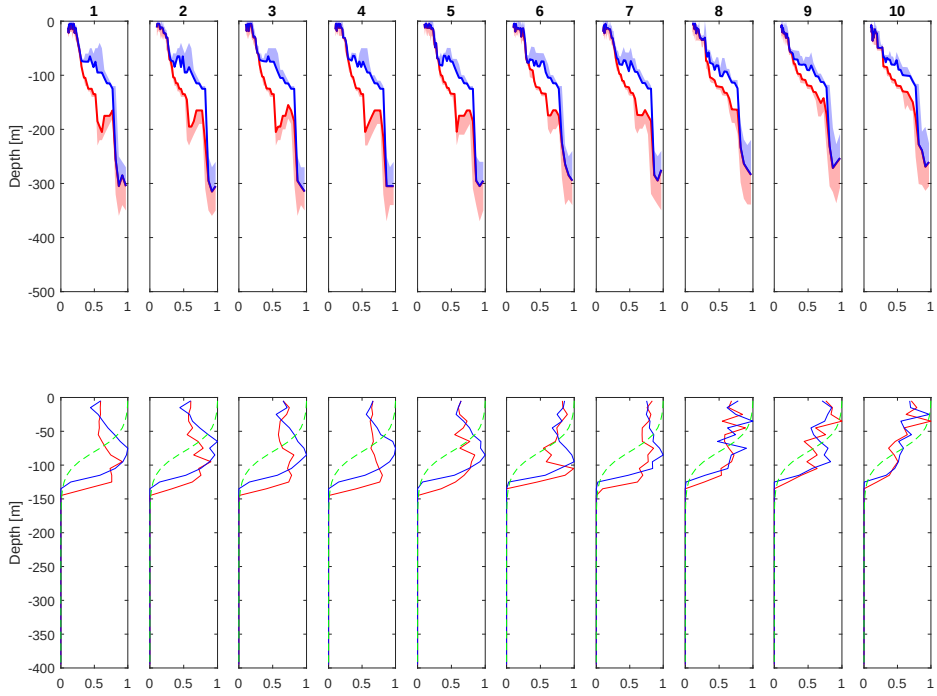

Figure 8.6: Sensitivity to the maximum irradiance. L_{max} varied linearly from 100 (panel 1) to 1000 (panel 10) Wm^{-2}. First line shows the day (red) and night (blue) mean distribution (and 1^{st} and 3^{rd} quartile) of copepods as a function of depth, and the second line shows the day (red) and night (blue) normalized distribution of fish as well as the distribution of phytoplankton and microzooplankton (green) as a function of depth.

overall shape remains, but the migration envelope of copepods get smaller as the maximum irradiance increases. The night residency remains more or less constant, whereas the day residency seems to get closer to the surface for intermediate-sized copepods. This result

may seem counter-intuitive as we would expect that under lighter conditions prey need to go deeper to hide in darker places. But zooplankton need to optimise not only survival but growth, and so the optimal trade-off may be to actually go closer to the surface to feed more, even if it means suffering a higher mortality rate.

Light-saturation parameter

As an agglomerate of several parameters that are hard to define, the exact signification of K_e

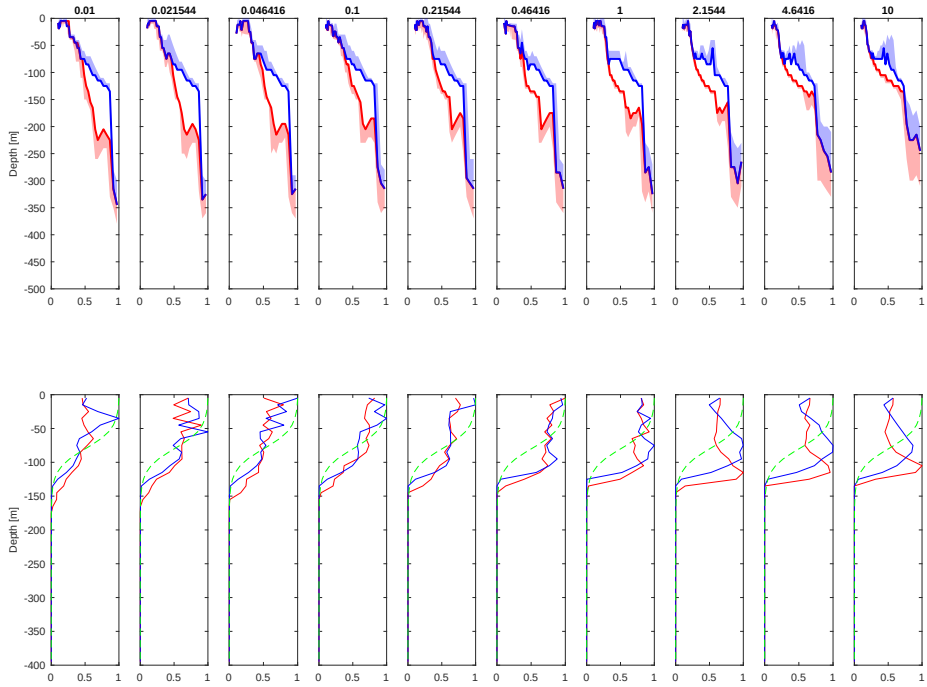

Figure 8.7: Sensitivity to the composite light-saturation parameter. K_e varied linearly from 0.01 (panel 1) to 10 (panel 10) Wm^{-2}.

and its possible range is uncertain (Aksnes and Utne, 1997). It has some influence on the trade-off experienced by copepods and fish, and thus on the migration envelope of copepods and the distribution of fish. It can be understood as the sensitivity of fish to light. With a higher K_e, fish will saturate faster and thus see less under low light conditions. This enables copepods to go higher in the water column, reducing their day residency depth.

Detritus

Increment

This parameter has a strong influence on the migration envelope of copepods. If there is no

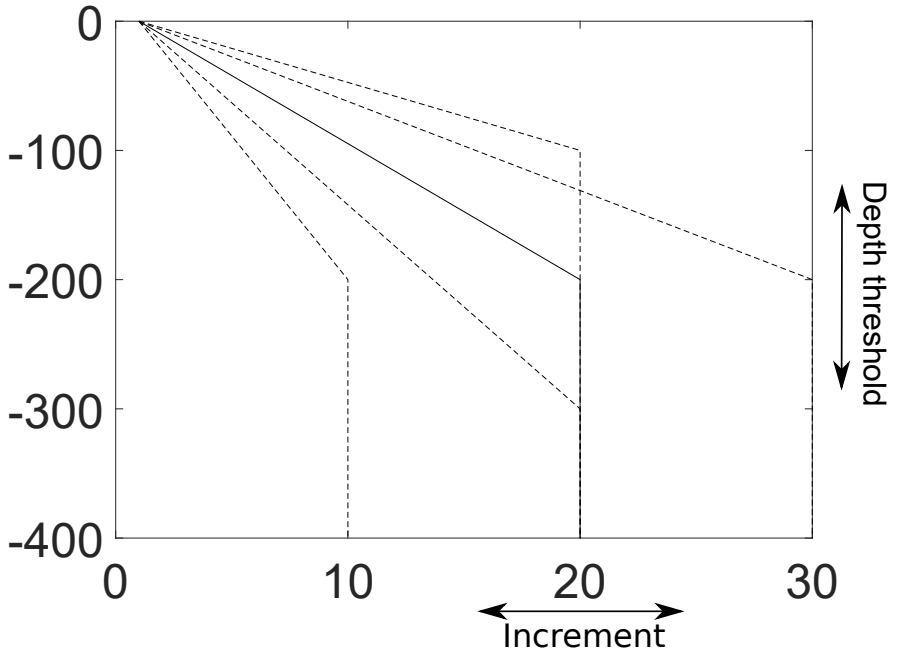

Figure 8.8: The detritus preference function. In full line is the baseline scenario, and dashed lines are functions for different values of depth threshold and increment.

added benefit to feed on detritus at depth compared to the surface (panel 1), the migration envelope of copepods is different, and there is no complete residency at depth for the biggest copepods. As soon as there is an advantage (panel 2 to 10), the migration envelope has the usual shape. Moreover, the bigger the increment, the wider the migration envelope is, and the deeper the bigger copepods reside. We can note that if this increment has a big consequence on the distribution of copepods, it has very little influence on the distribution of fish.

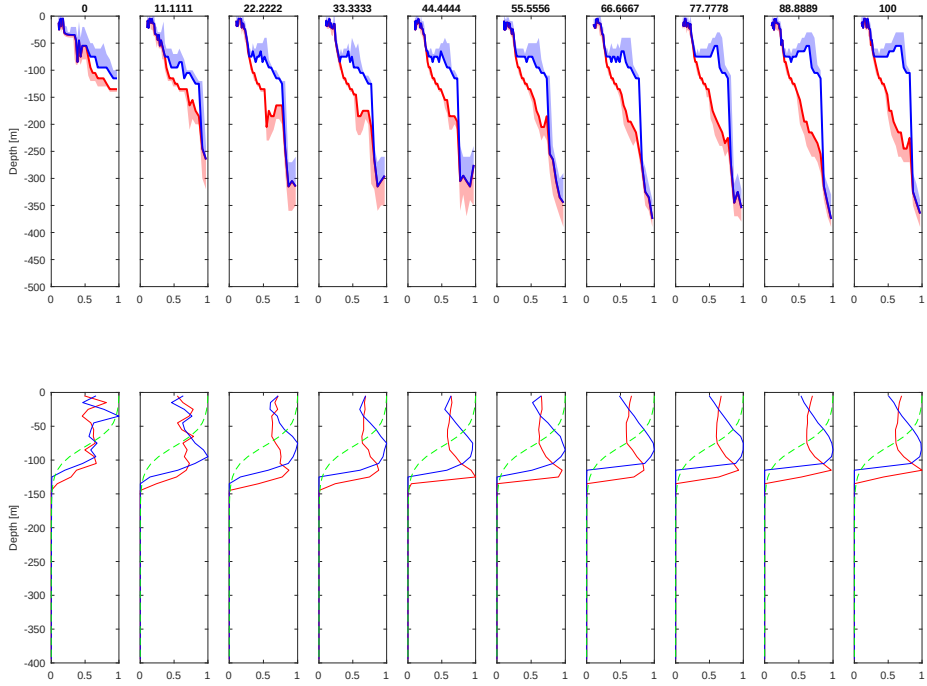

Figure 8.9: Sensitivity to the increment. The increment varied from 0 (panel 1) to 100 (panel 10).

Depth threshold

Overall, the depth threshold has very little influence on the migration patterns of fish and copepods.

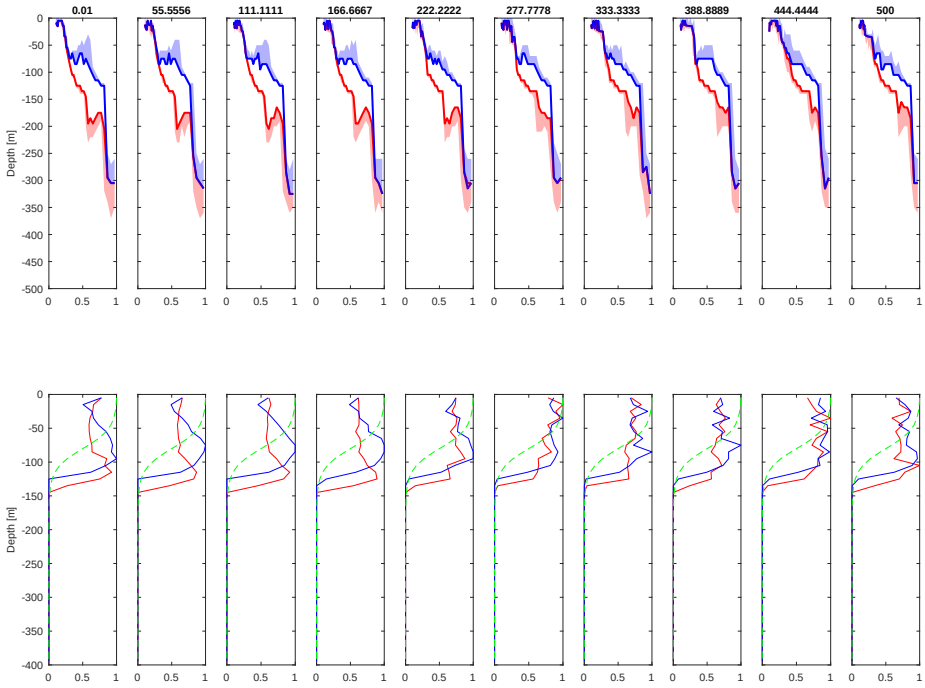

Figure 8.10: Sensitivity to the depth threshold. The threshold varied from 0 (panel 1) to 500 m (panel 10).

Sheldon spectrum

We multiplied each concentration by a factor $\frac{(\xi-1)l_{mean}+l_{f,mean}-\xi l_{P,mean}}{l_{P,mean}-l_{f,min}}$ with l_{mean} the mean length of the organisms in the considered group. ξ is a factor varying between 0.1 and 1. $\xi = 1$ means that the length distribution of organisms follows a Sheldon spectrum, and $\xi = 0.1$ means that the concentration of fish is 10% of what it would be with a Sheldon spectrum. Figure 8.11 shows the concentrations of copepods for different values of ξ.

This parameter has relatively little influence on the copepods. With a lower ξ, the predation pressure from the higher trophic levels is reduced, allowing the copepods to remain closer to the surface. On the contrary, this parameter changes a lot the optimal distribution of fish, from a regime with a low number of individuals performing migrations (panel 10) to a regime with a more pronounced DVM of the community (panel 1).

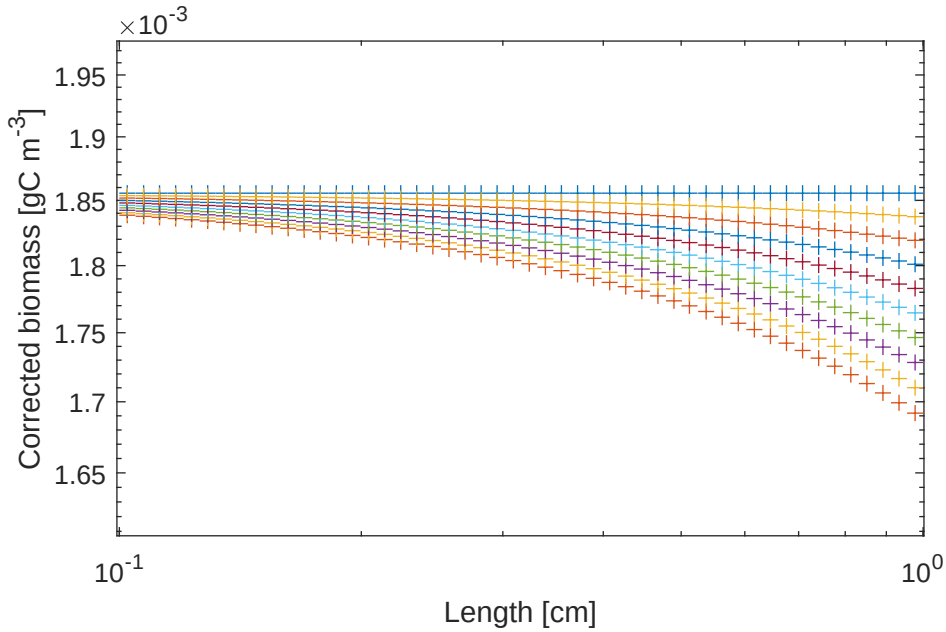

Figure 8.11: Concentration of the different classes of copepods for several values of ξ. Note that we corrected the concentration to account for the difference in length intervals (i.e. we multiplied by the mean size of organisms and divided by the class width, so that a Sheldon spectrum is represented by a straight line.)

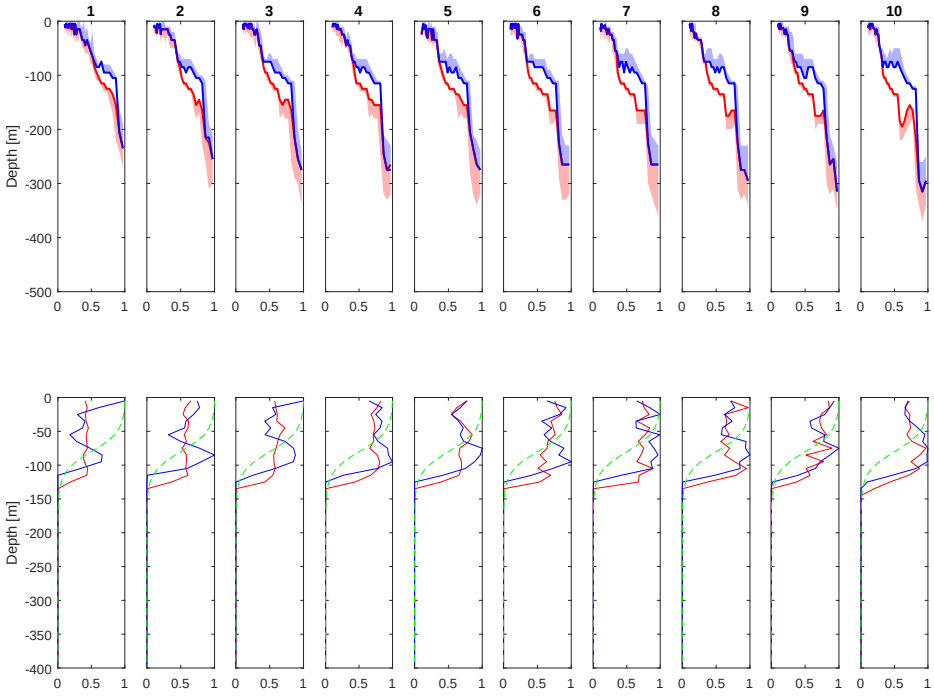

Figure 8.12: Sensitivity to the abundance of organisms with their size (tilt of the Sheldon spectrum). The parameter ξ varied between 0.1 (panel 1) and 1 (panel 10).

Distribution of active and passive feeders

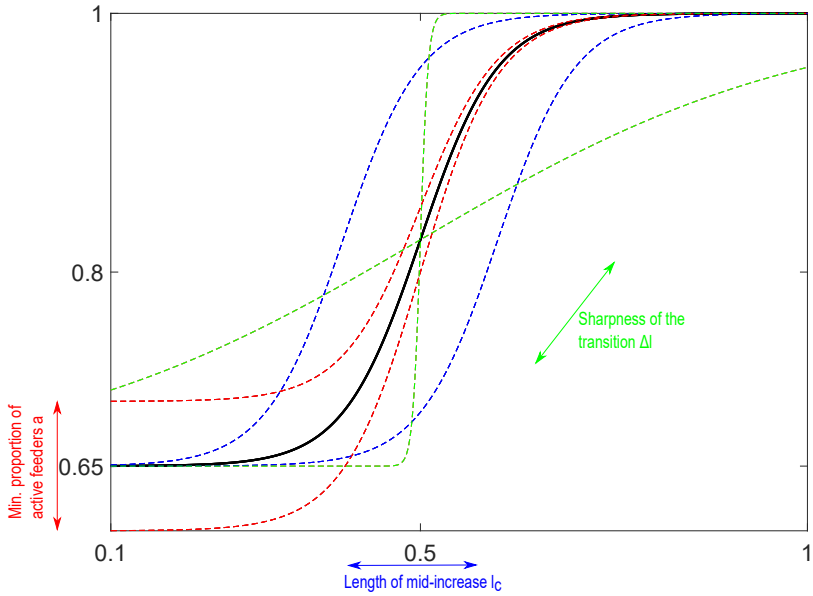

Figure 8.13: Length-dependent proportion of active feeders. Note the influence of the different parameters on the shape of the function. In black is the baseline scenario, and in dashed are examples of how the shape of the function changes with changing one parameter, the two others held constant.

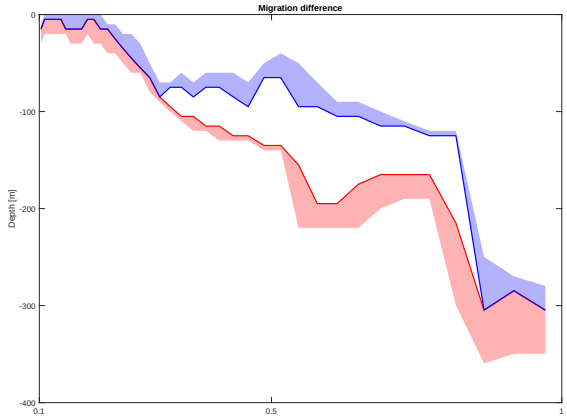

Figure 8.14: Migration patterns with only active feeders.

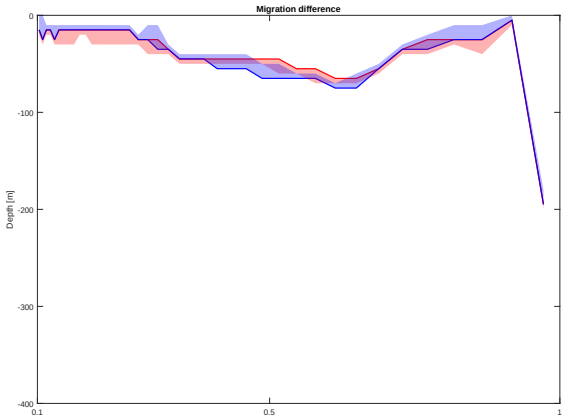

Figure 8.15: Migration patterns with only passive feeders.

Before moving on to more in-depth analysis of the influence of β on the migration patterns, we can see that having only active feeders or only passive feeders yields very different migration patterns. As seen in the main article (figure 3), active feeders do exhibit a migration envelope, but passive feeders tend to remain at the same depth all the time. This depth is close to the surface but varies a bit with the size of the individual.

Critical length l_c

When the critical length increases, the migration envelope of copepods narrows down. This is the consequence of having more passive copepods in the system that tend to remain at the surface (figure 8.15).

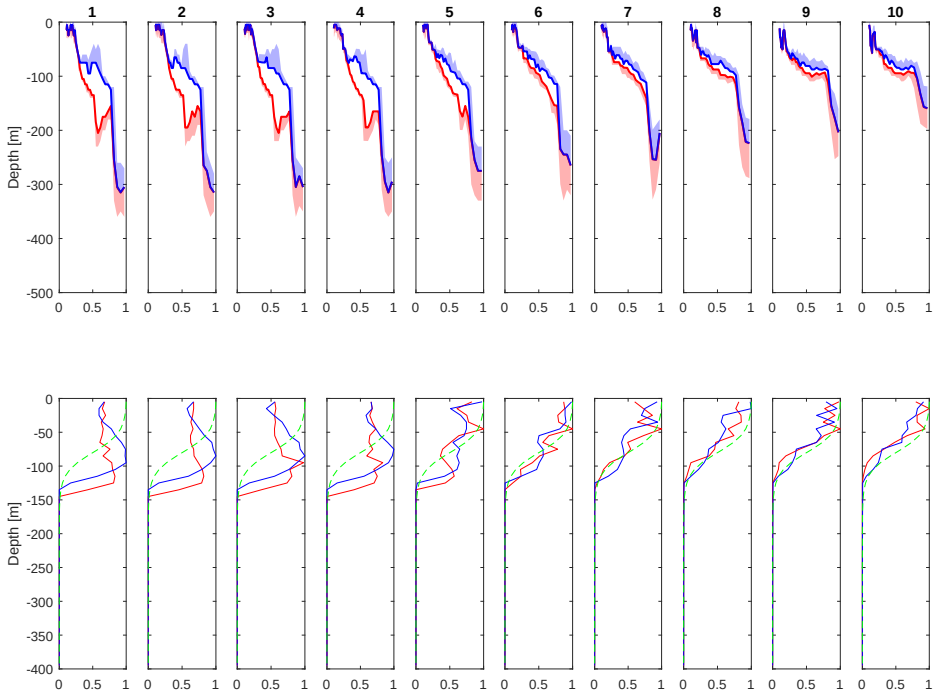

Figure 8.16: Sensitivity to the critical length. l_c varied between 0 and 1 cm.

Initial proportion a

The initial proportion a has very little influence on the migration patterns of the different groups. This is because all small copepods (no matter their feeding mode) remain at the surface, and the transition to an active-feeders dominated size class happens early (the default value was 0.25 cm).

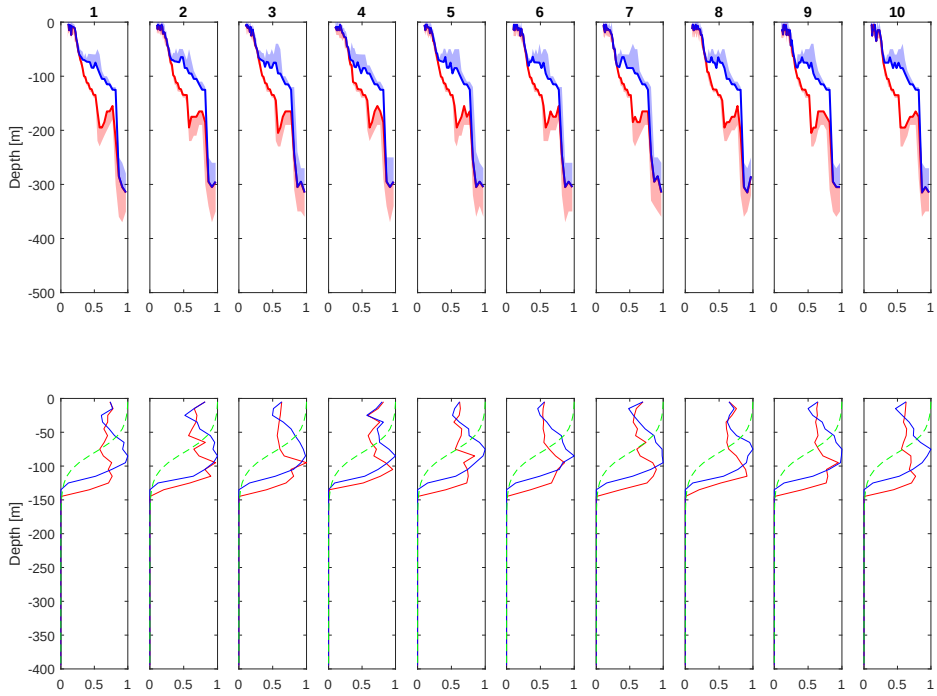

Figure 8.17: Sensitivity to the initial proportion. a varied between 0 and 1.

Transition zone Δl

Δl has a limited influence on the migration patterns of copepods and fish. If Δl increases (i.e. we have a smoother transition towards an active-feeders dominated size class, and so more passive predators at higher size classes), the migration envelope of copepods is narrower, as it is when l_c gets bigger.

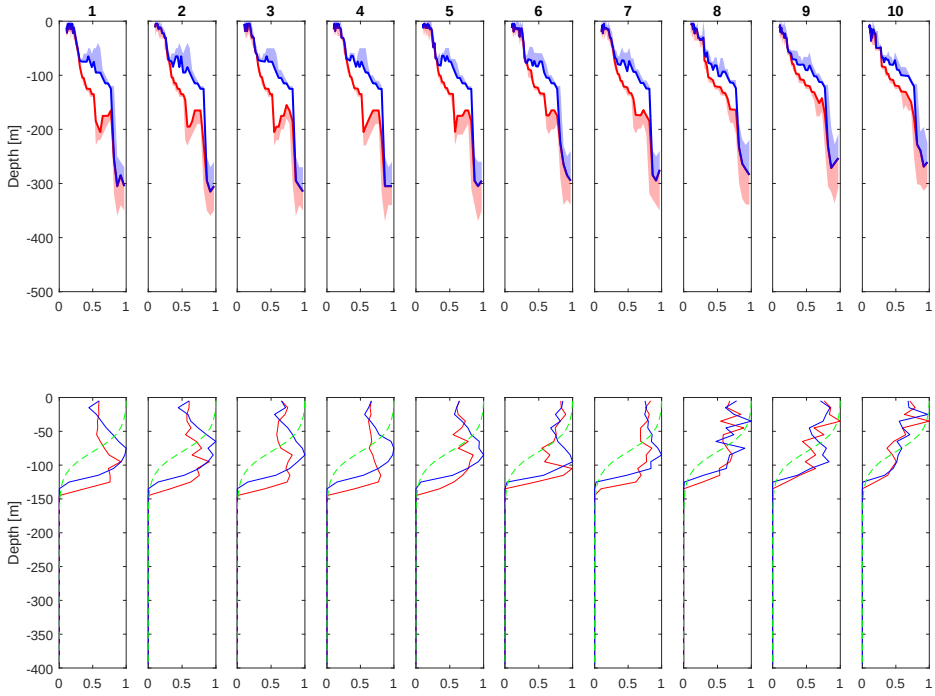

Figure 8.18: Sensitivity to the transition zone width Δl. Δl varied logarithmically between 0.05 and 0.5 cm.

Summary of all parameters used

Table 8.7: Glossary of parameters

Parameter	Unit	Value	Signification	Source
Z	m	-	Depth of the water column	
M	-	-	Number of depth layers	
z_0	m	table 8.6	Depth of the mixed layer	
z_m	m	table 8.6	Thickness of the transition zone	
l	cm	-	Size of an organism	
W_w	g	-	Wet weight of an organism	
W_c	gC	-	Carbon weight of an organism	
P_0	gC m^3	table 8.6	Surface concentration of phytoplankton	
P_{mean}	gC m^{-3}	eq. 8.4	Mean concentration of phytoplankton	
M_{Z_0}	gC m^3	-	Surface concentration of microzooplankton	
$M_{Z,mean}$	gC m^{-3}	eq. 8.5	Mean concentration of microzooplankton	
$P(z)$	gC m^{-3}	eq. 8.3	Concentration of phytoplankton at depth z	Ji and Franks (2007)
$M_Z(z)$	gC m^{-3}	eq. 8.3	Concentration of microzooplankton at depth z	Ji and Franks (2007)
k	-	40	Number of copepod size classes	
Z_i	gC m^{-3}	eq. 8.1	Mean concentration of copepods i	Sheldon et al. (1972)
F_0	gC m^{-3}	eq. 8.1	Mean fish concentration in the water column	Sheldon et al. (1972)
$l_{min/max/mean}$	cm	-	Min (max or mean) length of organisms of a generic class X	
$l_{P,mean}$	cm	$2.1 \cdot 10^{-4}$	Mean size of phytoplankton	
X	gC m^{-3}	eq. 8.1	Concentration of a generic community of minimum size l_{min} and of maximum size l_{max}	Sheldon and Parsons (1967); Sheldon et al. (1972)
$\beta(l)$	-	eq. 8.2 and 8.39	Proportion of active feeders at size l	Brun et al. (2016)
Fit	day^{-1}	eq. 8.6	Fitness of an organism	Kiørboe et al. (2018a)
$Growth$	day^{-1}	eq. 8.26	Growth rate	
$Mort$	day^{-1}	eq. 8.27 and 8.28	Mortality rate	
σ	-	0.6	Fraction of daytime during a day	
ν^k	gC day^{-1}	eq. 8.7	Assimilation rate of an organism k	
F_k^i	gC day^{-1}	eq. 8.8	Ingestion rate of organisms i by an individual k	Holling (1959)
E_k^i	gC day^{-1}	eq. 8.10	Attack rate of organisms i by an individual k	
V_k^i	m^3 day^{-1}	eq. 8.12 and 8.19	Clearance rate of an organism k for prey i	Titelman and Fiksen (2004); van Someren Gréve et al. (2017)
I_{max}^k	gC m^{-3}	eq. 8.9	Maximum ingestion rate of an organism k	Andersen et al. (2017)
φ_k	-	0.65 (fish) or 0.7 (copepods)	Assimilation efficiency	Acuña et al. (2011b)
$\Phi(k,i)$	-	eq. 8.11	Preference function for an organism k on prey i	Hartvig et al. (2011)
ψ	-	table 8.4	Preferred predator-prey ratio of an organism	Andersen et al. (2017); Kiørboe (2016)
σ_{pref}	-	table 8.4	Standard deviation of the preferred predator-prey ratio of an organism	Andersen et al. (2017); Kiørboe (2016)
$R_{k,i}$	m	eq. 8.14 and 8.16	Detection distance of predator k for prey i	van Someren Gréve et al. (2017); Bianchi et al. (2013a)
u	m s^{-1}	eq. 8.13	Length-dependent swimming speed	Huntley and Zhou (2004)
$V_{is-i,fish}$	m^3 day^{-1}	eq. 8.15	Visual clearance rate of a fish for a prey i	Titelman and Fiksen (2004)

Table 8.7 – continued from previous page

Parameter	Unit	Value	Signification	Source
γ	-	0.5	Cross-sectional area efficiently scanned by fish	Titelman and Fiksen (2004)
$\Lambda(z, day)$	W m^{-2}	eq. 8.17	Light level at depth z and time day	Bianchi et al. (2013b)
k_{light}	m^{-1}	table 8.6	Light attenuation coefficient in the water column	Ohman and Romagnan (2016)
ρ_l	-	1 (day) or 10^{-5} (night)	Light attenuation coefficient for day or night	Bollens and Frost (1991a); Webster et al. (2013)
L_0	W m^{-2}	800	Surface irradiance during daytime	Naraghi and Etienne (2012)
K_e	W m^{-2}	1	Composite light-saturation parameter	Aksnes and Utne (1997)
R_0	m	0.5	Reference detection distance for a prey of size l_{ref}	
l_{ref}	cm	1	Reference size for the detection distance R_0	
$F_{ilt-i,fish}$	m^3 day^{-1}	eq. 8.18	Potential filtering rate of a fish on a prey i	
ζ	-	0.5	Filtering efficiency for fish	
T	day^{-1}	eq. 8.20 and 8.21	Metabolic rate	Kiørboe and Hirst (2014b)
μ_0	day^{-1}	0.2	Background mortality rate for copepods	Visser (2007)
D_r	kg m s^{-2}	eq. 8.22	Hydrodynamic drag	Kiørboe et al. (2010)
ρ	kg m^{-3}	1028	Density of seawater	
C_D	-	eq. 8.23	Drag coefficient	Kiørboe et al. (2010)
Re	-	eq. 8.24	Reynolds number	
ν_w	m^2 s^{-1}	$1.3 \cdot 10^{-6}$	Kinematic viscosity of seawater	Visser (2007)
C_{migr}	gC	eq. 8.25	Migration cost for an organism	
ϵ	-	0.01	Swimming efficiency	Visser (2007)
D_0	gC m^{-3}	eq. 8.29	Background detritus concentration	Martin et al. (1987)
D	gC m^{-3}	eq. 8.38	Size-dependent detritus concentration	
S_D	gC m^{-3}	table 8.6	Surface detritus concentration	
$F_{PV}(l)$	μm^3	eq. 8.30	Fecal pellet volume for a copepod of length l	Stamieszkin et al. (2015)
η, θ, τ, ϕ	-	table 8.5	Fecal pellet-related parameters	Stamieszkin et al. (2015)
α	day^{-1}	0.1	Degradation rate of detritus	
$S_R(l)$	m day^{-1}	eq. 8.31	Sinking rate of detritus	Stamieszkin et al. (2015)
$F_{PC}(l, z)$	gC m^{-3}	eq. 8.32 and 8.33	Concentration of fecal pellets of size l at depth z	Stamieszkin et al. (2015)
Φ_{det}	-	eq. 8.34	Depth-dependent increase in encounter rate for copepods and detritus	
λ	-	0.5	Proportion of available detritus that can be eaten in a day	
$\mathbf{n}^k$	-	–	Matrix of strategies for a class of organisms k	
n_{ij}^k	-	eq. 8.36	Proportion of individuals from class k exhibiting strategy ij	
δt	-	eq. 8.37	Dynamic rate of increase during the replicator equation	
λ_{inc}	-	0.05	Max. growth in population that a strategy can achieve at each time step	
p	-	0.1	Damper for the calculation of the new value of the detritus concentration	
ξ	-	0 (default)	Tilt in the Sheldon spectrum. Varied only in the sensitivity analysis.	
a	-	0.65 (default)	Proportion of active feeders of 0.1 mm	
l_c	cm	0.25 (default)	Length of mid-increase in active feeders	
Δl	cm	0.1 (default)	Sharpness of the transition in β	

Bibliography

Acuña, J. L., López-Urrutia, Á., and Colin, S. (2011a). Faking giants: The evolution of high prey clearance rates in jellyfishes. *Science*, 333(6049):1627–1629.

Acuña, J. L., López-Urrutia, Á., and Colin, S. (2011b). Supplementary material- Faking giants: The evolution of high prey clearance rates in jellyfishes. *Science*, 333(6049):1627–1629.

Aksnes, D. L. and Utne, A. C. W. (1997). A revised model of visual range in fish. *Sarsia*, 4827(September):37–41.

Andersen, K. H. (2019). *Fish Ecology, Evolution, and Exploitation : A New Theoretical Synthesis*. Princeton University Press, monographs edition.

Andersen, K. H., Berge, T., Gonçalves, R., Hartvig, M., Heuschele, J., Hylander, S., Jacobsen, N., Lindemann, C., Martens, E., Neuheimer, A., Olsson, K., Palacz, A., Prowe, A., Sainmont, J., Traving, S., Visser, A. W., Wadhwa, N., and Kiørboe, T. (2016). Characteristic Sizes of Life in the Oceans, from Bacteria to Whales. *Annual Review of Marine Science*, 8(1):217–241.

Andersen, N. G., Lundgren, B., Neuenfeldt, S., and Beyer, J. E. (2017). Diel vertical interactions between Atlantic cod Gadus morhua and sprat Sprattus sprattus in a stratified water column. *Marine Ecology Progress Series*, 583:195–209.

Andersen, V. and Sardou, J. (1992). The diel migrations and vertical distributions of zooplankton and micronekton in the Northwestern Mediterranean Sea. 1. Euphausiids, mysids, decapods and fishes. *Journal of Plankton Research*, 14(8):1129–1154.

Ariza, A., Landeira, J. M., Escánez, A., Wienerroither, R., Aguilar de Soto, N., Røstad, A., Kaartvedt, S., and Hernández-León, S. (2016). Vertical distribution, composition and migratory patterns of acoustic scattering layers in the Canary Islands. *Journal of Marine Systems*, 157:82–91.

Atkinson, A., Ward, P., Williams, R., and Poulet, S. A. (1992). Diel vertical migration and feeding of copepods at an oceanic site near South Georgia. *Marine Biology*, 113(4):583–593.

Aumont, O., Maury, O., Lefort, S., and Bopp, L. (2018). Evaluating the potential impacts of the diurnal vertical migration by marine organisms on marine biogeochemistry. *Global Biogeochemical Cycles*, pages 1–22.

Bianchi, D., Galbraith, E. D., Carozza, D. A., Mislan, K. A. S., and Stock, C. A. (2013a). Intensification of open-ocean oxygen depletion by vertically migrating animals. *Nature Geoscience*, 6(7):545–548.

Bianchi, D., Stock, C., Galbraith, E. D., and Sarmiento, J. L. (2013b). Diel vertical migration: Ecological controls and impacts on the biological pump in a one-dimensional ocean model. *Global Biogeochemical Cycles*, 27(2):478–491.

Bollens, S. M. and Frost, B. W. (1991a). Diel Vertical Migration in Zooplankton - Rapid Individual-Response to Predators. *Journal of Plankton Research*, 13(6):1359–1365.

Bollens, S. M. and Frost, B. W. (1991b). Ovigerity , selective predation , and variable diel vertical migration in Euchaeta elongata (Copepoda : Calanoida). *Oecologia*, 87:155–161.

Boukal, D. S. (2014). Trait- and size-based descriptions of trophic links in freshwater food webs: Current status and perspectives. *Journal of Limnology*, 73(1 SUPPL):171–185.

Broom, M. and Rychtář, J. (2014). Asymmetric Games in Monomorphic and Polymorphic Populations. *Dynamic Games and Applications*, 4(4):391–406.

Brown, J. H., Gillooly, J. F., Allen, A. P., Savage, V. M., and West, G. B. (2004). Toward a metabolic theory of ecology. *Ecology*, 85(7):1771–1789.

Brun, P., Payne, M. R., and Kiørboe, T. (2016). Trait biogeography of marine copepods – an analysis across scales. *Ecology Letters*, 19(12):1403–1413.

Brun, P., Stamieszkin, K., Visser, A. W., Licandro, P., Payne, M. R., and Kiørboe, T. (2019). Climate change has altered zooplankton-fuelled carbon export in the North Atlantic. *Nature Ecology and Evolution*, 3:416–423.

Cohen, J. H. and Forward Jr, R. B. (2009). Zooplankton Diel Vertical Migration — A Review Of Proximate Control. *Oceanography and Marine Biology*, 47:77–110.

Daase, M., Eiane, K., Aksnes, D. L., and Vogedes, D. (2008). Vertical distribution of Calanus spp. and Metridia longa at four Arctic locations. *Marine Biology Research*, 4(3):193–207.

Daufresne, M., Lengfellner, K., and Sommer, U. (2009). Global warming benefits the small in aquatic ecosystems. *Proceedings of the National Academy of Sciences*, 106(31):12788–12793.

Davis, R. E., Ohman, M. D., Rudnick, D. L., Sherman, J. T., and Hodges, B. (2008). Glider surveillance of physics and biology in the southern California Current System. *Limnology and Oceanography*, 53(5-2):2151–2168.

De Robertis, A. (2002). Size-dependent visual predation risk and the timing of vertical migration: An optimization model. *Limnology and Oceanography*, 47(4):925–933.

De Robertis, A., Jaffe, J. S., and Ohman, M. D. (2000). Size-dependent visual predation risk and the timing of vertical migration. *Limnology and Oceanography*, 45(8):1838–1844.

Falkenhaug, T., Tande, K. S., and Semenova, T. (1997). Diel, seasonal and ontogenetic variations in the vertical distributions of four marine copepods. *Marine Ecology Progress Series*, 149(1-3):105–119.

Fiksen, Ø. (1995). Vertical distribution and population dynamics of copepods by dynamic optimization. *ICES Journal of Marine Science*, 52(3-4):483–503.

Flint, M. V., Drits, A. V., and Pasternak, A. F. (1991). Characteristic features of body composition and metabolism in some interzonal copepods. *Marine Biology*, 111(2):199–205.

Frank, T. M. and Widder, E. A. (2002). Effects of a decrease in downwelling irradiance on the daytime vertical distribution patterns of zooplankton and micronekton. *Marine Biology*, 140(6):1181–1193.

Garzke, J., Hansen, T., Ismar, S. M., and Sommer, U. (2016). Combined effects of ocean warming and acidification on copepod abundance, body size and fatty acid content. *PLoS ONE*, 11(5):1–22.

Garzke, J., Ismar, S. M., and Sommer, U. (2015). Climate change affects low trophic level marine consumers: warming decreases copepod size and abundance. *Oecologia*, 177(3):849–860.

Gilbert, J. J. and Williamson, C. E. (1983). Sexual Dimorphism in zooplankton (copepoda, cladocera, and rotifera). *Annual Review of Ecology and Systematics*, 14(1):1–33.

Gilliam, J. F. and Fraser, D. F. (1987). Habitat Selection Under Predation Hazard: Test of a Model with Foraging Minnows. *Ecology*, 68(6):1856–1862.

Green, S. J. and Côté, I. M. (2014). Trait-based diet selection: Prey behaviour and morphology predict vulnerability to predation in reef fish communities. *Journal of Animal Ecology*, 83(6):1451–1460.

Hansen, A. N. and Visser, A. W. (2016). Carbon export by vertically migrating zooplankton: An optimal behavior model. *Limnology and Oceanography*, 61(2):701–710.

Hartvig, M., Andersen, K. H., and Beyer, J. E. (2011). Food web framework for size-structured populations. *Journal of Theoretical Biology*, 272(1):113–122.

Hofbauer, J. and Sigmund, K. (2003). Evolutionary Game Dynamics. *Bulletin (New Series) of the American mathematical society*, 40(403):479–519.

Holliland, P. B., Ahlbeck, I., Westlund, E., and Hansson, S. (2012). Ontogenetic and seasonal changes in diel vertical migration amplitude of the calanoid copepods Eurytemora affinis and Acartia spp. in a coastal area of the northern Baltic proper. *Journal of Plankton Research*, 34(4):298–307.

Holling, C. (1959). Some characteristics of simple types of predation and parasitism. *The Canadian Entomologist*, 91(7):385–398.

Huntley, M. E. and Zhou, M. (2004). Influence of animal on turbulence in the sea. *Marine Ecology Progress Series*, 273:65–79.

Irigoien, X., Conway, D. V., and Harris, R. P. (2004). Flexible diel vertical migration behaviour of zooplankton in the Irish Sea. *Marine Ecology Progress Series*, 267(2):85–97.

Jackson, G. A. and Checkley Jr, D. M. (2011). Particle size distributions in the upper 100m water column and their implications for animal feeding in the plankton. *Deep Sea Research Part I*, 58:283–297.

Jackson, G. A. and Kiørboe, T. (2004). Zooplankton use of chemodetection to find and eat particles. *Marine Ecology Progress Series*, 269:153–162.

Ji, R. and Franks, P. (2007). Vertical migration of dinoflagellates: model analysis of strategies, growth, and vertical distribution patterns. *Marine Ecology Progress Series*, 344:49–61.

Kaartvedt, S., Røstad, A., Fiksen, Ø., Melle, W., Torgersen, T., Breien, M. T., and Klevjer, T. A. (2005). Piscivorous fish patrol krill swarms. *Marine Ecology Progress Series*, 299:1–5.

Kampa, E. M. (1975). Observations of a sonic-scattering layer during the total solar eclipse 30 June, 1973. *Deep-Sea Research and Oceanographic Abstracts*, 22(6).

Kiørboe, T. (2016). Foraging mode and prey size spectra of suspension-feeding copepods and other zooplankton. *Marine Ecology Progress Series*, 558(October 2016):15–20.

Kiørboe, T., Andersen, A., Langlois, V. J., and Jakobsen, H. H. (2010). Unsteady motion: escape jumps in planktonic copepods, their kinematics and energetics. *Journal of The Royal Society Interface*, 7(52):1591–1602.

Kiørboe, T., Andersen, K., and Dam, H. G. (1990). Coagulation efficiency and aggregate formation in marine phytoplankton. *Marine Biology*, 107:235–245.

Kiørboe, T. and Hirst, A. G. (2014a). Shifts in Mass Scaling of Respiration, Feeding, and Growth Rates across Life-Form Transitions in Marine Pelagic Organisms. *The American Naturalist*, 183(4):E118–E130.

Kiørboe, T. and Hirst, A. G. (2014b). Shifts in Mass Scaling of Respiration, Feeding, and Growth Rates across Life-Form Transitions in Marine Pelagic Organisms. *The American Naturalist*, 183(4):E118–E130.

Kiørboe, T., Saiz, E., Tiselius, P., and Andersen, K. H. (2018a). Adaptive feeding behavior and functional responses in zooplankton. *Limnology and Oceanography*, 63(1):308–321.

Kiørboe, T., Visser, A., and Andersen, K. H. (2018b). A trait-based approach to ocean ecology. *ICES Journal of Marine Science*.

Klevjer, T. A., Irigoien, X., Røstad, A., Fraile-Nuez, E., Benítez-Barrios, V. M., and Kaartvedt, S. (2016). Large scale patterns in vertical distribution and behaviour of mesopelagic scattering layers. *Scientific Reports*, 6(1):19873.

Leising, A. W., Pierson, J. J., Cary, S., and Frost, B. W. (2005). Copepod foraging and predation risk within the surface layer during night-time feeding forays. *Journal of Plankton Research*, 27(10):987–1001.

Longhurst, A. R. (1985). Relationship between diversity and the vertical structure of the upper ocean. *Deep Sea Research Part A, Oceanographic Research Papers*, 32(12):1535–1570.

Martin, J. H., Knauer, G. A., Karl, D. M., and Broenkow, W. W. (1987). VERTEX: carbon cycling in the northeast Pacific. *Deep Sea Research Part A. Oceanographic Research Papers*, 34(2):267–285.

Mehner, T. and Kasprzak, P. (2011). Partial diel vertical migrations in pelagic fish. *Journal of Animal Ecology*, 80(4):761–770.

Moraitou-Apostolopoulou, M. (1971). Vertical distribution, diurnal and seasonal migration of copepods in Saronic Bay, Greece. *Marine Biology*, 9(2):92–98.

Morales, C. E. (1999). Carbon and nitrogen fluxes in the oceans: the contribution by zooplankton migrants to active transport in the North Atlantic during the Joint Global Ocean Flux Study. *Journal of Plankton Research*, 21(9):1799–1808.

Naraghi, M. H. and Etienne, G. (2012). Solar Panel Orientation and Modeling Based on Hourly Clearness Index. *ASME 2012 6th International Conference on Energy Sustainability, Parts A and B*, (July 2012):105.

Nash, J. (1951). Non-Cooperative Games. *The Annals of Mathematics*, 54(2):286.

Netburn, A. N. and Koslow, J. A. (2015). Dissolved oxygen as a constraint on daytime deep scattering layer depth in the southern California current ecosystem. *Deep-Sea Research Part I*, 104:149–158.

Nicol, S. and O'dor, R. K. (1985). Predatory behaviour of squid (Illex illecebrosus) feeding on surface swarms of euphausiids. *Canadian Journal of Zoology*, 63:15–17.

O'Driscoll, R. L. and McClatchie, S. (1998). Spatial distribution of planktivorous fish schools in relation to krill abundance and local hydrography off Otago, New Zealand. *Deep-Sea Research Part II: Topical Studies in Oceanography*, 45(7):1295–1325.

Ohman, M. D. (1990). The Demographic Benefits of Diel Vertical Migration by Zooplankton. *Ecological Monographs*, 60(3):257–281.

Ohman, M. D., Frost, B. W., and Cohen, E. B. (1983). Reverse diel vertical migration: An escape from invertebrate predators. *Science*, 220(4604):1404–1407.

Ohman, M. D. and Romagnan, J.-B. (2016). Nonlinear effects of body size and optical attenuation on Diel Vertical Migration by zooplankton. *Limnology and Oceanography*, 61(2):765–770.

Onsrud, M. S. and Kaartvedt, S. (1998). Diel vertical migration of the krill Meganyctiphanes norvegica in relation to physical environment, food and predators. *Marine Ecology Progress Series*, 171(Dvm):209–219.

Partridge, B. L. (1982). The structure and function of fish schools. *Scientific American*, 246(6):90–100.

Passow, U. and Carlson, C. A. (2012). The biological pump in a high CO2 world. *Marine Ecology Progress Series*, 470(2):249–271.

Pinti, J. and Visser, A. W. (2019). Predator-Prey Games in Multiple Habitats Reveal Mixed Strategies in Diel Vertical Migration. *The American Naturalist*, 193(3):E000–E000.

Richardson, K. (2000). Subsurface phytoplankton blooms fuel pelagic production in the North Sea. *Journal of Plankton Research*, 22(9):1663–1671.

Roe, H. S. (1984). The diel migrations and distributions within a mesopelagic community in the North East Atlantic. 4. The copepods. *Progress in Oceanography*, 13(3-4):353–388.

Sainmont, J., Andersen, K. H., Thygesen, U. H., Fiksen, Ø., and Visser, A. W. (2015). An effective algorithm for approximating adaptive behavior in seasonal environments. *Ecological Modelling*, 311:20–30.

Salonen, K., Sarvala, J., Hakala, I., and Viljanen, M. L. (1976). The relation of energy and organic carbon in aquatic invertebrates. *Limnology and Oceanography*, 21 (5)(5):724–730.

Schuster, P. and Siegmund, K. (1983). Replicator Dynamics. *Journal of Theoretical Biology*, 100:533–538.

Sewell, R. B. S. and Fage, L. (1948). Minimum Oxygen Layer in the Ocean. *Nature*, 162(4129):949–951.

Sheldon, R. and Parsons, T. (1967). A Continuous Size Spectrurn for Particulate Matter in the Sea. *Journal of the Fisheries Board of Canada*, 24(5):909–915.

Sheldon, R. W., Prakash, A., and Sutcliffe, W. H. (1972). The Size Distribution of Particles in the Ocean. *Limnology and Oceanography*, 17(3):327–340.

Solberg, I. and Kaartvedt, S. (2017). The diel vertical migration patterns and individual swimming behavior of overwintering sprat Sprattus sprattus. *Progress in Oceanography*, 151:49–61.

Sourisseau, M., Simard, Y., and Saucier, F. J. (2008). Krill diel vertical migration fine dynamics, nocturnal overturns, and their roles for aggregation in stratified flows. *Canadian Journal of Fisheries and Aquatic Sciences*, 65(4):574–587.

Spitz, J., Ridoux, V., and Brind'Amour, A. (2014). Let's go beyond taxonomy in diet description: Testing a trait-based approach to prey-predator relationships. *Journal of Animal Ecology*, 83(5):1137–1148.

Sprules, W. G. and Munawar, M. (1986). Plankton size spectra in relation to ecosystem productivity, size, and perturbation. *Canadian Journal of Fisheries and Aquatic Sciences*, 43:1789–1794.

Stamieszkin, K., Pershing, A. J., Record, N. R., Pilskaln, C. H., Dam, H. G., and Feinberg, L. R. (2015). Size as the master trait in modeled copepod fecal pellet carbon flux. *Limnology and Oceanography*, 60(6):2090–2107.

Steinberg, D. K. and Landry, M. R. (2017). Zooplankton and the Ocean Carbon Cycle. *Annual Review of Marine Science*, 9(1):413–444.

Taylor, A. G. and Landry, M. R. (2018). Phytoplankton biomass and size structure across trophic gradients in the southern California Current and adjacent ocean ecosystems. *Marine Ecology Progress Series*, 592:1–17.

Thygesen, U. H. and Patterson, T. A. (2018). Oceanic diel vertical migrations arising from a predator-prey game. *Theoretical Ecology*, pages 1–13.

Titelman, J. and Fiksen, Ø. (2004). Ontogenetic vertical distribution patterns in small copepods: field observations and model predictions. *Marine Ecology Progress Series*, 284(1):49–63.

Trueman, C. N., Johnston, G., O'Hea, B., and MacKenzie, K. M. (2014). Trophic interactions of fish communities at midwater depths enhance long-term carbon storage and benthic production on continental slopes. *Proceedings. Biological sciences*, 281(1787):20140669.

Tsuda, A., Saito, H., and Hirose, T. (1998). Effect of gut content on the vulnerability of Copepods To Visual Predation. *Limnology and Oceanography*, 43(8):1944–1947.

van Someren Gréve, H., Almeda, R., and Kiørboe, T. (2017). Motile behavior and predation risk in planktonic copepods. *Limnology and Oceanography*, 62(5):1810–1824.

Visser, A. W. (2007). Motility of zooplankton: Fitness, foraging and predation. *Journal of Plankton Research*, 29(5):447–461.

Visser, A. W. and Kiørboe, T. (2006). Plankton motility patterns and encounter rates. *Oecologia*, 148(3):538–546.

Webster, C. N., Varpe, Ø., Falk-Petersen, S., Berge, J., Stübner, E., and Brierley, A. S. (2013). Moonlit swimming: vertical distributions of macrozooplankton and nekton during the polar night.

Woodworth-Jefcoats, P. A., Polovina, J. J., Dunne, J. P., and Blanchard, J. L. (2013). Ecosystem size structure response to 21st century climate projection: large fish abundance decreases in the central North Pacific and increases in the California Current. *Global Change Biology*, 19(3):724–733.

CHAPTER 9

The global importance of fish to the biological carbon pump

Pinti J., DeVries T., Norin T., Serra-Pompei C., Proud R., Siegel D.A., Kiørboe T., Petrik C.M., Andersen K.H., Brierley A., Visser A.W. (*in prep*)

Abstract Diel Vertical Migration – the daily movement of aquatic organisms between surface waters and depths – is a ubiquitous behaviour that generates an active transport of organic carbon from the ocean surface to depth. While recognised as a potentially significant contribution to the biological pump, neither the global magnitude nor the relative contribution of different functional groups such as forage and mesopelagic fish are currently known. Here, we use a 1D behavioural model based on game theory to assess the optimal vertical migration patterns of different functional groups simultaneously. We run the model on a global scale and track the fate of the ingested organic carbon transported by the functional groups considered. Organic carbon is transformed into dissolved inorganic carbon (DIC), either by respiration (animal respiration pathway) or by bacterial respiration due to degradation of fecal pellets (fecal pellets pathway). We couple these DIC production sources with OCIM, an inverse ocean circulation model, to estimate how much carbon originating from the different pathways and functional groups considered is sequestered in the global ocean. The modelled global particulate export below the euphotic zone, due to meso zooplankton and higher trophic levels, is estimated to be 4.8 PgC/yr. The associated total carbon sequestration is 875 PgC. Our results point out that fish, especially forage fish and mesopelagic are more important contributors to carbon sequestration than previously assumed (they are responsible for the sequestration of 94 and 158 PgC respectively). We argue that fish should be considered and included in global biological pump assessments.

Keywords— Diel Vertical Migrations, Food-webs, Game theory, Biological carbon pump, Carbon sequestration, Mesopelagic fish

9.1 Introduction

Large sectors of marine pelagic communities – from zooplankton to fish – perform diel vertical migration (DVM) (McLaren, 1963; Onsrud et al., 2004; Kaartvedt et al., 2007; O'Driscoll et al., 2009; Klevjer et al., 2016). The main explanation for DVM is a trade-off between feeding opportunity and predator avoidance. For instance, organisms grazing on phytoplankton stay close to the surface during nighttime to feed and migrate to depth to take refuge in deep dark waters during daytime, where the effectiveness of visual predators is reduced (Zaret and Suffern, 1976; Stich and Lampert, 1981; Lampert, 1993). Higher trophic levels have their own imperative to organise their vertical migration to take advantage of their migrating prey while avoiding predators. Seen in this sense, DVM with a marine pelagic community is the product of co-adaptive game as various actors seek to optimize their migration patterns in terms of the migration patterns of their respective prey, predators and conspecifics (Hugie and Dill, 1994; Iwasa, 1982; Sainmont et al., 2015; Thygesen and Patterson, 2018; Pinti and Visser, 2019; Pinti et al., 2019).

These interacting DVM patterns do not only affect trophic interactions (Hays, 2003), but also global biogeochemical cycles. Indeed, organisms feeding at the surface and

migrating to depths carry with them organic carbon that can be respired or excreted at depth (Buesseler and Boyd, 2009). This process, termed the active biological pump, is highly efficient as carbon escapes remineralization processes, contrarily to passive sinking particles. The biological pump is one of the ocean's key ecosystem services, as it mediates the transport of atmospheric carbon dioxide to depths (Falkowski et al., 1998), where it is stored for time scales ranging from decades to centuries (DeVries et al., 2012).

Several studies explored the effects of DVM on carbon export (Archibald et al., 2019; Aumont et al., 2018; Gorgues et al., 2019), mainly focusing on exports mediated by zooplankton (Longhurst et al., 1990; Dam et al., 1995; Steinberg et al., 2000; Hansen and Visser, 2016; Archibald et al., 2019; Gorgues et al., 2019). Recent biogeochemical models estimated that active carbon fluxes (mediated by vertical migrants) range between 1 and 30 $\mathrm{mgCm^{-2}day^{-1}}$ on a global scale (Archibald et al., 2019; Aumont et al., 2018).

However, the global contribution of fish to the active biological pump is currently unknown. In particular, the contribution of mesopelagic fish is potentially of great importance, in part because of their high biomass. Mesopelagic fish biomass estimates have recently been revised by an order of magnitude (Irigoien et al., 2014), spurring researchers to reconsider the importance of this group for pelagic ecosystem functioning. With a median biomass estimate around 11-15,000 million tonnes, mesopelagic fish harbour a huge potential for active carbon sequestration through their diel vertical migrations that span several hundred meters Klevjer et al. (2016); O'Driscoll et al. (2009); Davison et al. (2013).

Here, we investigate the global carbon export and sequestration potential of different groups of a pelagic food-web (meso and macro zooplankton, forage fish, mesopelagic fish, top predators and jellyfish). We start by computing the optimal DVM patterns of all components of the food-web simultaneously, taking into account the feedbacks that individual behaviours can have on each other, as well as the consequences of light levels, temperature and oxygen concentration on the vital rates of the organisms. We use spatially resolved realistic estimates of global biomasses to compute the equilibrium DVM patterns of the different populations, and we use these global patterns to compute active carbon export mediated by each group considered, both in terms of respiration and particulate flux through fecal pellets excretion. Finally, we combine our results with an inverse ocean circulation model. With DIC (Dissolved Inorganic Carbon) source terms as an input, we use OCIM (DeVries and Primeau, 2011; DeVries, 2014) to estimate the amount of carbon that can be sequestered in the global ocean. DIC originates either from animal respiration (respiration pathway) or from bacterial respiration due to fecal pellets degradation (fecal pellets pathway), for all functional groups. By dividing carbon sequestered by the corresponding DIC source term (either global respiration rate or fecal pellets excretion), we obtain a measure of the time scale on which carbon is stored in the oceans, i.e. of the efficiency of the pathway in focus.

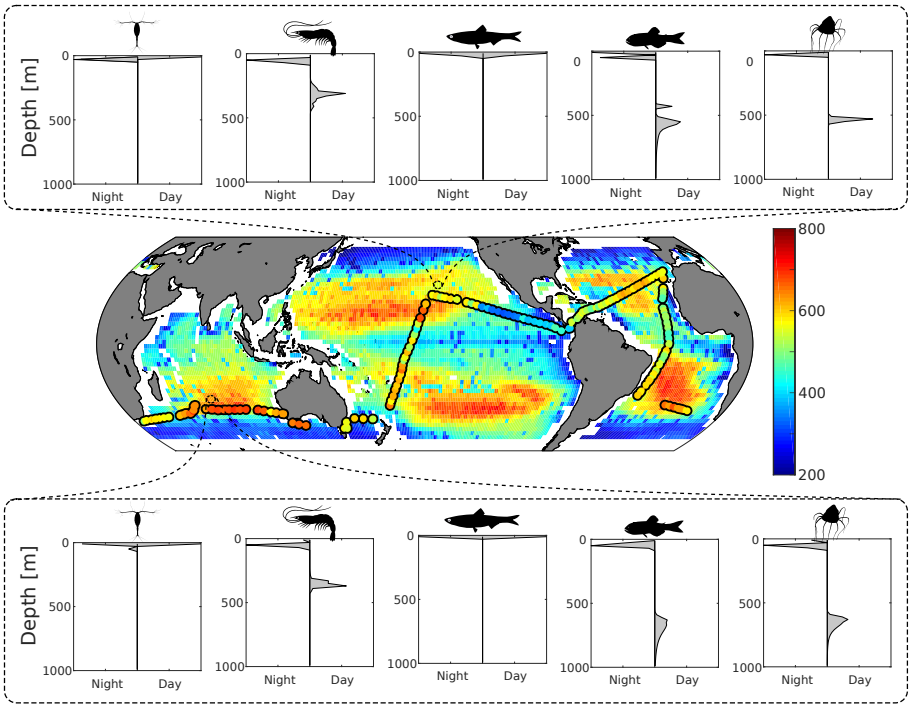

Figure 9.1: Top & Bottom panels: predicted day and night distribution of mesozooplankton, macrozooplankton, forage fish, mesopelagic fish an jellyfish at 26°N 152°W and 25°S 78°E respectively. Large pelagic fish distribution is not pictured as they are assumed to be scattered throughout the water column at all times. Middle panel: Predicted depth of the deep scattering layer during daytime. Overlaid is the observed deep scattering layer depth Klevjer et al. (2016).

9.2 Results

The DVM patterns of the different functional groups match their usual niches: meso zooplankton and forage fish remain close to the surface, whereas macro zooplankton and mesopelagic fish (as well as jellyfish) perform vertical migrations throughout the globe, sometimes with multimodal distributions during part of the day (figure 9.1). The global deep scattering layer (DSL) depths (taken as the daytime depths of maximum mesopelagic fish abundance) closely match observations of DSL obtained during the circumglobal Malaspina expedition (Klevjer et al., 2016). The DSL is deeper in oceanic gyres (between 500-700m deep), and shallower along the coast and at the Equator (between 200-400m). The main geographical region where discrepancies are observed is the Southern Ocean, where our model predicts no or very little DVM for macrozooplankton and mesopelagic fish.

This global distribution of organisms enables us to compute the strengths of trophic couplings between different functional groups (figure 9.4). In particular, mesopelagic fish (total biomass of 0.32 PgC) are strongly coupled with macro zooplankton (they ingest 2.9 PgC of macrozooplankton annually).

Fecal pellets excretion of all functional groups results in a global sinking flux below the euphotic zone of 4.8 PgC/yr (see figure 9.3 for local estimates). Additionally, 0.6 PgC/yr of fecal pellets are excreted below the euphotic zone, and the global community respires 1.0 PgC/yr below the euphotic zone (see figures 9.14 and 9.15 for local estimates). Table 9.1 provides an overview of the production of DIC due to the two different pathways – respiration and fecal pellets – for all functional groups. Assuming the system is at steady state, we can also estimate the contributions of the different functional groups to carbon sequestration, as well as the corresponding sequestration time. In total, 124 PgC are stored through the respiration pathway, and 751 PgC are stored via the fecal pellets pathway. Zooplankton are the most important contributors to carbon sequestration (meso and macro zooplankton fecal pellets degradation sequesters 275 and 279 PgC respectively), followed by mesopelagic fish (158 PgC sequestered in total) and forage fish (94 PgC sequestered in total). Carbon sequestered via the fecal pellets pathway remains in the ocean on a longer time scale than carbon sequestered via respiration (146 years vs. 46 years for all functional groups). In addition, carbon sequestered via degradation of fast-sinking fish fecal pellets is stored on much longer time scales (up to 499 years for large pelagic fish) than carbon sequestered via pathways of slower-sinking fecal pellets such as mesozooplankton (71 years).

On a regional level, the absolute magnitude of the fecal pellets flux below the euphotic zone varies significantly (from less than 10 to more than 120 $\mathrm{mgC/m^2/day}$, see figure 9.3 – subtropical gyres have lower export than tropics, upwelling areas, North Atlantic and North Pacific), but the relative contribution of the different functional groups to carbon sequestration appears quite steady across the different regions of the oceans (figure 9.13). Zooplankton dominate carbon sequestration via fecal pellets degradation (between 70 and 80%), followed by mesopelagic and forage fish (between 20 and 30%). Large pelagic fish and mesopelagic fish always dominate carbon sequestration via the respiration pathway (more than 85% of the total).

Only scarce datasets are available for comparing model predictions with observations. First, DSL depths match the scarce observations of deep scattering layer available (figure 9.1 and 9.11, Klevjer et al. (2016)). Second, we compare the simulated sinking flux with sediment traps data (Lutz et al., 2007). While there are some differences between data and observations for some locations (up to 20 $\mathrm{mgC/m^2/day}$, see figure 9.11), there is no regional bias in these differences (figure 9.12) and the predicted fluxes are of the same order of magnitude as those observed.

Because of the very high number of parameters and high computational cost of each simulation, a complete sensitivity analysis could not be completed. However, we tested the model sensitivity to 5 parameters (bacterial degradation rate, fecal pellets sinking speed, biomass of all functional groups, biomass of mesopelagic fish only, assimilation efficiency). These parameters are anticipated to be the ones to which

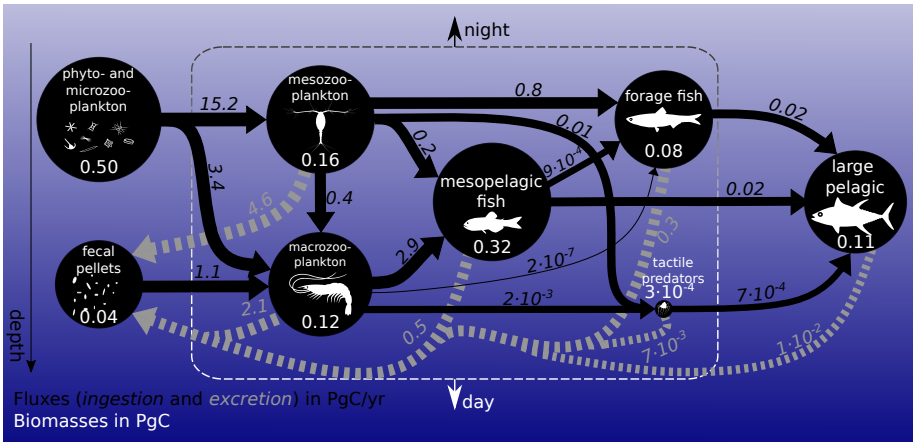

Figure 9.2: Food-web of the model. Biomasses and fluxes are integrated values over the global ocean. Arrow widths and circle diameters are proportional to the logarithm of the fluxes and biomasses they represent.

carbon export and sequestration are the most sensitive. Overall, the DVM patterns observed are very robust (figures 9.16-9.27). Carbon exported and sequestered varies significantly, but mostly within the ranges of the parameter variations (±50%, table S1-S13), supporting the robustness of our results.

9.3 Discussion

Our model is built on simple principles defining the interactions between different individuals. These interactions lead to local and global vertical migration patterns that

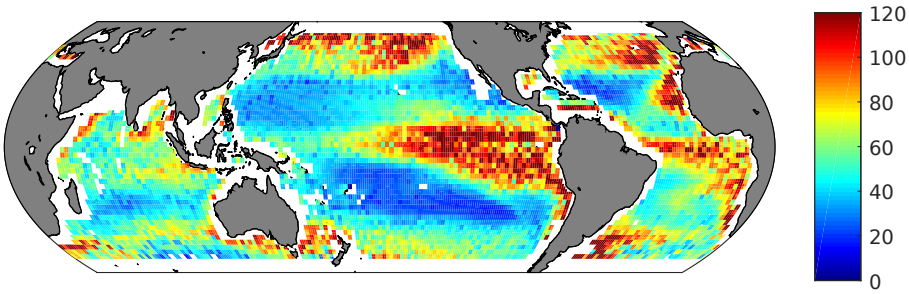

Figure 9.3: Predicted fecal pellets sinking flux below the euphotic zone (in mgC/m^2/day).

Table 9.1: Total DIC produced, corresponding sequestration and residence time for the different pathways considered in the model. Respiration pathway corresponds to animal respiration, and fecal pellets pathway to bacterial respiration due to fecal pellets degradation.

Organism	Respiration pathway			Fecal pellets pathway		
	DIC production [PgC / yr]	Sequestration [PgC]	Residence time [yr]	DIC production [PgC / yr]	Sequestration [PgC]	Residence time [yr]
Meso zooplankton	0.9	0.2	0.2	3.9	275	71
Macro zooplankton	0.4	7	19	1.9	279	151
Mesopelagic	1.0	65	63	0.4	93	217
Forage fish	0.07	0.2	3	0.3	94	341
Large pelagic	0.3	51	158	2e-2	8	499
Jellyfish	1e-3	0.05	46	7e-3	2	296
Total	**2.7**	**124**	**46**	**6.4**	**751**	**116**

are coupled to a global ocean circulation model to assess global carbon sequestration. The results are, to our knowledge, the first global mechanistic estimates of DVM patterns for different functional groups (including global deep scattering layer depth estimates), and the first global estimates of fish-mediated carbon export, including forage and mesopelagic fish. This demonstrates that fish are much more important to the global carbon cycle than usually assumed – an hypothesis only suggested by previous local estimates (Saba and Steinberg, 2012; Davison et al., 2013; Hudson et al., 2014).

Current global particulate export (below the euphotic zone) estimates range between 4 and 12 PgC/yr (Henson et al., 2011; Siegel et al., 2014; Law, 2000), with several estimates clustered around 9-10 PgC/yr (Schlitzer, 2002; Dunne et al., 2005; DeVries and Weber, 2017) – higher than our estimate of 4.8 PgC/yr. The first reason for this discrepancy is that our model does not include coastal areas (shallower than 500 m) nor polar latitudes. Coastal areas were not included because they do not have mesopelagic depths, and polar areas were not included because of their seasonality. Seasonality can lead to large changes in DVM behaviour throughout the year (Prihartato et al., 2015; Darnis et al., 2017; Blachowiak-Samolyk et al., 2006), including zooplankton dormancy for up to several months (Bandara et al., 2016) that can be of importance to carbon export (Jónasdóttir et al., 2015; Visser et al., 2017). With the same spatial coverage as our model, the SIMPLE-TRIM model (predicting an export flux of ∼9 PgC/yr globally, including coasts and polar latitudes, DeVries and Weber, 2017) predicts an export flux out of the euphotic zone of ∼6 PgC/yr. The remaining difference with our study could be due to the lack of algal cells, aggregates and microzooplankton in our model: they account for around 13% of the global flux Siegel et al. (2014).

When it comes to the active part of the biological pump, studies assessing the global contribution of vertical migrants to carbon export rely on a few heuristics and not on mechanistic principles, and do not consider the functional groups separately to assess their relative importance (Aumont et al., 2018; Archibald et al., 2019). Aumont et al. (2018) estimated that all migrating organisms export about 1.0 PgC/yr below 150m, and Archibald et al. (2019) found that zooplankton organisms are responsible for the export of about 0.8 PgC/yr below the euphotic zone. Our model predicts a total active export below the euphotic zone of 1.6 PgC/yr due to vertical migrants (respiration and excretion of organisms below the euphotic zone), of which 0.9 PgC/yr is due to macro zooplankton. Our results predict about the same export due to macro zooplankton DVM as Archibald et al. (2019), but predicts a larger total export than Aumont et al. (2018). This can be due to several factors. They consider the export below a 150m deep reference, whereas we consider the export below the euphotic zone that is always shallower than 150 m (figure 9.8). Further, their study considered biomasses as model outputs, which may underestimate the biomass of functional groups such as mesopelagic fish. Local mesopelagic fish-mediated carbon export measurements estimate that between 15-17 % of the carbon flux is due to mesopelagic fish (Davison et al., 2013), a ratio in agreement with our results (18 % of the flux due to mesopelagic fish).

Our results are relatively robust, as a factor 2 change in the most sensitive parameter values lead to a factor 2 change in exports. One of the most sensitive inputs is biomasses, and their global estimates are still relatively inaccurate. For example, global mesopelagic estimates vary because of the difficulty to translate acoustic backscatter into biomass estimates (Proud et al., 2018). Gelatinous zooplankton biomass estimates are still highly imprecise (Lucas et al., 2014), but these organisms are potentially of considerable importance. A recent study (Luo et al., 2020) estimated that gelatinous zooplankton was responsible for a global export of 1.6-5.2 PgC/yr below 100m.

In addition to its inherent sensitivity, our model is limited by some of its building assumptions. As mentioned earlier, not all sinking particles are considered, and no aggregation or coagulation process is explicitly considered. No gut transit time is considered (contrarily to Brun et al., 2019; Archibald et al., 2019), but this is probably not an issue when compared to the temporal resolution of the model (12h). We built our model by assuming general principles, and all biological parameters were applied globally. Inputs variability (temperature, oxygen, biomasses) are the only drivers of behaviour. Because of this, our model is not based on a closed carbon budget. As a consequence, the carbon budget (see e.g. figure 9.4 and table 9.1) is not balanced. In a dynamic context, functional groups that are currently net carbon sinks (e.g. mesozooplankton, all fish) would increase in biomass, and functional groups that are net carbon sources (macro zooplankton) would decrease in biomass or seek food from other sources. Finally, the results presented here only consider basal respiration, and not respiration due to activities (e.g. hunting, digesting...). But total respiration cost, even though hardly ever assessed in the field, can be as high as twice basal respiration costs. With parameters tuned so that all functional groups are net carbon sinks, a solution to balance the carbon budget is to consider that all the extra fitness is respired by the organisms. This is acceptable as carbon not currently considered in the fitness expenditure would either be respired or used for reproduction (meaning that it would still be respired later by offsprings).

Other non-modelled organisms and behaviours could also modify the strength of the biological carbon pump. Because of the temporal resolution of our model, our model predicts that the mesopelagic community migrates entirely to the surface. While this is counter to what happens in nature as acoustic backscatter is always detected at night (Klevjer et al., 2016), the exact proportion of migrating organisms in unknown. In addition, as seafloor depth increases, another functional group of fish appears: bathypelagic fish. These fish constantly live below $\sim$1000m, potentially migrating daily between bathyal depths (up 4000m deep) and the mesopelagic zone (Vinogradov, 1962). These organisms, feeding on mesopelagic fish, would tend to increase the efficiency of the active biological carbon pump. A copepod fecal pellet sinking from the surface would take several days to reach bathypelagic depths (and only a fraction of it would reach such depths as it would get greatly degraded along the way), but the carbon content of a copepod eaten at the surface by a mesopelagic fish, in turn eaten by a bathypelagic fish the day afterwards would reach depths of 4000m in less than two days. Bathypelagic fish biomass is, however, even more unreliably estimated

than mesopelagic fish biomass. As such, their potential contribution to global carbon export and sequestration is very hard to assess. We can only postulate that, carbon sequestrated because of bathypelagic fish migrations would be sequestrated for very long time scales given the depths at which these organisms live.

As anthropogenic pressures accumulates on Earth, the last realm to remain somewhat undisturbed nor exploited is the mesopelagic zone. This may change soon because of commercial incentives to fish on the vast resource that mesopelagic fish represents (St. John et al., 2016). However, it would be wise to reflect on the potential benefits of maintaining mesopelagic fish biomass intact before starting such exploitation. St. John et al. (2016) suggested that 50 % of the existing mesopelagic biomass could be sustainably extracted. Without investigating the changes that such a change in biomass would incur on trophic interactions and food-web structure in the pelagic, we can make a rapid calculation of the net worth of this resource for climate sequestration. If mesopelagic fish are now responsible for the sequestration of 158 PgC, we can assume that half of them are responsible for the sequestration of 79 PgC (which is equivalent to 290 Pg CO_2). With a price of 25 € by ton of CO_2, this would mean that 50% of mesopelagic biomass would be valued at 7.25 billion €. While this is a simple academic exercise, it shows that mesopelagic ecosystems can have other advantages than harbouring a vast food resource.

9.4 Methods

The behavioural part of our model is a 1D model depicting a pelagic community, from surface waters to mesopelagic depths (figure 9.4). The migrating functional groups considered are meso zooplankton, macro zooplankton, forage fish, large pelagic fish, jellyfish, mesopelagic fish, and detritus (see figure 9.4), as well as phytoplankton & microzooplankton as non-migrating resources. The biomass of all groups is fixed. The vertical distribution of resources depends on the mixed layer depth. Large pelagic fish are assumed to be uniformly distributed in the water column as they are proficient swimmers and are able to move up and down the water column several times a day (Holland et al., 1992; Thygesen et al., 2016). Detritus is created by organisms (through fecal pellet production), sinks and becomes degraded along the way, and can also be ingested by copepods. All other functional groups can move in the water column and our model computes the optimal day and night distribution of all organisms in the water column simultaneously.

The optimal strategy (i.e. day and night positions) of an organism is that which maximises its fitness given the position of all other organisms in the water column. As an individual selects a strategy, the fitness of its prey, predators and conspecifics also varies. Hence, the optimal strategy of all individuals is intrinsically linked to the optimal strategy of all other players. The optimal strategies for all individuals is attained at the Nash equilibrium (Nash, 1951), where no individual can increase its fitness by changing its strategy. The Nash equilibrium is found using the replicator

equation (Hofbauer and Sigmund, 2003; Pinti and Visser, 2019). In short, the fraction of the population following a particular strategy grows proportionally to the fitness related to that strategy, before renormalization to ensure fixed population sizes.

The fitness measure (Gilliam's rule, growth divided by mortality, Houston et al., 1993) is calculated from simple trait-based mechanistic principles. In the water column, abiotic conditions (temperature, light levels, oxygen concentration) vary vertically, impacting vital rates and trophic interactions between organisms, in turn affecting the fitness of organisms. Light levels also vary between day and night, creating the possibility for organisms to perform DVM – if the optimal strategy is to change vertical position during day and night.

The growth rate of organisms is taken as the assimilation rate minus standard metabolic rate and migration cost (calculated assuming organisms are steadily translating spheres), and the mortality rate is the mortality due to predation plus a small background mortality rate. Predators and prey swim at a constant speed and encounter each other depending on the clearance rate of the predator (for visual predators, this varies vertically and between day and night). The probability of capture for each encounter event depends on the escape speed of prey and the attack speed of predators, both varying with the aerobic scope of the corresponding organism (which depends on the local oxygen and temperature conditions). The ingestion rate of each organism is modulated by a type II functional response, except for jellyfish that follow a type I functional response with no saturation at high prey concentrations (Holling, 1959). An ingested prey is then assimilated by with a certain efficiency. The fraction not assimilated is excreted as fecal pellets. All details, equations and parameters for fitness calculations are given section 9.5.

This 1D behavioural model is then run on a global scale, informed by global biomass, temperature and oxygen levels estimates. Global biomass estimates of plankton are outputs of the COBALT model (Stock et al., 2014, 2017), forage fish and large pelagic fish biomasses are outputs of the FEISTY model (Petrik et al., 2019), and mesopelagic fish biomass is calculated from acoustic backscatter (Proud et al., 2017, 2018). Environmental drivers are taken from the World Ocean Atlas 2018 (Locarnini et al., 2019; Garcia et al., 2019). Global inputs are pictured figures 9.8 and 9.9.

Once the global behaviour of organisms is computed, we compute the amount of carbon respired or excreted as fecal pellets by each functional group. This directly provides us with global carbon export estimates. The animal respiration and bacterial respiration (due to fecal pellets degradation) rates are then coupled to the OCIM model (Ocean Circulation Inverse Model, a steady-state ocean circulation model, DeVries and Primeau, 2011; DeVries, 2014), giving us estimates of the amount of carbon sequestered in the oceans via the different pathways, assuming equilibrium conditions. Dividing the amount of carbon sequestered by the corresponding global respiration rate yields the sequestration time, a measure of the time scale on which carbon is sequestered (the 'efficiency' of the considered pathway).

Data, code and material

The source code (written in MATLAB) supporting this article has been uploaded as part of the supplementary material and is available at: `https://github.com/JeromeAqua/Global_contribution_fish`.

Acknowledgements

This work was supported by the Centre for Ocean Life, a VKR Centre of excellence funded by the Villum Foundation, and by the Gordon and Betty Moore Foundation (grant #5479).

9.5 Supplementary material

1D diel vertical migration model

Food-web set-up

The model depicts a pelagic community, from surface waters to mesopelagic depths. We consider phytoplankton resources, two zooplankton populations (meso zooplankton and macro zooplankton), forage fish, top predator (large pelagic fish), tactile predators (e.g. jellyfish), mesopelagic fish, and detritus (figure 9.4). The water column is discretized in n different water layers. The average biomass of all functional groups in the water column is fixed. The vertical distribution of phytoplankton is fixed, with organisms distributed in the surface mixed layer. Large pelagic fish are very fast organisms able to move up and down the water column several times every day (Holland et al., 1992; Thygesen et al., 2016), so we consider their distribution fixed and uniform in the water column. The vertical distribution of all other groups (meso and macro zooplankton, forage fish, mesopelagic fish and tactile predators) is not fixed, and organisms can perform DVM. The day is divided in two periods of time – daytime and nighttime –, and organisms can change their position during daytime and during nighttime according to fitness-optimization rules detailed below. Detritus are created by organisms (through fecal pellet excretion), sink and get degraded along the way, but can also be ingested by zooplankton.

A summary of all parameters and functions used in this document (along with, for each parameter, a short description, its corresponding parameter value or defining equation, and unit) is provided tables 9.15, 9.16, 9.17, 9.18 and 9.19.

We call $\tilde{X}$ the mean concentration of population X in the water column in gC m^{-3}. Here and in the rest of this document, X is a placeholder referring to the different groups of individuals considered: meso zooplankton C, macro zooplankton P, forage fish F, mesopelagic fish M, large pelagic organisms A or tactile predators J. X_{ij} is the proportion of population X following strategy ij (we call strategy the set of day-night positions an individual adopts). In the following of this document, i and j will either refer to a water layer or to the depth of this specific water layer. By definition, we have

$$\sum_{i=1}^{n}\sum_{j=1}^{n} X_{ij} = 1. \tag{9.1}$$

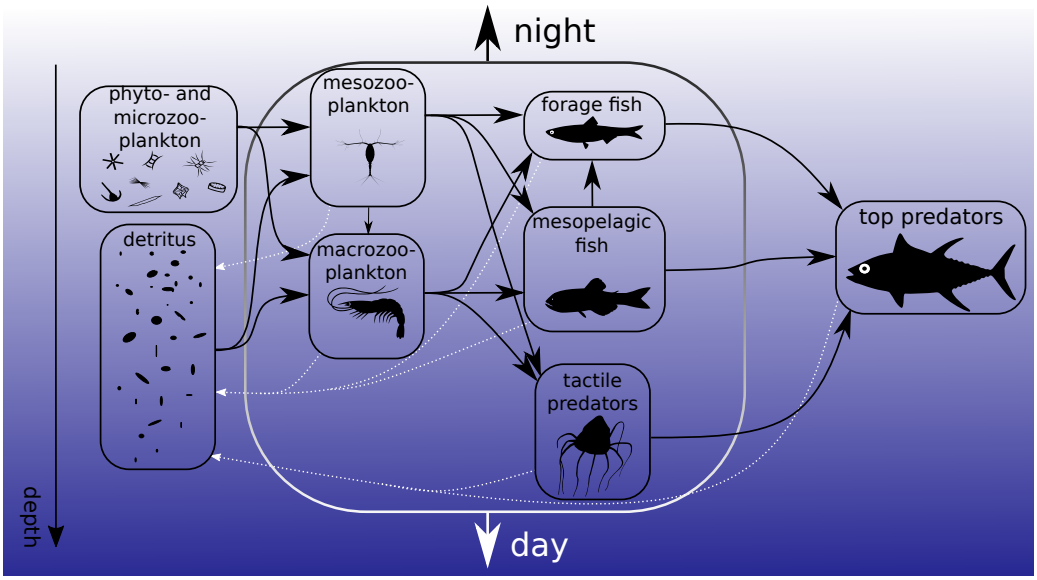

Figure 9.4: Outline of the pelagic food-web considered.

The concentration of organisms in water layer i during daytime is

$$X(i, day) = \tilde{X} n \sum_{k=1}^{n} X_{ik}, \tag{9.2}$$

with a similar expression for the concentration of organisms in layer j during nighttime.

In the water column, abiotic conditions (temperature, light levels, oxygen concentration) vary vertically, impacting the fitness W_X of organisms. Light levels also change between day and night, creating the possibility for organisms to perform DVM — if the optimal strategy is to change vertical position during day and night. The goal of performing DVM is to optimize one's fitness. As an individual selects a strategy, the fitness of its prey, predators and conspecifics also varies. Hence, the optimal strategy of each individual is intrinsically linked to the optimal strategy of the other players. The optimal strategies for all individuals is attained at the Nash equilibrium (Nash, 1951), where no individual can increase its fitness by changing its strategy. The Nash equilibrium is found using the replicator equation (Hofbauer and Sigmund, 2003; Pinti and Visser, 2019, see section 9.5). In short, the fraction of the population following a particular strategy grows proportionally to the fitness related to that strategy, before renormalization to ensure fixed population sizes.

Effects of temperature and oxygen on standard metabolic rate, maximum metabolic rate and aerobic scope

While the effect of temperature T on vital rates is fairly well understood and modelled (e.g. with Q_{10} temperature coefficients), oxygen concentration is rarely considered in popu-

lation models of zooplankton and fish. The way oxygen concentration affects the standard metabolic rate (SMR) and the maximum metabolic rate (MMR) of organisms depends on whether they are oxygen regulators or oxygen conformers (figure 9.5). Oxygen regulators (i.e. fish) have an SMR depending only on temperature (Ekau et al., 2010; Rogers et al., 2016) – at least at oxygen concentrations above the critical oxygen tension (p_{crit}), below which the animal will start accumulating an oxygen debt (see also section 9.5) and eventually die if continually exposed to hypoxia or anoxia – whereas oxygen conformers (i.e. zooplankton and jellyfish) have the ability to decrease their oxygen requirements when the oxygen partial pressure p_{O_2} drops below p_{reg} (typically below 60% oxygen saturation, Kiko et al. (2016)). For both oxygen regulators and conformers, the MMR drops when p_{O_2} decreases below p_{reg} (Seibel and Deutsch, 2020).

p_{crit} is the oxygen partial pressure at which MMR equals SMR, and p_{reg} the partial pressure above which the MMR cannot increase.

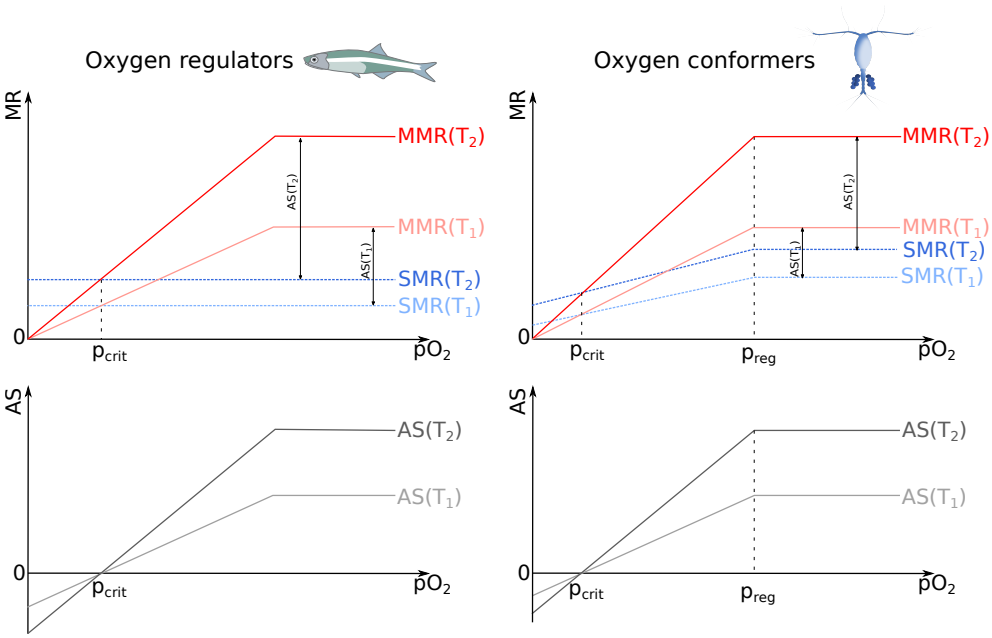

Figure 9.5: Outline of typical maximum metabolic rates (MMR), standard metabolic rates (SMR) and aerobic scopes (AS=MMR-SMR) of oxygen regulator and oxygen conformer organisms. Here, $T_1 < T_2$.

The aerobic scope AS (defined as MMR-SMR, Ern et al. (2016); Claireaux et al. (2000)) is what defines the extra oxygen that organisms can use for their activities. As such, we assume that it scales linearly with rates such as maximum ingestion rate or activities such as swimming speed. Few expressions of aerobic scope of pelagic fish or zooplankton as a function of both temperature and oxygen are available in the literature, and for simplicity we transformed the expression of Claireaux et al. (2000) in a piece-wise linear function (figure 9.5) for both oxyconformers and oxyregulators.

(i) Rates for oxygen conformers

In the following, we drop the dependencies in X, T and p_{O_2} for readability. We also call $s(T)$ the function:

$$s(T) = SMR_0 Q_{10}^{\frac{min(T,T_{max})-T_{ref}}{10}}, \tag{9.3}$$

where T is temperature, SMR_0 the standard metabolic rate at T_{ref}, and T_{max} the temperature of maximum aerobic scope.

The following equations are derived from the facts that the maximum metabolic rate is equal to the standard metabolic rate at p_{crit} (by definition of p_{crit}) and that the maximum metabolic rate is 0 under complete anoxia (figure 9.5, Ultsch and Regan (2019)).

The SMR is:

$$\begin{aligned} SMR &= s(T) && \text{if } p_{O_2} > p_{reg} = 0.6 p_{max} \\ &= s(T)\left[1 + \left(\Delta_{MR}\frac{p_{crit}}{p_{reg}} - 1\right)\frac{p_{reg}-p_{O_2}}{p_{reg}-p_{crit}}\right] && \text{if } p_{O_2} \leq p_{reg}, \end{aligned} \tag{9.4}$$

with p_{O_2} the oxygen partial pressure and Δ_{MR} the factor of increase of MMR compared to SMR under normoxia.

Similarly, the MMR of an oxygen conformer is:

$$\begin{aligned} MMR &= \Delta_{MR} s(T) && \text{if } p_{O_2} > p_{reg} = 0.6 p_{max} \\ &= \Delta_{MR} s(T)\frac{p_{O_2}}{p_{reg}} && \text{if } p_{O_2} \leq p_{reg}. \end{aligned} \tag{9.5}$$

(ii) Rates for oxygen regulators

With the same conventions as section 9.5, the SMR is (figure 9.5):

$$SMR = s(T), \tag{9.6}$$

and the maximum metabolic rate is:

$$MMR = \min\left(s(T)\frac{p_{O_2}}{p_{crit}}, \Delta_{MR} s(T)\right). \tag{9.7}$$

(iii) Diel context

For some combinations of temperature and oxygen concentration, the aerobic scope of the organism is negative (figure 9.5), meaning that it has a deficit in oxygen supply compared to its oxygen demand.

Organisms can build up and sustain an oxygen debt (typically building lactates, Seibel (2011); Seibel et al. (2016)) for a period of time. Fish can usually sustain this oxygen deficiency for a period of a few minutes to a few hours (Speers-Roesch et al., 2013; Nilsson and Östlund-Nilsson, 2008), whereas zooplankton can withstand such low oxygen conditions for several hours and up to half a day (Ekau et al., 2010). As the hypoxic tolerance of fish is below the temporal resolution of our model, habitats yielding negative metabolic scopes (and their related strategies) are not available to fish populations (figure 9.6), except large pelagic fish that are scattered in the water column.

Some zooplankton can, however, maintain an anaerobic metabolism for a period of half a day. When in anaerobic mode, they build up an oxygen debt that needs to be repaid later.

In our case, we consider that the oxygen debt taken during one part of the day (daytime or nighttime) will be repaid during the other part of the day, decreasing the available aerobic scope. Once again, the aerobic scope is set to a minimum of 0, so oxygen debts cannot be repaid in all cases: for example, a day and a night residency at low oxygen levels is not a viable strategy as it would create a oxygen debt that can never be repaid (not to mention the fact that a constant aerobic scope of 0 means that the organism does not feed, see figure 9.6). In cases where the oxygen debt can be repaid (for example a day oxygen debt repaid at night), the available aerobic scope during nighttime $S_X(i, j, day = 0)$ is equal to its original value plus the negative daytime aerobic scope $\tilde{S_X}(i, j, day = 1) = AS(z = i)$, modulated by the proportion of daylight hours in a day:

$$S_X(i, j, 0) = (1 - \sigma)\tilde{S_X}(i, j, 0) + \sigma\tilde{S_X}(i, j, 1). \tag{9.8}$$

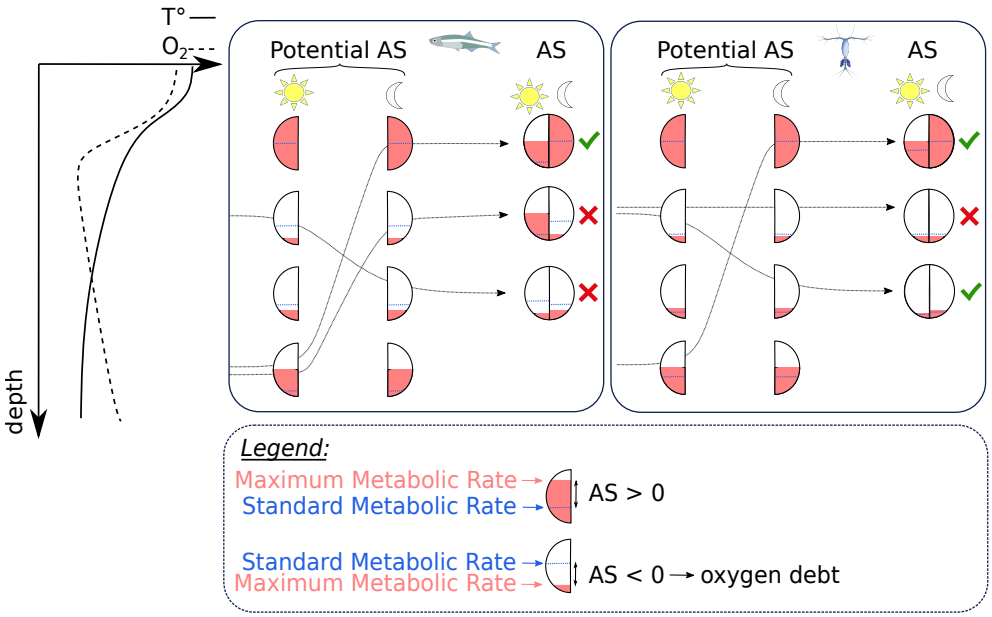

Figure 9.6: Example of possible strategies for copepods and fish. As depth increases, their standard metabolic rate decreases, and their maximum metabolic rate (and hence aerobic scope) scope changes because of changing oxygen and temperature levels. The SMR also decreases because of decreasing temperatures. When the potential aerobic scope gets negative, zooplankton can build up an oxygen debt which can be repaid during the other part of the day, but fish cannot – making any habitat with a negative aerobic scope unsuitable. For zooplankton, the total balance cannot be negative: the oxygen debt contracted during part of the day has to be repaid during the other part of the day.

Fitness

The fitness W of an individual from population X following strategy ij (i.e. being at depth i during day and j during night) is defined, following Gilliam's rule, as its growth rate divided

by its mortality rate (Gilliam and Fraser, 1987; Houston et al., 1993):

$$W_X(i,j) = \frac{g_X(i,j)}{m_X(i,j)}. \tag{9.9}$$

The fitness of phytoplankton and of large predatory fish is not considered here as we constrain their vertical distributions.

Growth g is equal to the assimilation rate ν due to predation minus a standard metabolic cost Q and a migration cost C_{migr}. Mortality m is due to predation μ and to a background mortality μ_0.

(i) Metabolic rate

The standard metabolic cost experienced by an individual X following strategy ij is:

$$Q_X(i,j) = \sigma\tilde{Q_X}(i) + (1-\sigma)\tilde{Q_X}(j), \tag{9.10}$$

with σ the proportion of daylight hours in a day and $\tilde{Q}(z)$ the metabolic cost experienced at depth z. $\tilde{Q}(z)$ is the standard metabolic rate with the conditions encountered at depth z:

$$\tilde{Q}(z) = SMR(T(z), p_{O_2}(z)). \tag{9.11}$$

The reference metabolic rate at T_{ref} is SMR_0, defined as (Kiørboe and Hirst, 2014):

$$\begin{aligned} SMR_0 &= 0.0014 w_X^{-0.25} \text{ for zooplankton and fish,} \\ &= 0.0011 w_X^{-0.25} \text{ for tactile predators.} \end{aligned} \tag{9.12}$$

(ii) Assimilation rate

As for the metabolic rate, the total assimilation rate is the mean of the assimilation rate during day and night:

$$\nu_X(i,j) = \sigma\tilde{\nu}_{X,i,j}(i) + (1-\sigma)\tilde{\nu}_{X,i,j}(j), \tag{9.13}$$

with $\tilde{\nu}_{X,i,j}(z)$ the assimilation rate of X at depth z ($z = i$ during day and j during night). The calculation of $\tilde{\nu}$ is tedious as it depends on the feeding mode of the predator, on the concentration of prey at the considered depth but also on the environmental conditions encountered both during day and during night. Indeed, the assimilation rate is related to the swimming speed u and the maximum ingestion rate I_{max} of an individual, both of which are impacted by temperature and oxygen concentration in the water column as they scale linearly with the aerobic scope S of the organism. We express u and I_{max} as:

$$\begin{aligned} u_{X,i,j}(z) &= u_{0,X}\frac{S_X(i,j,z)}{S_0}, \\ I_{max,X,i,j}(z) &= \max\left[10^{-10}, I_{max0,X}\frac{S_X(i,j,z)}{S_0}\right], \end{aligned} \tag{9.14}$$

with $u_{0,X}$ and $I_{max0,X}$ the terms measured when the organism experienced an aerobic scope of S_0.

The reference swimming speed $u_{0,X}$ is defined as (Huntley and Zhou, 2004):

$$\begin{aligned} u_{0,X} &= 7.87 \cdot 10^4 l^{0.825} \text{ for zooplankton and fish,} \\ &= 2.68 \cdot 10^4 l^{0.75} \text{ for tactile predators,} \end{aligned} \tag{9.15}$$

and the reference maximum ingestion rate is (Andersen, 2019):

$$\begin{aligned} I_{max0,X} &= 0.0542 w_X^{3/4} \text{ for zooplankton,} \\ &= 226.6 l_X^{2.55} \text{ for fish.} \end{aligned} \tag{9.16}$$

The assimilation rate $\tilde{\nu}(z)$ can be first expressed as:

$$\tilde{\nu_X}(z) = \sum_{preyY} \varphi_X F_X^Y(z), \tag{9.17}$$

with φ the assimilation efficiency and $F_X^Y(z)$ the ingestion rate of prey Y by predator X at depth z. Note that for both zooplankton populations, prey also include the detritus pool.

Ingestion rate:

The ingestion rate $F_X^Y(z)$ is defined as:

$$F_X^Y(z) = \frac{1}{w_X} \frac{I_{maz,X}(z) E_X^Y(z)}{I_{maz,X}(z) + \sum_{preyY'} E_X^{Y'}(z)}, \tag{9.18}$$

with E_X^Y the encounter rate of prey Y by predator X. It is equal to:

$$E_X^Y(day, z) = \Gamma_X^Y(z, day) V_X^Y(day, z) \Phi(X, Y) Y(day, z), \tag{9.19}$$

where Γ_X^Y is the capture probability, V_X^Y the clearance rate of X on Y, Φ the preference function (whose values are given table 9.18) and Y the concentration of prey organisms at the time and depth considered. As in eq. 9.8 and for the rest of this section, *day* is a boolean taking value 1 during daytime and 0 during nighttime.

Clearance rate:

For fish, the clearance rate depends on the light level at the time and depth considered. The visual range $\Lambda_X^Y(z, day)$ of a fish X preying on Y is expressed as:

$$\Lambda_X^Y(z, day) = R_{0,X}^Y \sqrt{\frac{light(z, day)}{K_{e,X} + light(z, day)}}, \tag{9.20}$$

with $R_{0,X}$ the reference visual range, K_{eX} the half-saturation constant for light and $light(z, day)$ the light level at the time and depth considered. Light levels are expressed as:

$$light(z, day) = \rho_l(day) L_{max} \exp(-\kappa z), \tag{9.21}$$

with ρ_l the attenuation coefficient between day and night (1 and day, 10^{-5} at night), L_{max} the surface daytime irradiance and κ the light attenuation coefficient of the water. We assume that the visual range of a fish is always at least 10% of its body length, and the clearance

rate of fish is then:

$$V_X^Y(day, z) = \gamma\pi \max\left[\Lambda_X^Y(z, day)^2, (0.1l_X)^2\right] u_X(z), \tag{9.22}$$

with γ the cross-sectional area efficiently scanned and u_X the predator swimming speed. For zooplankton, the clearance rate is:

$$V_C^Y(day, z) = \pi(2l_C)^2 u_C(z), \tag{9.23}$$

with $2l_C$ the extension of the predator fluid signal (van Someren Gréve et al., 2017). Finally, for tactile predators, the clearance rate is (Acuña et al., 2011):

$$V_J^Y(day, z) = f\pi(l_J/2)^2 u_J(z), \tag{9.24}$$

with f the filtering efficiency of tactile predators.

Capture probability:

The capture probability $\Gamma_X^Y(z, day)$ is based on the maximum swimming speed of organisms and on the prey visual range (Caparroy et al., 2000, see figure 9.7). During an attack event, the organisms do not swim at their cruising speeds u but at their maximum swimming speed u_{max}, defined as (Domenici, 2001):

$$u_{max} = \begin{cases} 1.15w_c^{0.16} & \text{for zooplankton and fish} \\ 0.51w_c^{0.16} & \text{for jellyfish.} \end{cases} \tag{9.25}$$

Once a predator X encounters a prey Y, the attack event starts when the distance between the two is the prey detection distance $r_{detec} = \Lambda_Y^X(z, day)$ – if the prey detects the predator before the predator detects the prey, we assume that the prey always escapes before the predator detects it, and as such it is not captured. Similarly, the capture probability of non-motile prey (resource, detritus) is 1. When the attack starts, the predator jumps towards the prey, and the prey tries to escape by jumping a distance r_{esc} into a random direction. For simplicity, we assume here that the prey jumps for as much time as it takes the predator to reach its initial position, so we have:

$$r_{esc} = \frac{r_{detec}}{AS_X(z)u_{max,X}} AS_Y(z)u_{max,Y}. \tag{9.26}$$

The predator jumps until it reaches the end of the sphere of all possible escape jumps of the copepod (figure 9.7), so:

$$r_{attac} = r_{detec} + r_{esc}. \tag{9.27}$$

The predator can capture the prey on a disc of radius $r_{capt} = 0.1l_X$. As the prey can jump in any direction with no preference *a priori*, we assume that the capture probability is the fraction v_{capt} of the escape sphere v_{esc} swept by the predator as it moves through it:

$$\Gamma_X^Y(z, day) = \frac{v_{capt,X}^Y(z, day)}{v_{esc,X}^Y(z, day)}. \tag{9.28}$$

(iii) Mortality

For all migrating populations, mortality is the sum of a predation mortality rate μ_X and

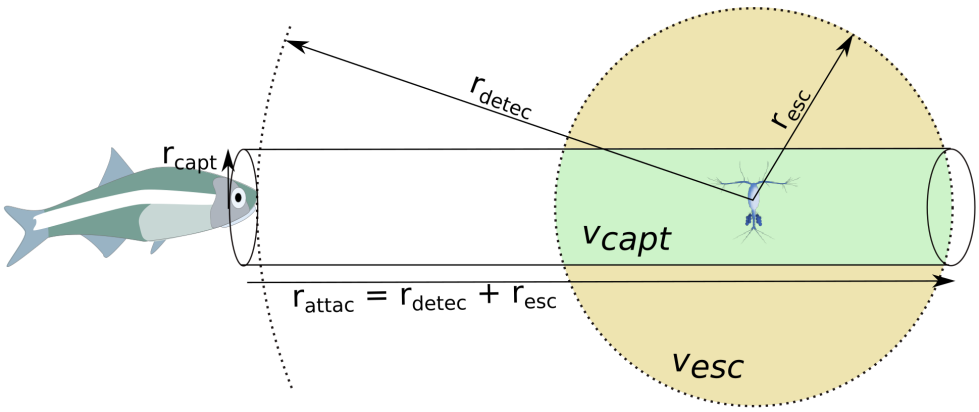

Figure 9.7: The zooplankton capture probability by the fish is the ratio between the green volume (intersection between the predator capture area and the zooplankton potential escape location) and the beige volume (sphere of potential escapes of the zooplankton).

of a background mortality rate $\mu_{0,X}$. For macrozooplankton and mesopelagic fish, $\mu_{0,X}$ is light-dependent. As for metabolic and assimilation rates, the total mortality rate of an individual following a strategy ij is the mean of the mortality rates experienced during day and during night:

$$\mu_{Y,i,j} = \sigma\tilde{\mu}_Y(i,1) + (1-\sigma)\tilde{\mu}_Y(j,0), \tag{9.29}$$

with $\tilde{\mu}_Y(z, day)$ the mortality rate experienced by $Y(i,j)$ during day (depth i) or during night (depth j). Note that, contrarily to ingestion rates, mortality rates are not dependent on the aerobic scope of the individual, but only on the aerobic scopes of its predators. Therefore, the mortality rate of a prey population during *day* at z is:

$$\tilde{\mu}_Y(z, day) = \sum_{pred.X} \sum_{\substack{compatible \\ strat.ij}} F_X^Y X_{ij} \frac{1}{Y(z, day)}, \tag{9.30}$$

$Y(z, day)$ being the concentration of prey Y at depth z during *day*. The compatible strategies are the strategies that overlap with prey at the time and depth considered (so being at i during daytime, or a j during nighttime depending on the value of *day*).

(iv) Migration cost

The migration cost $C_{migr,X}$ of an organism X is calculated similarly to Pinti et al. (2019), where organisms are simply assumed to be steadily translating spheres. We start by computing the hydrodynamic drag $D_{r,X}$ of the body (Kiørboe et al., 2010):

$$D_{r,X} = \frac{1}{2}\pi C_D \rho \frac{((10^{-2}\ \text{m cm}^{-1})l)^2}{4} u_X^2 \qquad [\text{kg m s}^{-2}], \tag{9.31}$$

with ρ the density of the fluid, u_X the speed of the organism and $C_{D,X}$ its drag coefficient. We can relate this drag coefficient to the Reynolds number Re_X (Kiørboe et al., 2010):

$$C_{D,X} = \frac{24}{Re_X} + \frac{5}{\sqrt{Re_X}} + \frac{2}{5}, \tag{9.32}$$

with the Reynolds number defined as:

$$Re_X = \frac{10^{-2} l_X u_X}{\nu_w}. \tag{9.33}$$

ν_w is the kinematic viscosity of sea water. The normalized energy spent migrating is then:

$$\begin{aligned} C_{migr,X} &= 2\tfrac{1}{w_X}\tfrac{1}{46\cdot 10^3}\textstyle\int_{migr\ event}\tfrac{D_{r,X}}{\epsilon}u_X \mathrm{d}t \\ &= \tfrac{D_{r,X}}{46\cdot 10^3 \epsilon w_X} 2\Delta Z \qquad [\,\mathrm{day}^{-1}]. \end{aligned} \tag{9.34}$$

ϵ is the efficiency with which internal energy is converted to motion (Visser, 2007) and ΔZ is the distance migrated. The factor 2 is there because the migration cost accounts for the migration at dawn and at dusk. The migration cost is converted to grams of carbon using a generic ratio of 46 kJ gC^{-1} (Salonen et al., 1976).

(v) Detritus

In this model, detritus are fecal pellets created by organisms. We do not consider aggregation mechanisms explicitly, but it can influence particle encounter rates in two direct ways (Pinti et al., 2019): bigger particles sink faster and are detected from further away. This has little influence in the upper levels of the water column, as the characteristic size of detritus is much smaller than the characteristic size of zooplankton, but it becomes increasingly important with depth. Zooplankton may also be able to sense aggregates from further away due to an increased odour plume (Jackson and Kiørboe, 2004). To account for this process, we introduced a depth-dependent preference function on the encounter rate of detritus (Pinti et al., 2019):

$$\Phi_{det}(z) = \begin{cases} 1 + \frac{19z}{200} & \text{if } z < 700 \text{ m} \\ 20 & \text{if } z > 700 \text{ m}. \end{cases} \tag{9.35}$$

Each population creates fecal pellets of different sizes and sinking speeds. $D_X(z)$ refers to the concentration at depth z of fecal pellets created by population X. Fecal pellets are the part of the food ingested that is not assimilated, and is therefore created at the rate

$$D_{crea,X}(z) = (1 - \varphi_X) \sum_{preyY} F_X^Y(z). \tag{9.36}$$

Zooplankton organisms can also feed on detritus, and the consumption rate of detritus is

$$D_{conso,X}(z) = F_C^{D_X}(z) + F_P^{D_X}(z). \tag{9.37}$$

It is worth noting that in our model with no population or detritus dynamics (i.e resources do not get depleted as they are eaten), the daily consumption of detritus in a water layer can be more important than the concentration of detritus in that layer. As a solution to this artefact, we impose a limit ψ of the proportion of the detritus in a water layer that can be

consumed daily:

$$\begin{aligned}\tilde{F}_C^{D_X}(z) &= \min\left[\frac{\psi D_X(z)}{D_{conso,X}(z)}F_C^{D_X}(z), F_C^{D_X}(z)\right],\\ \tilde{F}_P^{D_X}(z) &= \min\left[\frac{\psi D_X(z)}{D_{conso,X}(z)}F_P^{D_X}(z), F_P^{D_X}(z)\right].\end{aligned} \tag{9.38}$$

Further, if a rescaling is used for zooplankton detritus ingestion rates, the rescaling factor $\frac{\psi D_X(z)}{D_{conso,X}(z)}$ is also applied to detritus encounter rates, so that it modifies in turn the zooplankton ingestion rate of phytoplankton (section 9.5, eq. 9.18).

All this considered, the creation term of detritus $\zeta^X(z)$ is:

$$\zeta^X(z) = D_{crea,X}(z) - \tilde{F}_C^{D_X}(z) - \tilde{F}_P^{D_X}(z). \tag{9.39}$$

The steady state concentration of detritus D^X in the water column is obtained by solving the following transport equation:

$$\frac{\partial D}{\partial t} = -\alpha(z)D^X - \omega_X\frac{\partial D}{\partial z} + \zeta^X = 0, \tag{9.40}$$

where ω_X is the sinking speed of fecal pellets and α is the depth-dependent bacterial degradation rate of detritus:

$$\alpha(z) = \alpha_0 Q_{bac}^{\frac{T-T_{ref}}{10}}\frac{p_{O_2}}{K_{O_2}+p_{O_2}}, \tag{9.41}$$

with α_0 the maximum degradation rate, Q_{bac} the Q_{10} factor of bacterial respiration and K_{O_2} the half-saturation constant of the oxygen dependency of the degradation rate.

Eq. 9.40 is solved numerically using a Euler scheme.

Nash equilibrium

The optimal vertical migration patterns of all organisms is attained when the system is at its Nash equilibrium (Nash, 1951). At this point in the strategy space, no organism can increase its fitness by changing unilaterally its behaviour. Only a subset of the available strategies (i.e. set of depths ij) may be populated at this point, and all the populated strategies of a population will have identical fitness. Formally, this translates in:

$$\begin{aligned}&W_X(i,j) = W_X^0 \text{ for all } \textit{(i,j)} \text{ such that } X_{i,j} > 0,\\ &W_X(i,j) \leq W_X^0 \text{ for all } \textit{(i,j)} \text{ such that } X_{i,j} = 0.\end{aligned} \tag{9.42}$$

The Nash equilibrium of the system is found using the Replicator equation (Schuster and Siegmund, 1983). The Replicator equation is a two-step process, during which we allow the proportion of individuals following strategy ij of a population to grow proportionally to its fitness, before renormalisation to ensure that populations do not grow in size:

$$\begin{aligned}X'_{ij}(t+\delta t) &= X_{ij}(t) + \lambda_t W_X(i,j)X_{i,j}(t),\\ X_{ij}(t+\delta t) &= \frac{X'_{ij}(t+\delta t)}{\sum_k\sum_l X'_{kl}(t+\delta t)}.\end{aligned} \tag{9.43}$$

λ_t is a factor chosen to ensure a rapid transition to equilibrium. As a practical compromise, λ_t is chosen so that $\lambda_t \max(W_X(i,j)) = 0.05$.

At each time step, the detritus flux and concentrations are also updated, and taken as the weighted mean of the equilibrium flux and concentrations given by the population distribution at time t (90%) and $t + \delta t$ (10%).

Global model

In order to get global DVM patterns of the considered population, we run the previous model on the global ocean discretised in 1x1 degree cells. The water column model is run independently in each cell, ignoring possible interactions between the different cells.

To run the model on a global scale, physical and biological inputs are needed:

- Global 3D temperature field ;
- Global 3D oxygen concentration field ;
- Global surface irradiance and light attenuation coefficient ;
- Global biomasses (not resolved vertically - but only horizontally) of the different populations of the model: phytoplankton and microzooplankton, mesozooplankton, macrozooplankton, forage fish, mesopelagic fish, large pelagic fish and jellyfish ;
- Global mixed layer depth estimate, to assess the vertical distribution of phytoplankton in the water column.

We ignore seasonal fluctuations and use only annually averaged inputs. The global temperature and oxygen fields are averaged from the world ocean atlas (Locarnini et al., 2019; Garcia et al., 2019). The light attenuation coefficient comes from the MODIS GMIS-AQUA climatology of the European Commission (Melin, 2013). These three physical parameters were averaged over the period 2003-2017.

The day surface irradiance is calculated for each latitude following Naraghi and Etienne (2012):

$$L_{max} = \frac{1}{365} G_{SG} \sum_{d=1}^{365} \sin(\beta) \left[1 + 0.033 \cos(360 \frac{d-3}{365}) \right], \tag{9.44}$$

with G_{SG} the solar constant equal to 1367 W/m^2, d the day number of the year and β the solar altitude angle, defined as

$$\sin(\beta) = \cos(lat)\cos(\delta)\cos(h) + \sin(lat)\sin(\delta), \tag{9.45}$$

with lat the latitude considered, h the hour angle (equal to 0 here as we are looking for the irradiance at solar midday), and δ the solar inclination angle equal to $23.45 \sin(360 \frac{d+284}{365})$. The resulting yearly-averaged surface irradiance is pictured figure 9.8.

Mixed layer depth is calculated using a temperature criterion of $\pm$ 0.2 degrees from temperature at 10 m (de Boyer Montégut et al., 2004, figure 9.8). The mixed layer depth is calculated to assess the distribution of the non-migrating resource in the water column. If z_0 is the mixed layer depth, the resource is distributed following (Ji and Franks, 2007):

$$R(z) \propto 1 - \tanh\left(\frac{2(z - z_0)}{z_0} \right). \tag{9.46}$$

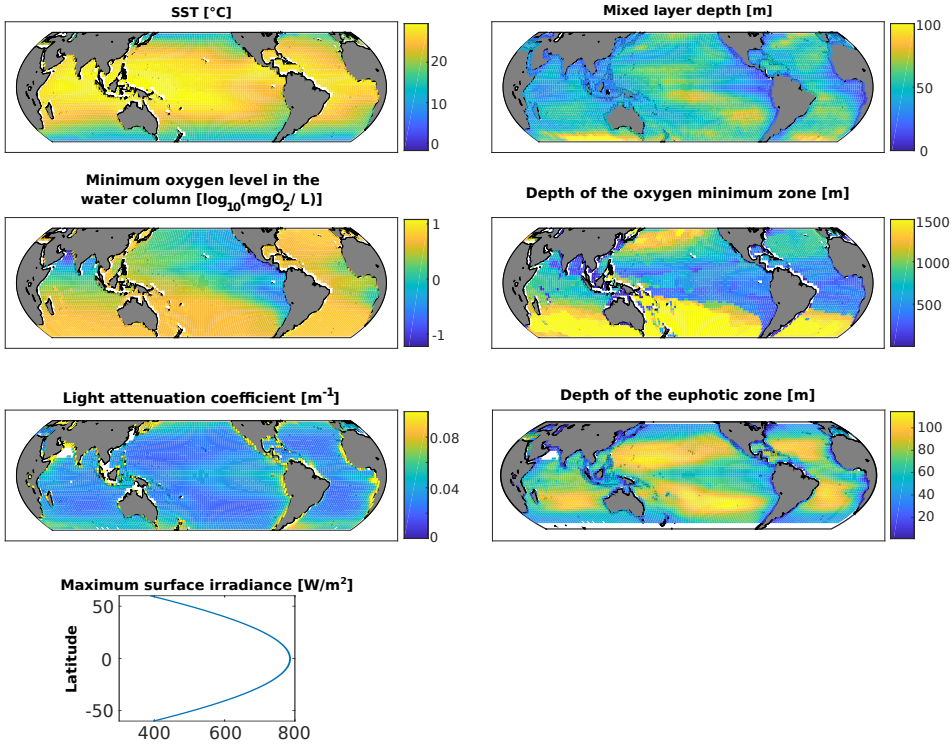

Figure 9.8: Physical inputs for the global model. Here, the depth of the oxygen minimum zone is capped to 1500 m and the light attenuation coefficient to 0.1 day^{-1}.

The global estimates of zooplankton are the outputs of the COBALT model (Stock et al., 2017), that are also used in the FEISTY model that provides the abundances of forage fish and large predators (Petrik et al., 2019).

The predicted global median mesopelagic fish biomass value of 3.833 Pg (Proud et al., 2018) (wet weight, assuming all fish retain gas-filled swimbladders throughout their life-cycles) is distributed proportionally by mesopelagic province (Proud et al., 2017) using the province values of predicted 38 kHz mesopelagic echo energy (i.e. the predicted total amount of echo-energy backscattered by the mesopelagic community when insonified using an echosounder operating at 38 kHz):

$$\text{Meso fish province biomass} = \frac{(\text{total biomass}) \cdot (\text{province 38 kHz meso echo energy})}{(\text{global 38 kHz meso echo energy})}. \tag{9.47}$$

The global abundance of jellyfish is unknown and likely to vary, both temporally and spatially. Our model incorporates this functional group, but their abundance is too low to confidently assess their contribution to the global carbon cycle. As such, we set their biomass to a constant and conservative estimate of $10^{-3}\,\mathrm{gCm}^{-2}$. Our model can be used to estimate the sensibility of the carbon fluxes to the abundance of these predators. Global biomasses of zooplankton and fish are pictured figure 9.9.

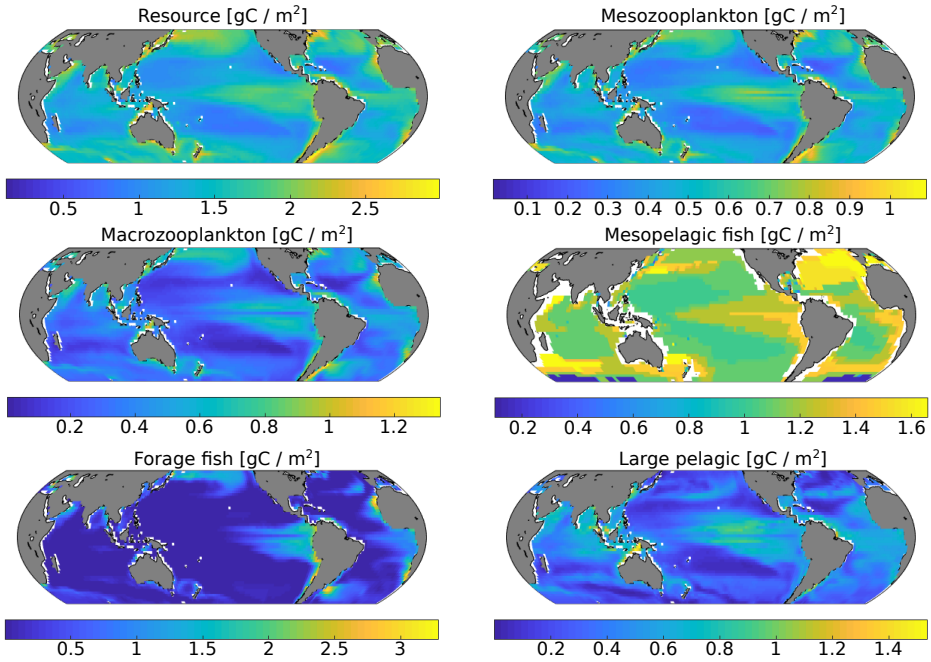

Figure 9.9: Biomasses of the different functional groups considered in gC / m^2.

Carbon export and sequestration

The global model outputs provide us with the 3D distribution of organisms, along with their ingestion, excretion and respiration rates. This allows us to compute how much carbon is respired by organisms in the global ocean, and how much carbon is excreted as fecal pellets. Assuming the sinking rate and degradation rates of fecal pellets (table 9.17 and eq. 9.41), we compute the flux of fecal material below any depth, but also the amount of fecal material that is turned into DIC (Dissolved Inorganic Carbon) by bacterial respiration.

The depth of the water column in the global model is set to 1000 m, and we extend here the water column to the *real* depth of the seafloor at the location considered. Fecal pellets then sink (and get degraded) below 1000 m and down to the seafloor. We consider that all material reaching the seafloor is respired. Figure 9.10 shows the globally average DIC source from animal respiration and bacterial respiration due to the degradation of sinking fecal pellets.

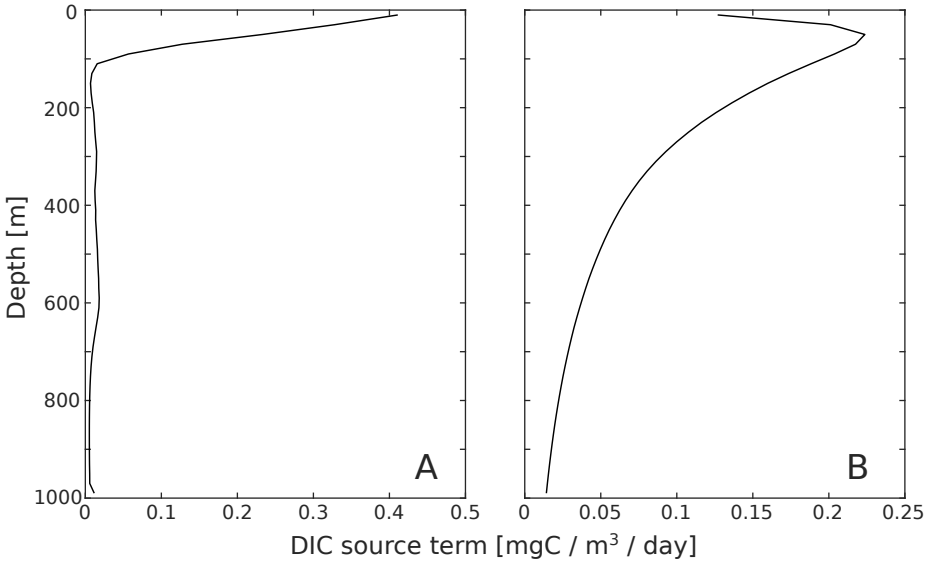

Figure 9.10: Globally averaged DIC source from (A) animal respiration and (B) bacterial respiration due to fecal pellets degradation.

We couple the respiration DIC source terms to OCIM, the Ocean Circulation Inverse Model (DeVries, 2014; DeVries and Weber, 2017). OCIM is a non-seasonal global ocean circulation model based on a transport matrix, allowing us to assess how much carbon is stored in the oceans through the different pathways (fecal pellets or respiration of the different functional groups considered). This measure is more representative than a global flux below an artificially chosen depth. First, a depth chosen arbitrarily has no biological meaning, unless it is chosen as the mixed layer depth below which carbon is effectively removed from phytoplankton (Buesseler et al., 2020). Second, a high carbon flux does not necessarily mean that a high amount of carbon will be stored. For example, carbon sinking below the euphotic

zone but in upwelling areas may get back to the surface quickly. Consequently, computing how much carbon the global ocean sequesters is a more robust way of assessing the efficiency of the biological carbon pump.

The concentration of biologically sequestered DIC is computed by solving the equation

$$\frac{dC_{in}}{dt} = \mathbf{A}C_{in} + J_{res}, \tag{9.48}$$

where $\mathbf{A}$ is the advection-diffusion matrix transport operator from the OCIM, J_{res} is the source of DIC from respiration, and C_{in} is dissolved inorganic carbon due to respiration. This equation is solved subject to a boundary condition of $C = 0$ at the sea surface, mimicking instantaneous air-sea CO_2 equilibration, and this calculation is repeated for each considered pathway.

After solving for C_{in} in equation (9.48), we volume integrate to obtain the total sequestered carbon inventory due to each mechanism (in PgC). Finally, dividing the total sequestered carbon inventory for each mechanisms by the source term of carbon (in PgC yr^{-1}) yields a sequestration time (in yr), an indication of the efficiency of the considered pathway.

Additional results

DSL depth and computed POC flux comparison with data

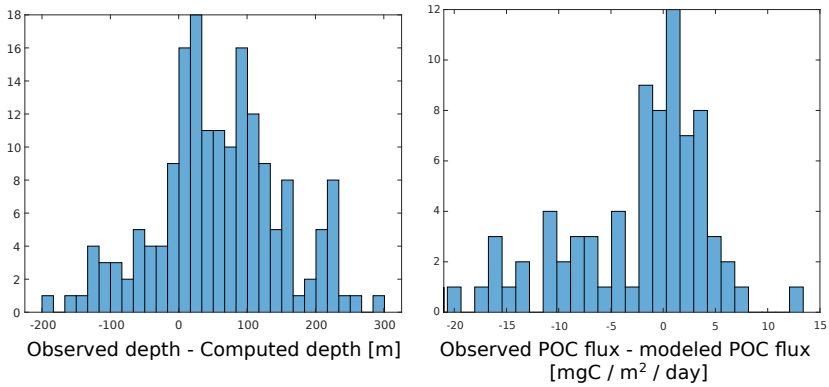

Figure 9.11: Comparison with data. Left panel: Histogram of the differences between the observed (from the Malaspina expedition, Klevjer et al. (2016)) and the computed depth of the deep scattering layer. Right panel: Difference between the observed (from sediment traps data, Lutz et al. (2007)) and modeled POC flux.

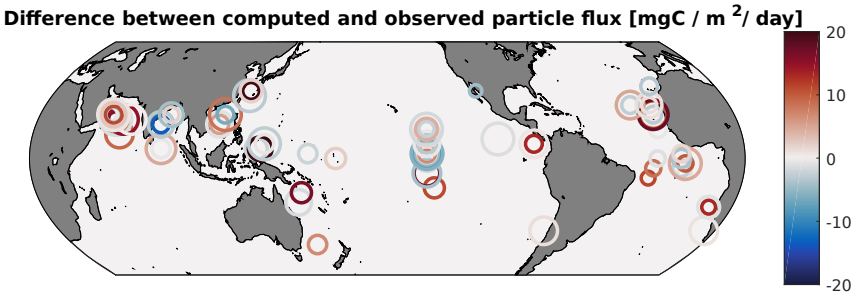

Figure 9.12: Difference between observed (from sediment traps data, Lutz et al. (2007)) and modeled POC flux. The size of the circle is proportional to the depth of the compared flux.

Regional sequestration potential

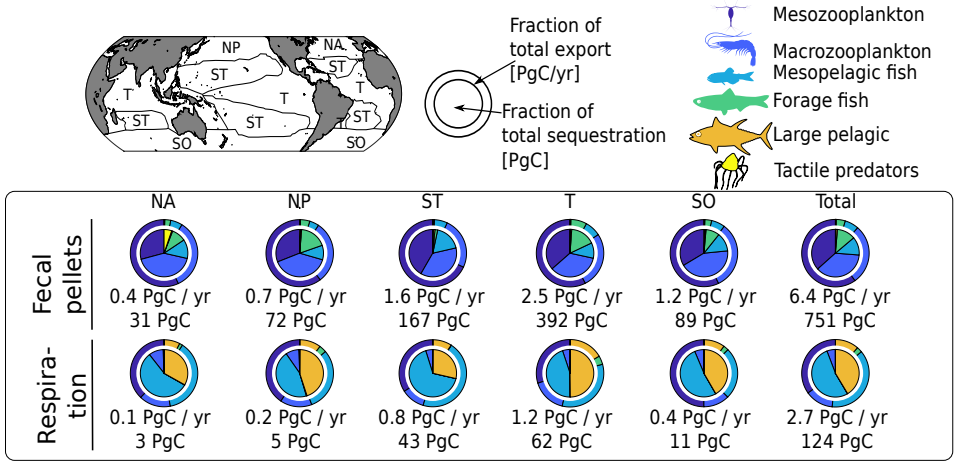

Figure 9.13: Geographical and functional breakout of carbon exported and sequestrated. NA stands for North Atlantic, NP for North Pacific, ST for subtropical gyres, T for tropics and upwelling zones, and SO for Southern Oceans. The figures below each pie chart represent the global contribution of the geographical zone in focus to carbon export and sequestration.

Respiration and excretion below the euphotic zone

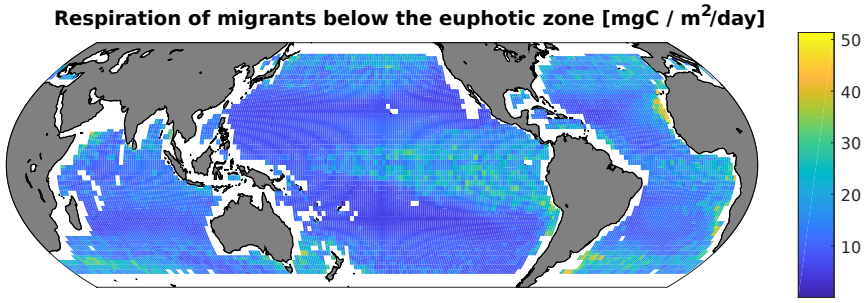

Figure 9.14: Total respiration of organisms below the euphotic zone.

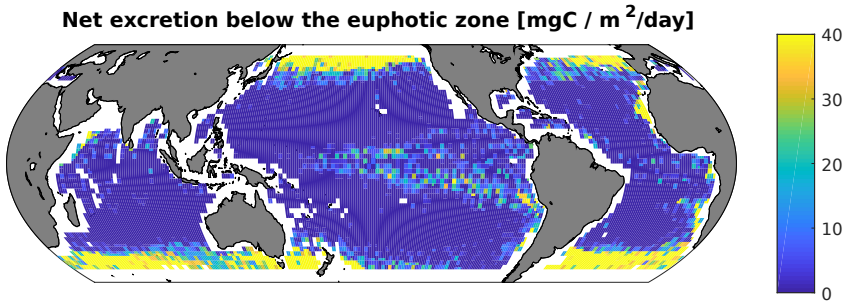

Figure 9.15: Net excretion (= fecal pellet excretion - consumption) of carbon below the euphotic zone.

Sensitivity analysis

Due to the very high number of parameters and high computational cost of each simulation, a complete sensitivity analysis could not be completed. As such, we performed an analysis of the most sensitive parameters with regards to carbon export, i.e. biomasses, fecal pellets sinking rates, bacterial degradation rate and assimilation efficiency. For the biomasses, two different scenarios were investigated: one where all biomasses are modified, and one where only mesopelagic fish biomass varies, as mesopelagic biomass is likely the estimate with the least confidence (except maybe tactile predators).

Overall, our results are quite robust. Despite small relative variations, the global trends in DSL depths are consistent between the different simulations. The total carbon sequestered via to respiration varies between 58.5 and 187 PgC, and the total carbon sequestered via fecal pellets degradation varies between 300 and 1764 PgC. The amount of carbon sinking below the euphotic zone varies between 1.85 and 10.6 PgC / yr, the amount of carbon respired below the euphotic zone varies between 0.5 and 1.61 PgC / yr, and the net amount of fecal pellets excreted below the euphotic zone varies between 0.21 and 1.46 PgC / yr.

The results are the most sensitive to variations in assimilation efficiencies, fecal pellets sinking rates and biomasses. Details of the variations for the different parameters are given below.

Total biomass

With biomass levels of 50 % the reference levels, the export below the euphotic zone is 1.85 PgC/yr, the respiration below the euphotic zone is 0.50 PgC/yr and the net excretion below the euphotic zone is 0.21 PgC/yr. With biomass levels of 150 % the reference levels, the export below the euphotic zone is 8.10 PgC/yr, the respiration below the euphotic zone is 1.61 PgC/yr and the net excretion below the euphotic zone is 1.02 PgC/yr. The DSL depths are still relatively close to the reference values (figures 9.16 and 9.17) and the total carbon sequestrated is roughly 50 % and 150% of the carbon sequestrated with reference biomass levels (tables 9.2 and 9.3).

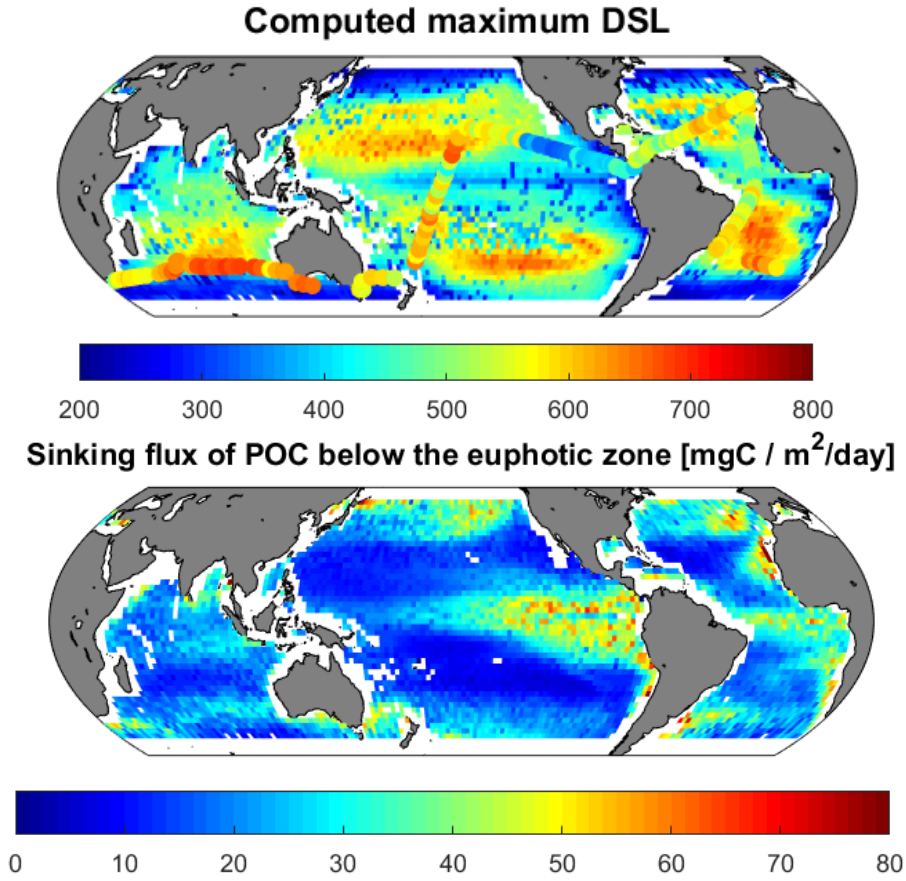

Figure 9.16: Top panel: Computed DSL depth. Bottom panel: Sinking flux of fecal pellets below the euphotic zone. Model run with biomasses equal to 50 % the reference value.

Table 9.2: Total carbon respired or excreted, corresponding sequestration and residence time for the different pathways considered in the model. Model run with biomasses equal to 50 % the reference value.

Organism	Respiration			Fecal pellets		
	Source [PgC / yr]	Sequestration [PgC]	Residence time [yr]	Source [PgC / yr]	Sequestration [PgC]	Residence time [yr]
Meso zooplankton	0.47	0.08	0.2	1.4	97	72
Macro zooplankton	0.18	3.5	19	0.8	114	146
Mesopelagic	0.50	29	59	0.2	44	217
Forage fish	0.02	0.05	1.97	0.1	42	339
Large pelagic	0.16	26	157	5.8e-3	3	504
Jellyfish	5e-4	0.02	41	1.8e-3	1	293
Total	1.3	58.5	45	2.5	300	122

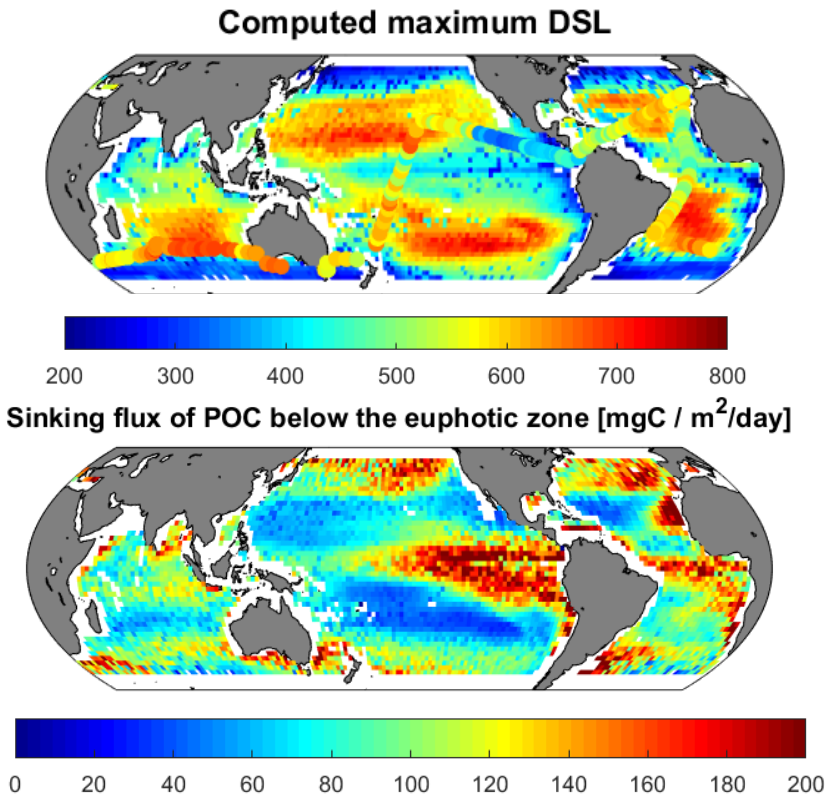

Figure 9.17: Top panel: Computed DSL depth. Bottom panel: Sinking flux of fecal pellets below the euphotic zone. Model run with biomasses equal to 150 % the reference value.

Table 9.3: Total carbon respired or excreted, corresponding sequestration and residence time for the different pathways considered in the model. Model run with biomasses equal to 150% the reference value.

Organism	Respiration			Fecal pellets		
	Source [PgC / yr]	Sequestration [PgC]	Residence time [yr]	Source [PgC / yr]	Sequestration [PgC]	Residence time [yr]
Meso zooplankton	1.41	0.4	0.3	6.7	477	71
Macro zooplankton	0.54	10.5	19	3.0	461	153
Mesopelagic	1.55	101	65	0.7	143	217
Forage fish	0.11	0.4	4	0.4	150	342
Large pelagic	0.49	77	157	0.03	13	501
Jellyfish	2e-3	0.09	52	0.01	4	296
Total	4.1	189	46	10.8	1248	116

Biomass of mesopelagic fish

Contrarily to other parameters that were varied of ± 50 %, the mesopelagic fish biomass varied between 20 and 200 % of the reference value, following current uncertainty estimates (Proud et al., 2018).

When varying only the biomass of mesopelagic fish, all carbon export values and rates remain relatively constant (table 9.4) except the export and sequestration values directly related to mesopelagic fish that varies according to the variation in mesopelagic biomass (tables 9.5, 9.6, 9.7 and 9.8).

Table 9.4: Global export, respiration and net excretion rates below the euphotic zone as the mesopelagic fish biomass varies.

% of the reference mesopelagic biomass	20 %	50%	100%	150%	200%
Export below the euphotic zone [PgC / yr]	4.6	4.6	4.8	5.0	5.2
Respiration below the euphotic zone [PgC / yr]	0.66	0.81	1.04	1.28	1.52
Net excretion below the euphotic zone [PgC / yr]	0.50	0.53	0.57	0.60	0.64

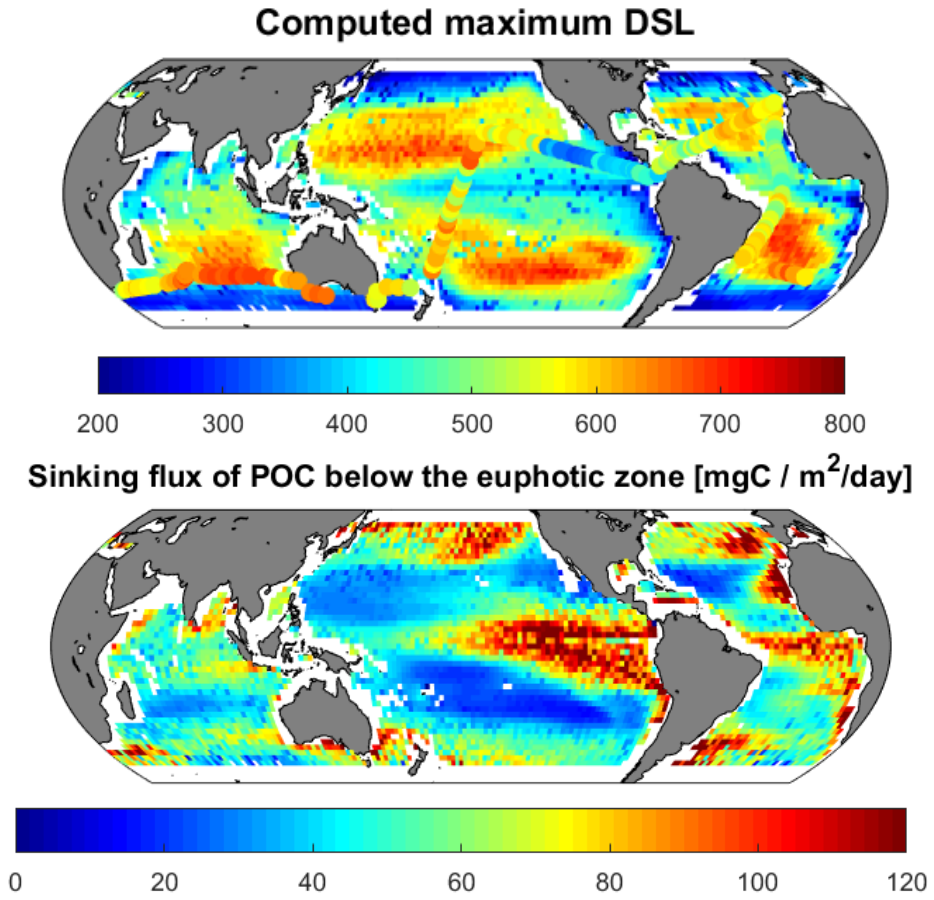

Figure 9.18: Top panel: Computed DSL depth. Bottom panel: Sinking flux of fecal pellets below the euphotic zone. Model run with mesopelagic biomass equal to 20 % the reference value.

Table 9.5: Total carbon respired or excreted, corresponding sequestration and residence time for the different pathways considered in the model. Model run with mesopelagic biomass equal to 20% the reference value.

Organism	Respiration			Fecal pellets		
	Source [PgC / yr]	Sequestration [PgC]	Residence time [yr]	Source [PgC / yr]	Sequestration [PgC]	Residence time [yr]
Meso zooplankton	0.95	0.1	0.1	4.0	280	71
Macro zooplankton	0.36	7.0	19	1.8	275	150
Mesopelagic	0.20	12.9	63	0.09	19	216
Forage fish	0.08	0.3	3.5	0.3	94	341
Large pelagic	0.32	51.1	157	1e-2	5	488
Jellyfish	1e-3	0.05	46	7e-3	21	292
Total	1.9	72	38	6.2	674	109

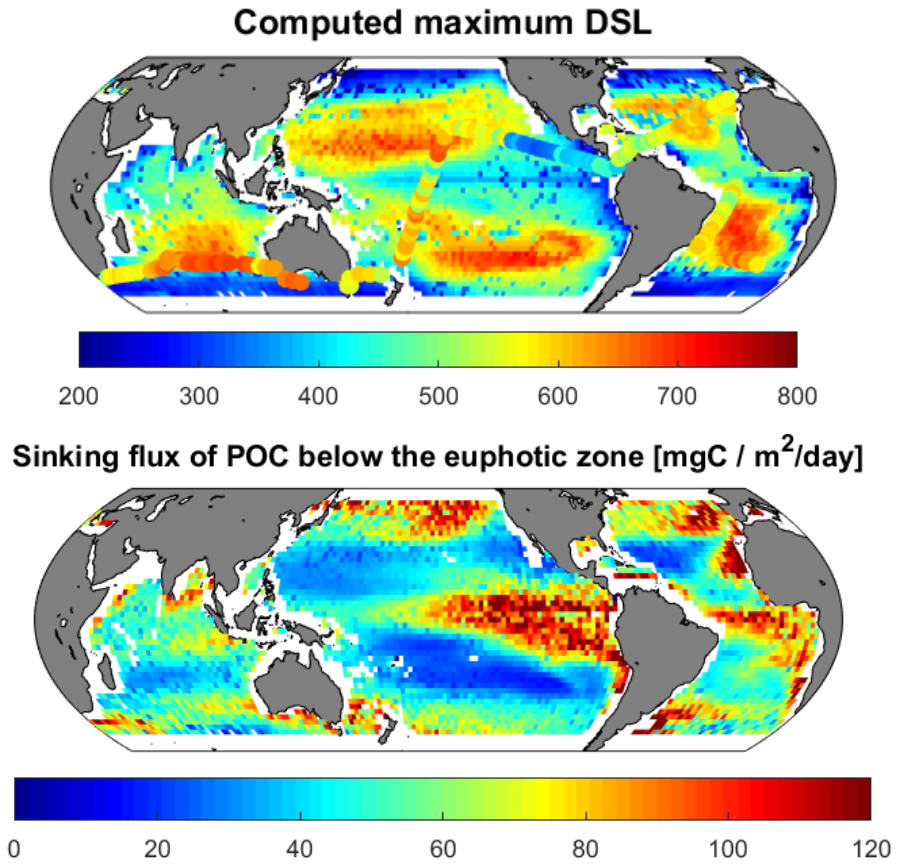

Figure 9.19: Top panel: Computed DSL depth. Bottom panel: Sinking flux of fecal pellets below the euphotic zone. Model run with mesopelagic biomass equal to 50 % the reference value.

Table 9.6: Total carbon respired or excreted, corresponding sequestration and residence time for the different pathways considered in the model. Model run with mesopelagic biomass equal to 50% the reference value.

Organism	Respiration			Fecal pellets		
	Source [PgC / yr]	Sequestration [PgC]	Residence time [yr]	Source [PgC / yr]	Sequestration [PgC]	Residence time [yr]
Meso zooplankton	0.94	0.2	0.2	3.9	275	71
Macro zooplankton	0.36	6.9	19	1.9	277	150
Mesopelagic	0.51	32.3	63	0.2	46	216
Forage fish	0.07	0.2	3	0.3	94	342
Large pelagic	0.32	51.1	157	0.01	6	495
Jellyfish	1e-3	0.05	47	7e-3	2	293
Total	2.2	90.8	41	6.2	700	113

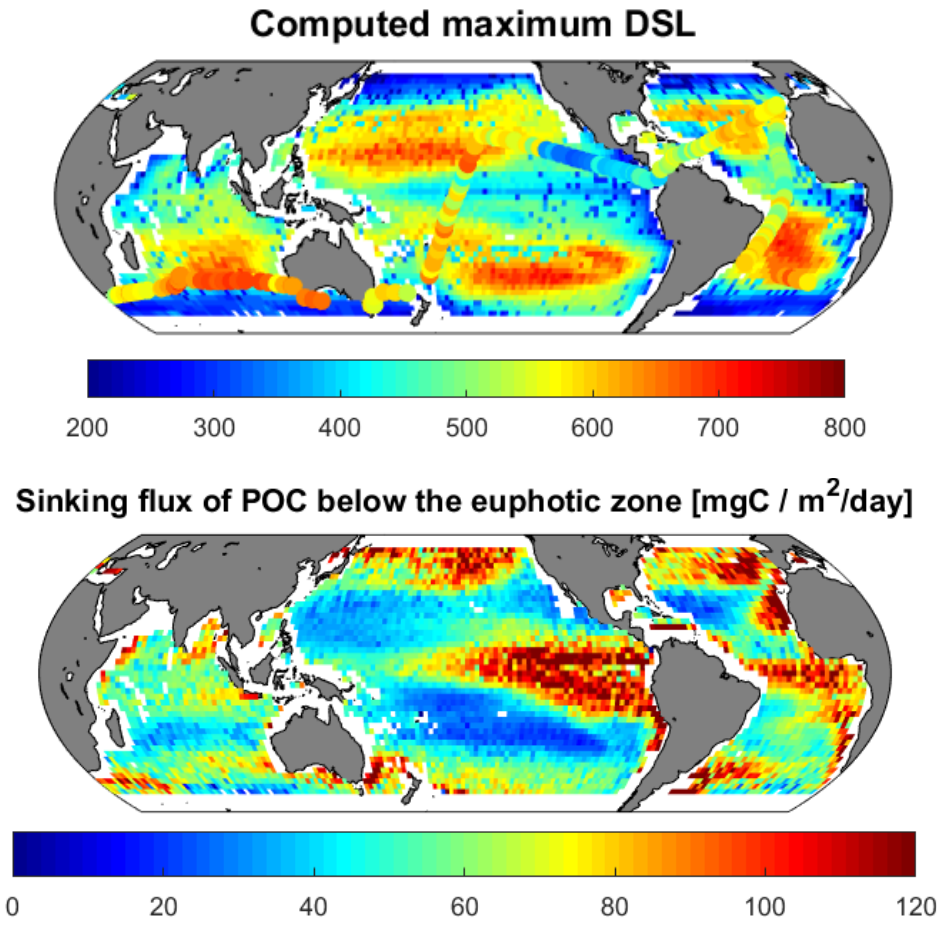

Figure 9.20: Top panel: Computed DSL depth. Bottom panel: Sinking flux of fecal pellets below the euphotic zone. Model run with mesopelagic biomass equal to 150 % the reference value.

Table 9.7: Total carbon respired or excreted, corresponding sequestration and residence time for the different pathways considered in the model. Model run with mesopelagic biomass equal to 150 % the reference value.

Organism	Respiration			Fecal pellets		
	Source [PgC / yr]	Sequestration [PgC]	Residence time [yr]	Source [PgC / yr]	Sequestration [PgC]	Residence time [yr]
Meso zooplankton	0.94	0.3	0.3	3.8	274	71
Macro zooplankton	0.36	7.0	20	1.9	283	151
Mesopelagic	1.53	96	63	0.6	138	217
Forage fish	0.06	0.19	3	0.3	91	339
Large pelagic	0.32	51	157	0.02	8	505
Jellyfish	1e-3	0.05	48	7e-3	2	294
Total	3.2	155	48	6.6	796	121

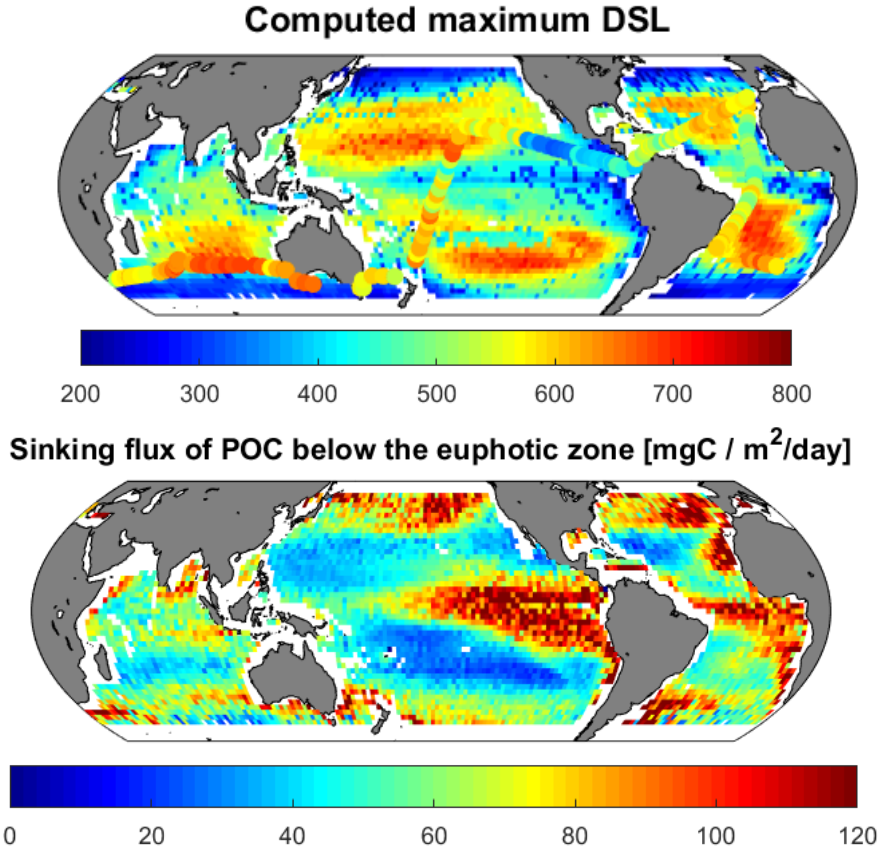

Figure 9.21: Top panel: Computed DSL depth. Bottom panel: Sinking flux of fecal pellets below the euphotic zone. Model run with mesopelagic biomass equal to 200 % the reference value.

Table 9.8: Total carbon respired or excreted, corresponding sequestration and residence time for the different pathways considered in the model. Model run with mesopelagic biomass equal to 200 % the reference value.

Organism	Respiration			Fecal pellets		
	Source [PgC / yr]	Sequestration [PgC]	Residence time [yr]	Source [PgC / yr]	Sequestration [PgC]	Residence time [yr]
Meso zooplankton	0.94	0.2	0.3	3.8	272	71
Macro zooplankton	0.36	7.0	20	1.9	286	152
Mesopelagic	2.04	128.6	63	0.9	185	217
Forage fish	0.05	0.2	3	0.3	94	338
Large pelagic	0.32	51	157	0.02	9	508
Jellyfish	1e-3	0.05	47	7e-3	2	296
Total	3.7	187	51	6.9	848	123

Fecal pellets sinking rates

With variations between 50-150 % of the reference levels, the carbon export below the euphotic zone varies between 3.91 and 5.19 PgC/yr. The respiration below the euphotic zone varies very little, between 1.04 and 1.06 PgC/yr, and the net excretion below the euphotic zone varies also little, between 0.56 and 0.59 PgC/yr. However, and as anticipated, the total carbon sequestered through the fecal pellet degradation pathway varies significantly, between 334 and 1153 PgC (tables 9.9 and 9.10).

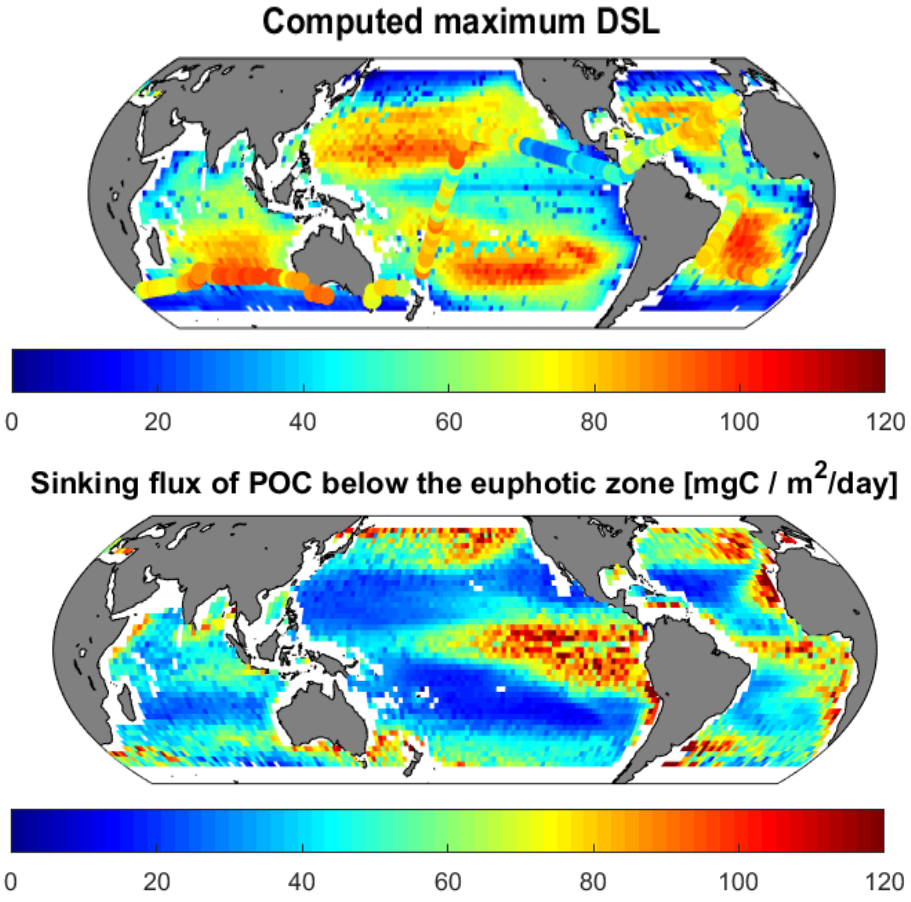

Figure 9.22: Top panel: Computed DSL depth. Bottom panel: Sinking flux of fecal pellets below the euphotic zone. Model run with fecal pellets sinking rates equal to 50 % the reference value.

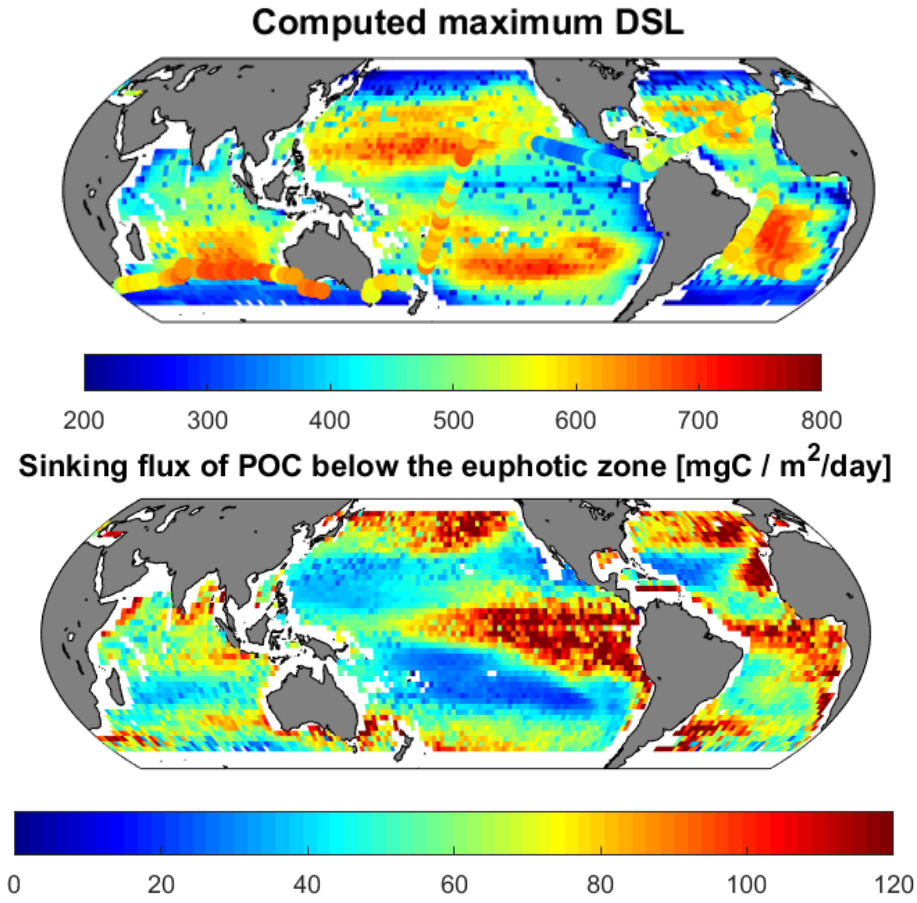

Figure 9.23: Top panel: Computed DSL depth. Bottom panel: Sinking flux of fecal pellets below the euphotic zone. Model run with fecal pellets sinking rates equal to 150 % the reference value.

Table 9.9: Total carbon respired or excreted, corresponding sequestration and residence time for the different pathways considered in the model. Model run with fecal pellets sinking rates equal to 50 % the reference value.

Organism	Respiration			Fecal pellets		
	Source [PgC / yr]	Sequestration [PgC]	Residence time [yr]	Source [PgC / yr]	Sequestration [PgC]	Residence time [yr]
Meso zooplankton	0.94	0.3	0.3	3.8	105	28
Macro zooplankton	0.36	6.7	19	1.8	131	73
Mesopelagic	1.02	65	64	0.4	41	100
Forage fish	0.07	0.2	3	0.3	51	196
Large pelagic	0.32	51	157	0.01	5	365
Jellyfish	1e-3	5e-2	47	7e-3	1	156
Total	2.7	123	46	6.3	334	53

Table 9.10: Total carbon respired or excreted, corresponding sequestration and residence time for the different pathways considered in the model. Model run with fecal pellets sinking rates equal to 150 % the reference value.

Organism	Respiration			Fecal pellets		
	Source [PgC / yr]	Sequestration [PgC]	Residence time [yr]	Source [PgC / yr]	Sequestration [PgC]	Residence time [yr]
Meso zooplankton	0.95	0.3	0.3	4.0	470	119
Macro zooplankton	0.36	7	20	1.9	413	221
Mesopelagic	1.02	65	64	0.44	139	312
Forage fish	0.07	0.2	3	0.3	119	419
Large pelagic	0.32	51	157	0.02	9	554
Jellyfish	1e-3	0.05	46	7e-3	3	379
Total	2.7	124	46	6.6	1153	175

Bacterial degradation rate

The bacterial degradation rate has a relatively minor influence on export and rates below the euphotic zone, as a variation between 50-150 % of the reference level implies an export below the euphotic zone between 4.37-5.31 PgC/yr, a respiration below the euphotic zone between 1.04-1.05 PgC/yr and a net excretion of fecal pellets below the euphotic zone between 0.52-0.60 PgC/yr. The total carbon sequestered through respiration does not vary much either, but the amount of carbon sequestered through the bacterial degradation of fecal pellets varies significantly, between 515 and 1102 PgC/yr (tables 9.11 and 9.12).

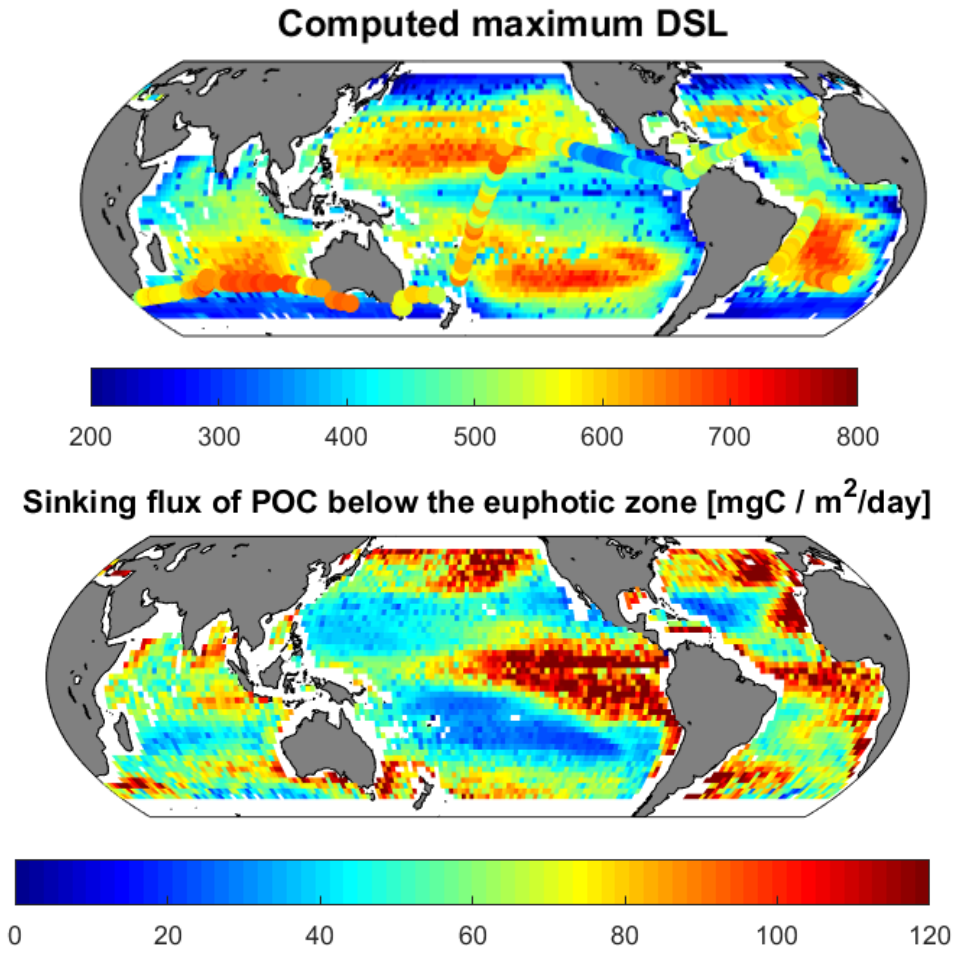

Figure 9.24: Top panel: Computed DSL depth. Bottom panel: Sinking flux of fecal pellets below the euphotic zone. Model run with bacterial degradation rate equal to 50 % the reference value.

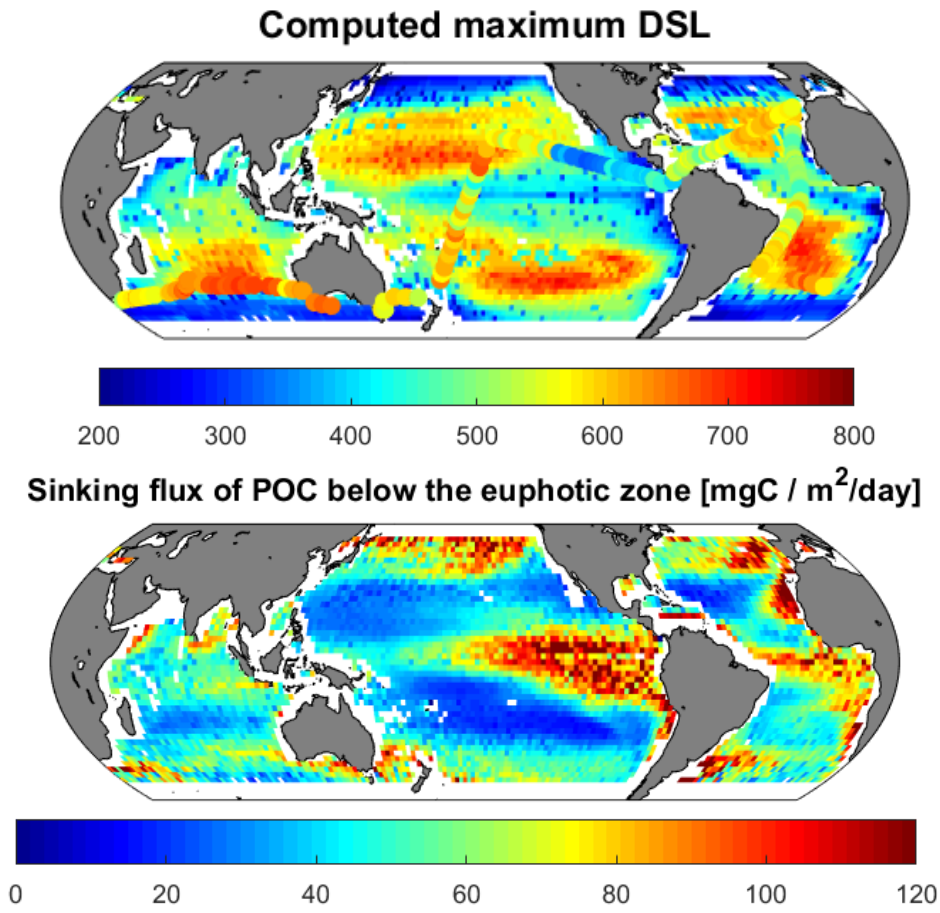

Figure 9.25: Top panel: Computed DSL depth. Bottom panel: Sinking flux of fecal pellets below the euphotic zone. Model run with bacterial degradation rate equal to 150 % the reference value.

Table 9.11: Total carbon respired or excreted, corresponding sequestration and residence time for the different pathways considered in the model. Model run with bacterial degradation rate equal to 50 % the reference value.

Organism	Respiration			Fecal pellets		
	Source [PgC / yr]	Sequestration [PgC]	Residence time [yr]	Source [PgC / yr]	Sequestration [PgC]	Residence time [yr]
Meso zooplankton	0.94	0.3	0.3	3.3	486	146
Macro zooplankton	0.36	7.0	19	1.7	419	248
Mesopelagic	1.02	65	63	0.3	108	335
Forage fish	0.07	0.2	3	0.2	82	445
Large pelagic	0.32	51	157	9e-3	5	592
Jellyfish	1e-3	5e-2	47	5e-3	2	403
Total	2.7	123	46	5.5	1102	200

Table 9.12: Total carbon respired or excreted, corresponding sequestration and residence time for the different pathways considered in the model. Model run with bacterial degradation rate equal to 150 % the reference value.

Organism	Respiration			Fecal pellets		
	Source [PgC / yr]	Sequestration [PgC]	Residence time [yr]	Source [PgC / yr]	Sequestration [PgC]	Residence time [yr]
Meso zooplankton	0.94	0.2	0.2	4.1	175	43
Macro zooplankton	0.36	7.0	20	1.7	177	101
Mesopelagic	1.02	64.0	64	0.5	68	150
Forage fish	0.07	0.21	3	0.3	85	266
Large pelagic	0.32	51	157	0.02	8	429
Jellyfish	1e-3	0.05	47	8e-3	1.7	222
Total	2.7	123	46	6.6	515	78

Assimilation efficiencies

Contrarily to the other parameters, assimilation efficiencies levels cannot be set to 150 % of the reference levels as they cannot be greater than 1. As such, when conducting this sensitivity analysis, the upper bound of the assimilation efficiency was taken as the mean between the reference value and 1. For example, a reference value of $\varphi = 0.85$ gave an upper bound of 0.925 in this analysis. The lower bound of the sensitivity analysis was kept to 50% of the reference values (i.e. a reference value of 0.85 had a lower bound of 0.425 here).

The assimilation efficiency is one of the parameters with the biggest influence on carbon sequestration, as it controls directly the fraction of ingested carbon that will be excreted as fecal pellets. Here, the export below the euphotic zone varies between 2.43 and 10.06 PgC/yr. The respiration below the euphotic zone is quite stable, varying between 1.02 and 1.06 PgC/yr, but the net excretion below the euphotic zone varies significantly, between 0.25 and 1.46 PgC/yr. This results in a total carbon sequestered through the fecal pellet degradation pathway varying between 373 and 1764 PgC.

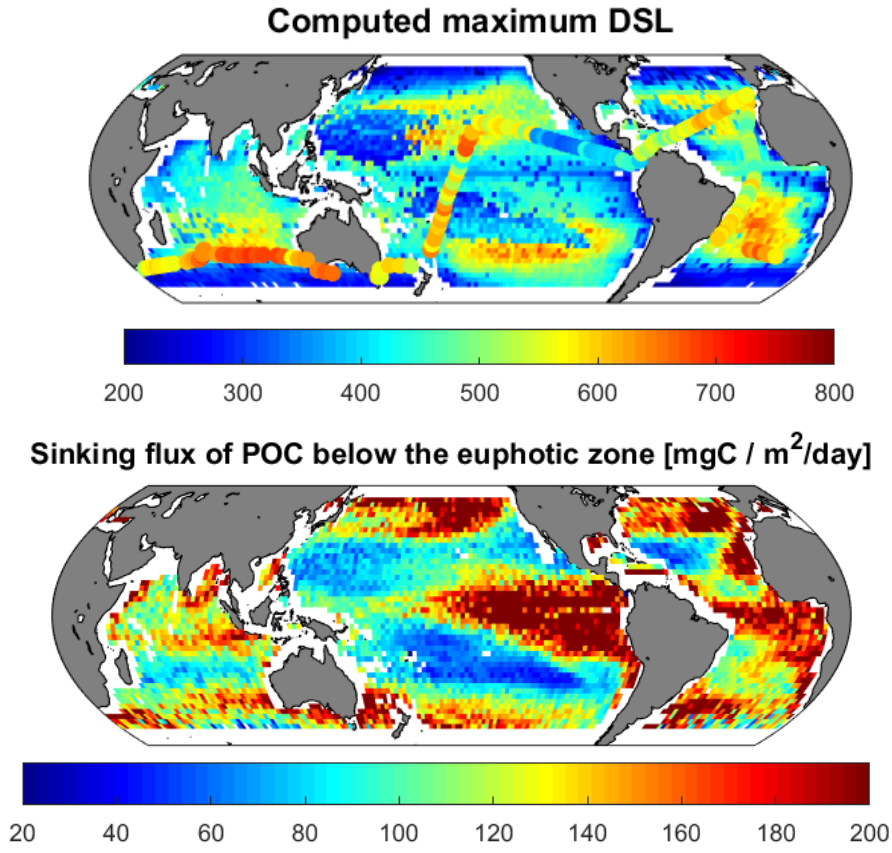

Figure 9.26: Top panel: Computed DSL depth. Bottom panel: Sinking flux of fecal pellets below the euphotic zone. Model run with assimilation efficiencies equal to 50 % the reference values.

Table 9.13: Total carbon respired or excreted, corresponding sequestration and residence time for the different pathways considered in the model. Model run with assimilation efficiencies equal to 50 % the reference values.

Organism	Respiration			Fecal pellets		
	Source [PgC / yr]	Sequestration [PgC]	Residence time [yr]	Source [PgC / yr]	Sequestration [PgC]	Residence time [yr]
Meso zooplankton	0.94	0.2	0.2	8.1	611	75
Macro zooplankton	0.36	6.6	18	3.6	525	146
Mesopelagic	0.95	49.6	52	1.9	421	220
Forage fish	0.02	0.03	1	0.5	186	342
Large pelagic	0.32	51.1	157	0.03	18	514
Jellyfish	1e-3	0.04	44	1e-2	3	301
Total	2.59	107.6	42	14.2	1764	124

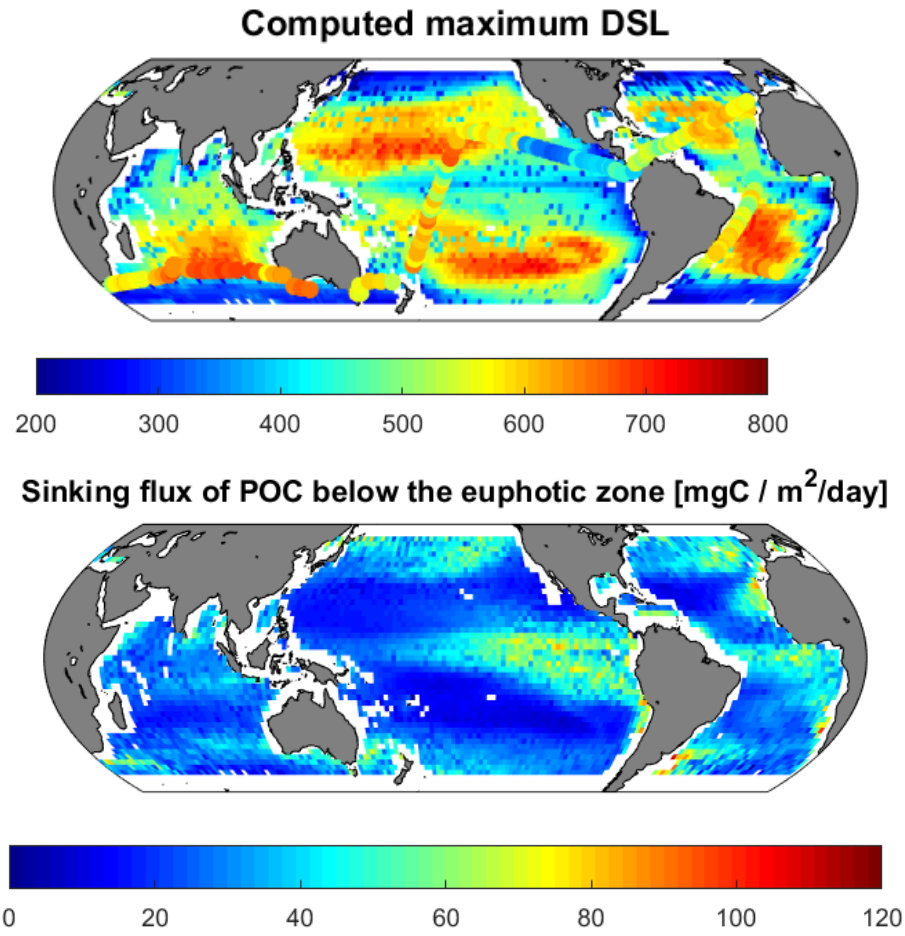

Figure 9.27: Top panel: Computed DSL depth. Bottom panel: Sinking flux of fecal pellets below the euphotic zone. Model run with assimilation efficiencies equal to the mean between 1 and the reference values.

Table 9.14: Total carbon respired or excreted, corresponding sequestration and residence time for the different pathways considered in the model. Model run with assimilation efficiencies equal to the mean between 1 and the reference values.

Organism	Respiration			Fecal pellets		
	Source [PgC / yr]	Sequestration [PgC]	Residence time [yr]	Source [PgC / yr]	Sequestration [PgC]	Residence time [yr]
Meso zooplankton	0.95	0.26	0.3	1.9	129	68
Macro zooplankton	0.36	7	19	1.0	151	154
Mesopelagic	1.02	66	64	0.2	44	215
Forage fish	0.09	0.44	5	0.1	45	338
Large pelagic	0.32	51	157	7e-3	3.6	501
Jellyfish	1e-3	6e-2	51	5e-3	1	291
Total	2.74	125	46	3.2	373	116

Glossary of parameters

Table 9.15: Glossary of non-population-specific parameters and values

Parameter	Signification	Value	Unit
σ	Fraction of daylight hours in a day	0.5	-
z	Depth	-	m
i, j	Daytime (Nighttime) depth or corresponding water layer	-	m/-
day	Boolean for dayttime (1) or nighttime (0)	-	-
n	Number of water layers	50	-
ΔZ	Width of each water layer	20	m
Z_{MAX}	Maximum depth of the 1D model	$n \cdot \Delta Z = 1000$	m
T	Temperature	-	$^{\circ}$C
O_2	Oxygen concentration	-	$\mathrm{mgO_2\ L^{-1}}$
p_{O_2}	Oxygen partial pressure	-	kPa
$light$	Light level	eq. 9.21	$\mathrm{W\ m^{-2}}$
L_{max}	Maximum irradiance at the surface	eq. 9.44	$\mathrm{W\ m^{-2}}$
ρ_l	Attenuation coefficient between day and night	1 or 10^{-5}	-
κ	Light attenuation coefficient of the water	see figure 9.8	$\mathrm{m^{-1}}$
ρ	Density of seawater	1028	$\mathrm{kg\ m^{-3}}$
ν_w	Kinematic viscosity of seawater	$1.3 \cdot 10^{-6}$	$\mathrm{m^2\ s^{-1}}$
G_{SG}	Solar constant	1367	$\mathrm{W\ m^{-2}}$
d	Day of the year	-	-
β	Solar altitude angle	eq. 9.45	rad
h	Hour angle	0	rad
δ	Solar inclination angle	$23.45 \sin(360 \frac{d+284}{365})$	rad
z_0	Mixed layer depth	see figure 9.8	m
R	Vertical profile of resources	eq. 9.46	$\mathrm{gC\ m^{-3}}$
Φ_{det}	Increase in zooplankton-fecal pellets encounter rate	eq. 9.35	-
ψ	Maximum fraction of detritus that can be consumed daily	0.8	$\mathrm{day^{-1}}$
$\tilde{F}_X^{D_Y}$	Corrected F with the maximum ingestion of detritus (only valid for $X = C$ and $X = P$)	eq. 9.38	
α	Bacterial degradation rate of fecal matter	eq. 9.41	$\mathrm{day^{-1}}$
α_0	Maximum bacterial degradation rate	0.5	$\mathrm{day^{-1}}$
Q_{bac}	Q_{10} factor for bacterial degradation	1.1	-
$T_{ref,bac}$	Reference temperature for bacterial degradation rate	$\frac{1}{200} \int_0^{200} T(z)dz$	$^{\circ}$ C
K_{O_2}	Half-saturation constant for bacterial degradation	10	$\mathrm{mgO_2\ L^{-1}}$
λ_t	Rescaling factor in the Replicator equation	$0.05/\max(W_X(i,j))$	-
δ_t	Time step of the Replicator equation	-	-
$\mathbf{A}$	Advection-diffusion matrix transport operator from OCIM	-	-

Table 9.16: Glossary of population-specific functions and rates

Symbol	Signification	Expression	Unit
X	Placeholder for the different populations: C (mesozooplankton), P (macrozooplankton), M (mesopelagic), F (forage), A (large pelagic), J (jellyfish), or D_X (fecal pellets produced by X)	-	-
X_{ij}	Fraction of population X following strategy ij	eq. 9.43	-
D_X	Concentration of fecal pellets created by X in the water column	eq. 9.40	gC m^{-3}
$X(i, day)$	Concentration of organisms X at i during day	eq. 9.2	gC m^{-3}
$W_X(i,j)$	Fitness of an individual X with strategy ij	eq. 9.9	-
$g_X(i,j)$	Growth rate of an individual X with strategy ij	$\nu_X - Q_X - C_{migr,X}$	day^{-1}
$m_X(i,j)$	Mortality rate of an individual X with strategy ij	$\mu_X + \mu_{0X}$	day^{-1}
$Q_X(i,j)$	Strategy-dependent standard metabolic rate	eq. 9.10	day^{-1}
$C_{migr,X}(i,j)$	Migration cost	eq. 9.34	day^{-1}
$\tilde{Q}_X(z)$	Depth-dependent standard metabolic cost	eq. 9.11	day^{-1}
$\nu_X(i,j)$	Strategy-dependent assimilation rate	eq. 9.13	day^{-1}
$\tilde{\nu}_{X,i,j}(z)$	Depth-dependent assimilation rate	eq. 9.17	day^{-1}
$u_{X,i,j}(z)$	(Cruising) swimming speed	eq. 9.14	mday^{-1}
$u_{max,X}$	Maximum swimming speed	eq. 9.25	ms^{-1}
$I_{max,X,i,j}(z)$	Maximum ingestion rate	eq. 9.14	gC day^{-1}
$SMR_{0,X}$	Standard metabolic cost at T_{ref}	eq. 9.12	day^{-1}
$u_{0,X}$	Reference swimming speed	eq. 9.15	m day^{-1}
$I_{max0,X}$	Reference max. ingestion rate	eq. 9.16	gC day^{-1}
s	Function used for SMR and MMR	eq. 9.3	day^{-1}
SMR	Standard Metabolic Rate	eq. 9.4 and 9.6	day^{-1}
MMR	Maximum Metabolic Rate	eq. 9.5 and 9.7	day^{-1}
AS	Aerobic scope	$MMR - SMR$	day^{-1}
$\tilde{S}_X(i,j,day)$	$AS(z=i)$ if $day=1$, $AS(z=j)$ if $day=0$	-	day^{-1}
$S_X(i,j,z)$	Available aerobic scope	eq. 9.8	day^{-1}
$S_{0,X}$	Reference metabolic scope for u_0 & I_{max0}	$\max S_X$	day^{-1}
$F_X^Y(z)$	Depth-dependent specific ingestion rate of prey Y by pred. X	eq. 9.18	day^{-1}
$E_X^Y(z)$	Depth-dependent encounter rate of Y by X	eq. 9.19	gC day^{-1}
$\Phi(X,Y)$	Preference function of X for Y	table 9.18	-
$\Gamma_X^Y(z, day)$	Capture probability of Y by X during an attack event	eq. 9.28	-
r_{esc}	Length of escape jump by prey	eq. 9.26	m
r_{detec}	Prey detection distance of predator	$\Lambda_Y^X(z, day)$	m
r_{capt}	Capture distance for predator	$0.1 l_X$	m
r_{attac}	Length of attack jump for predator	eq. 9.27	
v_{esc}	Volume of the escape sphere	$\frac{4}{3}\pi r_{esc}^3$	m^3
v_{capt}	Volume of the escape sphere swept by predator	-	m^3
$V_X^Y(z)$	Clearance rate of X for Y	eq. 9.22, 9.23, 9.24	m^3 day^{-1}
$\Lambda_X^Y(z, day)$	Visual range of X	eq. 9.20	m
$\mu_{X,i,j}$	Mortality rate due to predation for strategy ij	eq. 9.29	day^{-1}
$\tilde{\mu}_X(z, day)$	Mortality rate due to predation at (z,day)	eq. 9.30	day^{-1}
Dr_X	Hydrodynamic drag	eq. 9.31	kg m s^{-2}
C_D	Drag coefficient	eq. 9.32	-
Re_X	Reynolds number	eq. 9.33	-
W_X^0	Fitness of population X at the Nash equilibrium	eq. 9.42	-
X'_{ij}	Intermediate value in the Replicator equation	eq. 9.43	-

Table 9.16 – continued from previous page

Symbol	Signification	Expression	Unit
$D_{crea,X}$	Creation rate of fecal pellets by X	eq. 9.36	$\mathrm{gCm^{-3}day^{-1}}$
$D_{conso,X}$	Consumption rate of fecal pellets X	eq. 9.37	$\mathrm{gCm^{-3}day^{-1}}$
ζ_X	Source term of detritus X in each water layer	eq. 9.39	$\mathrm{gCm^{-3}day^{-1}}$
J_{res}	Source of DIC	-	$\mathrm{gCm^{-3}day^{-1}}$
C_{in}	DIC due to respiration	eq. 9.48	$\mathrm{gCm^{-3}}$

Table 9.17: Glossary of population-dependent parameters. Subscript $_X$ was omitted for readability. * The half-saturation constant for large pelagic fish is different for mesopelagic (1) and for the other organisms (10^{-1}), as mesopelagic organisms are dark and adapted to hiding in very low light conditions.

Param.	Signification	Unit	Mesozoo-plankton	Macrozoo-plankton	Mesopelagic fish	Forage fish	Large pelagic fish	Tactile predators
l	Length of a typical individual	m	$5 \cdot 10^{-4}$	$4 \cdot 10^{-3}$	0.03	0.2	1	0.2
w	Carbon weight of a typical individual	gC	10^{-5}	$5 \cdot 10^{-4}$	0.18	15.2	1900	11.8
$\tilde{X}$	Biomass in the water column	gCm^{-2}	fig. 9.9	fig. 9.9	fig. 9.9	fig. 9.9	fig. 9.9	10^{-3}
Q_{10}	Temperature coefficient	-	2	2	2	1.5	2	3
T_{ref}	Reference temperature	°C	$\frac{1}{100}\int_0^{100} T(z)dz$	15	6	$\frac{1}{200}\int_0^{200} T(z)dz$	$T(z = 200\,\mathrm{m})$	10
T_{max}	Maximum temperature	°C	$\frac{1}{20}\int_0^{20} T(z)dz$	20	15	$\max T(z)$	$\max T(z)$	18
φ	Assimilation efficiency	-	0.7	0.7 (0.1 if detritus)	0.85	0.65	0.65	0.39
R_0	Maximum detection distance	m	$2l_C$	$2l_P$	table 9.19	table 9.19	table 9.19	0.5
K_e	Half-saturation constant for light	Wm^{-2}	-	-	10^{-4}	1	$10^{-1}, 1*$	-
γ	Cross-sectionnal area efficiently scanned	-	-	0.5	0.5	0.5	0.5	-
f	Filtering efficiency of tactile predators	-	-	-	-	-	-	0.089
μ_0	Background mortality rate	day^{-1}	0.1	$0.05+\frac{light(z_i,1)+light(z_j,0)}{light(0,1)+light(0,0)}$	$0.05+\frac{light(z_i,1)+light(z_j,0)}{light(0,1)+light(0,0)}$	0.05	0.05	0.05
p_{crit}	Critical oxygen partial pressure	kPa	3.5	0.5	0.2	5	0.5	1
p_{reg}	Transition between oxy- regulation and conformism	% oxy. satur.	0.6	0.6	-	-	-	0.6
Δ_{MR}	Maximum AS compared to SMR	-	3	3	6	6	6	2
ω	Fecal pellet sinking speed	mday^{-1}	120	180	300	500	1000	500
ϵ	Swimming efficiency	-	0.01	0.01	0.01	0.01	0.01	0.01

Table 9.18: Preference function values. Predators are in line, prey in column.

	Resource	Detritus	MesoZPK	MacroZPK	Forage	Meso	Tact
MesoZPK	1	0	-	0	0	0	0
MacroZPK	1	1	1	-	0	0	0
Forage	0	0	1	1	-	1	0
Meso	0	0	0.1	1	0	-	0
Tact	0	0	1	1	0	0	-
Top	0	0	0	0	1	0.2	0.1

Table 9.19: Maximum visual range in m. Visual "viewers" (predators or prey) are in lines, and their targets are in columns.

	MesoZPK	MacroZPK	Meso	Forage	Tact	Large pelagic
Mesopelagic	0.05	0.2	-	0.3	0.3	1
Forage fish	0.2	2	2	-	-	3
Large pelagic	-	-	10	3	5	-

Bibliography

Acuña, J. L., López-Urrutia, Á., and Colin, S. (2011). Supplementary material- Faking giants: The evolution of high prey clearance rates in jellyfishes. *Science*, 333(6049):1627–1629.

Andersen, K. H. (2019). *Fish Ecology, Evolution, and Exploitation : A New Theoretical Synthesis*. Princeton University Press, monographs edition.

Archibald, K. M., Siegel, D. A., and Doney, S. C. (2019). Modeling the impact of zooplankton diel vertical migration on the carbon export flux of the biological pump. *Global Biogeochemical Cycles*.

Aumont, O., Maury, O., Lefort, S., and Bopp, L. (2018). Evaluating the potential impacts of the diurnal vertical migration by marine organisms on marine biogeochemistry. *Global Biogeochemical Cycles*, pages 1–22.

Bandara, K., Varpe, Ø., Søreide, J. E., Wallenschus, J., Berge, J., and Eiane, K. (2016). Seasonal vertical strategies in a high-Arctic coastal zooplankton community. *Marine Ecology Progress Series*, 555:49–64.

Blachowiak-Samolyk, K., Kwasniewski, S., Richardson, K., Dmoch, K., Hansen, E., Hop, H., Falk-Petersen, S., and Mouritsen, L. T. (2006). Arctic zooplankton do not perform diel vertical migration (DVM) during periods of midnight sun. *Marine Ecology Progress Series*, 308(Dvm):101–116.

Brun, P., Stamieszkin, K., Visser, A. W., Licandro, P., Payne, M. R., and Kiørboe, T. (2019). Climate change has altered zooplankton-fuelled carbon export in the North Atlantic. *Nature Ecology and Evolution*, 3:416–423.

Buesseler, K. O. and Boyd, P. W. (2009). Shedding light on processes that control particle export and flux attenuation in the twilight zone of the open ocean. *Limnology and Oceanography*, 54(4):1210–1232.

Buesseler, K. O., Boyd, P. W., Black, E. E., and Siegel, D. A. (2020). Metrics that matter for assessing the ocean biological carbon pump. *Proceedings of the National Academy of Sciences*, 117(18):201918114.

Caparroy, P., Thygesen, U. H., and Visser, A. W. (2000). Modelling the attack success of planktonic predators: patterns and mechanisms of prey size selectivity. *Journal of Plankton Research*, 22(10):1871–1900.

Claireaux, G., Webber, D. M., Lagardère, J.-P., and Kerr, S. R. (2000). Influence of water temperature and oxygenation on the aerobic metabolic scope of Atlantic cod (Gadus morhua). *Journal of Sea Research*, 44:257–265.

Dam, H. G., Roman, M. R., and Youngbluth, M. J. (1995). Downward export of respiratory carbon and dissolved inorganic nitrogen by diel-migra1nt mesozooplankton at the JGOFS Bermuda time-series station. *Deep Sea Research Part I: Oceanographic Research Papers*, 42(7):1187–1197.

Darnis, G., Hobbs, L., Geoffroy, M., Grenvald, J. C., Renaud, P. E., Berge, J., Cottier, F., Kristiansen, S., Daase, M., E. Søreide, J., Wold, A., Morata, N., and Gabrielsen, T. (2017). From polar night to midnight sun: Diel vertical migration, metabolism and biogeochemical role of zooplankton in a high Arctic fjord (Kongsfjorden, Svalbard). *Limnology and Oceanography*, 62(4):1586–1605.

Davison, P. C., Checkley, D. M., Koslow, J. A., and Barlow, J. (2013). Carbon export mediated by mesopelagic fishes in the northeast Pacific Ocean. *Progress in Oceanography*, 116:14–30.

de Boyer Montégut, C., Madec, G., Fischer, A. S., Lazar, A., and Iudicone, D. (2004). Mixed layer depth over the global ocean: An examination of profile data and a profile-based climatology. *Journal of Geophysical Research C: Oceans*, 109(12):1–20.

DeVries, T. (2014). The oceanic anthropogenic CO2 sink: Storage, air-sea fluxes, and transports over the industrial era. *Global Biogeochemical Cycles*, 28(7):631–647.

DeVries, T. and Primeau, F. (2011). Dynamically and observationally constrained estimates of water-mass distributions and ages in the global ocean. *Journal of Physical Oceanography*, 41(12):2381–2401.

DeVries, T., Primeau, F., and Deutsch, C. (2012). The sequestration efficiency of the biological pump. *Geophysical Research Letters*, 39(13):1–5.

DeVries, T. and Weber, T. (2017). The export and fate of organic matter in the ocean: New constraints from combining satellite and oceanographic tracer observations. *Global Biogeochemical Cycles*, 31(3):535–555.

Domenici, P. (2001). The scaling of locomotor performance in predator–prey encounters: from fish to killer whales. *Comparative Biochemistry and Physiology Part A: Molecular & Integrative Physiology*, 131(1):169–182.

Dunne, J. P., Armstrong, R. A., Gnnadesikan, A., and Sarmiento, J. L. (2005). Empirical and mechanistic models for the particle export ratio. *Global Biogeochemical Cycles*, 19(4):1–16.

Ekau, W., Auel, H., Portner, H. O., and Gilbert, D. (2010). Impacts of hypoxia on the structure and processes in pelagic communities (zooplankton, macro-invertebrates and fish). *Biogeosciences*, 7(5):1669–1699.

Ern, R., Norin, T., Gamperl, A. K., and Esbaugh, A. J. (2016). Oxygen dependence of upper thermal limits in fishes. *The Journal of Experimental Biology*, 219(21):3376–3383.

Falkowski, P. G., Barber, R. T., and Smetacek, V. (1998). Biogeochemical controls and feedbacks on ocean primary production. *Science*, 281(5374):200–206.

Garcia, H., Weathers, C., Paver, C., Smolyar, I., Boyer, T., Locarnini, R., Zweng, M., Mishonov, A., Baranova, O., Seidov, D., and Reagan, J. (2019). WORLD OCEAN ATLAS 2018 Volume 3: Dissolved Oxygen, Apparent Oxygen Utilization, and Dissolved Oxygen Saturation. Technical report, Silver Spring, MD.

Gilliam, J. F. and Fraser, D. F. (1987). Habitat Selection Under Predation Hazard: Test of a Model with Foraging Minnows. *Ecology*, 68(6):1856–1862.

Gorgues, T., Aumont, O., and Memery, L. (2019). Simulated changes in the particulate carbon export efficiency due to diel vertical migration of zooplankton in the North Atlantic. *Geophysical Research Letters*, 46(10):5387–5395.

Hansen, A. N. and Visser, A. W. (2016). Carbon export by vertically migrating zooplankton: An optimal behavior model. *Limnology and Oceanography*, 61(2):701–710.

Hays, G. C. (2003). A review of the adaptive significance and ecosystem consequences of zooplankton diel vertical migrations. *Hydrobiologia*, 503:163–170.

Henson, S. A., Sanders, R., Madsen, E., Morris, P. J., Le Moigne, F., and Quartly, G. D. (2011). A reduced estimate of the strength of the ocean's biological carbon pump. *Geophysical Research Letters*, 38(4):10–14.

Hofbauer, J. and Sigmund, K. (2003). Evolutionary Game Dynamics. *Bulletin (New Series) of the American mathematical society*, 40(403):479–519.

Holland, K. N., Brill, R. W., Chang, R. K., Sibert, J. R., and Fournier, D. A. (1992). Physiological and behavioural thermoregulation in bigeye tuna (Thunnus obesus). *Nature*, 358(6385):410–412.

Holling, C. (1959). Some characteristics of simple types of predation and parasitism. *The Canadian Entomologist*, 91(7):385–398.

Houston, A. I., McNamara, J. M., and Hutchinson, J. M. C. (1993). General results concerning the trade-off between gaining energy and avoiding predation. *Philosophical Transactions of the Royal Society of London. Series B: Biological Sciences*, 341(1298):375–397.

Hudson, J. M., Steinberg, D. K., Sutton, T. T., Graves, J. E., and Latour, R. J. (2014). Myctophid feeding ecology and carbon transport along the northern Mid-Atlantic Ridge. *Deep-Sea Research Part I: Oceanographic Research Papers*, 93:104–116.

Hugie, D. M. and Dill, L. M. (1994). Fish and Game: a game theoretic approach to habitat selection by predators and prey. *Journal of Fish Biology*, 45(Supplement A):151–169.

Huntley, M. E. and Zhou, M. (2004). Influence of animal on turbulence in the sea. *Marine Ecology Progress Series*, 273:65–79.

Irigoien, X., Klevjer, T. A., Røstad, A., Martinez, U., Boyra, G., Acuña, J. L., Bode, A., Echevarria, F., Gonzalez-Gordillo, J. I., Hernandez-Leon, S., Agusti, S., Aksnes, D. L., Duarte, C. M., and Kaartvedt, S. (2014). Large mesopelagic fishes biomass and trophic efficiency in the open ocean. *Nature communications*, 5:3271.

Iwasa, Y. (1982). Vertical migration of zooplankton: a game between predator and prey. *The American naturalist*, 120(2):171–180.

Jackson, G. A. and Kiørboe, T. (2004). Zooplankton use of chemodetection to find and eat particles. *Marine Ecology Progress Series*, 269:153–162.

Ji, R. and Franks, P. (2007). Vertical migration of dinoflagellates: model analysis of strategies, growth, and vertical distribution patterns. *Marine Ecology Progress Series*, 344:49–61.

Jónasdóttir, S. H., Visser, A. W., Richardson, K., and Heath, M. R. (2015). Seasonal copepod lipid pump promotes carbon sequestration in the deep North Atlantic. *Proceedings of the National Academy of Sciences*, 112(39):12122–12126.

Kaartvedt, S., Klevjer, T. A., Torgersen, T., Sørnes, T. A., and Røstad, A. (2007). Diel vertical migration of individual jellyfish (Periphylla periphylla). *Limnology and Oceanography*, 52(3):975–983.

Kiko, R., Hauss, H., Buchholz, F., and Melzner, F. (2016). Ammonium excretion and oxygen respiration of tropical copepods and euphausiids exposed to oxygen minimum zone conditions. *Biogeosciences*, 13(8):2241–2255.

Kiørboe, T., Andersen, A., Langlois, V. J., and Jakobsen, H. H. (2010). Unsteady motion: escape jumps in planktonic copepods, their kinematics and energetics. *Journal of The Royal Society Interface*, 7(52):1591–1602.

Kiørboe, T. and Hirst, A. G. (2014). Shifts in Mass Scaling of Respiration, Feeding, and Growth Rates across Life-Form Transitions in Marine Pelagic Organisms. *The American Naturalist*, 183(4):E118–E130.

Klevjer, T. A., Irigoien, X., Røstad, A., Fraile-Nuez, E., Benítez-Barrios, V. M., and Kaartvedt, S. (2016). Large scale patterns in vertical distribution and behaviour of mesopelagic scattering layers. *Scientific Reports*, 6(1):19873.

Lampert, W. (1993). Ultimate causes of diel vertical migration of zooplankton: New evidence for the predator-avoidance hypothesis. *Archiv her Hydrobiologie, Beiheft Ergebnisse der Limnologie*, 39:79–88.

Law, R. (2000). Fishing, selection, and phenotypic evolution. *ICES Journal of Marine Science*, 57(3):659–668.

Locarnini, R., Mishonov, A., Baranova, O., Boyer, T., Zweng, M., Garcia, H., Reagan, J., Seidov, D., Weathers, K., Paver, C., and Smolyar, I. (2019). World Ocean Atlas, Volume 1: Temperature.

Longhurst, A., Bedo, A., Harrison, W., Head, E., and Sameoto, D. (1990). Vertical flux of respiratory carbon by oceanic diel migrant biota. *Deep Sea Research Part A. Oceanographic Research Papers*, 37(4):685–694.

Lucas, C. H., Jones, D. O., Hollyhead, C. J., Condon, R. H., Duarte, C. M., Graham, W. M., Robinson, K. L., Pitt, K. A., Schildhauer, M., and Regetz, J. (2014). Gelatinous zooplankton biomass in the global oceans: Geographic variation and environmental drivers. *Global Ecology and Biogeography*, 23(7):701–714.

Luo, J. Y., Condon, R. H., Stock, C. A., Duarte, C. M., Lucas, C. H., Pitt, K. A., and Cowen, R. (2020). Gelatinous zooplankton-mediated carbon flows in the global oceans: a data-driven modeling study. *Global Biogeochemical Cycles*, 34(e2020GB006704).

Lutz, M. J., Caldeira, K., Dunbar, R. B., and Behrenfeld, M. J. (2007). Seasonal rhythms of net primary production and particulate organic carbon flux to depth describe the efficiency of biological pump in the global ocean. *Journal of Geophysical Research: Oceans*, 112(10).

McLaren, I. A. (1963). Effects of Temperature on Growth of Zooplankton, and the Adaptive Value of Vertical Migration. *Journal of the Fisheries Research Board of Canada*, 20(3):685–727.

Melin, F. (2013). GMIS - MODIS-AQUA Monthly climatology sea surface diffuse attenuation coefficient at 490nm (9km) in mˆ-1. Technical report, European Commision, Joint Research Centre (JRC).

Naraghi, M. H. and Etienne, G. (2012). Solar Panel Orientation and Modeling Based on Hourly Clearness Index. *ASME 2012 6th International Conference on Energy Sustainability, Parts A and B*, (July 2012):105.

Nash, J. (1951). Non-Cooperative Games. *The Annals of Mathematics*, 54(2):286.

Nilsson, G. E. and Östlund-Nilsson, S. (2008). Does size matter for hypoxia tolerance in fish? *Biological Reviews*, 83(2):173–189.

O'Driscoll, R. L., Gauthier, S., and Devine, J. A. (2009). Acoustic estimates of mesopelagic fish: as clear as day and night? *ICES Journal of Marine Science*, 66(6):1310–1317.

Onsrud, M. S. R., Kaartvedt, S., Røstad, A., and Klevjer, T. A. (2004). Vertical distribution and feeding patterns in fish foraging on the krill Meganyctiphanes norvegica. *ICES Journal of Marine Science*, 61(8):1278–1290.

Petrik, C. M., Stock, C. A., Andersen, K. H., van Denderen, P. D., and Watson, J. R. (2019). Bottom-up drivers of global patterns of demersal, forage, and pelagic fishes. *Progress in Oceanography*, 176(June):102124.

Pinti, J., Kiørboe, T., Thygesen, U. H., and Visser, A. W. (2019). Trophic interactions drive the emergence of diel vertical migration patterns: a game-theoretic model of copepod communities. *Proceedings of the Royal Society B: Biological Sciences*, 286(1911):20191645.

Pinti, J. and Visser, A. W. (2019). Predator-Prey Games in Multiple Habitats Reveal Mixed Strategies in Diel Vertical Migration. *The American Naturalist*, 193(3):E000–E000.

Prihartato, P. K., Aksnes, D. L., and Kaartvedt, S. (2015). Seasonal patterns in the nocturnal distributionand behavior of the mesopelagic fish Maurolicus muelleri at high latitudes. *Marine Ecology Progress Series*, 521:189–200.

Proud, R., Cox, M. J., and Brierley, A. S. (2017). Biogeography of the Global Ocean's Mesopelagic Zone. *Current Biology*, 27(1):113–119.

Proud, R., Cox, M. J., Handegard, N. O., Kloser, R. J., and Brierley, A. S. (2018). From siphonophores to deep scattering layers: an estimation of global mesopelagic fish biomass. *ICES Journal of Marine Science*, (May).

Rogers, N. J., Urbina, M. A., Reardon, E. E., McKenzie, D. J., and Wilson, R. W. (2016). A new analysis of hypoxia tolerance in fishes using a database of critical oxygen level (Pcrit). *Conservation Physiology*, 4(1):1–19.

Saba, G. K. and Steinberg, D. K. (2012). Abundance, composition, and sinking rates of fish fecal pellets in the santa barbara channel. *Scientific Reports*, 2:1–6.

Sainmont, J., Andersen, K. H., Thygesen, U. H., Fiksen, Ø., and Visser, A. W. (2015). An effective algorithm for approximating adaptive behavior in seasonal environments. *Ecological Modelling*, 311:20–30.

Salonen, K., Sarvala, J., Hakala, I., and Viljanen, M. L. (1976). The relation of energy and organic carbon in aquatic invertebrates. *Limnology and Oceanography*, 21 (5)(5):724–730.

Schlitzer, R. (2002). Carbon export fluxes in the Southern Ocean: Results from inverse modeling and comparison with satellite-based estimates. *Deep-Sea Research Part II: Topical Studies in Oceanography*, 49(9-10):1623–1644.

Schuster, P. and Siegmund, K. (1983). Replicator Dynamics. *Journal of Theoretical Biology*, 100:533–538.

Seibel, B. A. (2011). Critical oxygen levels and metabolic suppression in oceanic oxygen minimum zones. *Journal of Experimental Biology*, 214(2):326–336.

Seibel, B. A. and Deutsch, C. (2020). Oxygen supply capacity in animals evolves to meet maximum demand at the current oxygen partial pressure regardless of size or temperature. *Journal of Experimental Biology*, 223(12).

Seibel, B. A., Schneider, J. L., Kaartvedt, S., Wishner, K. F., and Daly, K. L. (2016). Hypoxia Tolerance and Metabolic Suppression in Oxygen Minimum Zone Euphausiids: Implications for Ocean Deoxygenation and Biogeochemical Cycles. *Integrative and Comparative Biology*, 56(4):510–523.

Siegel, D. A., Buesseler, K. O., Doney, S. C., Sailley, S. F., Behrenfeld, M. J., and Boyd, P. W. (2014). Global assessment of ocean carbon export by combining satellite observations and food-web models. *Global Biogeochemical Cycles*, 28(3):181–196.

Speers-Roesch, B., Mandic, M., Groom, D. J., and Richards, J. G. (2013). Critical oxygen tensions as predictors of hypoxia tolerance and tissue metabolic responses during hypoxia exposure in fishes. *Journal of Experimental Marine Biology and Ecology*, 449:239–249.

St. John, M. A., Borja, A., Chust, G., Heath, M. R., Grigorov, I., Mariani, P., Martin, A. P., and Santos, R. S. (2016). A Dark Hole in Our Understanding of Marine Ecosystems and Their Services: Perspectives from the Mesopelagic Community. *Frontiers in Marine Science*, 3(March):1–6.

Steinberg, D. K., Carlson, C. A., Bates, N. R., Goldthwait, S. A., Madin, L. P., and Michaels, A. F. (2000). Zooplankton vertical migration and the active transport of dissolved organic and inorganic carbon in the Sargasso Sea. *Deep Sea Research Part I*, 47(1):137–158.

Stich, H.-B. and Lampert, W. (1981). Predator evasion as an explanation of diurnal vertical migration by zooplankton. *Nature*, 293(5831):396–398.

Stock, C. A., Dunne, J. P., and John, J. G. (2014). Global-scale carbon and energy flows through the marine planktonic food web: An analysis with a coupled physical-biological model. *Progress in Oceanography*, 120:1–28.

Stock, C. A., John, J. G., Rykaczewski, R. R., Asch, R. G., Cheung, W. W., Dunne, J. P., Friedland, K. D., Lam, V. W., Sarmiento, J. L., and Watson, R. A. (2017). Reconciling fisheries catch and ocean productivity. *Proceedings of the National Academy of Sciences of the United States of America*, 114(8):E1441–E1449.

Thygesen, U. H. and Patterson, T. A. (2018). Oceanic diel vertical migrations arising from a predator-prey game. *Theoretical Ecology*, pages 1–13.

Thygesen, U. H., Sommer, L., Evans, K., and Patterson, T. A. (2016). Dynamic optimal foraging theory explains vertical migrations of Bigeye tuna. *Ecology*, 97(7):1852–1861.

Ultsch, G. R. and Regan, M. D. (2019). The utility and determination of Pcrit in fishes. *Journal of Experimental Biology*, 222(22):1–9.

van Someren Gréve, H., Almeda, R., and Kiørboe, T. (2017). Motile behavior and predation risk in planktonic copepods. *Limnology and Oceanography*, 62(5):1810–1824.

Vinogradov, M. (1962). Feeding of the deep-sea zooplankton. *ICES reports*, (18):114–120.

Visser, A. W. (2007). Motility of zooplankton: Fitness, foraging and predation. *Journal of Plankton Research*, 29(5):447–461.

Visser, A. W., Grønning, J., and Jónasdóttir, S. H. (2017). Calanus hyperboreus and the lipid pump. *Limnology and Oceanography*, 62(3):1155–1165.

Zaret, T. M. and Suffern, S. (1976). Vertical migration in zooplankton as a predator avoidance mechanism. *Limnology and Oceanography*, 21(6):804–813.

CHAPTER A

Appendices

Appendix A: Pinti et al. 2020

Jérôme Pinti, Antonio Celani, Uffe H. Thygesen and Patrizio Mariani

Optimal navigation and behavioural traits in oceanic migrations. Published in *Theoretical Ecology* (2020)

Abstract

Many organisms perform regular migrations over long distances. These movements are often related to feeding and reproductive periods and regulated by oceanographic conditions as well as physiological and behavioural traits. Different individual traits and their associated evolutionary constraints will ultimately shape the migratory strategy (and route) of individuals. Optimality theory can provide a framework to assess these inherent trade-offs in individual migrations and identify optimal migration routes in different conditions. Here, we present a model that describes the behavioural trade-off between migration time and energy expenditure and identifies optimal migration routes in realistic ocean conditions. The model explicitly includes a behavioural factor for individual risk management, including risks associated with moving in a stochastic environment. We test this model in three different case studies, one in an idealized theoretical context and two in realistic conditions for sea turtle migrations. We show that behavioural traits can largely influence the optimal routes in long-distance migrations, resulting in major changes in migratory pathways. Further, we assess the ability of the model to infer back behavioural traits given a set of synthetic individual tracks and show relatively good performances. However, further tests are needed to evaluate performances when accurate observations of migrations are used.

Appendix B: Serra-Pompei et al. (*in prep*)

Camila Serra-Pompei, Ben Ward, Jérôme Pinti, André W. Visser, Thomas Kiørboe, Ken H. Andersen

Role of zooplankton trophic dynamics in driving carbon export efficiency (*in prep*)

Abstract

Copepods largely contribute to carbon export and sequestration in the ocean. However, whether copepod increase or decrease carbon export efficiency is still unclear. We investigated the role of copepods in regulating export efficiency of particles (pe-ratio). We used a mechanistic plankton-ecosystem model (unicellular protists and copepods) coupled to a global ocean circulation model. The model generates an emergent planktonic community and the size distribution of all organisms and associated sinking particles. We tested several hypothesis relating the role of mesozooplankton in driving carbon export efficiency. We show that high carbon export efficiency is related to the flux of carbon going through the copepod compartment. Biomass of large copepod was related to high pe-ratios, but total copepod biomass did not show a clear pattern. Copepods consumed a large fraction of the detritus produced, but respiration losses did not strongly attenuate the particle flux. Trophic coupling between phytoplankton and zooplankton did not reduce pe-ratio. In this case pe-ratio was regulated by the size of the predators. Finally, we did not find a clear relation between NPP and pe-ratio. By resolving the size-distribution of copepods and associated faecal pellets we improve the understanding of the mechanisms driving carbon export efficiency.